

Modeling of Pile Footings and Drilled Shafts for Seismic Design

by

I. PoLam, M. Kapuskar and D. Chaudhuri

Earth Mechanics, Inc.
17660 Newhope Street, Suite E
Fountain Valley, California 92708

Technical Report MCEER-98-0018

December 21, 1998

REPRODUCED BY
U.S. DEPARTMENT OF COMMERCE
NATIONAL TECHNICAL
INFORMATION SERVICE
SPRINGFIELD, VA 22161

This research was conducted at Earth Mechanics, Inc. and was supported by the
Federal Highway Administration under contract number DTFH61-92-C-00112.

NOTICE

This report was prepared by Earth Mechanics, Inc. as a result of research sponsored by the Multidisciplinary Center for Earthquake Engineering Research (MCEER) through a contract from the Federal Highway Administration. Neither MCEER, associates of MCEER, its sponsors, Earth Mechanics, Inc., nor any person acting on their behalf:

- a. makes any warranty, express or implied, with respect to the use of any information, apparatus, method, or process disclosed in this report or that such use may not infringe upon privately owned rights; or
- b. assumes any liabilities of whatsoever kind with respect to the use of, or the damage resulting from the use of, any information, apparatus, method, or process disclosed in this report.

Any opinions, findings, and conclusions or recommendations expressed in this publication are those of the author(s) and do not necessarily reflect the views of MCEER or the Federal Highway Administration.

50272 - 101			
REPORT DOCUMENTATION PAGE	1. Report No. MCEER-98-0018	2.	3. Recipient's Accession No.
4. Title and Subtitle Modeling of Pile Footings and Drilled Shafts for Seismic Design		5. Report Date December 21, 1998	
7. Authors I. PoLam, M. Kapuskar and D. Chaudhuri		6.	
9. Performing Organization Name and Address Earth Mechanics, Inc., 17660 Newhope Street, Suite E, Fountain Valley, California 92708		8. Performing Organization Report No.	
		10. Project/Task/Work Unit No. 112-D-3.5 and 112-D-3.6	
12. Sponsoring Organization Name and Address Multidisciplinary Center for Earthquake Engineering Research State University of New York at Buffalo Red Jacket Quadrangle, Buffalo, NY 14261		11. Contract (C) or Grant (G) No. (C) DTFH61-92-C-00112 (G)	
		13. Type of Report & Period Covered Technical report	
		14.	
15. Supplementary Notes This research was conducted at Earth Mechanics, Inc. and was supported by the Federal Highway Administration under contract number DTFH61-92-C-00112.			
16. Abstract (limit 200 words) This report documents two studies that were conducted to review, assess, and provide recommendations regarding the seismic design of bridge foundations. Specifically, the report addresses modeling approaches and parameters that affect the seismic design and response of pile groups and drilled shafts. The report attempts to bridge the interface between the structural and geotechnical design process by describing a two-step design and analysis procedure for these bridge foundation components. Recent research results on pile group effects and the design of pile foundations to resist lateral spreading of liquefiable soils are also reviewed. Recommendations are provided concerning: modifications to p-y curves to account for cyclic loading conditions, pile group effects and soil-pile interaction behavior, and development of p-y curves for the design of drilled shafts.			
17. Document Analysis a. Descriptors Earthquake engineering. Seismic design. Drilled shaft foundations. Pile group foundations. Bridges. Loading. Modeling. Stiffness. Lateral ground spreading. Seismic response. Soil-pile interaction.			
b. Identifiers/Open-Ended Terms			
c. COSATI Field/Group			
18. Availability Statement Release unlimited.		19. Security Class (This Report) Unclassified	21. No. of Pages 151
		20. Security Class (This Page) Unclassified	22. Price
(see ANSI_Z39.18)			

MOEER

1999 MAY 11 PM 1:51



Modeling of Pile Footings and Drilled Shafts For Seismic Design

by

I. PoLam¹, M. Kapuskar² and D. Chaudhuri³

Publication Date: December 21, 1998

Submittal Date: January 31, 1998

Technical Report MCEER-98-0018

Task Numbers 112-D-3.5 and 112-D-3.6

FHWA Contract Number DTFH61-92-C-00112

PROTECTED UNDER INTERNATIONAL COPYRIGHT
ALL RIGHTS RESERVED.
NATIONAL TECHNICAL INFORMATION SERVICE
U.S. DEPARTMENT OF COMMERCE

- 1 Principal, Earth Mechanics, Inc., Fountain Valley, California
- 2 Project Engineer, Earth Mechanics, Inc., Fountain Valley, California
- 3 Staff Engineer, Earth Mechanics, Inc., Fountain Valley, California

MULTIDISCIPLINARY CENTER FOR EARTHQUAKE ENGINEERING RESEARCH
University at Buffalo, State University of New York
Red Jacket Quadrangle, Buffalo, NY 14261

Preface

The Multidisciplinary Center for Earthquake Engineering Research (MCEER) is a national center of excellence in advanced technology applications that is dedicated to the reduction of earthquake losses nationwide. Headquartered at the University at Buffalo, State University of New York, the Center was originally established by the National Science Foundation in 1986, as the National Center for Earthquake Engineering Research (NCEER).

Comprising a consortium of researchers from numerous disciplines and institutions throughout the United States, the Center's mission is to reduce earthquake losses through research and the application of advanced technologies that improve engineering, pre-earthquake planning and post-earthquake recovery strategies. Toward this end, the Center coordinates a nationwide program of multidisciplinary team research, education and outreach activities.

MCEER's research is conducted under the sponsorship of two major federal agencies, the National Science Foundation (NSF) and the Federal Highway Administration (FHWA), and the State of New York. Significant support is also derived from the Federal Emergency Management Agency (FEMA), other state governments, academic institutions, foreign governments and private industry.

The Center's FHWA-sponsored Highway Project develops retrofit and evaluation methodologies for existing bridges and other highway structures (including tunnels, retaining structures, slopes, culverts, and pavements), and improved seismic design criteria and procedures for bridges and other highway structures. Specifically, tasks are being conducted to:

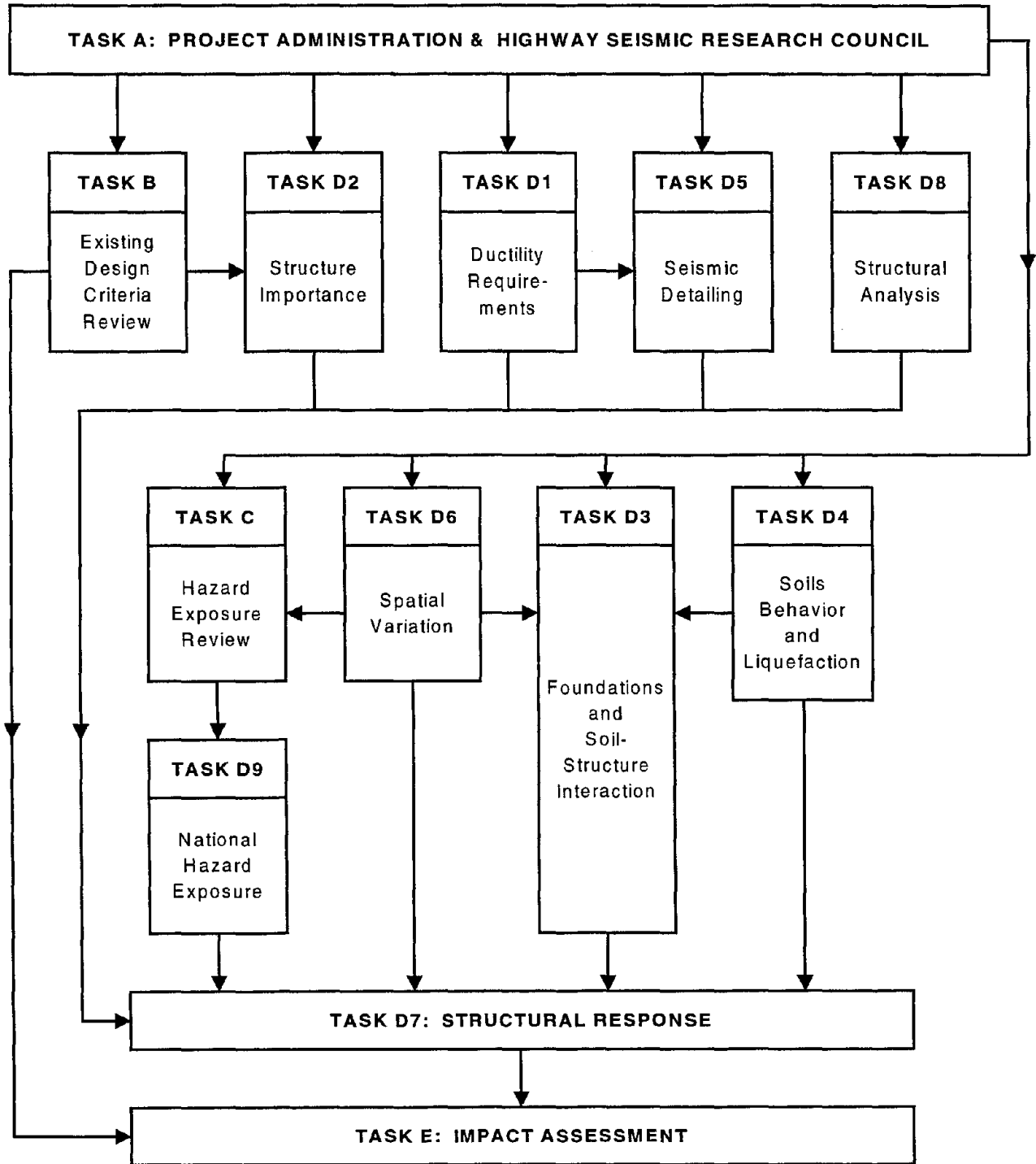
- assess the vulnerability of highway systems, structures and components;
- develop concepts for retrofitting vulnerable highway structures and components;
- develop improved design and analysis methodologies for bridges, tunnels, and retaining structures, which include consideration of soil-structure interaction mechanisms and their influence on structural response;
- review and recommend improved seismic design and performance criteria for new highway structures.

Highway Project research focuses on two distinct areas: the development of improved design criteria and philosophies for new or future highway construction, and the development of improved analysis and retrofitting methodologies for existing highway systems and structures. The research discussed in this report is a result of work conducted under the new highway structures project, and was performed within Task 112-D-3.5(a), "Develop Analysis and Design Procedures for Pile Footings" and Task 112-D-3.6, "Develop Analysis and Design Procedures for Drilled Shafts" as shown in the flowchart on the following page.

The overall objective of these tasks was to develop seismic design procedures for two types of typical bridge foundations: pile footings and drilled shafts. This report reviews, assesses and provides recommendations concerning design guidelines for each of these foundation types. For both types of foundations, a two-step process was developed and various parameters that affect predicted foundation response are identified. The implications of the foundation modeling process in

estimating structural response is described. The research examined the applicability of conventional p-y formulations in modeling soil-pile behavior, and assessed modifications to account for cyclic loading conditions, pile group effects, and soil-pile interaction behavior in liquefied soil. For both types of foundations, the report attempts to integrate the structural and geotechnical engineering points of view.

SEISMIC VULNERABILITY OF NEW HIGHWAY CONSTRUCTION
FHWA Contract DTFH61-92-C-00112



ABSTRACT

This report documents two studies that were conducted to review, assess, and provide recommendations regarding the seismic design of bridge foundations. Specifically, the report addresses modeling approaches and parameters that affect the seismic design and response of pile groups and drilled shafts. The report attempts to bridge the interface between the structural and geotechnical design process - in so doing, it describes a two-step design and analysis procedure for these bridge foundation components. Recent research results on pile group effects and the design of pile foundations to resist lateral spreading of liquefiable soils are also reviewed. Recommendations are provided concerning: modifications to p-y curves to account for cyclic loading conditions, pile group effects and soil-pile interaction behavior, and development of p-y curves for the design of drilled shafts.

ACKNOWLEDGMENTS

This research was funded by the Multidisciplinary Center for Earthquake Engineering Research, Buffalo through a contract with the Federal Highway Administration. In an attempt to implement research findings into design practice, the authors have extracted results from research reported in the literature, especially those funded by the FHWA/MCEER highway research programs. This support gratefully acknowledged.

The authors acknowledge Dr. Hubert Law for his contributions in the production of this report. Dr. Ricardo Dobry of Rensselaer Polytechnic Institute and Dr. Kyle Rollins of Brigham Young University were very helpful in providing their centrifuge and full-scale pile load test data, and their assistance is greatly acknowledged.

TABLE OF CONTENTS

SECTION	TITLE	PAGE
1	INTRODUCTION	
1.1	Overview	1
1.2	Objectives	3
1.3	Organization of the Report	3
2	MODELING OF PILE FOOTINGS	5
2.1	Introduction	5
2.2	Two-Step Seismic Design Process	6
2.2.1	Step 1: Determination of Seismic Demand and Foundation Stiffness	6
2.2.1.1	Displacement Demand	8
2.2.1.2	Force Demand Associated with Load Fuses	8
2.2.1.3	Governing Load Case for Foundation Design	10
2.2.1.4	Other Loading Mechanisms	10
2.2.1.5	Foundation Damping	10
2.2.2	Step 2: Capacity Analysis	11
2.2.3	Prevalent Practice for Conservatism	12
2.3	Single Pile-Head Stiffness	13
2.3.1	General Form	13
2.3.2	Appropriate Foundation Stiffness Matrix	14
2.3.2.1	Fundamental Assumptions	14
2.3.2.2	Stiffness Matrix from Nonlinear Analysis	16
2.3.3	Pile-Head Stiffness for Axial Load	17
2.3.3.1	Simplified Graphical Procedure	17
2.3.3.2	Stiffness for Uplift Loading	19
2.3.3.3	Selection of Secant Stiffness	19
2.3.4	Pile-Head Stiffness for Lateral Loading	20
2.3.4.1	Linear Subgrade Modulus	22
2.3.4.2	Embedment Effect	29
2.3.4.3	Relationship Between Subgrade Modulus and Soil Modulus	29
2.3.4.4	Presumptive Lateral Stiffness	34
2.3.5	Foundation Displacement/Rotation Criteria	35
2.4	Pile-Group Stiffness	35
2.4.1	Rigorous Method Using Static Equilibrium	35
2.4.1.1	Special Case of Plumb Pile Group	37
2.4.2	Simplified Method Using an Equivalent-Cantilever Approach	37
2.4.2.1	Equivalent Cantilever Model Parameter for Lateral Loading	40
2.4.2.2	Cantilever Model Matched to Diagonal Stiffness	40
2.4.2.3	Cantilever Model Matched to Translational and Cross Coupling Stiffness	41
2.4.2.4	Axial and Torsional Stiffness	41

TABLE OF CONTENTS - Cont'd

SECTION	TITLE	PAGE
2.5	Pilecap Stiffness	42
2.5.1	Previous Research on Interaction Between Pile and Pile Cap	42
2.5.2	Recommendation for Incorporating Pile Cap Stiffness	43
2.5.3	Passive Earth Pressure for Sand	45
2.5.4	Passive Earth Pressure for General $c-\phi$ Soils	47
2.5.5	Typical Earth Pressure Coefficients for Design	47
2.5.6	Pile Cap Displacement	47
2.6	Nonlinear Load-Deflection Sensitivity Study	50
2.6.1	Background on p-y Curves	50
2.6.2	p-y Curves versus Terzaghi's Subgrade Modulus	50
2.6.3	Sensitivity to Various Aspects of Soil-Pile Modeling Assumptions	54
2.6.4	Pile Group Effects for Typical Pile Footings	56
2.6.4.1	Group Effects from Elastic Halfspace Theory	57
2.6.4.2	Group Effects from Experimental Studies	57
2.6.5	Group Effects for Extremely Large Pile Groups	62
2.6.6	Pile Design in Liquefiable Soils	65
2.6.6.1	Design for Structural Loading	65
2.6.6.2	Design Issues Related to Lateral Ground Spread	70
3	MODELING OF DRILLED SHAFTS	75
3.1	Introduction	75
3.2	Seismic Design Procedure For Drilled Shafts	76
3.2.1	Step 1: Modeling of Foundation Stiffness	76
3.2.1.1	Coupled Foundation Stiffness Matrix	77
3.2.1.2	Equivalent Cantilever Beam	79
3.2.1.3	Uncoupled Foundation Springs	83
3.2.1.4	Foundation Nonlinearity	83
3.2.1.5	Foundation Geometry	85
3.2.1.6	Boundary Conditions	87
3.2.1.7	Other Considerations	89
3.2.2	Step 2: Estimating Foundation Capacity	89
3.2.2.1	Prevalent Practice for Conservatism	91
3.2.2.2	Formation of Plastic Hinge	91
3.2.2.3	Shear Capacity	92
3.2.2.4	Minimum Pile Length	95
3.3	p-y Model For Drilled Shafts	96
3.3.1	Effects of Various Parameters	98
3.3.1.1	Soil Properties	99
3.3.1.2	Degradation Effect	99
3.3.1.3	Embedment and Gapping or Scouring	99

TABLE OF CONTENTS - Cont'd

SECTION	TITLE	PAGE
	3.3.2 Load Transfer Mechanism of Laterally Loaded Piles	103
	3.3.3 Installation Procedure	106
	3.3.4 Observation From Load Test Data	106
	3.3.5 Observations From Analytical Results	107
4	SUMMARY AND CONCLUSIONS	
	4.1 Summary	109
	4.2 Conclusions and Recommendations	109
5	REFERENCES	113

LIST OF ILLUSTRATIONS

FIGURE	TITLE	PAGE
1-1	Pile Foundation Configurations	2
2-1	Equivalent Linear Stiffness from Nonlinear Response	7
2-2	Typical Locations of Plastic Hinges (after Caltrans, 1990)	9
2-3	Coordinate System and Stiffness Directions	15
2-4	Axial Load-Displacement Graphical Solution	18
2-5	Typical Characteristics of Friction versus End-Bearing Piles	21
2-6	Lateral Pile-Head Stiffness (Fixed-Head Condition)	23
2-7	Rotational Pile-Head Stiffness	24
2-8	Cross-Coupling Pile-Head Stiffness	25
2-9	Lateral Pile-Head Stiffness (Free-Head Condition)	26
2-10	Recommended Coefficient f of Variation in Subgrade Modulus with Depth for Sand	27
2-11	Recommended Coefficient f of Variation in Subgrade Modulus with Depth for Clay	28
2-12	Adjustment Factors for Effective Stiffness for Concrete Piles	30
2-13	Lateral Embedded Pile-Head Stiffness	31
2-14	Embedded Pile-Head Rotational Stiffness	32
2-15	Embedded Pile Cross-Coupling Pile-Head Stiffness	33
2-16	Modeling Piles Using Equivalent Cantilever Beams	39
2-17	Method for Passive Pressure Capacity of Pile Cap	44
2-18	Coefficients for Friction Component of Passive Pressure Capacity	46
2-19	Elastic Stiffness Based on Elastic Soil Modulus	49
2-20	Correlation of p-y Curves with Terzaghi's Subgrade Stiffness for Sands	51
2-21	Correlation of p-y Curves with Terzaghi's Subgrade Stiffness for Clays	53
2-22	Sensitivity Study of Various Uncertainties in Pile Loading Analysis	55
2-23	Results of 4x4 Pile Group Tests in Sand	60
2-24	Pile Group Effects Reflected by p-y Curve on Pile Response	61
2-25	3-D FE Analysis using Periodic Boundary Condition for Infinite Pile Groups	63
2-26	Results of Group Effects at 3 Spacings for Infinite Pile Group	64
2-27	Loading Mechanism in Soil-Pile Interaction Problem	67
2-28	Degradation Coefficient C_u versus Pore-Pressure Ratio from Liu and Dobry	68
2-29	Two Generic Soil Conditions for Lateral Spread Pile Loading Problem	73
2-30	Bending Moment from Centrifuge Lateral Spread Loading Experiment	74
3-1	Pile Head Stiffness Representation	78
3-2	SPT Blowcount vs. Cantilever Length of Pile in Sand (After Caltrans,1990)	81
3-3	SPT Blowcount vs. Cantilever Length of Pile in Clay (After Caltrans,1990)	82
3-4	Pile Configuration and Load Resistance Mechanism	86
3-5	Boundary Condition and Pile Response	88
3-6	Modeling Soil-Pile System in Step 2 Analyses	90
3-7	Plastic Hinge Formation in Pile (after Priestley, 1996)	93

LIST OF ILLUSTRATIONS - Cont'd

FIGURE	TITLE	PAGE
3-8	Effect of Near Ground Support	94
3-9	Stability Ratios of Two Piles	97
3-10	Effect of Soil Properties on Pile Response	100
3-11	Example of p-Multiplier on p-y Curves	101
3-12	Effect of p-Multiplier on Pile Response	102
3-13	Effect of Scouring and Embedment on Pile Response	104
3-14	Load Transfer Mechanisms of a Drilled Shaft (After Lam and Martin, 1986)	105

LIST OF TABLES

TABLES	TITLE	PAGE
2-1	p-Multipliers (Cycle-1 Loading) from Various Experiments at 3D Center-to-Center Spacing for 3x3 Pile Groups	57

SECTION 1 INTRODUCTION

1.5 Overview

In this report, discussion is focused on the modeling and seismic design of pile group and drilled shaft foundations for bridge structures. Although the modeling approach for seismic loading is similar for various pile types, important differences exist due to installation procedures. These procedures significantly effect the appropriate input parameters as a result of i) how they are constructed, ii) specific properties of the pile type, and iii) specific connection details at the pile head-pile footing.

There are two general configurations where pile foundations are connected to the superstructure as shown in figure 1-1. Figure 1-1a shows an arrangement where piles are connected by a pile cap that supports the bridge pier or bent. This kind of arrangement is usually adopted for conventional small diameter pile groups. Figure 1-1b shows an example of a pile extension where the pile is extended as a structural unit to support the bridge superstructure. The load supporting mechanism and response of these two types of foundations are different and hence the modeling approach must account for these differences. In fact, the foundation types mentioned above fall into one of the two configurations shown in figure 1-1.

The first part of this report is dedicated to pile group foundations, as they are the most common foundation type used in bridge structures. The treatment for this type of configuration requires an understanding of pile behavior under both axial and lateral loading. Moreover, the combined effect of shear and overturning moment on pile footing behavior must be carefully addressed in modeling as well as from a seismic design standpoint. In the second part, the discussion is geared toward lateral loading on drilled shafts or pile extension type structures. In this type of structure, the overall as well as individual pile behavior is generally governed by the lateral loads on the bridge deck which in turn is reacted by the induced shear and bending moment on the drilled shafts. The bridge response is relatively insensitive to axial pile response in contrast to pile footings.

In general, structural behavior under seismic loading is a function of its dynamic response characteristics. Moreover, it is well known that overall structural dynamic properties are influenced by the relevant foundation properties. Therefore, for realistic evaluation of the structural response, it is necessary to model the force-deformation characteristics of the foundation and incorporate them in the analytical model of the structure.

The procedures currently used to analyze and design pile foundations under lateral and/or axial loads are generally based on the theory of beam on elastic foundation and its nonlinear variations as embodied in p-y formulations proposed by several researchers (e.g., Hetenyi, 1946; Matlock, 1970; Reese et al., 1974; Murchison and O'Neill, 1983; O'Neill and Gazioglu, 1984). Among the various sources of nonlinearities within the soil-pile interaction zone are the geometric nonlinearity such as gapping, material nonlinearity in the soil behavior, etc. Since these nonlinearities would have a

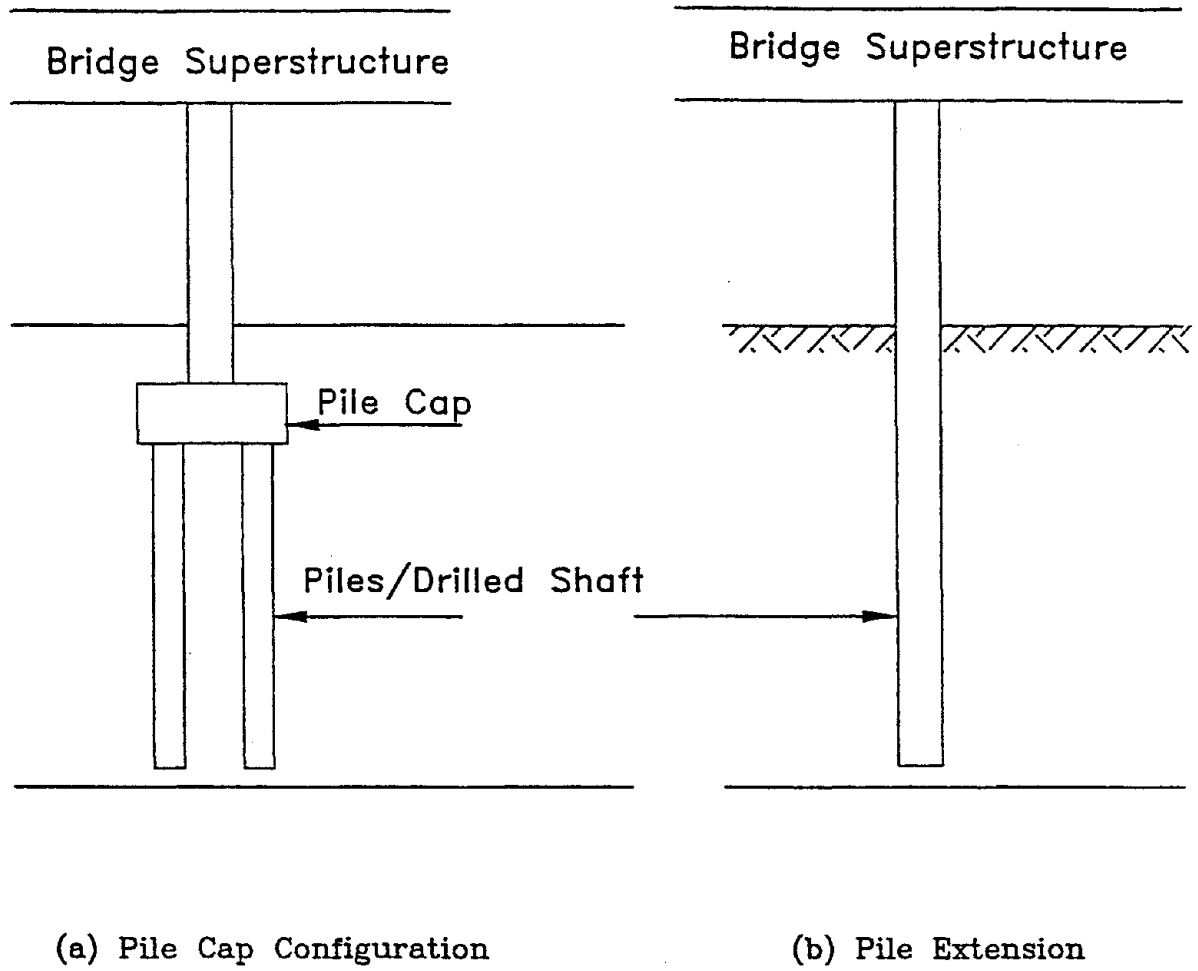


Figure 1-1 Pile Foundation Configurations

direct effect on the structural response, the most desirable way to evaluate the overall response is to integrate the total foundation system in the analytical model of the structure. However, this procedure is expensive in terms of computational effort, and not suitable for routine analysis and design. Moreover, given the uncertainties involved in predicting the ground motion and in characterizing the nonlinear behavior of structural and foundation elements, such a procedure may not improve the solution. In practice, foundation stiffnesses are represented in simpler forms that can be readily incorporated in the structural model. Since such procedures involve some simplifications and assumptions, the structural designer needs to be aware of the simplifying procedure and its implication in assessing the performance of the overall structural and foundation system.

1.2 Objectives

This report deals with the modeling of pile footings and drilled shaft foundations. It is recognized that a technically sound bridge and supporting foundation design requires full cooperation among structural and foundation engineers. Therefore, this report attempts to provide an integrated viewpoint that addresses issues of importance to both structural and foundation engineers. In doing so, the principal objectives are to:

- (1) Evaluate the effect of assumptions made in modeling the actual foundation behavior on the overall response of the structure.
- (2) Evaluate the effect of assumptions made in modeling the actual foundation behavior on the estimated displacement and force demand on the foundation as well as the overall bridge system.
- (3) Summarize different methods used to characterize the stiffness of pile footings and drilled shaft foundations, and discuss their limitations.
- (4) Provide guidelines on foundation modeling for seismic response and in subsequent foundation capacity analysis.
- (5) Provide seismic design guidelines.

1.3 Organization of the Report

This report consists of two main sections on the modeling aspects of pile footings and drilled shaft foundations for seismic design and analysis, respectively.

Pile footings are discussed in Section 2. This section discusses the steps involved in the overall design process for seismic loading and reviews the role of foundation modeling in the design process. A general methodology to develop the stiffness matrix of individual piles is provided. Various approaches to integrate individual pile-head stiffness matrices into the pile group model are discussed, as are the effects of soil resistance acting on the pile cap. Guidelines are given to account

for the additional stiffness. Finally, some nonlinear load-deflection soil-pile interaction analyses are provided and various sensitivity issues are discussed. Background information on the widely used p-y curve criteria with reference to the classical Terzaghi's linear subgrade theory, findings from recent studies on pile group effects, and issues related to design of piles in liquefiable soils are presented.

Section 3 discusses seismic design procedures for drilled shaft foundations. Applicability of conventional p-y models for drilled shaft foundation analysis is examined.

Section 4 contains a list of conclusions and recommendations regarding the seismic design of pile footings and drilled shafts from a geotechnical standpoint.

SECTION 2 MODELING OF PILE FOOTINGS

2.1 Introduction

In this section, various aspects of modeling, analysis and design of one of the most common foundation types, namely, pile group foundations (pile footings) are discussed. This type of foundation is typically used to support bridge superstructures. Pile foundations are used in a variety of substructure configurations, such as single column, multiple column bents on common or separate pile footings, pier walls, abutment walls and very large pile groups (with several hundred piles) to support pier towers in major water crossings and pile extensions where individual piles are extended above the mudline to support the superstructure directly. Moreover, pile types used in the above-mentioned foundations may vary depending on the specific site and design requirement. Among the various types of piles are driven steel pipe or HP piles, driven precast concrete piles, driven timber piles, cast-in drilled-hole (CIDH) piles, and a variety of cast-in-place (CIP) piles.

In general, seismic design procedures involve various steps [at least] one of which requires a reliable computational as well as analytical model of the structural system under consideration. Moreover, the overall structural system may be modeled and designed as uncoupled subsystems to avoid possible difficulties that may be encountered during the design process. These subsystems can be later combined to evaluate the overall system performance. One good example of such an approach, namely, substructuring approach, is usually used in modeling pile group foundations for bridges. This technique overcomes some of the difficulties (due to large number of piles) involved with the modeling of each pile member individually and complexities related to modeling realistic soil behavior. In the substructuring modeling approach, the overall bridge is divided into two sub-models: i) the structural model (commonly referred to as the global bridge model) which typically includes the bridge deck superstructure and portion of the substructure extending down to the foundation and ii) a foundation substructure. Typically, geotechnical engineers are responsible for foundation modeling (or input parameters to the foundation model), whereas the structural engineers are responsible for modeling the global model. The first step in modeling the foundation would be to establish, with input from the structural engineers, the appropriate interface between the two sub-models (e.g. at the base of the column, at the centroid of the pile cap, or at the base of the pile cap, etc.). The following sections discuss various aspects of the procedures used for the foundation substructuring approach.

Depending on the type of analysis/design procedure adopted, relevant linear, nonlinear and/or equivalent linear properties of the modeled elements should be determined. Such properties can be best incorporated in analyses in terms of stiffness of pile elements which are determined based on specific pile force-deformation behavior. Moreover, load transfer – load supporting mechanisms should be identified prior to any attempt to model the structural system. As mentioned before, overall seismic response of pile group foundations generally depend on the individual pile response under both axial and lateral loadings. Therefore, stiffness characteristics of various components in pile group foundations are discussed in the following sections for these types of loadings.

It has been a common practice to use p-y curves or Terzaghi's linear subgrade modulus theory (which in effect is a form of p-y curves) in developing stiffness properties of piles in the surrounding soil. These curves (p-y) are developed empirically based on observations of pile load tests of mostly smaller-diameter piles installed by impact hammer driving. Some recent studies suggest that the conventional p-y curves may need to be modified for the analysis and design of large-diameter drilled shafts. This issue will be further discussed in Section 3.

2.2 Two-Step Seismic Design Process

It is important to recognize that most of the soil-structure interaction analyses conducted by geotechnical engineers are usually performed to support structural engineers in the design of the structural and foundation system. It is important for geotechnical engineers to gain some degree of appreciation of the overall structural design process. In general, a seismic design process involves a two-step process. These steps are discussed in the following subsections.

2.2.1 Step 1: Determination of Seismic Demand and Foundation Stiffness

The first step to determine the seismic demand imposed on the structural system is to determine the response level implied by the design earthquake. Unlike static loading, dynamic loads on a structure depends on the overall period of the structure, which in turn depends on the foundation stiffness. Therefore, a realistic estimation of foundation stiffness and integration into the structural analysis is important because it plays an important role in the assessment of seismic demand. In general, the overall structural system (including the foundation) responds nonlinearly to the applied load for typical seismic load levels. However, for practical purposes, linear response analyses are the most common analysis types in designing bridges in which a linear stiffness representation of the foundation is incorporated in the analytical model. Structural designers and geotechnical engineers should be aware of the modeling procedure of the foundation system and the inherent limitations associated with the process of the linearization as discussed below.

In Step 1, emphasis is placed on characterizing the proper foundation stiffness to be incorporated in the overall global structural model such that the seismic demand from the earthquake can be determined. Figure 2-1 shows generic load-deflection characteristics of the foundation system. Unlike structural properties, which typically have a reasonably well-defined elastic stiffness, soils are intrinsically nonlinear, starting from extremely small load levels. For this reason, the choice of an equivalent-linear soil modulus would be rather complex and potentially requires an iterative process such that the adopted stiffness would be compatible to the deflection level. It can be assumed that a secant stiffness at peak load/deflection would represent the lower bound stiffness occurring only at an infinitesimal duration in time during peak earthquake load. Such a stiffness might be too soft to be representative for the overall duration of the earthquake. A secant stiffness at a smaller deflection might be a better candidate to serve as the effective foundation stiffness representative for a longer time frame over the duration of the earthquake.

In the widely used equivalent-linear site response analysis procedure, Idriss and Sun (1992) proposed to establish the equivalent secant soil modulus at an effective strain value equal to the peak strain

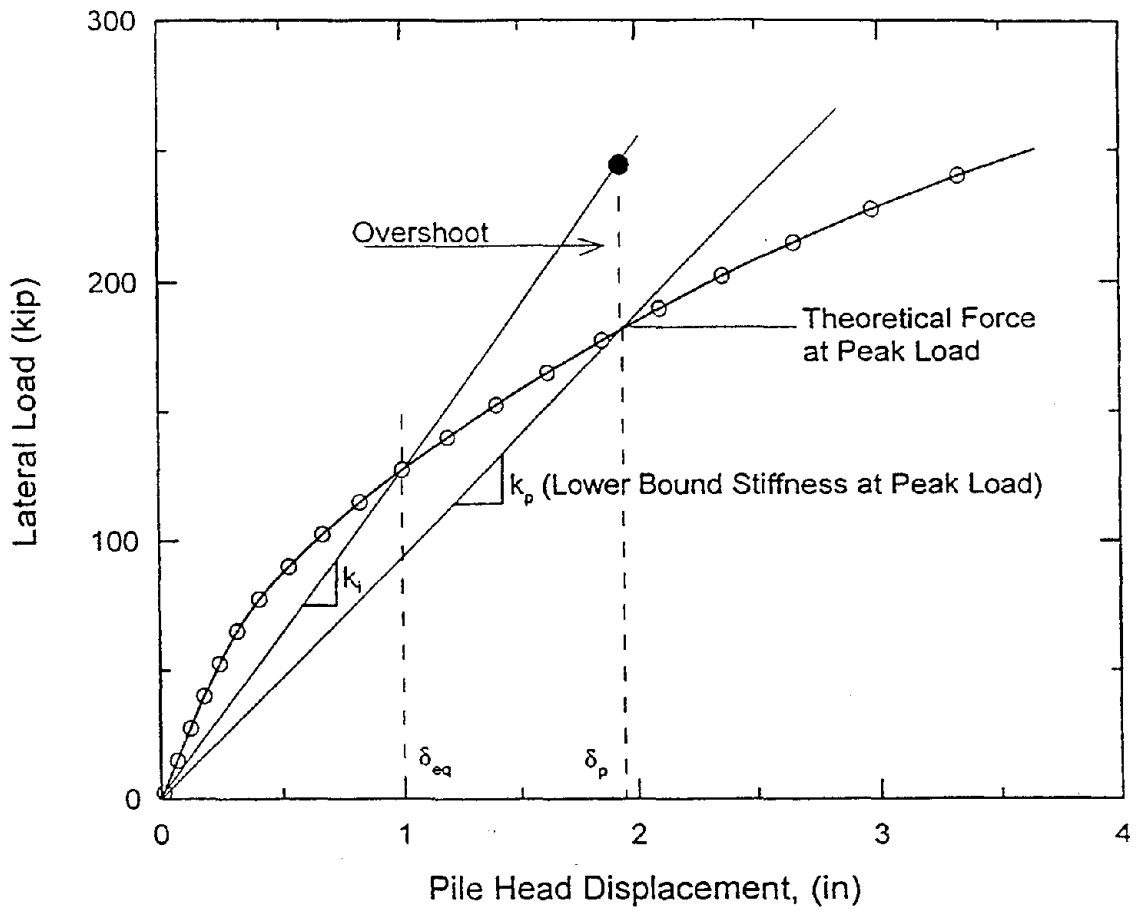


Figure 2-1 Equivalent Linear Stiffness from Nonlinear Response

multiplied by a scaling factor $n = (M_w - 1)/10$ where M_w is the earthquake magnitude (Moment magnitude). The above recommendations by Idriss and Sun, or the simple establishment of a secant foundation stiffness at 0.5 to 0.65 of peak deflection, would provide a better basis for developing foundation stiffness than the lower-bound stiffness at peak deflection.

2.2.1.1 Displacement Demand

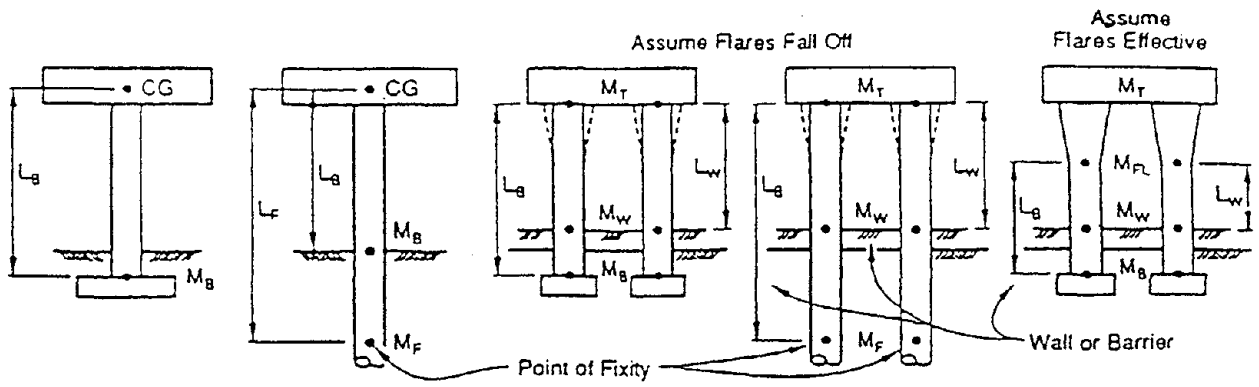
Various researchers (e.g., Miranda, 1991) have concluded that solutions from linear response analysis generally give reasonable peak superstructure displacement solutions (referred to as the equal-displacement principle for long period systems). Therefore, it can generally be assumed that if an appropriate equivalent-linear stiffness is chosen, the linear dynamic response analysis can predict the peak displacement. However, as shown in figure 2-1, a secant stiffness selected at a deflection δ_{eq} below peak deflection δ_p overestimates the load at peak deflection for a typical nonlinear load-deflection curve. The dilemma is that a secant stiffness at below the peak load should be used in order to capture the average stiffness characteristics rationally, which in turn forms the basis to predict the proper level of peak displacement. For this reason, solutions from a linear dynamic response analysis can only provide a rational basis for the displacement demand for a system that is designed to yield (premise of a modern seismic ductile design principle).

Since the linear response analysis generally overestimates the load demand, a pseudo-static nonlinear pushover analysis is needed in a subsequent capacity analysis to account for forces corresponding to the displacement demand predicted in Step 1. The above inherent limitations in a linear response analysis imply that a nonlinear dynamic response analysis would be needed to solve for both forces and displacement simultaneously in a one-step analysis for a system that has significant inherent nonlinearities.

2.2.1.2 Force Demand Associated with Load Fuses

In modern seismic design, the ductility principle is used to design the superstructure and to size the column, so that a plastic hinge can form at a predetermined location (typically at the columns) during a seismic event to limit the load transfer to the foundation and also to provide a mechanism to dissipate energy. This design strategy allows for an economical foundation system and also protects embedded foundations which are difficult to inspect for damage. Such strategies are very sound and necessary, not just from an economic standpoint but also because of uncertainty in our knowledge of the earthquake load. Therefore, it would be a good practice to control the behavior under potential over-load conditions such that damage would be limited to preferred locations associated with ductile behavior in the overall system.

Figure 2-2 was extracted from the Caltrans BDS which illustrates typical locations of plastic hinges (load fuses) and how the corresponding lateral shear load is determined based on the plastic hinge moment for foundation design. In the overall design process, it is important to design the system so that the limit state is governed by the plastic moment capacity rather than by the shear capacity of the column, to ensure an overall ductile behavior. There has been a significant number of cases where an overly soft characterization of a foundation stiffness has misled the designer to an



$$V = \frac{M_B}{L_B}$$

$$V = \frac{M_B}{L_B} \text{ or } V = \frac{M_F}{L_F}$$

$$V = \frac{M_T + M_W}{L_W}$$

$$V = \frac{M_T + M_W}{L_W}$$

$$V = \frac{M_{FL} + M_W}{L_W}$$

$$\text{or}$$

$$V = \frac{M_T + M_B}{L_B}$$

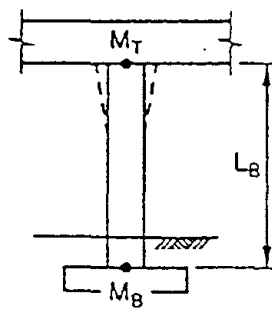
$$\text{or}$$

$$V = \frac{M_T + M_F}{L_F}$$

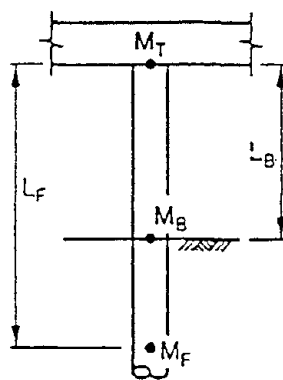
$$\text{or}$$

$$V = \frac{M_{FL} + M_B}{L_B}$$

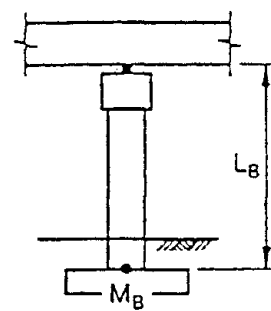
(a) Transverse



$$V = \frac{M_T + M_B}{L_B}$$



$$V = \frac{M_T + M_B}{L_B} \text{ or } V = \frac{M_T + M_F}{L_F}$$



$$V = \frac{M_B}{L_B}$$

(b) Longitudinal

Figure 2-2 Typical Locations of Plastic Hinges (after Caltrans, 1990)

overly soft overall system behavior (e.g. overly deep plastic hinge locations for drilled shafts, or concrete barriers placed around columns led to shorter column lengths than as designed), which in turn led to underestimating the shear demand in the column, resulting in catastrophic failure in earthquakes.

2.2.1.3 Governing Load Case for Foundation Design

Theoretically, the governing foundation load should be the lower of the two conditions: (1) forces from a nonlinear pushover analysis compatible with the displacement demand from dynamic response analysis, or (2) forces associated with load fuses inherent in the structural system (e.g., forces associated with the plastic hinge moment of the columns). The objective in Step 1 is to quantify the seismic demand implied by the design earthquake for the overall bridge system, which can then be compared with the capacity obtained from the subsequent pseudo-static pushover analysis (see Step 2 below) to determine the adequacy of the design.

2.2.1.4 Other Loading Mechanisms

The above design process is geared toward designing for the inertial loads on the superstructure induced by the design earthquake. It should be recognized that there are other loading mechanisms associated with earth pressure loading on the bridge through the foundation. However, this latter load case has not been fully developed in current design codes. At poor-soil sites, especially where there is a potential ground instability (lateral spread associated with liquefaction or slope deformation), this type of loading has caused most of the historical catastrophic failure of bridges. Unfortunately, the studies that investigate various design alternatives for this load case are still in a rudimentary stage. Therefore, designers need to be cognizant of the potential of the other loading mechanisms, especially at poor-soil sites. Design for this type of loading is rather complex and requires a higher degree of interaction with geotechnical engineers in order to implement proper measures into the design process. Some comments on sound engineering practice for good engineering design for these conditions are provided in Section 2.6.6.

2.2.1.5 Foundation Damping

Theoretically, various forms of damping (radiation and material or hysteretic dampings are major sources of foundation damping) should be accounted for in design analysis. In practice, implementation of foundation damping in design often leads to difficulties, and some default values are assumed. In addition, precautions must be exercised to avoid misuse of damping in design (i.e. resulting in an overly damped design). Some of the difficulties include: (1) radiation damping is rate dependent and becomes less significant especially for long-span structures which typically have long periods (typically several seconds fundamental period), (2) damping implied from elasto-dynamic approach is frequency dependent, which is difficult to be implemented into nonlinear time history analyses (the analysis approach adopted for important bridge structures), (3) elasto-dynamic approach has been known to over-predict damping because of its inherent simplification that foundations are bonded to the soil mass, and (4) material damping is strain dependent and theoretically should be related to the seismic load level. It is the authors' experience that radiation

damping involves more implementation difficulties, whereas, accounting for hysteretic material damping might be more reliable and implementable. Ultimately, one major difficulty is how to implement foundation damping in the overall bridge model in a practical manner. Very close interaction between structural and geotechnical experts is required to implement foundation damping properly. Several highway bridge research projects provided some indication that abutment damping might play an important role in typical overcrossing bridge structures. From system identification studies using actual strong motion recordings on bridge structures, as much as 30 percent abutment damping has been observed for specific modes of response of the bridge involving displacement of the abutments. For toll bridge projects in California, where state-of-the-art soil-structure interaction analyses are implemented in retrofit and new design projects, about 10-percent foundation damping (without the superstructure) has been sometimes adopted (based on consensus opinion), unless special studies are conducted on a case by case basis. When this 10-percent foundation damping is implemented into a more massive global bridge model, a much smaller damping ratio for the overall bridge structure will result in only those specific modes involving foundation displacement. From the author's experience, for long period bridges, foundation damping (especially compatible to a design strategy to achieve essentially elastic response in the foundations) is a secondary design issue.

2.2.2 Step 2: Capacity Analysis

Because a linear response analysis usually over-predicts the load level (see previous section), another analytical step is usually needed to calculate a more realistic force in the system (including foundation forces) if the seismic demand arises from a linear dynamic response analysis. In Step 2, the complete structure and foundation with the surrounding soil is usually modeled, including structural nonlinearity in a static (pushover) analysis of the bridge-foundation system to determine the displacement level where structural yielding is initiated (i.e., to determine yield displacement) and how the load is distributed to various structural components at various load levels (up to the design earthquake load level).

On the basis of the analyses, the foundation capacity is evaluated and compared to the demand determined from Step 1 to determine the adequacy for structural integrity for the design earthquake. The ratio of the displacement demand versus yield displacement is the ductility demand which can be used to evaluate whether there is adequate capacity as compared to the seismic demand associated with the earthquake.

It is our experience that in Step 2 capacity solution, it is more important to properly account for the structural nonlinearity than soil nonlinearity. However, within the context of the pseudo-static monotonic loading condition, the currently available numerical tools can incorporate nonlinear soil behavior rather easily and we encourage that nonlinear soil behavior (e.g., p-y curves) be included in pushover analysis (Step 2). In many cases, a linearized representation of soil stiffness such as the Terzaghi's subgrade modulus approach could provide reasonable solutions for design applications.

For a laterally-loaded pile problem, usually there is ample soil capacity (ultimate passive pressure from soil) distributed over the entire pile length. The foundation system capacity is usually controlled by the structural capacity or the tolerable displacement of the overall bridge. The

appropriate analysis to determine the foundation capacity for lateral earthquake load relates to the assessment of the magnitude of lateral deflection that can be tolerated by the bridge and the foundation's ability to provide vertical support to structures within acceptable performance (settlement). For earthquake design (which usually implies extremely high loads in states with high seismicity, but at a relatively low probability of occurrence), the structural system is expected to be damaged and will undergo some level of yielding. At any rate, the state-of-practice in the Step-2 analysis usually involves a higher degree of sophistication in terms of system modeling (e.g., involving some form of nonlinearity) as compared to the Step 1 seismic demand analysis. Because the demand and capacity models are usually incompatible, it is important to discuss how results in the seismic demand solutions from Step 1 are related to the capacity solutions from Step 2.

As discussed earlier, results in the Step 1 dynamic analysis are usually used to establish the displacement demand. In the Step 2 static pushover analysis, the first step would be to determine whether one should conduct the analysis to the level of prescribed displacement or force. As mentioned earlier, if the demand arises from a linear dynamic response analysis, the force level directly from the solution might be too high and an alternate static pushover analysis would be more valid to determine the load demand at the displacement amplitude determined from Step 1. Therefore, results from a linear dynamic response analysis is typically used to establish the level of displacement demand. However, if the governing foundation load arises from forces corresponding to plastic hinge moment of the column, then it would be more valid to treat the loading condition in this Step 2 analysis as prescribed load, even if an existing equivalent linear stiffness was used for the foundation. The governing load on the foundation is the lower of the two cases (i.e. forces from nonlinear pushover to the displacement demand or forces associated with plastic hinge moment).

2.2.3 Prevalent Practice for Conservatism

Because of uncertainties in soil behavior, geotechnical engineering tends to involve some inherent conservatism in traditional practice. Both geotechnical and structural engineers often assume that a softer soil stiffness and a lower soil capacity will lead to a more conservative design. This assumption is true only when the foundation is designed in a force-controlled analysis, such as dead load in settlement analyses or when the design force is associated with plastic hinging at the column. For that fixed-load case, a softer soil will obviously develop a greater displacement and a lower factor of safety. However, as discussed above, a seismic design process often involves a static pushover analysis to a specified displacement rather than to a well defined load. In such cases, a softer soil stiffness in the analysis will often imply a lower force in the structural components and would be unconservative.

Another example that prevalent conservatism might be counter-productive is that a softer foundation stiffness often results in a more even distribution of the structural load (e.g. column load) among individual columns or foundations. This is particularly true for battered pile groups where the load distribution to foundations are controlled by kinematic constraints rather than static equilibrium considerations, and a softer pile stiffness will usually result in a more even load distribution among various piles.

For drilled shaft foundations, an overly soft soil stiffness also can mislead the designers to conclude that the plastic hinge will occur at a deeper location below grade which often leads to underestimating the shear demand in the shaft.

From our experience, it can be counter-productive to introduce arbitrary conservatism in geotechnical recommendations for seismic design. It is recommended that analysis and design for the seismic load case be conducted using a best-estimated scenario. However, this statement only applies to the seismic load case, especially for situations where the seismic demand is associated with dynamic response solutions, rather than associated with plastic hinge mechanisms (e.g. for pier walls in the transverse loading direction). Traditional conservatism should be maintained in foundation design for other load cases, where the loads are usually better defined to allow engineers to judge the level of conservatism. A better approach to account for uncertainty in the soil behavior would be to characterize a range of potential foundation and soil behavior (i.e., to provide best estimates as well as upper and lower-bound recommendations) which imply the need to design for multiple sets of foundation conditions. However, this could result in undue complexity and conservatism in the design process resulting in costly foundations. Therefore, it is also important to gain an appreciation where such higher level of complexity is necessary.

2.3 Single Pile-Head Stiffness

2.3.1 General Form

Characterization of the stiffness characteristics of an individual pile involves an evaluation of the pile load-displacement behavior for both axial and lateral loading conditions. The overall pile-soil stiffness can be estimated in a number of ways, and the method used should reflect the soil characteristics (e.g., type, strength and nonlinearity) and the structural properties of the pile (e.g., type, axial and bending stiffnesses, diameter, length and structural constraints).

The stiffnesses of a single pile can be represented by a positive definite, symmetric matrix in the local coordinate system of the pile with the following coefficients:

$$K_{pile} = \begin{bmatrix} K_x & 0 & 0 & 0 & 0 & 0 \\ & K_y & 0 & 0 & 0 & K_{y'\theta_z'} \\ & & K_z & 0 & -K_{z'\theta_y'} & 0 \\ & & & K_{\theta_x'} & 0 & 0 \\ (symm.) & & & & K_{\theta_y'} & 0 \\ & & & & & K_{\theta_z'} \end{bmatrix} \quad (2-1)$$

where K_x is the axial stiffness,
 K_y and K_z are the lateral stiffnesses,
 $K_{y'\theta_z'}$ and $K_{z'\theta_y'}$ are corresponding coupled stiffnesses between shear and overturning moment,

$K_{\theta'}$ is the torsional stiffness, and
 $K_{\theta'}$ and $K_{\theta'}$ are the bending stiffnesses.

The coordinate system and stiffness orientations are defined in figure 2-3. The axial translational and torsional stiffness terms are diagonal coefficients, uncoupled with other degrees of freedom. In a pile group, the overall torsional moments are resisted mostly by shear and torsional stiffnesses of the individual piles. The individual pile torsional stiffness, $K_{\theta'}$, would be small and can be assumed to be zero or very small to avoid artificially constraining the torsional motion of the bridge. The lateral translational stiffnesses are coupled with rocking rotations through the $K_{y'\theta'}$ and $K_{z'\theta'}$ coefficients.

Eq. (2-1) also shows that there is no cross-coupling between lateral loading in the two orthogonal x' - y' and x' - z' planes (e.g., no coupling between loading in y' and z' directions), so separate analyses can be conducted for the two lateral loading directions, thereby reducing the mathematical problem of lateral loading in either x' - y' or x' - z' planes to three coefficients (the diagonal translational and rotational plus the off-diagonal cross-coupling stiffness). For piles with symmetrical cross-sections (e.g., round, square or octagonal piles), the two lateral stiffness coefficients $K_{y'}$ and $K_{z'}$, the two lateral coupled stiffnesses $K_{y'\theta'}$ and $K_{z'\theta'}$, and the two bending stiffness coefficients $K_{\theta'y'}$ and $K_{\theta'z'}$ would be equal to each other. Conversely, if the pile section is non-symmetric (e.g., it has weak and strong bending axes such as an H-pile), the coefficients for the two orthogonal planes will differ.

2.3.2 Appropriate Foundation Stiffness Matrix

2.3.2.1 Fundamental Assumptions

A foundation stiffness matrix (either in terms of local single pile or a global pile group) must be positive-definite and symmetric for it to be suitable for implementation in global model analysis and design. The correct way to obtain pile-head or pile group stiffness matrices would be to conduct the quasi-dynamic analyses by applying loading (either as forces or displacements) at the interface node between the superstructure and foundation model using only linearized pile and soil spring representation.

A stiffness matrix can be obtained by prescribing for each of the six degrees of freedom (three translational and three rotational d.o.f.) a unit displacement vector (i.e., unity in translational displacement or rotation, while keeping the other five degrees of freedom zero). The resultant force vector corresponding to the unit displacement vector can be used to form the corresponding column vector in the stiffness matrix. Conversely, a compliance matrix can be obtained by prescribing a unit force vector (i.e., unity in force or moment, while keeping the other five force components zero). The resultant displacement vector solution can be used to form the column vector in the compliance matrix. The inverse of the compliance matrix can then be used to form the foundation stiffness matrix. The unit load or unit displacement vector load-deflection solution to derive a unique foundation stiffness matrix requires the development of an equivalent-linear soil stiffness (e.g., linear Winkler springs) versus depth.

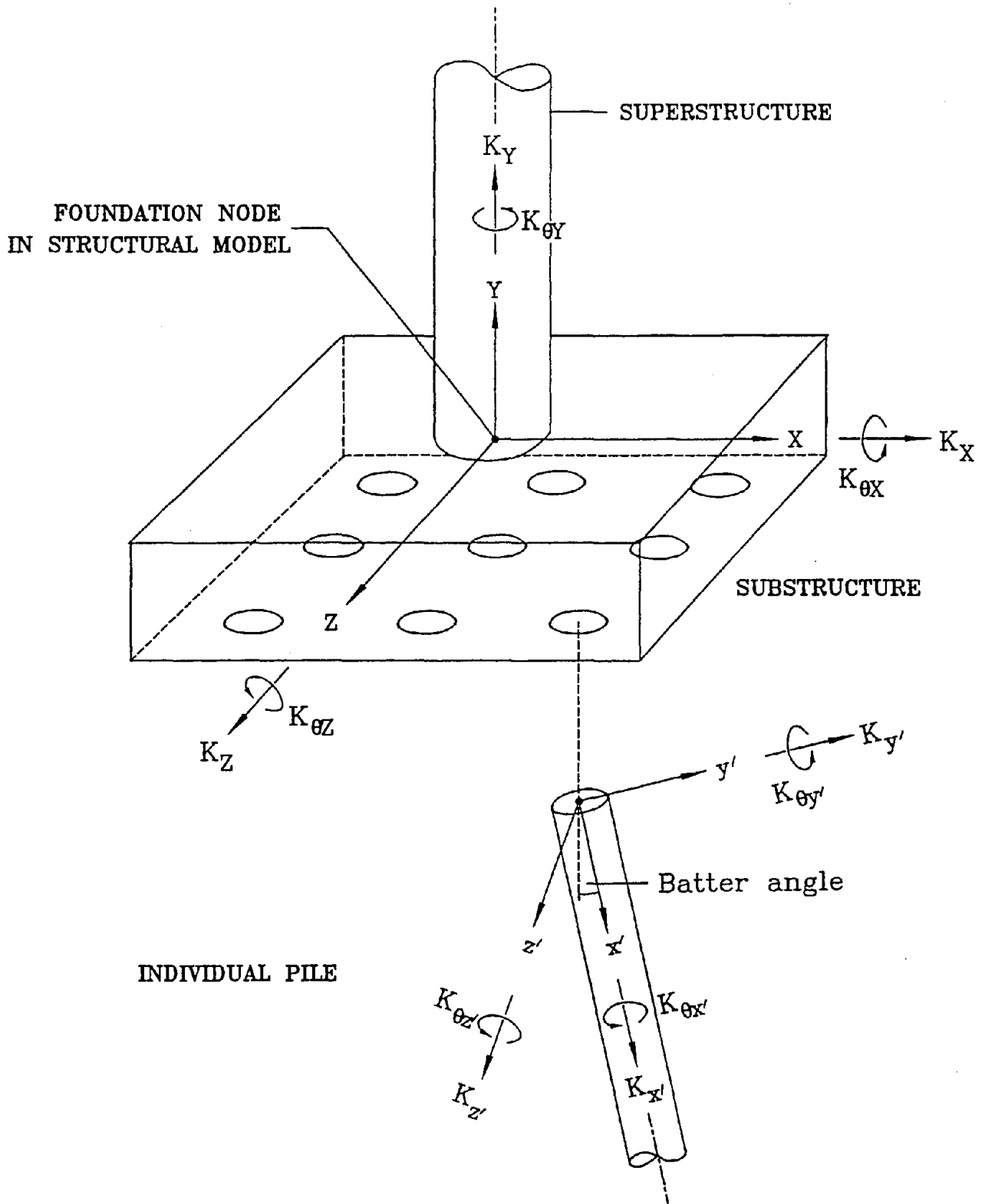


Figure 2-3 Coordinate System and Stiffness Directions

2.3.2.2 Stiffness Matrix from Nonlinear Analysis

There is an abundance of computer programs commercially available today that can perform nonlinear pushover analyses utilizing nonlinear p-y curves for either single piles (e.g., LPILE by ENSOFT, 1997; COM624 by Reese, 1980; BMCOL76 by Matlock et. al., 1981), or a pile group (e.g., GROUP by ENSOFT, 1997; PASS by Bryant et al., 1977). As a result, many geotechnical engineers derive the foundation stiffness matrix by conducting load-deflection analyses using elastic piles embedded in soils modeled by *nonlinear* p-y springs for lateral soil resistance and nonlinear t-z springs for axial soil resistance. Secant lateral shear and the corresponding coupled stiffnesses are then developed from the shear load vs. deflection and shear load vs. rotation curves. Similarly, secant rotational stiffnesses are developed from nonlinear moment vs. rotation curves. However, such procedures have led to ill-defined stiffness matrices (i.e., non-positive definite stiffness foundation matrices) in many projects and caused numerical problems when they are used in global response analyses. This is because the various terms of the stiffness matrix from these nonlinear load-deflection analyses (i.e. lateral, moment and coupled stiffnesses) are associated with different deformed pile shapes which would imply distinctly different sets of equivalent linear soil springs for each run. Even for a proportional loading condition, each point on the nonlinear load-deflection curve as shown in figure 2-1 implies its own stiffness matrix corresponding to a specific equivalent linear soil stiffness distribution with depth. The superposition of separate nonlinear load-deflection solutions to form a stiffness matrix violates the basis for linearity and uniqueness, and could therefore lead to an ill-defined stiffness matrix.

To ensure a well-conditioned, unique positive-definite and symmetric stiffness matrix, irrespective of the loading condition used for the dynamic analysis, the pile-soil system should be linearized. This can be done by conducting the above static pushover analysis with nonlinear soil support curves, and extracting linear secant p-y and t-z stiffness from the p-y and t-z curves on the basis of the deflected pile shape. The resultant equation of motion of the pile-soil system can then be statically condensed upward to the interface node to develop the 6x6 pile submatrix, or directly solved to obtain the load-deflection solutions. Such operation (static condensation or direct load-deflection solution) do not require any assumption of the form of the foundation stiffness matrix (such as that shown in eq. (2-1)). For a pile group involving irregular patterns or battered piles, the form of the foundation stiffness matrix can be rather complex and the discussed procedure should be used to systematically solve for both the form and the numerical values of the stiffness matrix coefficients.

One method to ensure that the stiffness matrix is positive-definite would be to invert the stiffness matrix to develop the compliance matrix and then check that the diagonal terms in the compliance matrix are all positive. Merely the fact that all diagonal terms of the stiffness matrix are positive does not guarantee a positive-definite stiffness matrix because of the cross-coupling stiffness terms. While shallow foundations can usually be represented adequately by diagonal stiffness matrices (i.e., all off-diagonal stiffness coefficients can be assumed to be zero), deeply embedded foundations generally imply a high degree of cross-coupling between the lateral translational and the rotational terms, and therefore the cross-coupling term must be properly taken into account in the derivation and implementation of the foundation stiffness and compliance matrices.

2.3.3 Pile-Head Stiffness for Axial Loading

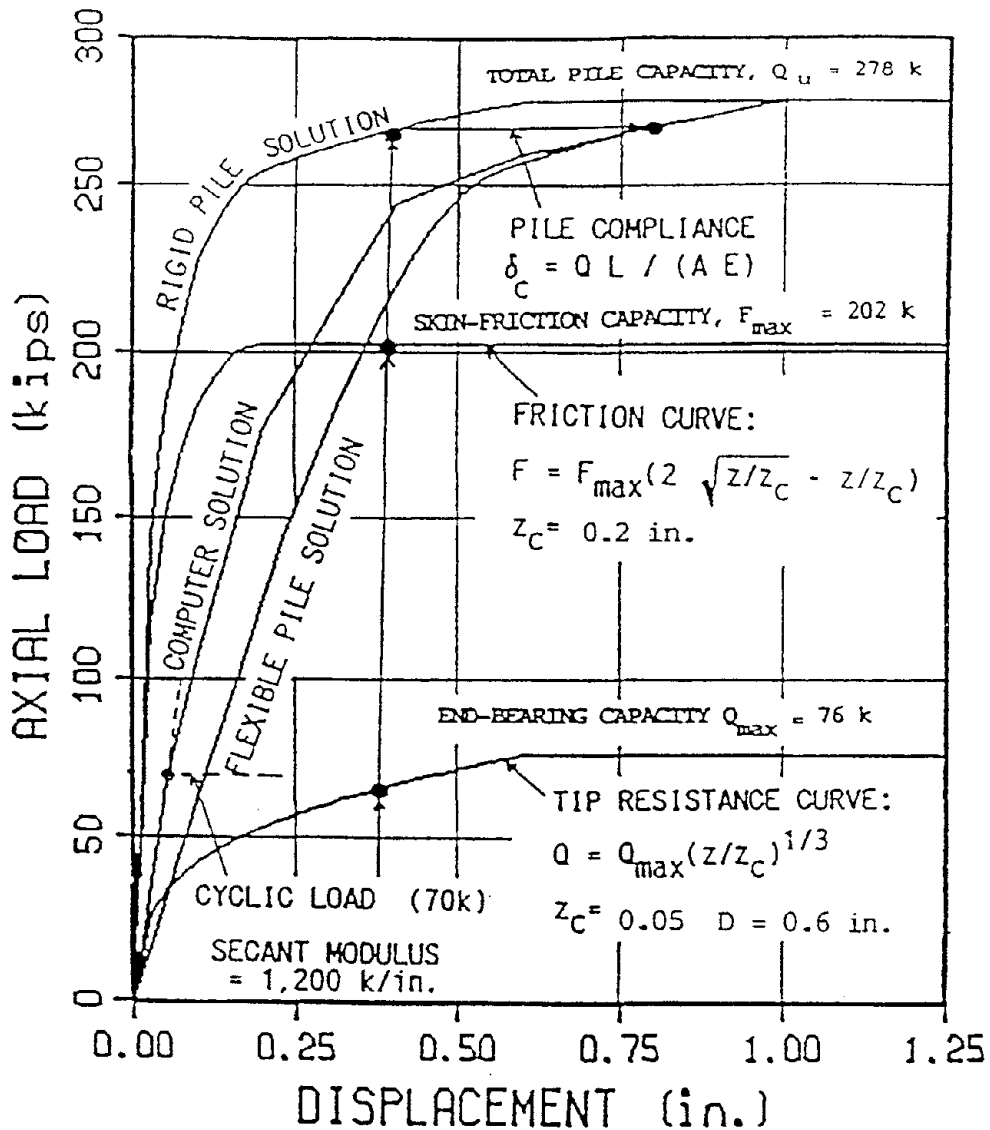
Generally, it can be assumed that the axial pile-head stiffness in the local pile coordinate axis is uncoupled with other degrees of freedom and it is rather trivial to avoid non-physically based (non-positive definite) stiffness matrices in the characterization of the axial pile stiffness term. Also, axial load-displacement characteristics can be assumed to be effectively uncoupled with the lateral load-deflection behavior because much of the soil resistance associated with axial loading will come from relatively deep elevations and thus is relatively insensitive to the shallower soil-structure interaction zone associated with lateral loading. However, since the overall soil resistance for axial loading is derived along a significant length of the pile (especially at the deeper soil strata), and the pile would be under a relatively large ambient dead load prior to the earthquake, a realistic consideration of axial pile characteristics requires the ability to account for inhomogeneous soil layering as well as plastic slippage in the upper part of the pile. Therefore, linear homogeneous analytical solutions would have relatively minor practical applications in axial pile loading problems.

2.3.3.1 Simplified Graphical Procedure

A simple graphical procedure has been developed by Lam and Martin (1986) for developing the axial pile stiffness coefficient (K_x). The method inherently accounts for both soil layering and plastic soil-pile slippage interface behavior. The procedure is illustrated in figure 2-4 and consists of the following steps:

- (1) Ultimate compressive capacity. Ultimate pile capacity is developed from a site-specific pile capacity analysis using conventional procedures for skin-friction and end-bearing capacities for the different soil layers. In assigning the skin-friction and end-bearing capacities, one should properly account for, among others, the construction method (e.g., predrilling, driving etc.), special conditions (e.g., consolidation due to surcharging, corrosion) and dynamic soil behavior (e.g., cyclic strength degradation, soil liquefaction) and strain-rate effects.
- (2) Rigid-pile load-displacement curve. Based on the estimated ultimate capacity, a pile load-displacement curve shape is developed using published skin-friction and end-bearing versus pile displacement relationships. The resulting load-displacement curve in figure 2-4 obtained as the sum of the skin-friction and end-bearing capacities at each axial pile displacements will result in a pile-head load-displacement relationship for a rigid pile assumption. This curve constitutes a lower bound for the actual pile displacements.
- (3) Flexible-pile load-displacement curve. When the pile is treated as a column without soil, the maximum additional compliance related to elastic deformation of the pile with a section modulus AE , a length L for an axial load Q can be developed as

$$\delta(Q) = \frac{QL}{AE} \tag{2-2}$$



Notes:

Load displacement curves for most soil and pile conditions will resemble rigid pile behavior at extremely small load levels, then progress to flexible pile behavior at higher load level (ultimate capacity range). Our experience indicates that for most design conditions, the average stiffness from the rigid and the flexible pile solutions will provide reasonable axial pile stiffness for earthquake design.

Figure 2-4 Axial Load-Displacement Graphical Solution

The flexible pile solution can then be obtained by adding the additional displacement values shown in eq. (2-2) to the rigid-pile load-displacement curve in figure 2-4 at different pile loads Q corresponding to the rigid pile load-displacement curve. This curve provides an upper bound for the actual pile displacements.

- (4) "Actual Anticipated" load-displacement curve. The appropriate axial load-displacement solution will be bounded by the two (rigid and flexible load-displacement) solutions derived in Steps 2 and 3. The actual load-displacement curve would depend on the specific pile-soil system. Generally, the average of both solutions will be a good approximation. For an end-bearing pile, the appropriate curve may be closer to the flexible pile solution. In general, at small load levels, the upper portion of the pile is compressed first, and thus the load-displacement curve will be closer to the rigid-pile curve at small load. At higher loads, slippage occurs along most of the pile and the solution might migrate closer to the flexible pile curve.
- (5) Axial pile stiffness. Finally, an axial secant stiffness to be implemented into the axial stiffness coefficient in eq. (2-1) can be estimated from the anticipated load-displacement curve compatible with the axial compression load or the considered displacement range. For dynamic analyses, the secant stiffness would typically extend from the curve's origin to the level of cyclic load amplitude. For regular highway bridge foundation piles, typical levels of cyclic compression loading would be in the range from 50 to 70% of the ultimate pile capacity.

2.3.3.2 Stiffness for Uplift Loading

If the axial stiffness is to be used for uplift loading only, the above procedure can be used to obtain the corresponding uplift load-displacement backbone curve by use of skin-friction capacity for uplift loading, ignoring the end-bearing capacity.

2.3.3.3 Selection of Secant Stiffness

The load-displacement curve (either the compression or the tension loading curves) represents the expected initial load-displacement (referred as the backbone curve) at the pile head. For axial loading, prior to the earthquake, the pile would be subjected to a large ambient static dead load and the appropriate secant stiffness for earthquake response should reflect the hysteretic loading, unloading and reloading behavior which can be approximated by the secant stiffness extending from the origin to the cyclic load amplitude in compression. A secant stiffness from the zero origin to the peak earthquake load (i.e., the sum of ambient static plus cyclic load) tends to be too soft to represent the stiffer unloading reloading stiffness.

More refined nonlinear solutions can be derived from computer analyses (e.g. Lam and Law, 1994) with distributed t-z curves to model the skin frictional behavior along the pile along with a Q-u curve to represent the end-bearing behavior. The actual axial loading behavior expected for earthquake condition can be rather complex. Other than the pile and soil condition, complexity for

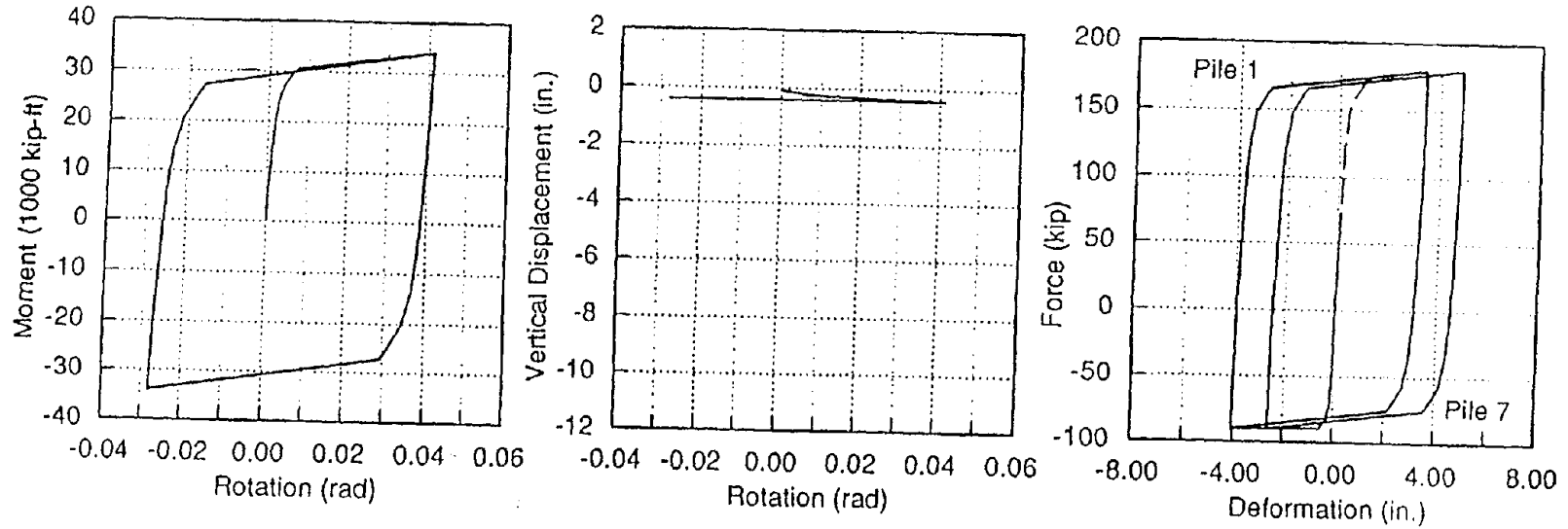
characterization of equivalent linear axial stiffness is compounded by the initial offset due to the static ambient pile load, as discussed previously. The axial stiffness for cyclic moment loading on the footing would vary depending on the position of the pile within the pile group as the outer piles would be much more heavily loaded.

Also, there is some fundamental difference in the cyclic response between skin friction and the end-bearing component of soil resistance. Figure 2-5 presents some representative hysteresis loops from overturning of a typical 3x3 pile group to illustrate differences in behavior between skin-friction versus end-bearing piles. The skin friction behavior resembles typical hysteretic behavior, whereas end-bearing piles could exhibit gapping behavior which is a form of geometric nonlinearity. Also, axial load-displacement characteristics vary depending on the magnitude of pile load and tend to exhibit perfectly plastic behavior (i.e. constant load for increasing displacement) if the displacement is sufficiently high to reach the plastic branch. Therefore, the axial stiffness can change drastically from a stiff scenario on the elastic branch to a much softer scenario on the plastic branch corresponding to highly nonlinear behavior. The degree of nonlinearity for load-deflection characteristics associated with lateral loading tends to be less severe than the axial load-displacement characteristics as discussed more fully in later sections. For some cases, especially for end-bearing piles with very shallow penetration, the behavior of a pile group can resemble shallow spread footings and the load-displacement characteristics could be dominated by uplifting of some of the piles and exhibit a high degree of geometric nonlinearity where it becomes more difficult to linearize.

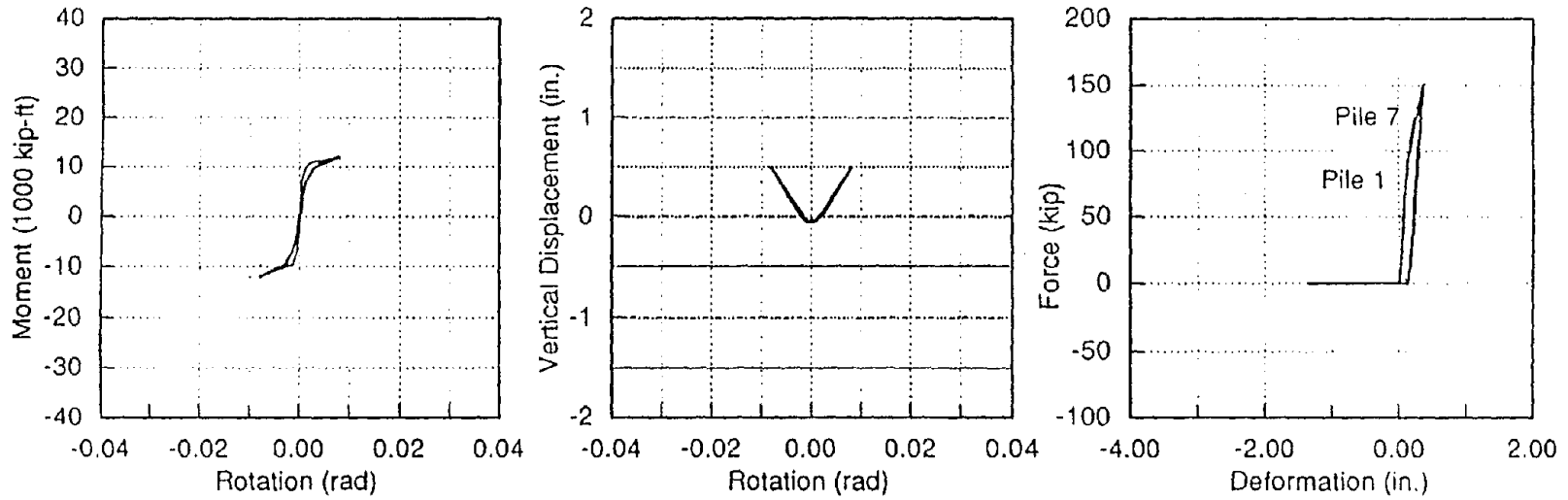
While most recent research on seismic design of foundations emphasize the lateral pile loading problem, the axial pile loading problem related to the rocking response of the pile group involves more complexity in both material and geometric nonlinearities. There is evidence that the overall response of the structure would be more sensitive to variations in the axial pile stiffness (i.e., rocking stiffness of the pile group) and therefore the axial pile loading problem deserves more attention (Douglas and Norris, 1983). Moreover, moment demand on a pile group generally should govern the foundation design (i.e., size of the pile group, number and length of piles) in typical situations, rather than the lateral load if the foundation is properly designed for typical soil conditions. This is the reason why the Caltrans Bridge Design Specifications contain explicit statements suggesting that the shear load should not govern the foundation design, and that the design for most existing foundations in high seismic region would be governed by the overturning moment load case.

2.3.4 Pile-Head Stiffness for Lateral Loading

In practice, the lateral pile load-deflection characteristics are determined by a pushover analysis using a beam supported by springs which are characterized by nonlinear (p-y) curves. This type of pseudo static soil structure interaction problem can be analyzed using a variety of methods including discrete beam-column and finite-element type analyses. Various authors have developed empirical deflection-dependent lateral soil resistance curves for sand and clays based on small-diameter pile load tests. The most commonly used p-y curves are those by Reese et al (1974) for sands and by Matlock (1970) for clays. As discussed in Section 2.3.2, these curves should be linearized to develop a consistent set of lateral, rocking and coupled stiffnesses.



(a) Behavior of Friction Pile



(b) Behavior of End-Bearing Pile

Note: Results shown are from overturning of a typical 3x3 pile group.

Figure 2-5 Typical Characteristics of Friction versus End-Bearing Piles

2.3.4.1 Linear Subgrade Modulus

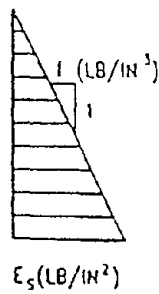
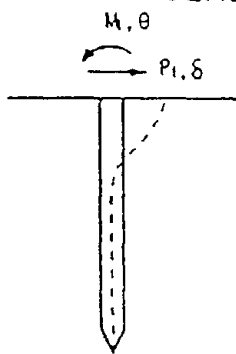
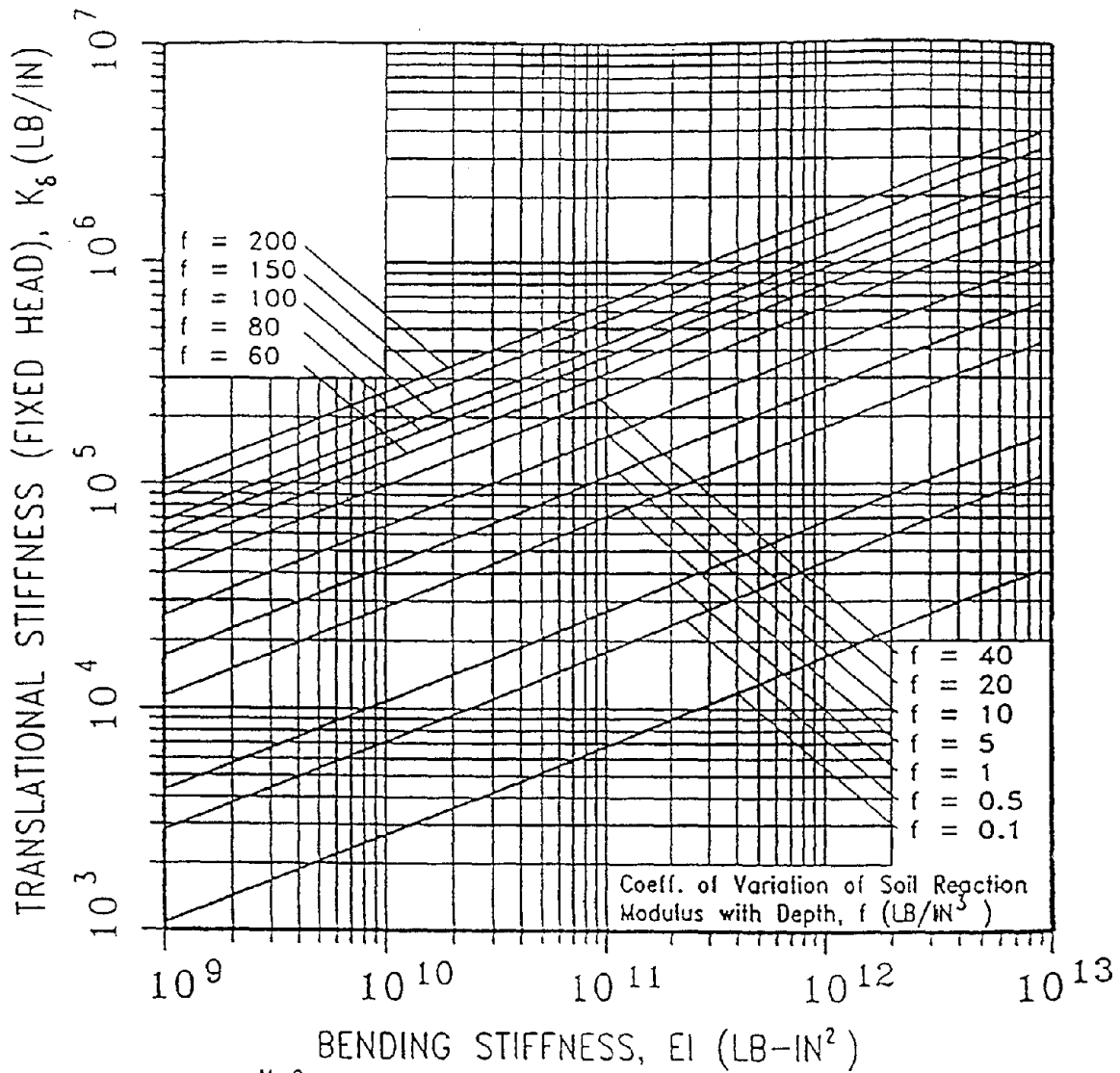
Lam and Martin (1986) found that lateral load-deflection characteristics representing the overall stiffness of the pile-soil system would only be mildly nonlinear because the elastic pile usually dominates the nonlinear soil stiffness. Furthermore, the significant soil-pile interaction zone is usually confined to a depth at the upper 5 to 10 pile diameters. Therefore, simplified single-layer pile-head stiffness design charts are appropriate for lateral loading. Some of such single-layer linear design charts are presented in figures 2-6 to 2-9 that make use of a discrete Winkler spring soil model in which stiffness increases linearly with depth from zero at grade level where the location of the pile-head is assumed. The representation of a subgrade stiffness increasing linearly with depth has been found to reasonably fit pile load test data for both sand and clay soil conditions. For this soil-pile representation, the system is reduced to two parameters: (1) the pile bending stiffness EI and (2) a coefficient of variation in elastic subgrade modulus with depth, f . The coefficient f has the unit of Force/Volume (FL^{-3}) and is used to define the subgrade modulus E_s at depth z , representing the soil stiffness per unit pile length (see figures 2-6 to 2-9):

$$E_s = f \cdot z \quad (2-3)$$

Values of f for normal design working loads have been published by Terzaghi (1955) and Murchison and O'Neill (1983) for piles embedded in sand as a function of corrected Standard Penetration Test (SPT) blowcount or density (see figure 2-10). Figure 2-11 shows a correlation of f values with cohesion of clay soils (Lam et al., 1991). For the purpose of selecting an appropriate f value, the soil condition at the upper 5 pile diameters should be used. The two charts presented in figures 2-10 and 2-11 were based on data for smaller-diameter (12-inch) piles, but can be used for piles up to about 24 inches in diameter.

Given a selected f value and the bending stiffness of the pile EI , lateral and rocking stiffnesses can be directly read-off the charts shown in figures 2-6 to 2-9 (Lam et al, 1991). The charts assume no pile top embedment, but also yield reasonable stiffnesses for shallow embedments not exceeding about 5 feet, in which case the soil above the pile top would be neglected. An additional set of design charts for lateral stiffness of a pinned -head (i.e. zero bending moment) condition are included in figure 2-9. If the ratio of variation in subgrade modulus as shown in figures 2-10 and 2-11 are used to derive the pile-head stiffness matrix from figures 2-6 to 2-9, the resultant pile-head stiffness matrix corresponds to the stiffness between about 0.25 and 2-inch pile-head deflection.

These stiffness charts are appropriate for embedded piles that are sufficiently long to approach the solution of an infinitely long ("flexible") pile condition (this is valid for most conditions). There is a theoretical characteristic length of the pile-soil system that depends on both the bending stiffness of the pile as well as the stiffness of the soil. When the ratio of the embedded pile length to this characteristic length exceeds a value of about 3, the pile can be regarded as an infinitely long pile for pile-head stiffness characterization. The following equation can be used to obtain the characteristic length of the pile soil system:



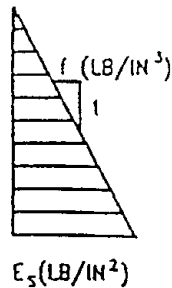
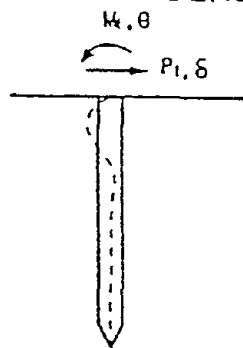
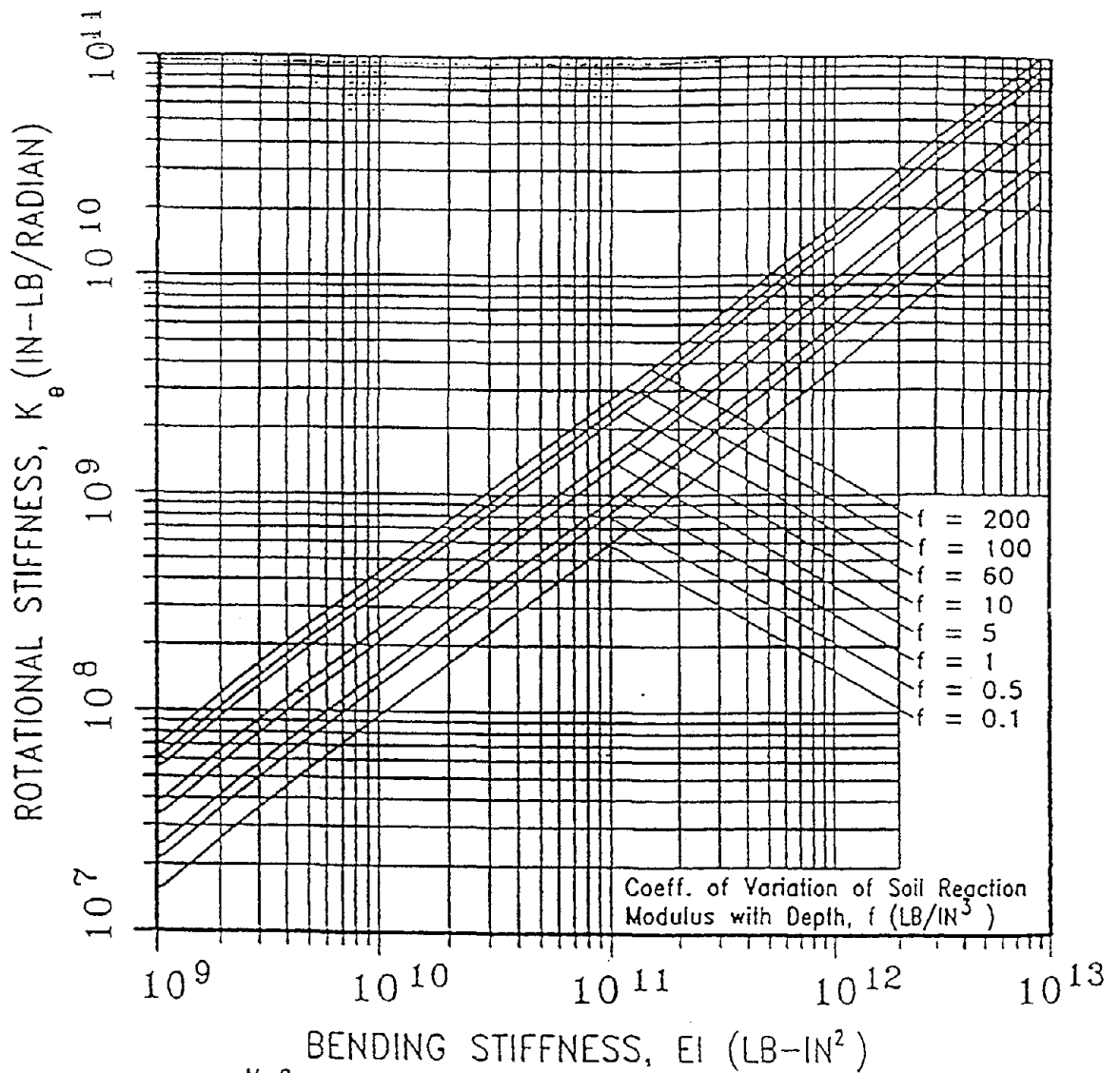
$$P_t = K_g \cdot \delta + K_{g\theta} \cdot \theta$$

$$M_t = K_{g\theta} \cdot \delta + K_g \cdot \theta$$

$$K_g = \frac{1.0765 \cdot E \cdot I}{T^3}$$

$$T = \left(\frac{E \cdot I}{f} \right)^{1/5}$$

Figure 2-6 Lateral Pile-Head Stiffness (Fixed-Head Condition)



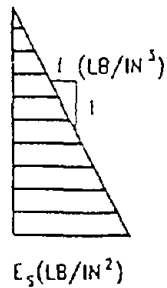
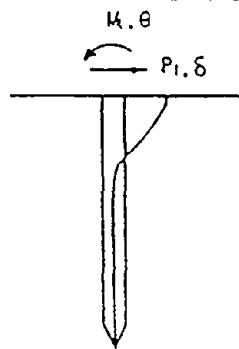
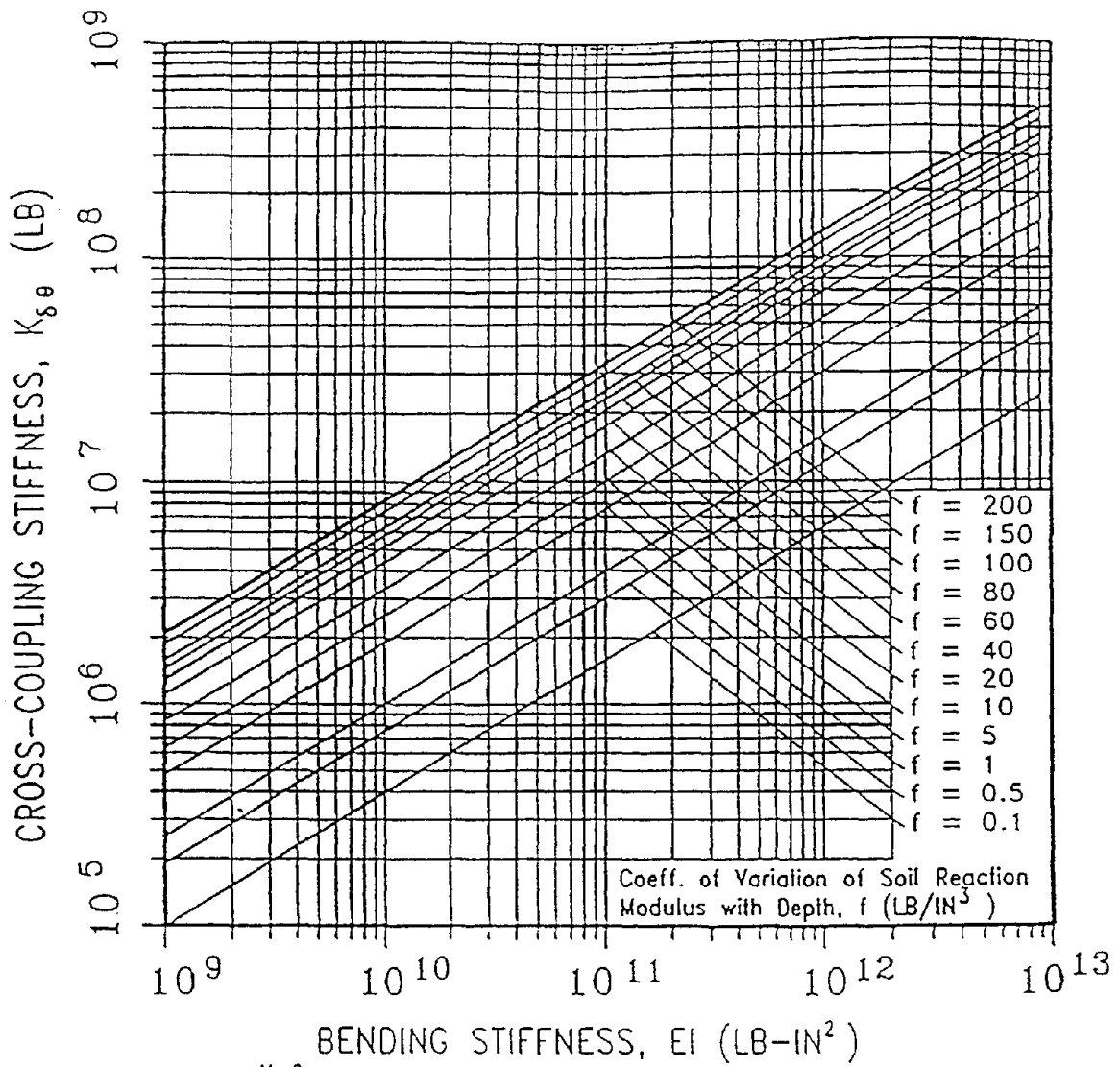
$$P_t = K_{\delta} \cdot \delta + K_{\theta} \cdot \theta$$

$$M_t = K_{\delta} \cdot \delta + K_{\theta} \cdot \theta$$

$$K_{\theta} = \frac{1.499 \cdot E \cdot I}{T}$$

$$T = \left(\frac{E \cdot I}{f} \right)^{1/5}$$

Figure 2-7 Rotational Pile-Head Stiffness



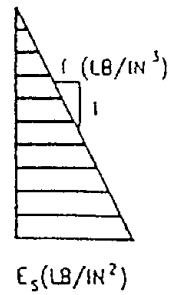
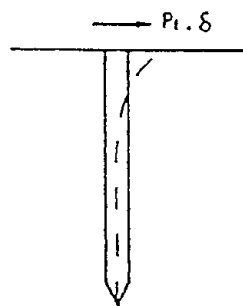
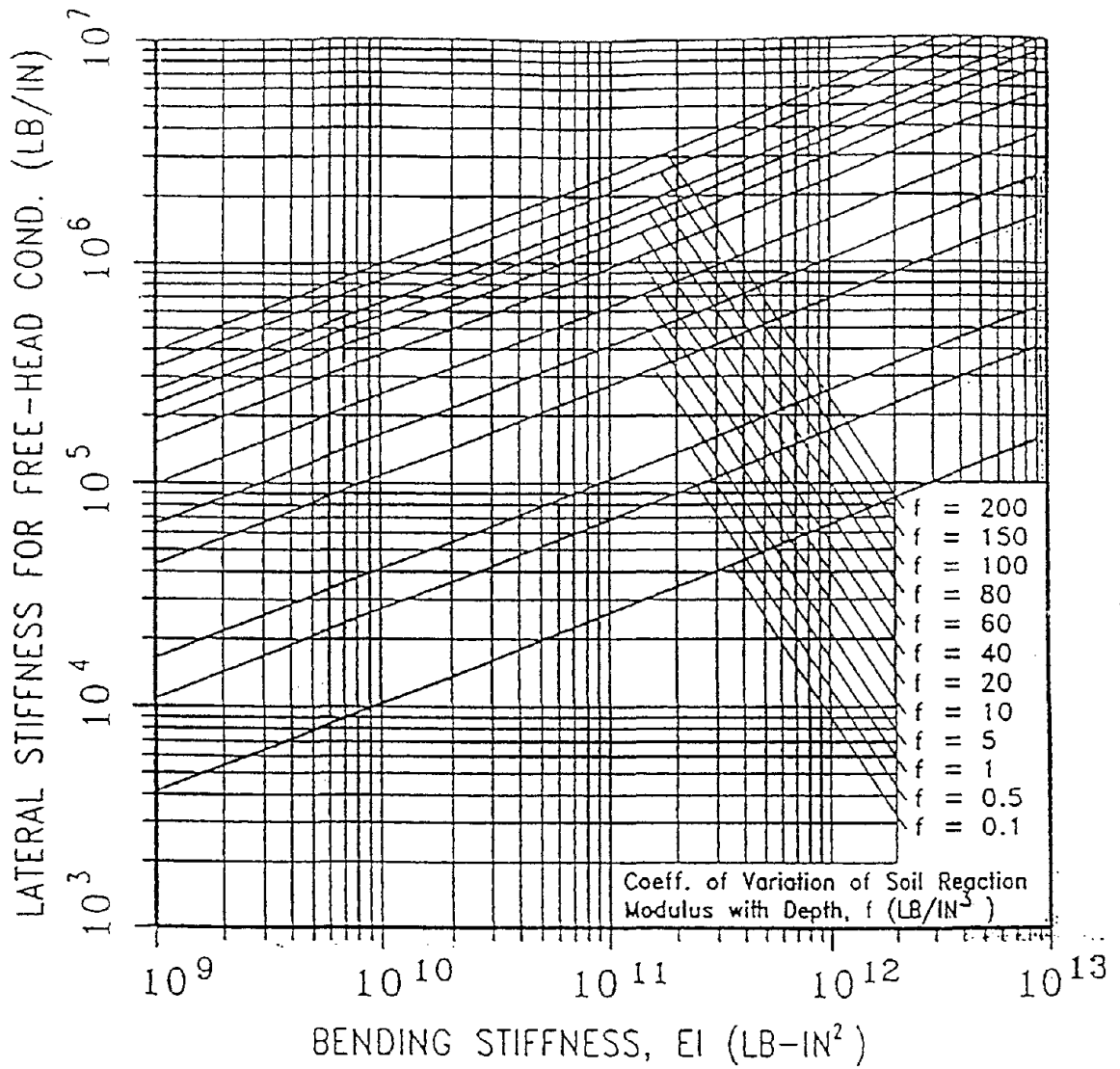
$$P_1 = K_s \cdot \delta + K_{\delta\theta} \cdot \theta$$

$$M_1 = K_{\delta\theta} \cdot \delta + K_\theta \cdot \theta$$

$$K_{\delta\theta} = \frac{0.999 \cdot E \cdot I}{T^2}$$

$$T = \left(\frac{E \cdot I}{f} \right)^{1/5}$$

Figure 2-8 Cross-Coupling Pile-Head Stiffness



FREE HEAD PILE STIFFNESS

$$= K_s - \frac{K_{se}^2}{K_e}$$

$$= 0.41 \frac{E \cdot I}{l^3}$$

$$T = \left(\frac{E \cdot I}{f} \right)^{1/5}$$

Figure 2-9 Lateral Pile-Head Stiffness (Free-Head Condition)

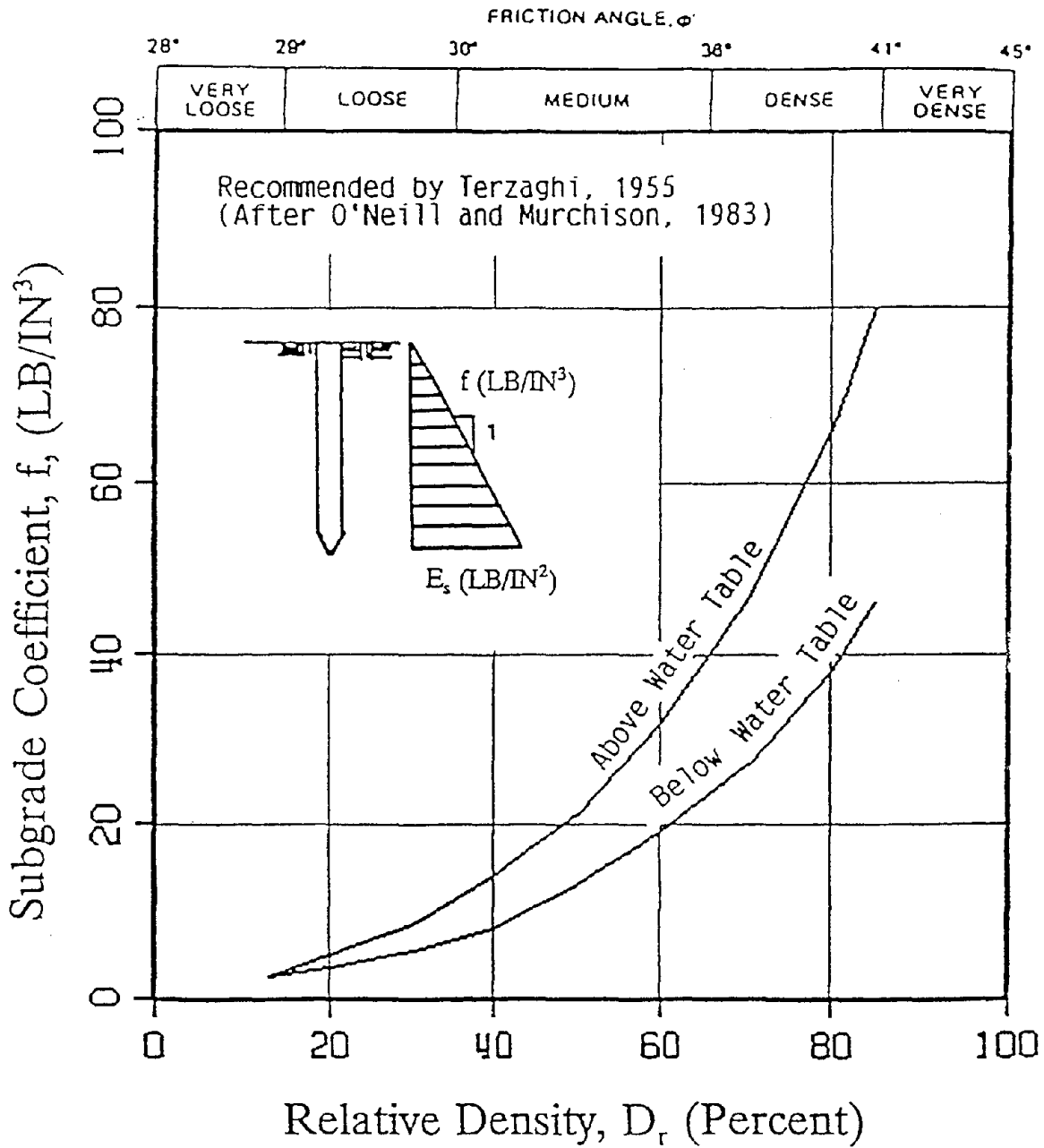


Figure 2-10 Recommended Coefficient f of Variation in Subgrade Modulus with Depth for Sand

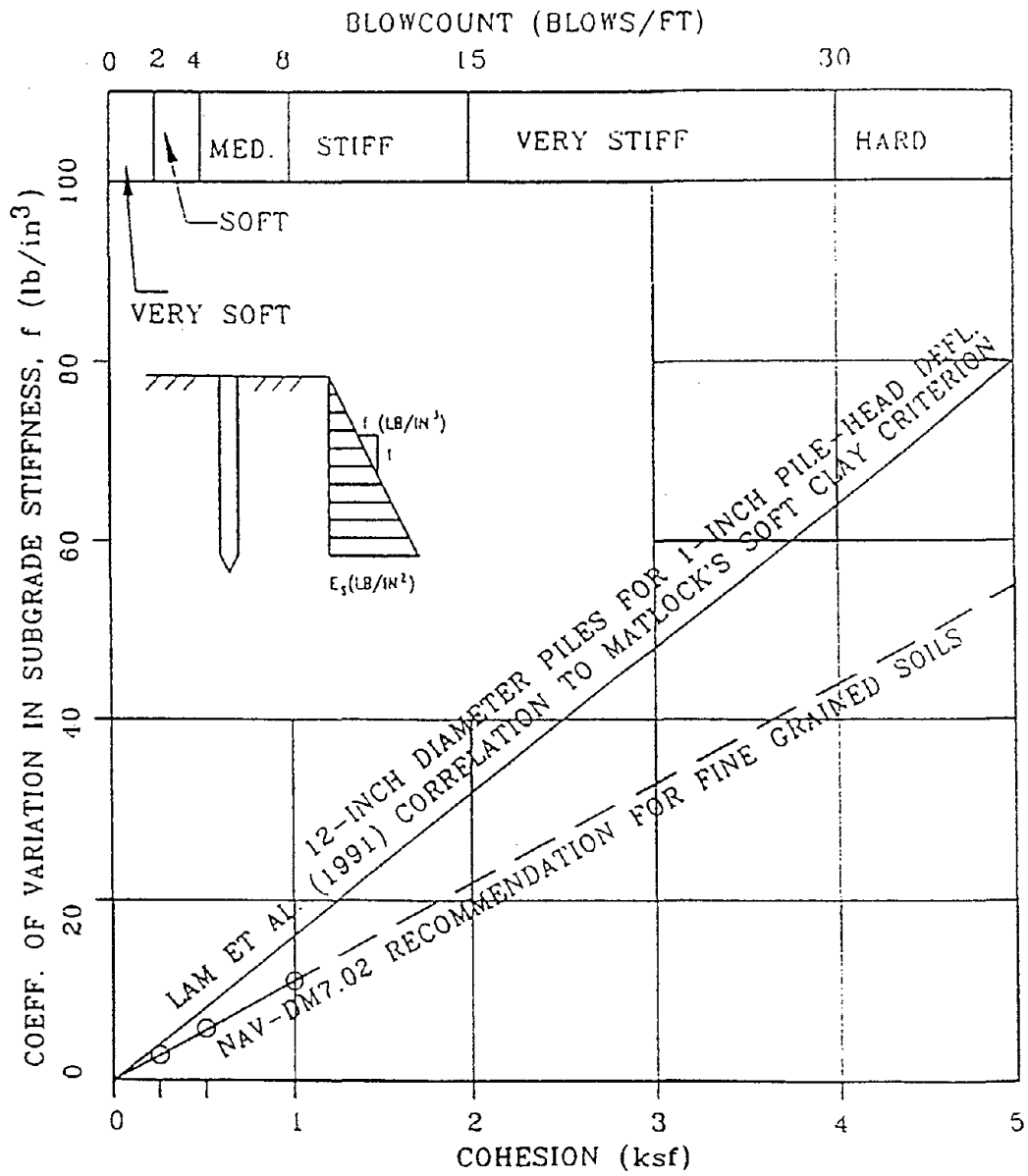


Figure 2-11 Recommended Coefficient f of Variation in Subgrade Modulus with Depth for Clay

$$\lambda = \sqrt[5]{\frac{EI_p}{f}} \quad \text{for subgrade stiffness increasing linearly with depth} \quad (2-4)$$

$$\lambda = \sqrt[4]{\frac{EI_p}{E_s}} \quad \text{for subgrade stiffness } E_s \text{ constant with depth} \quad (2-5)$$

The discussed procedures are appropriate for calculating pile-head stiffnesses for typical smaller-diameter piles. For larger-diameter piles (i.e., drilled shafts) drilled and grouted in place (similar to large-diameter drilled shafts), there are some evidence that the above recommended coefficient f of variation in subgrade modulus would be too soft. Some recommendations to adjust the soil stiffness parameters are recommended later in this report along with a mechanistic explanation for the apparent higher subgrade stiffness for large-diameter drilled shafts and other relevant topics (e.g., effective versus gross sectional properties). For concrete piles, it has been found that the choice of the pile bending stiffness (reflecting cracked sectional properties) is very important. Figure 2-12 has been taken from the structural design literature (Priestley et al., 1996) to provide adjustment factors for the effective (e.g., cracked) bending stiffness for concrete piles.

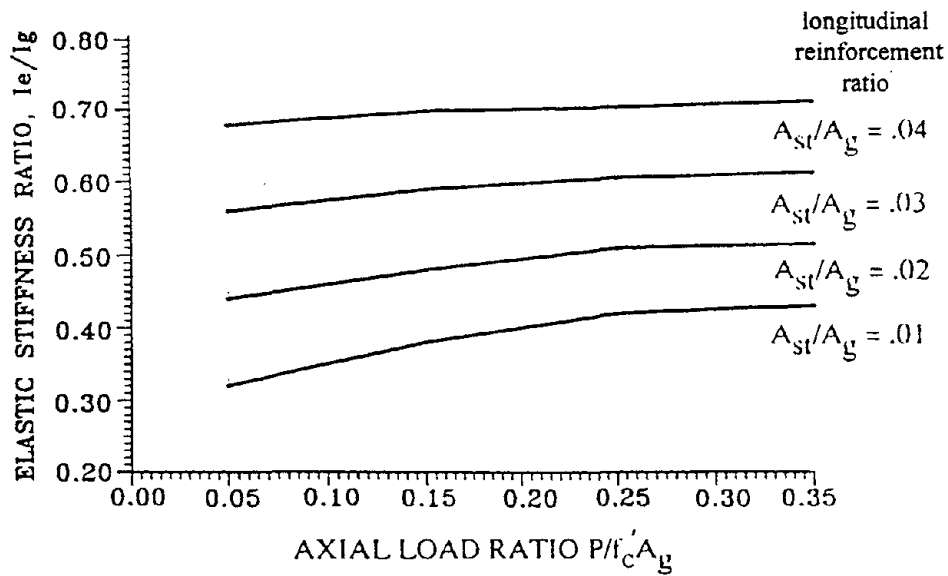
2.3.4.2 Embedment Effect

As a result of additional overburden, soil resistance on the pile increases and the stiffness coefficients increase with the depth of embedment. Figures 2-13 to 2-15 present pile-head stiffness coefficients for pile embedment depths of 5 and 10 ft based on a subgrade modulus which increases linearly with depth. It can be seen from these figures that the embedment effect on the stiffnesses is larger for slender piles and tends to diminish for stiffer piles, and that the lateral stiffness is affected the most. For example, for a pile cap embedded in slightly compact sand ($f=10$ pci), figure 2-13 shows an increase in embedment depth from 0 to 5 ft can increase the lateral pile-head stiffness by a factor of 2.3 (slender pile) to 1.3 (rigid pile). For a depth increase from 0 to 10 ft, the stiffness increases from 3.5 (slender pile) to 1.5 (rigid pile) times.

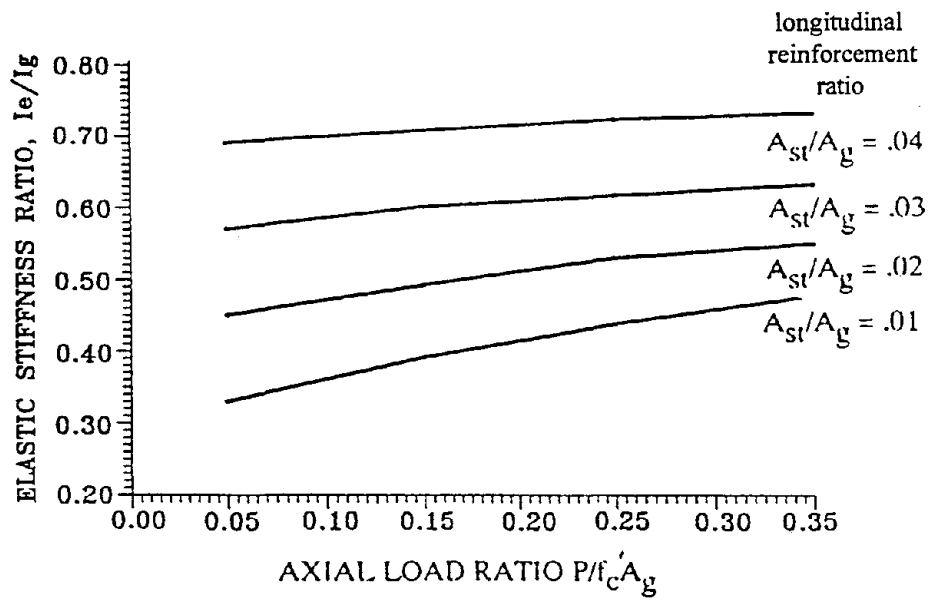
These figures also illustrate that the significance of the embedment depth effect is greater in dense sands. For example, for a 12-inch square concrete pile ($EI=6.22 \times 10^9$ lb-in²) embedded 5 ft, the lateral stiffness increases by a factor of 1.6 in slightly compact sand ($f=10$ pci) and 2.6 in dense sand ($f=100$ pci).

2.3.4.3 Relationship Between Subgrade Modulus and Soil Modulus

Vesic (1961) compared the solution for an infinitely-long beam resting on an elastic halfspace and arrived at the following relationship between the Winkler spring subgrade modulus E_s and the Young's modulus of the elastic halfspace E_{soil} :



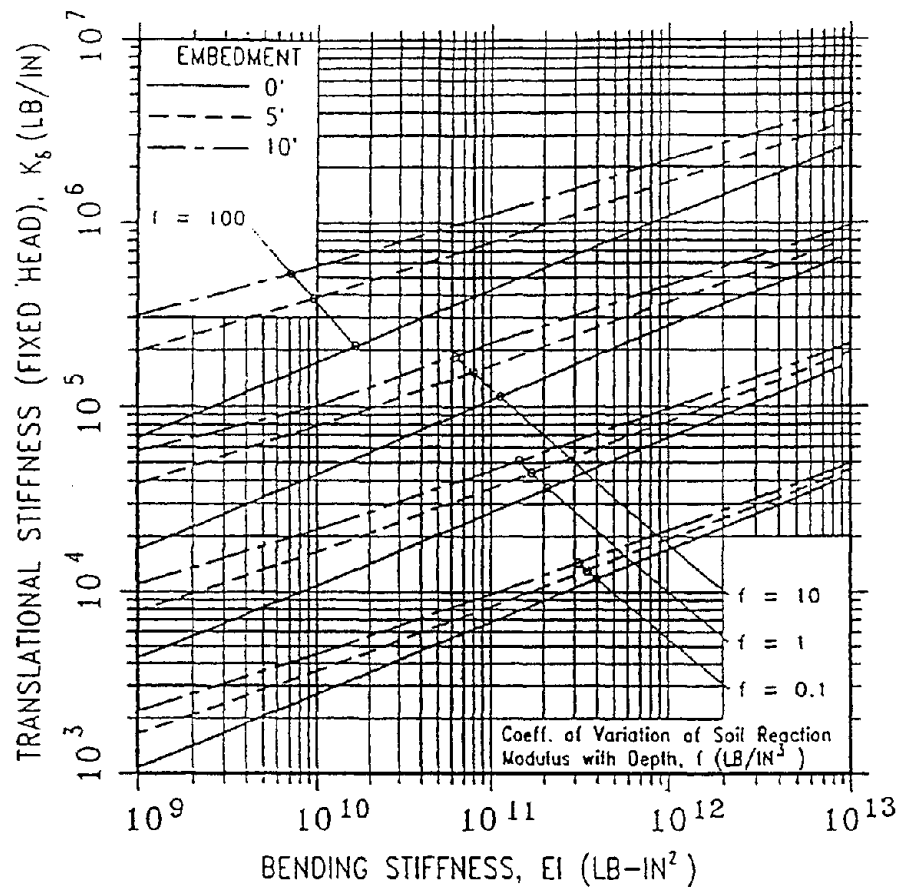
a) Circular Sections



b) Rectangular Sections

A_g = gross section area
 A_{st} = steel section area
 I_g = gross moment of inertia
 I_e = effective moment of inertia of cracked section
 f'_c = compressive strength of unconfined concrete
 P = applied axial compressive load

Figure 2-12 Adjustment Factors for Effective Stiffness for Concrete Piles (Priestley et al, 1996)



$$P_i = K_t \cdot \delta + K_{s0} \cdot \theta$$

$$M_i = K_{s0} \cdot \delta + K_t \cdot \theta$$

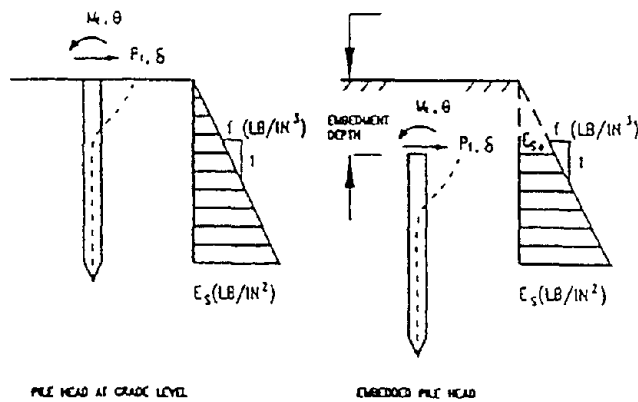
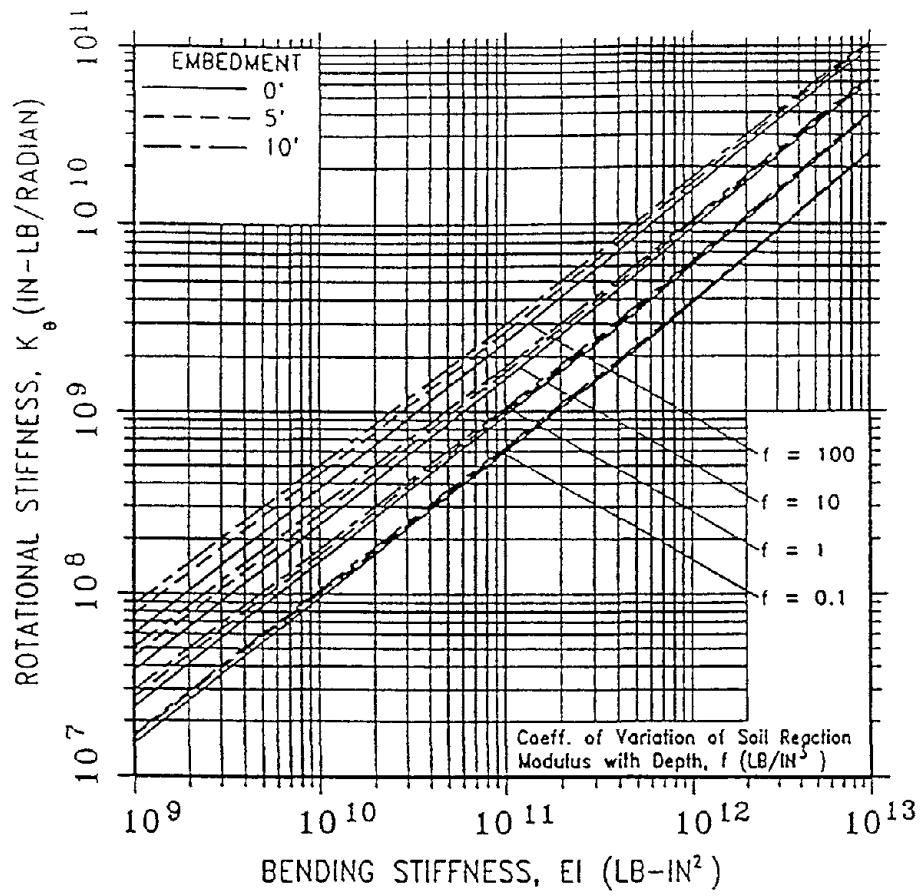


Figure 2-13 Lateral Embedded Pile-Head Stiffness



$$P_t = K_{\delta} \cdot \delta + K_{\theta} \cdot \theta$$

$$M_t = K_{\delta} \cdot \delta + K_{\theta} \cdot \theta$$

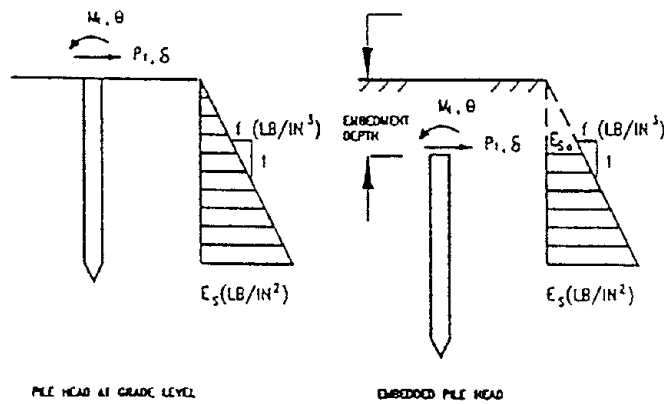
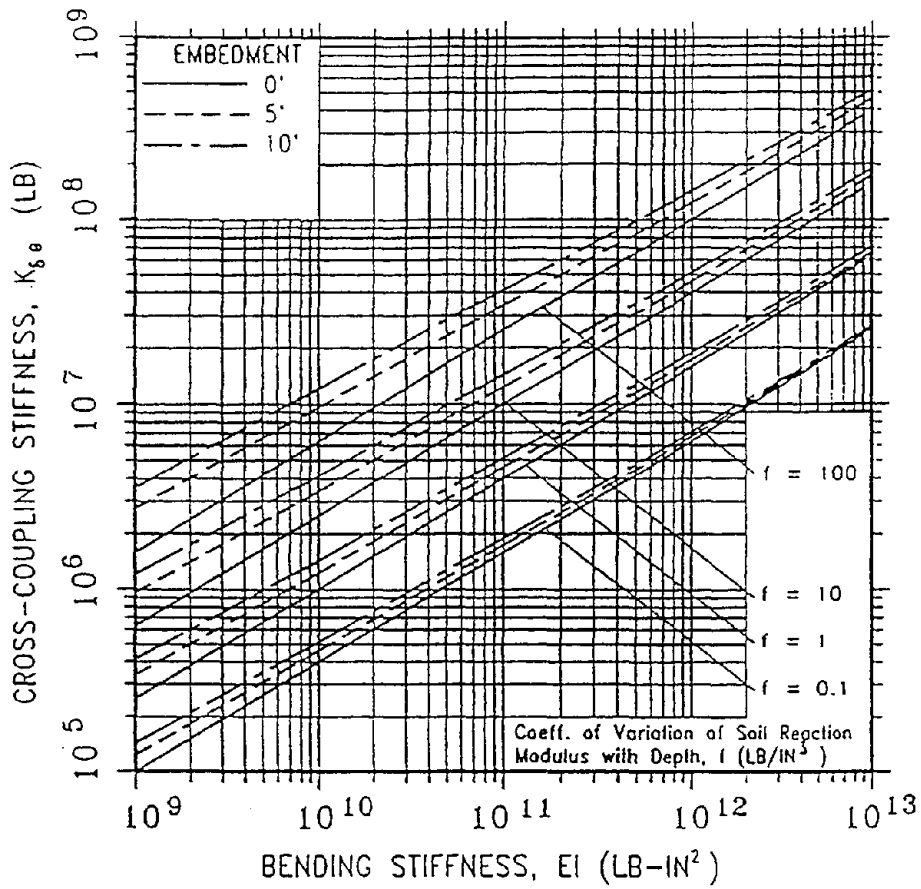


Figure 2-14 Embedded Pile-Head Rotational Stiffness



$$P_1 = K_{\delta} \cdot \delta + K_{\delta, \theta} \cdot \theta$$

$$M_1 = K_{\theta} \cdot \delta + K_{\theta} \cdot \theta$$

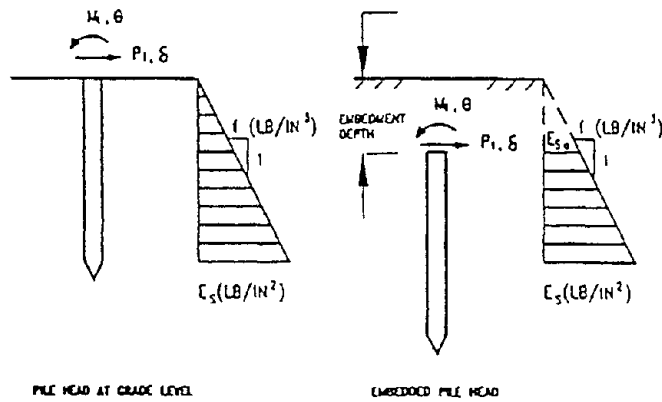


Figure 2-15 Embedded Pile Cross-Coupling Pile-Head Stiffness

$$E_s \approx 0.65 \frac{E_{soil}}{(1-\nu^2)} \quad (2-6)$$

for a Poisson's ratio, ν of 0.5, $E_s \approx E_{soil}$, or the subgrade modulus can be approximated by the Young's modulus of the soil.

2.3.4.4 Presumptive Lateral Stiffnesses

In addition to the above theoretical pile stiffness values, some presumptive stiffness values commonly adopted in practice by structural designers are provided for cross comparison. Section 4.3.4.8 of the Caltrans BDS (1993) gives the following lateral stiffnesses (termed K_y and K_z in eq. (1)) based on pile load tests:

<u>Pile type</u>	<u>Lateral pile-head stiffness (kips/in)</u>
16" CIDH	52
15" driven concrete pile	52
12" driven concrete pile	20
12" or 10" steel flange pile	20
8" steel flange pile	16
timber	20

These stiffnesses were recommended for piles in normal soil conditions with SPT blowcounts of 10 blows per foot and higher, and can be used for service load design (1/4-inch displacement criteria).

Pile load tests at the Cypress Viaduct interpreted by Yashinsky and Zelinski (1993) led to the following guidelines used for San Francisco double-deck viaduct retrofit:

<u>Pile type</u>	<u>Lateral pile-head stiffness (kips/in)</u>	
	<u>Soft soil</u>	<u>Stiff soil</u>
Steel	20 to 30	35
Concrete	20	40
Raymond step-tapered	40 max.	40

It should be noted that the above stiffnesses include contribution from the passive soil stiffness acting at the face of typical pile caps (see Section 2.4). The above presumptive stiffnesses in Caltrans BDS were originally recommended for service load design and to limit the foundation to an acceptable value of structural displacement due to the lateral force demands for service load cases.

The above Caltrans BDS recommended lateral stiffnesses were originally developed for service load design. However, the above tabulated stiffnesses values could also serve as a rule-of-thumb and as a crude check on more refined site-specific solutions or for the earthquake load case.

2.3.5 Foundation Displacement/Rotation Criteria

Allowable foundation displacement (rotation) is a very important subject. However, more research is needed to develop rational guidelines. The most comprehensive study on tolerable foundation displacement to-date is that conducted by Moulton et al. (1985) which suggests tolerable lateral deflections up to 2 inches, and differential settlements arising from rotations of 0.004 rad for continuous structures and 0.005 rad for simply supported structures based on observation of performance of existing bridges under normal service conditions. Moulton's study suggests that the conventional 0.25-inch service load criteria might be over conservative, especially for poor soil conditions or for cantilevered pile caps such as many water crossings.

To date, there are a few guidelines on what might be regarded as tolerable foundation movement for earthquake loading. Probably the only rational approach to determine tolerable movements for earthquake loading would be on the basis of the level of stress or strain on structural components and computed displacements at expansion joints. Nevertheless, the level of tolerable foundation displacement observed by Moulton for service load can be regarded as a conservative criterion for the more severe and relatively rare earthquake loading condition. A recent NCHRP project (1991) re-examined the data compiled by Moulton et al. and recommended an upper-bound limit of angular distortion of 0.004 rad for continuous bridges, but up to 0.008 rad for simple-span bridges. That report led to Commentary C4.5.1 of the ATC-32 (1996) suggesting presumptive tolerable foundation rotations of 0.008 rad and lateral deflections of up to 2-inch as presumptive and conservative seismic design criteria. It is recommended that the designers base their decisions on specific case by case examinations of the level of stress and strain and displacements on specific structures wherever possible for earthquake loading. Current design procedure is also too crude in many respect to accurately predict relative displacements (e.g., the current procedure cannot account for spatial variations in ground motion). Therefore, other traditional rules (e.g., minimum seat width) must still be observed in design practice.

2.4 Pile-Group Stiffness

2.4.1 Rigorous Method Using Static Equilibrium

A simplified, rigorous procedure to develop a linear 6x6 pile group stiffness matrix has been described in Lam and Martin (1986) and incorporated into a computer program by Lam et al (1986). The procedure can be applied to any number of piles and geometric pile group configurations and assumes that the pile cap is infinitely rigid. The stiffness of a pile group is found by static condensation of all pile-head stiffnesses into a single foundation node using basic matrix operations. The individual steps of this procedure are as follows (refer to figure 2-3):

- (1) Select one of the 6 degrees of freedom (three translational and three rotational) of the foundation node and apply a unit displacement or rotation to this degree of freedom. For the first degree of freedom, the pile group displacement vector would be as follows:

$$\mathbf{D} = \begin{bmatrix} \delta_x \\ \delta_y \\ \delta_z \\ \theta_x \\ \theta_y \\ \theta_z \end{bmatrix} = \begin{bmatrix} 1 \\ 0 \\ 0 \\ 0 \\ 0 \\ 0 \end{bmatrix} \quad (2-7)$$

- (2) Perform the following Steps (a) to (e) for each pile in the group:

- (a) Calculate the pile-head displacement and rotation that result from the applied pile group displacement vector \mathbf{D} , taking into account the pile group geometry (e.g., pile-head offsets ΔX , ΔY and ΔZ from the pile group node). This can be achieved using a geometric pile group-to-pile displacement transformation matrix \mathbf{A} :

$$\mathbf{d}_{\text{pile}} = \mathbf{A} \mathbf{D} \quad (2-8)$$

- (b) The local pile coordinate system usually differs from the pile group coordinate system. The induced pile-head displacements and rotations \mathbf{D}_{pile} can be transformed into the pile coordinate system using a pile group-to-pile coordinate transformation matrix \mathbf{T} :

$$\mathbf{d}_{\text{pile}} = \mathbf{T} \mathbf{D}_{\text{pile}} \quad (2-9)$$

- (c) Obtain the pile-head forces and moments resulting from the pile-head movements \mathbf{d}_{pile} by multiplying the movements by the pile-head stiffnesses \mathbf{K}_{pile} from Section 2.3:

$$\mathbf{f}_{\text{pile}} = \mathbf{K}_{\text{pile}} \mathbf{d}_{\text{pile}} \quad (2-10)$$

- (d) Transform the pile-head forces and moments back to the pile group coordinate system using the inverse of the coordinate transformation matrix \mathbf{T} :

$$\mathbf{F}_{\text{pile}} = \mathbf{T}^{-1} \mathbf{f}_{\text{pile}} \quad (2-11)$$

- (e) Calculate the pile group force and moment contributions resulting from the pile using the inverse of the geometric transformation matrix \mathbf{A} :

$$\mathbf{F} = \mathbf{A}^{-1} \mathbf{F}_{\text{pile}} \quad (2-12)$$

- (3) At the pile group node, superimpose the force and moment contributions from all piles:

$$\mathbf{F}_{\text{group}}^i = \sum_{\text{piles}} \mathbf{F} \quad (2-13)$$

- (4) The total pile group reactions $\mathbf{F}_{\text{group}}^i$ are due to a unit displacement \mathbf{D} applied in Step (1) to the i^{th} degree of freedom at the pile group node, and therefore represent the i^{th} row (and column) in the pile group stiffness matrix. Repeat steps (1) to (3) for the remaining 5 degrees of freedom to obtain the remaining column vectors. Superpose all 6 columns to obtain the full 6x6 pile group stiffness matrix:

$$\mathbf{F}_{\text{group}} = \mathbf{K}_{\text{group}} \mathbf{D}_{\text{group}} \quad (2-14)$$

2.4.1.1 Special Case of Plumb Pile Group

For a pile group consisting of only plumb (vertical) piles, the translational and cross-coupling stiffness of the group is simply the sum of the corresponding stiffnesses of all piles. For piles of symmetrical cross-sections (e.g., round, square or octagonal piles), the coupled terms in the pile group stiffness matrix are all equal. Conversely, if the pile layout is non-symmetric or involving battered piles, the matrix can differ from a single pile stiffness matrix as shown in eq. (2-1).

For the rocking stiffnesses of the pile group, however, the axial stiffnesses and cross-coupling stiffnesses of each pile need to be reflected in addition to each piles' rocking stiffnesses. The pile group rocking stiffness can be calculated as follows (refer to figure 2-3):

$$\left. \begin{aligned} \mathbf{K}_{\theta X} &= \sum_{\text{piles}} \mathbf{K}_{\theta y}^{\text{pile}} + \sum_{\text{piles}} \mathbf{K}_x^{\text{pile}} Z^2 \\ \mathbf{K}_{\theta Z} &= \sum_{\text{piles}} \mathbf{K}_{\theta z}^{\text{pile}} + \sum_{\text{piles}} \mathbf{K}_x^{\text{pile}} Y^2 \\ \mathbf{K}_{\theta Y} &= \sum_{\text{piles}} \mathbf{K}_y^{\text{pile}} X^2 + \sum_{\text{piles}} \mathbf{K}_z^{\text{pile}} Z^2 \end{aligned} \right\} \quad (2-15)$$

To avoid complexities in developing and entering complicated matrices into the structural model, an alternative simplified method is presented below.

2.4.2 Simplified Method Using an Equivalent-Cantilever Approach

The pile group matrix can also be developed using a simple elastic equivalent-cantilever model to approximate the individual pile-head stiffness matrix. The concept is to match the individual single-pile stiffness matrix coefficients of eq. (2-3), usually provided by the geotechnical engineer, with the following equivalent cantilever model:

$$\mathbf{K}_{pile} = \begin{pmatrix} \frac{AE}{L} & 0 & 0 & 0 & 0 & 0 \\ 0 & \frac{12EI_{z'}}{L^3} & 0 & 0 & 0 & \frac{6EI_{z'}}{L^2} \\ 0 & 0 & \frac{12EI_{y'}}{L^3} & 0 & -\frac{6EI_{y'}}{L^2} & 0 \\ 0 & 0 & 0 & \frac{GJ_t}{L^3} & 0 & 0 \\ 0 & 0 & 0 & 0 & \frac{4EI_{y'}}{L} & 0 \\ 0 & 0 & 0 & 0 & 0 & \frac{4EI_{z'}}{L} \end{pmatrix} \quad (2-16)$$

where L is the equivalent cantilever's length,
 A is the equivalent cantilever's uniform cross-sectional area,
 E is the equivalent cantilever's elastic modulus,
 G is equivalent the cantilever's shear modulus,
 $I_{y'}$ is the equivalent cantilever's moment of inertia about lateral y' -axis,
 $I_{z'}$ is the equivalent cantilever's moment's of inertia about lateral z' -axis, and
 J_t is the equivalent cantilever's torsional moment of inertia about axial x' -axis.

In this method, each pile is represented by a uniform elastic cantilever beam with unknown length, cross-section and moments of inertia (see figure 2-16) and with its bottom end (point of fixity) fixed. The characteristics of these cantilever beams can be obtained by matching the matrices in eq. (2-16) and (2-1). The beams can then be directly incorporated into the structural designer's complete pile group or global bridge model, to take into account the stiffness of the pile soil system as well as the orientation of each pile member. This approach is presented because only a beam element would be needed to account for the more complicated beam on Winkler spring or p-y curve model. The equivalent cantilever beam model can then be used in a global model to account for the soil, the pile stiffness and to explicitly inputting a rather complex pile layout along with battering effects of each pile. Implementing a pile group configuration by way of an equivalent cantilever model would also be manageable from the point of view of the needed number of degrees of freedom in a typical problem.

In seismic design, the equivalent cantilever model is normally established by matching displacements or stiffness of the soil-pile system in dynamic response analysis. The resultant model represents the foundation stiffness properly, but the calculated shear and bending moments in the cantilever may not bear any relevance to those in the actual pile. Therefore, this particular modeling approach is only suitable for the *first step* in the design process to represent foundation stiffness in a global dynamic response analysis of the bridge structure. To calculate pile forces, it is necessary

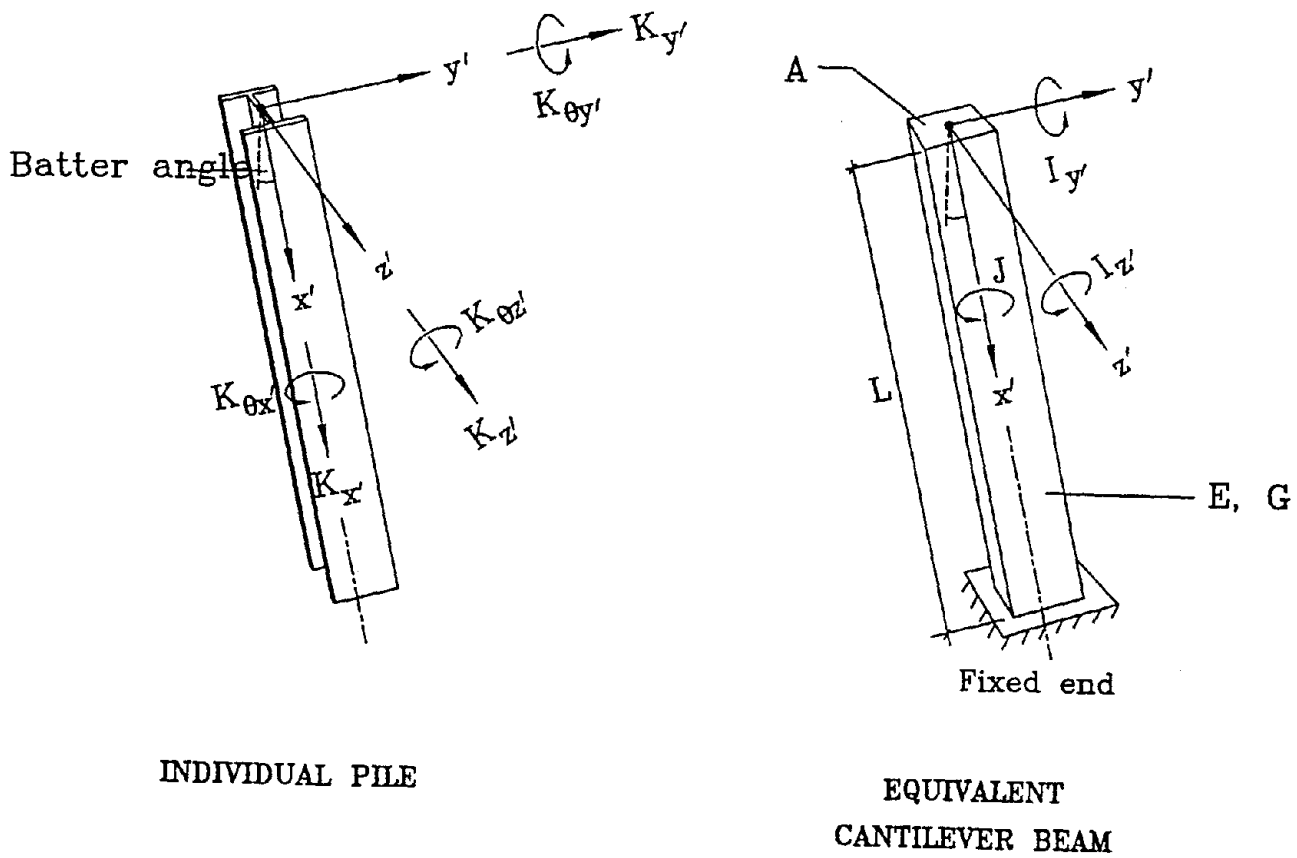


Figure 2-16 Modeling Piles Using Equivalent Cantilever Beams

to go through the second step (static pushover) analysis, where the complete, realistic pile with the surrounding soil is modeled.

2.4.2.1 Equivalent Cantilever Model Parameter for Lateral Loading

The process of developing an equivalent cantilever model to represent the foundation stiffness of a soil-pile system involves choosing the appropriate cantilever pile parameters such that eq. (2-16) would approximate the stiffness matrix of a given soil-pile system as defined in eq. (2-1). The equivalent cantilever model can be evaluated for each of the two orthogonal lateral loading directions independently. The foregoing discussions present the methodology to develop the equivalent cantilever model parameter for loading in a x-y plane (i.e. loading in the y direction in the local pile coordinate). The procedure can be repeated for the other orthogonal z loading directions.

For a pile of flexural stiffness EI_p embedded in a soil of linearly increasing subgrade modulus, the stiffness matrix at the pile head at the grade elevation can be calculated as (Lam et al., 1991)

$$K = \begin{bmatrix} K_{y'} & K_{y'\theta z'} \\ K_{y'\theta z'} & K_{\theta z'} \end{bmatrix} = EI_p \begin{bmatrix} \frac{1.06}{\lambda^3} & \frac{0.98}{\lambda^2} \\ \frac{0.98}{\lambda^2} & \frac{1.48}{\lambda} \end{bmatrix} \quad (2-17)$$

in which λ is the characteristic length of the pile soil system as defined in eq. (2-4) or (2-5).

2.4.2.2 Cantilever Model Matched to Diagonal Stiffnesses

The stiffness matrix for each pile with its soil support (as shown in eq. (2-17)) and for the lateral loading direction can be approximated by an equivalent cantilever beam column by choosing the appropriate EI_c and equivalent cantilever length L_c . It is obvious that these two cantilever model parameters are insufficient to satisfy all three stiffness coefficients (two diagonal stiffness and one cross-coupling stiffness coefficients) in eq. (2-17). The general approach would be to match the diagonal stiffness terms, leading to the following cantilever model parameters:

$$L_c = 2.05\lambda \quad (2-18)$$

$$EI_c = 0.757EI_p \quad (2-19)$$

The corresponding cantilever model, in terms of the actual diagonal stiffness coefficient of a pile-soil system (e.g. determined from actual load-deflection solutions by computer analysis) are given below.

$$L_c = 1.732 (K_{\theta z'})^{0.5} (K_{z'})^{-0.5} \quad (2-20)$$

$$EI_c = 0.433 (K_{\theta z'})^{1.5} (K_{z'})^{-0.5} \quad (2-21)$$

2.4.2.3 Cantilever Model Matched to Translational and Cross Coupling Stiffnesses

The basis of matching the diagonal stiffness coefficient in the above equivalent cantilever model appears generally sound, especially for a pile extension type configuration such as shown in figure 1-1(b).

For a pile footing type configuration such as shown in figure 1-1(a), the rotational stiffness of the pile group tends to be dominated by the axial pile stiffness as compared to the stiffness contribution from the bending stiffness of individual piles. Therefore, it might be possible to choose the equivalent cantilever model solely to match the lateral force versus deflection equation (i.e. the first of eq. (2-17), by matching the translational and the cross-coupling stiffness term), resulting in the following cantilever model:

$$L_c = 1.85\lambda \quad (2-22)$$

$$EI_c = 0.556EI_p \quad (2-23)$$

This approach can lead to a more appropriate lateral stiffness for a wider range of pile-head boundary (fixed and free-head) conditions. This cantilever model can be expressed in terms of the lateral and cross-coupling stiffness coefficients of a pile-soil system shown in eq. (2-1) as follows (e.g., determined from actual load-deflection solutions by computer analysis):

$$L_c = 2 (K_{y'_{ez'}}) (K_z)^{-1} \quad (2-24)$$

$$EI_c = 0.667 (K_{y'_{ez'}})^3 (K_z)^{-2} \quad (2-25)$$

2.4.2.4 Axial and Torsional Stiffnesses

The axial translational displacement stiffness coefficient is uncoupled with other stiffness coefficients in the local pile coordinates. While there are many complexities in establishing the appropriate axial pile stiffness, it is rather trivial to implement the axial pile stiffness term in a global model. In the equivalent cantilever model, with a beam length L_c calculated as shown above to match lateral load-deflection characteristics, the axial stiffness of the model would merely be:

$$AE_c = K_x \cdot L_c \quad (2-26)$$

The torsional stiffness of the overall pile group is usually dominated by the translational stiffnesses of individual piles in conjunction with the spacing between the pile and the neutral torsional axis of the pile group. The contribution of the torsional stiffness of individual piles tends to be very small. To avoid artificial overly constraining the torsional mode of response in the global bridge model, the torsional stiffness of an individual pile should be zero or an arbitrarily small value because of the lack of a well established method or procedure to derive the torsional pile stiffness.

2.5 Pilecap Stiffness

2.5.1 Previous Research on Interaction Between Pile and Pile Cap

In addition to the component of soil resistance acting on the piles, a pile footing involves an additional component of soil resistance acting on the pile cap. A research project has been conducted at the Rensselaer Polytechnic Institute led by Dobry to evaluate the component of soil resistance associated with the pile cap (Gadre, 1997). The research program initiated by centrifuge tests on embedded piles alone, then embedded pile cap without piles, followed by testing of embedded piles with a pile cap to investigate the various component of soil resistance and how they interact with each other. Static finite-element analyses were also used to extend the results of centrifuge tests to various pilecap geometries. Major conclusions from the research program are summarized as follows:

- (1) Pile-soil interaction analyses based on the p-y curve approach gives reasonable account of stiffness characteristics of the pile-soil interaction mechanism. Similar conclusions on the reasonableness of p-y curves have been confirmed by other numerous research projects.
- (2) Centrifuge test data for loading of the pile cap alone indicates that the overall load-deflection characteristics of the pile cap (both stiffness and internal damping energy) can be developed by summation of the various component of resistance: (i) passive pressure acting on the front face of the pile cap, (ii) side shears acting on the two vertical side surfaces of the pile cap and (iii) base shear acting on the bottom of the pile cap.

The most significant component of resistance arises from the passive pressure acting on the front face of the pile cap, which constitutes over 50% of the total resistance for the range of pile cap geometries studied. Classical earth pressure theories give reasonable account of this passive component of soil resistance. The wall-soil interface friction angle was found to be as high as the internal friction angle of soil. However, the soil resistance acting on the pile cap should be regarded as a force capacity rather than a stiffness because the displacement amplitude to reach the ultimate capacity occurs at a relatively small value, of the order of 1 to 2 inches. As a result, the secant stiffness mobilized by the pile cap decreases at increasing pile cap deflection within the range of design interest. At deflections exceeding 1 to 2 inch range, an ultimate capacity is reached and the secant modulus can be estimated by the ratio of the ultimate force capacity and the cap deflection.

- (3) Centrifuge data for pile embedded into pile cap shows that there is some degree of pile cap-pile interaction (i.e. the load-deflection characteristics associated with the pile cap and the pile varies to some degree depending on loading on the other component). This is because the load acting both on the pile cap and the piles will ultimately be resisted by the soil mass at the same zone. Also, the experiment confirms findings from both above items, that the component of soil resistance on the pile can be regarded as a form of stiffness, whereas the component of soil resistance on the pile cap would better be characterized as a constant force capacity.

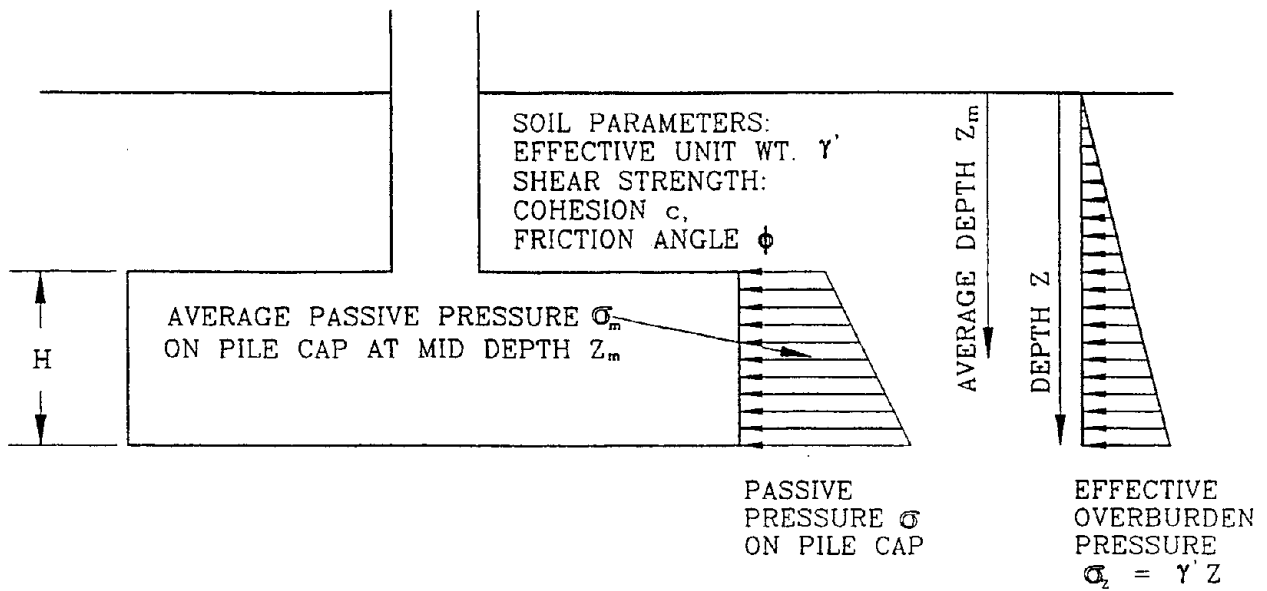
The above research findings will be used as a basis to develop the appropriate overall load-deflection characteristics of typical pile footings to account for both the pile cap and pile component of soil resistance.

Other full-scale experimental data on the passive soil resistance mobilized at the vertical pile cap face can be found from full-scale load tests reported by Abcarius (1991). This additional stiffness should be included only for stable soil sites and its resistance would be small and should be ignored for soft clay and liquefiable sites. The pile cap stiffness is the ultimate soil capacity divided by an estimated displacement to mobilize this capacity. Figure 2-17 illustrates a simple procedure to estimate the ultimate capacity.

2.5.2 Recommendation for Incorporating Pile Cap Stiffness

The following recommendations would be appropriate to incorporate the pile cap stiffness into the pile group based on various studies.

- (1) For stable level ground conditions (i.e., level ground and competent soils with blowcounts above 10 blows per foot), the component of the passive pressure soil resistance on the front vertical pile cap face can be added to the stiffness and resistance derived from the pile members. Because of potential interaction between the pile cap and the supporting piles, it is recommended to ignore other components of soil resistance acting on the pile cap, including the shear force at the bottom of the pile cap, and side shears on the two side surfaces.
- (2) The appropriate classical earth pressure theories can be used to calculate the ultimate passive pressure capacity. This ultimate capacity can be used to construct an elasto-plastic load-deflection curve to represent the characteristics of the pile cap. Such limiting-equilibrium solutions can be used to develop the ultimate passive pressure capacity on the front vertical pile cap face which can be used to form the ultimate capacity of the pile cap. Some further details on the passive earth pressure theories for various soil types will be discussed further.
- (3) An elastic slope would then be needed to form the elastic stiffness, along with the ultimate passive pressure capacity, to develop an elasto-perfectly plastic load-deflection curve to characterize the load-deflection characteristics of the pile cap. Theoretically, the elastic slope would depend on the configuration of the front vertical pilecap face (especially the thickness of the pile cap) and the modulus of the soil. Elastic solutions are available (e.g. Wilson, 1988) for this elastic stiffness. However, experimental data (Gadre, 1997) shows that the solution depends very strongly on the choice of the appropriate soil modulus. If shear wave velocity is used to derive the soil modulus, data shows that a rather low secant modulus to low-strain modulus ratio (less than 0.1) is needed to predict the initial stiffness from the experiment. Moreover, since the ultimate capacity is reached at rather small deflection values, the range where elastic half space theory applies would be rather limited.



RECOMMENDED METHOD FOR PASSIVE PRESSURE CAPACITY

- (I) FOR FRICTIONAL SOIL (ϕ ONLY):
AVERAGE PASSIVE PRESSURE CAPACITY = $K_p \gamma' Z_m$
 K_p BASED ON CAQUOT & KERISEL(1948) FOR
INTERFACE FRICTION ANGLE $\delta = 0.5 \phi$
- (II) FOR COHESIVE SOIL (c ONLY):
BASED ON RANKINE PRESSURE THEORY
AVERAGE PASSIVE PRESSURE CAPACITY = $\gamma' Z_m + 2c$
- (III) FOR c AND ϕ SOILS:
AVERAGE PASSIVE PRESSURE CAPACITY = $K_p \gamma' Z_m + 2c \tan(45^\circ + \phi/2)$

TOTAL FORCE CAPACITY ON PILE CAP PER UNIT WIDTH
= AVERAGE PASSIVE PRESSURE CAPACITY \times THICKNESS OF CAP (H)

Figure 2-17 Method for Passive Pressure Capacity of Pile Cap

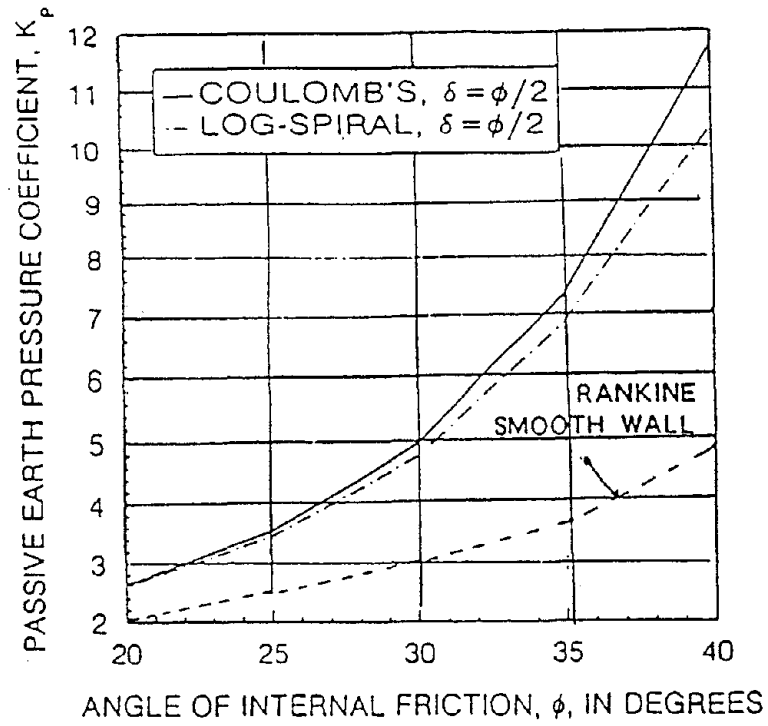
- (4) Experimental data (Gadre, 1997) further shows that the deflection level to reach the ultimate pile cap capacity occurs at about 0.03 to 0.05 times the embedment depth. When an elastic-perfectly plastic model is fitted to that data, however, the ultimate capacity occurs at a deflection of about 0.02 times the embedment depth, which is consistent with data from other wall-soil interaction experiments.
- (5) The above load-deflection characteristics can be used to develop the equivalent linear secant stiffness to be added to the stiffness of the piles.

The foregoing procedure to account for additional stiffness contributions of the pile cap only applies to typical conditions where the ground is level. For many cases, where the footing might be adjacent to embankment slopes (e.g. at abutments) and where the ground elevation is not level, or where poor soils exist, the pile cap stiffness would be significantly eroded, so that the contribution from the pile cap determined using the foregoing procedure would not be appropriate and must be dealt with on a case by case basis.

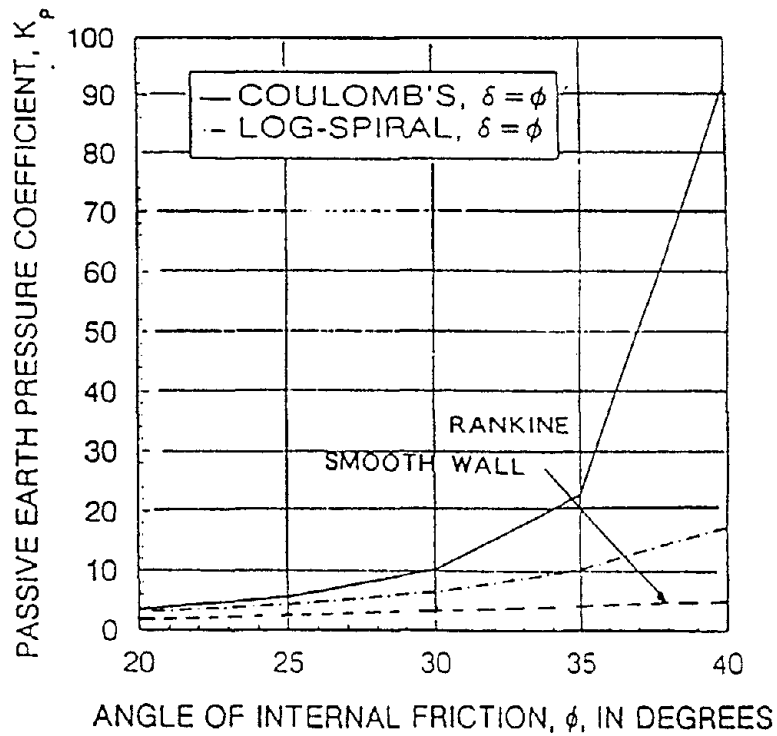
2.5.3 Passive Earth Pressure for Sand

The ultimate static soil resistance at the pile cap face can be determined based on classical passive earth pressure theories by treating the face as an embedded wall. A passive earth pressure condition arises when the pile cap is forced to move toward the soil mass (as opposed to an active earth pressure condition where the pile cap moves away from the soil, or an at-rest earth pressure condition where the pile cap is in at a neutral condition between the two active and passive condition).

Solutions based on various earth pressure theories are available in the literature, including: (1) Rankine's theory, which assumes that the wall-soil interface is perfectly smooth, (2) Coulomb theory, which accounts for interface friction, but assumes a planar failure mechanism, or (3) a logarithmic spiral-type failure mechanism in granular soils (Caquot and Kerisel, 1948), which can be regarded as an improvement over Coulomb's planar failure assumption. Among these three earth pressure theories, the log-spiral method can be regarded as technically correct for frictional sandy soils. Several experimental studies (Rollins et al., 1997; Gadre, 1997; and Maroney et al., 1994) confirmed the validity of Caquot and Kerisel's solution, and the measured wall-soil interface friction angle corresponding to the full internal friction angle of sand ($\delta=\phi$). On the basis of the evidence reviewed, the authors recommend adopting Caquot and Kerisel's log-spiral solution for general application as shown in figure 2-18. Based on available data, a wall-soil interface angle equal to the full internal friction angle of the soil would represent the best-estimated scenario. However, taking the interface friction angle to be half of the soil friction angle ($\delta=\frac{1}{2}\phi$) can be adopted for a conservative design, especially for poor soil sites where the soils could be degraded. Figure 2-17 summarizes how the earth pressure coefficient in figure 2-18 can be used to calculate the ultimate passive pressure capacity of the pile cap.



(a) $\delta = \phi/2$



(b) $\delta = \phi$

Figure 2-18 Coefficients for Friction Component of Passive Pressure Capacity

2.5.4 Passive Earth Pressure for General c - ϕ Soils

In addition to purely frictional soils (sands with friction angle ϕ with zero cohesion), Martin et al. (1997) also presented some numerical solutions for the passive pressure coefficient for purely cohesive (only c) soils and general c - ϕ soils. Proven solutions for general c - ϕ soils and wall-soil interface friction are not available in the literature. Following interim procedure is recommended to deduce passive pressure capacity for cohesive and c - ϕ soils:

- For purely frictional soils (i.e. only ϕ), adopt the above discussed log-spiral solutions for the frictional component of soil resistance.
- For purely cohesive soils (only c) develop the capacity based on the effective overburden pressure (self weight of the soil) plus an additional component equal to $2c$ as shown in figure 2-17.
- For a general combination of frictional and cohesive (i.e. c - ϕ) soils, use the combination rule as shown in figure 2-17.

2.5.5 Typical Earth Pressure Coefficients for Design

For seismic design, the effects of soil resistance at the pile cap under seismic loadings is not well understood. In absence of a common consensus, it is suggested that the seismic passive earth pressure coefficient K_{pe} for friction soils should be determined on the basis of a log-spiral type mechanism with high wall friction. For Caltrans standard wall structural backfill (Caltrans Bridge Design Specifications, 1990) with full friction, a K_{pe} of 16 can be justified. Large-scale cyclic wall load tests in sand documented by Maroney et al. (1994) have shown that an average maximum soil pressure of 369 kPa (7.7 ksf) can be justified for a 2.44-m (8-ft) high wall, which corresponds well with this K_{pe} value (Gadre, 1997). Dobry's centrifuge data confirmed the use of passive pressure theory. However, Dobry concluded that the conventionally assumed 7.7 ksf of passive pressure for a typical abutment wall could be too high. Also, soils around pile caps might not be as compacted as approach fills behind abutments. For the above reasons, it is recommended that passive pressure coefficient of about 10 could be regarded as typical for pile cap resistance.

The maximum pressure of 7.7 ksf is used by Caltrans for design of abutment walls of 8-ft height (Caltrans Memo to Designers 20-4, 1995). According to classical earth pressure theory for frictional soils, the average maximum pressure would depend on the wall height because soil pressure increases linearly with depth (e.g., proportional to overburden pressure). The integrated ultimate capacity would then be proportional to the square of the wall height. For wall heights less than 8 ft, the maximum pressure could then be obtained using a linear interpolation.

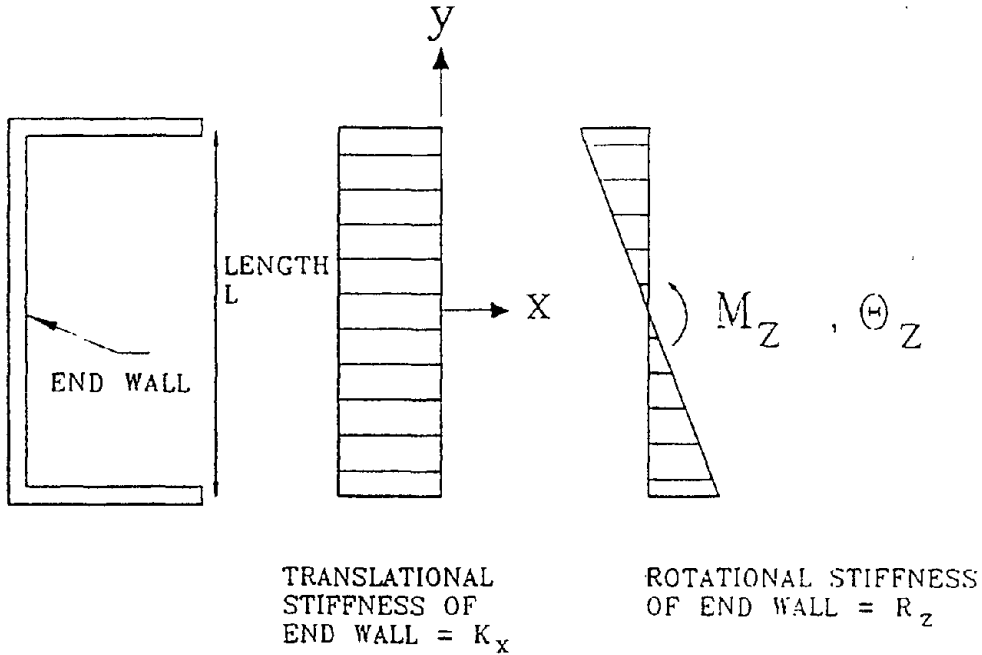
2.5.6 Pile Cap Displacement

The lateral deflection to mobilize the full passive pressure capacity must be estimated. Clough and Duncan (1991) suggested "wall" movements from 1% to 2% of the thickness of the embedded pile

cap. The elastic stiffness should theoretically depend on the configuration of the wall contact configuration as well as the modulus of the soil. Elastic stiffness solutions can be developed based on more rigorous numerical solutions or approximate elastic stiffness charts such as that from Wilson (1988) as shown in figure 2-19. However, use of this elastic stiffness chart is hampered by difficulty in choosing the appropriate elastic soil modulus. If a low-strain shear modulus is used from geophysical shear wave velocity data, it should be modified using a rather small multiplication factor (as low as 0.1) to reflect the much higher level of strain from the rather high structural loading as compared to the strain expected from free-field response. Also, elastic soil moduli are difficult or expensive to obtain for most applications. The criteria of 1% to 2 % of the thickness of the pile cap might be more practical. The choice of the 1% versus 2% might be guided by the specific soil type with the choice of higher displacement value for soft soils (e.g., for soft to medium clay and loose sands).

A bilinear elasto-plastic load-deflection curve can be developed by the use of aforementioned passive pressure theories to estimate the ultimate passive pressure soil resistance. The elastic stiffness can be developed based on the ratio of the ultimate capacity to the deflection level to fully mobilize the ultimate capacity. The stiffness at any deflection level can be deduced based on the equivalent-linear stiffness from the elasto-plastic load-deflection curve. As discussed in Section 2.2, a secant stiffness at about 0.5 to 0.65 of the peak foundation deflection from the global dynamic response model would be appropriate in an iterative solution process to establish the equivalent-linear secant modulus of the foundation. The 0.5 to 0.65 factor applied to peak foundation deflection differs from the iterative process used to develop equivalent linear abutment stiffness in bridge design. Because in the abutment modeling process, the intent is to introduce a softer abutment stiffness into the global bridge model in order to develop a sufficiently conservative load distribution to the columns for structural integrity assessment. In contrast, emphasis in foundation modeling should be placed on representing the foundation stiffness realistically such that the resultant global model would have the desirable dynamic response characteristics (i.e., fundamental period). The load distribution between the resistance on the pile cap versus the underlying piles can best be addressed in a separate nonlinear pseudo-static pushover analysis where the actual elasto-plastic pile cap load-deflection curves and nonlinear p-y curves along the piles are modeled.

The resultant pile cap stiffnesses can be added to the diagonal lateral translational stiffness coefficients in the pile group stiffness matrix developed in this section for the total pile group-pile cap stiffness matrix.



$$R_z = K_x L^2 / 12$$

$$K_x = \frac{E_s L}{(1-\nu^2) I}$$

where E_s is Young's Modulus of Soil

ν is Poisson Ratio of Soil

I is Shape Factor, a Function of the Ratio of Long vs. Short Dimension of the End Wall

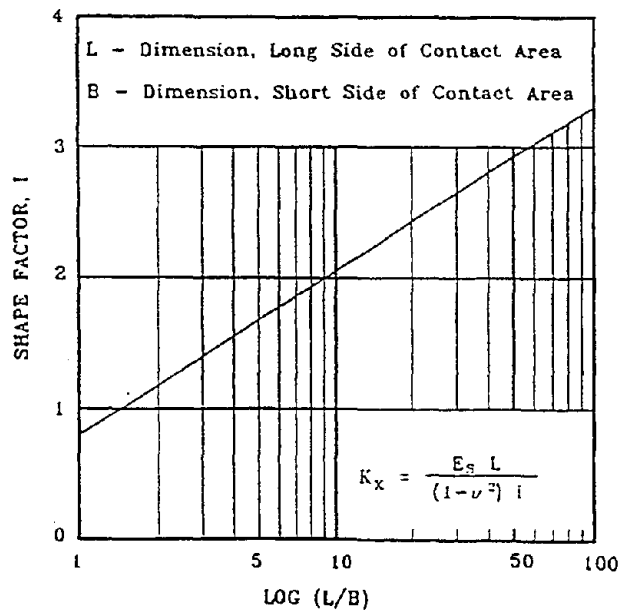


Figure 2-19 Elastic Stiffness Based on Elastic Soil Modulus

2.6 Nonlinear Load-deflection Sensitivity Study

2.6.1 Background on p-y Curves

This section presents a series of nonlinear load-deflection solutions based largely on p-y curve approaches to illustrate a number of sensitivity issues to aid the designers in the decision-making process in foundation design. Pile design based on p-y curves or the Terzaghi's subgrade modulus approach have been widely adopted by the industry for practical design for over 20 years. Numerous studies have been conducted and many major studies (sponsored by joint-industry research programs funded by oil companies or sponsored by state departments of transportation) have concluded that the Matlock and Reese p-y criteria (recommended for design in the API design code) give reasonable pile design solutions. These p-y criteria were originally conceived for design against storm wave loading conditions based on observation of monotonic static and cyclic pile load test data. The monotonic static loading data formed the static p-y criteria and are still applicable for developing the backbone p-y curves for seismic design applications. However, Matlock and Reese's cyclic p-y criteria were originally conceived for storm wave loading. The cyclic clay criteria have some implicit assumptions based on certain aspects of the storm wave loading characteristics which would not be appropriate for earthquake design applications. Therefore, Matlock and Reese's static p-y curves can serve as the benchmark for design to represent the initial monotonic loading path for typical smaller-diameter driven isolated single piles. There have been some recent advances in further development of p-y curves in the following aspects:

- (6) Pile load tests from fast-rate vibratory loading conditions have been presented by Crouse et al. (1993) and Lam and Cheang (1995) and have been compared to parallel slow cyclic pile load tests.
- (7) Full-scale pile group tests have become available to provide some guidance on the issue of pile group effects.
- (8) Some attention has been given to pile design in liquefied soil deposits.

Some comments are provided to summarize lessons learnt on the above subjects in the latter part of this section. In order to clarify the relationship between the p-y curves and the traditional Terzaghi's subgrade modulus approach is first discussed below.

2.6.2 p-y Curves versus Terzaghi's Subgrade Modulus

Figure 2-20 presents a series of pile load-deflection solutions for a 16-inch cast-in-drilled-hole (CIDH) concrete pile using both the standard Reese's static loading p-y curve criteria, compared to those based on Terzaghi's recommended subgrade modulus values. The comparison shows very reasonable agreement between the Terzaghi's linear subgrade modulus solution and the Reese's p-y criteria. Figure 2-21 presents a similar comparison for the same 16-inch CIDH pile for clay soils. Terzaghi recommended a subgrade modulus E_s constant with depth for clay. Matlock's soft clay p-y criteria for a clay with uniform undrained shear strength would result in an ultimate soil pressure capacity (i.e. p_{ult}) which varies with depth, increasing from $3c$ at mudline to $9c$ at a sufficiently large

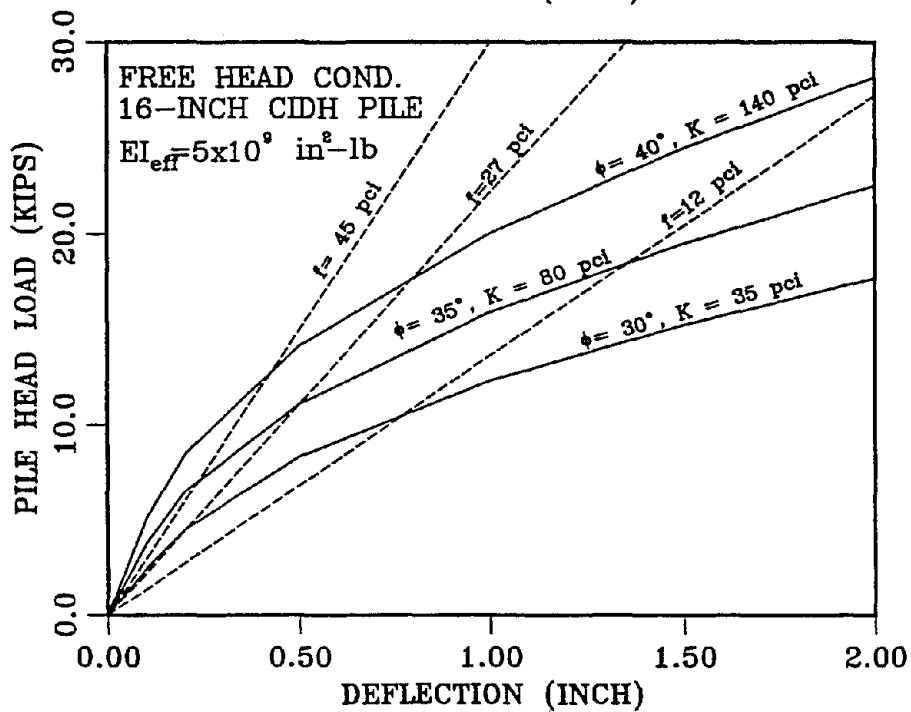
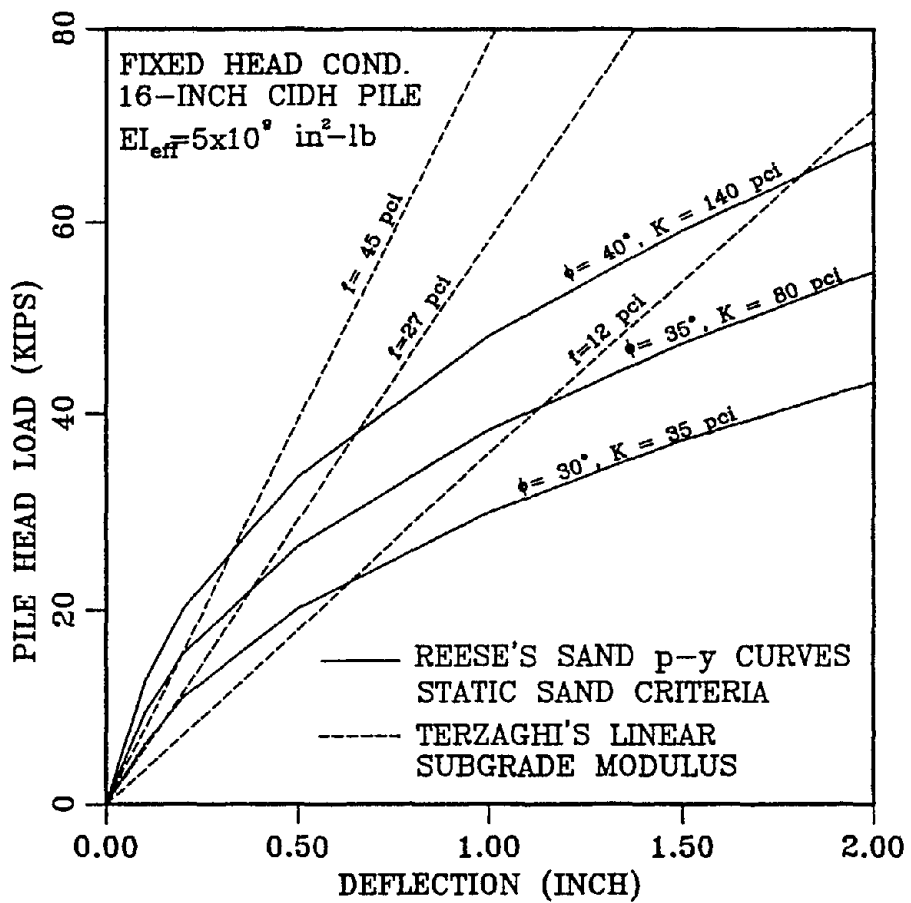


Figure 2-20 Correlation of p-y Curves with Terzaghi's Subgrade Stiffness for Sands

depth because of the difference in kinematic constraints between the shallow soil wedge heaving mechanism versus the mechanism of soil flow around the pile at deep depth. The subgrade stiffness model for clay shown in figure 2-11 deviates from Terzaghi's constant subgrade stiffness approach. In this report, the authors adopted the same subgrade model used for sand in which the stiffness increases linearly with depth for the following reasons:

- (1) Based on correlation to full-scale pile load test data, Matlock found that the linearly increasing subgrade stiffness approach led to better fit of the observed pile load test data compared to constant stiffness approach, especially for soft to medium stiff clay sites. This is because in most cases, one would expect a higher level of pile deflection at shallow depths, but the deflection decreases rapidly within the upper five pile diameters. Therefore, there is a higher degree of soil nonlinearity at the mudline which would lead to a softer equivalent secant modulus as compared to that at depth, even if the p-y characteristics might be identical within the soil-pile interaction zone.
- (2) The authors adopted a similar subgrade stiffness model for both sands and clays such that the same design charts can be used for both soil types to reduce unnecessary complexity and the need for numerous pile stiffness charts. It should be recognized that the Winkler spring stiffness is not an intrinsic soil property, but merely a tool to facilitate soil-pile interaction analyses. Therefore, it should be viewed as merely a computational tool that has proven to work well from ample design experience.

In figure 2-11, a correlation had been presented to aid in the selection of the coefficient f of variation in subgrade modulus with depth (see Section 2.3.4) for clays of different consistencies. This correlation proposed by Lam et al. (1991) was obtained for a specific pile type (12-inch diameter concrete pile with a fixed-head condition, calibrated to 1-inch pile-head deflection). The actual solutions from the correlation shows a nonlinear cohesion versus coefficient of variation of subgrade stiffness with depth, but Lam adopted a linear relationship (calibrated at an undrained shear strength of 1 ksf) for simplicity.

Figure 2-11 also presents some recommendations from the widely used Navy Design Manual (DM-7.02, 1986). The comparison shows that Lam's correlation gives a somewhat higher subgrade coefficient, but can be regarded to be in reasonable agreement with DM7 recommendations. While the correlations shown in figure 2-11 provides data for very stiff to hard clays (undrained shear strength up to 5 ksf), it should be cautioned that very stiff to hard clays often exhibit secondary structural characteristics in the soil matrix (i.e., cracks and fissures), and the intact strength of the clay can rarely be fully mobilized in these soils. As a result, p-y curves for very stiff to hard clays often exhibit rather drastic strength softening behavior. The authors feel that such secondary structural characteristics cannot be taken into account except on a case-by-case basis, and therefore the authors prefer the Matlock's soft clay p-y criteria (which is based more directly on mechanistic geomechanics theories) even for stiff to hard clays. However, users are cautioned on this issue, and it is suggested to adopt a conservative approach in the selection of the coefficient f for very stiff to hard clays, but setting a limiting value on the clay shear strength value to no higher than 5 ksf. Figure 2-21 presents comparison of the resultant pile-head stiffness between the Lam's recommended f value with the Matlock's p-y curves. Whereas, there is some discrepancies in the comparison,

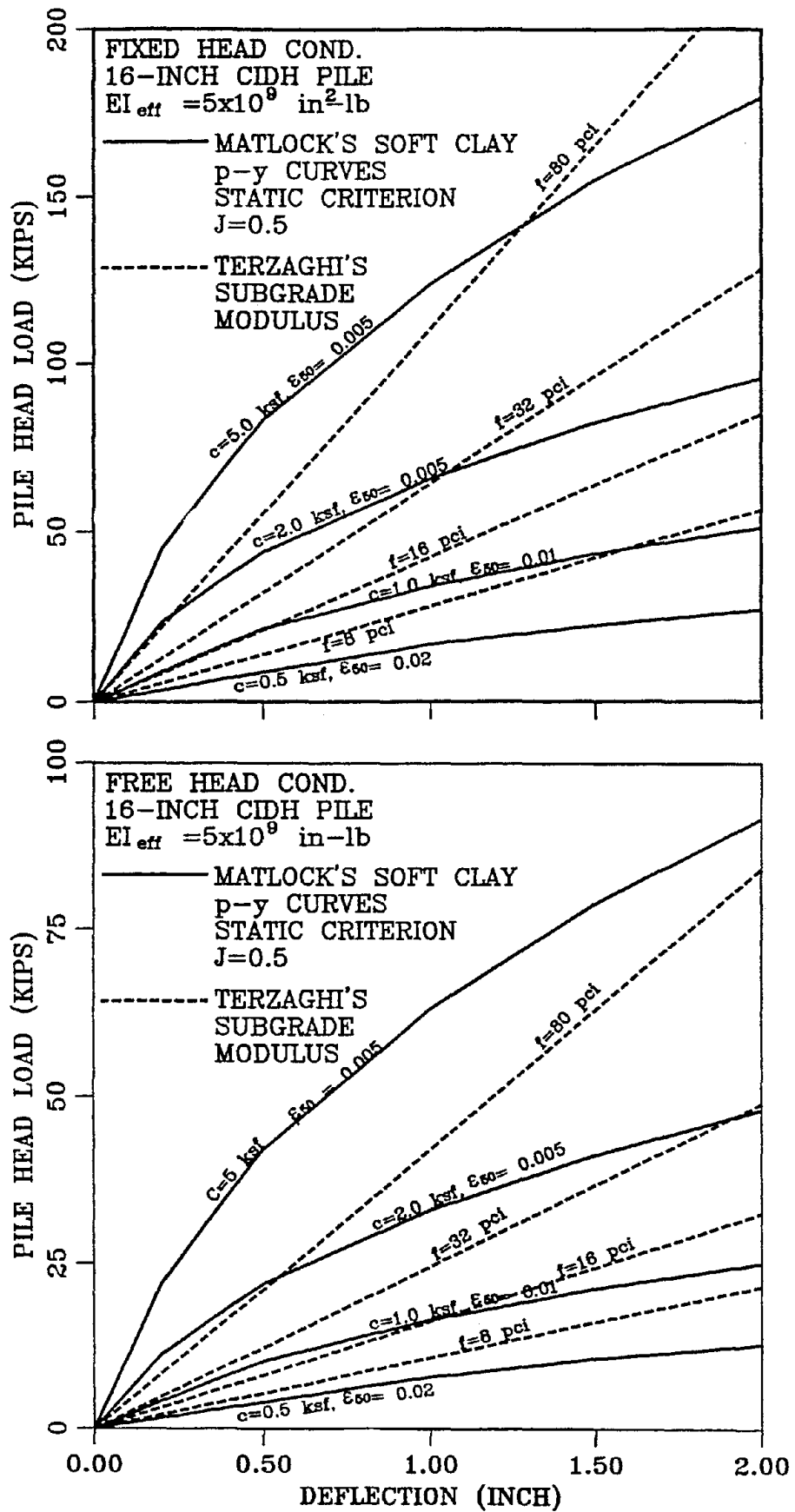


Figure 2-21 Correlation of p-y Curves with Terzaghi's Subgrade Stiffness for Clays

it can be seen that the correlation is reasonable for a 1-inch deflection and an undrained shear strength of 1 ksf, which was the basis of the original Lam et al. (1991) correlations.

The nonlinear p-y curve is a form of discrete spring model to account for the stiffness of the soil mass. Matlock's and Reese's nonlinear p-y approach can be regarded as an extension of the widely used Terzaghi's linear subgrade modulus approach (1955). Terzaghi's linear subgrade modulus can be regarded as the soil stiffness corresponding to the secant stiffness at normal working load range. If the Matlock soft clay and Reese sand p-y criteria are used in load-deflection analysis for typical smaller-diameter piles to develop a nonlinear load-deflection curve, they typically give solutions comparable to results from Terzaghi's linear subgrade modulus at a 0.5 to 2-inch pile-head deflection. As a matter of fact, Reese's sand p-y criteria utilize Terzaghi's working load modulus scaled by a factor of 3 to form the initial tangent stiffness in the p-y curves. As a result, solutions from p-y curves and the more simple Terzaghi's linear modulus approach usually can be cross-correlated to a reasonable degree. Terzaghi's linear approach can often form the basis in the Step-1 dynamic response analysis, and then the nonlinear p-y approach can be used for the Step-2 pushover analysis (see Section 2.2) where results from the apparently different approaches generally give reasonably compatible solutions in the design process.

2.6.3 Sensitivity to Various Aspects of Soil-Pile Modeling Assumptions

The case of the 16-inch CIDH pile embedded in medium dense sand (internal friction angle of 35°) in the previously discussed example problem will be used for a series of sensitivity studies in this section to investigate the significance of a number of design issues, including:

- (1) Uncertainties in p-y curve stiffnesses,
- (2) Gapping effects,
- (3) Fixity of the pile-head,
- (4) Choice of bending stiffness parameter for the piles, and
- (5) Embedment effects.

In the foregoing example problems, a benchmark case is established so that subsequent sensitivity cases can be compared against it for cross-references. The following input parameters are established for the benchmark case:

- (1) Reese's static p-y curves for a submerged sand condition with an effective (buoyant) unit weight of 50 pcf, 35° frictional angle with the initial tangent p-y stiffness based on f_0 of 80 pci.
- (2) 16-inch CIDH pile with an effective (cracked) bending stiffness (EI) taken as half of the gross bending stiffness.
- (3) Fixed pile-head condition.

Solutions for the conducted sensitivity studies have been compiled in figure 2-22 for both the pile-head load-deflection and the pile moment-pile load relationships. The following can be observed in figure 2-22:

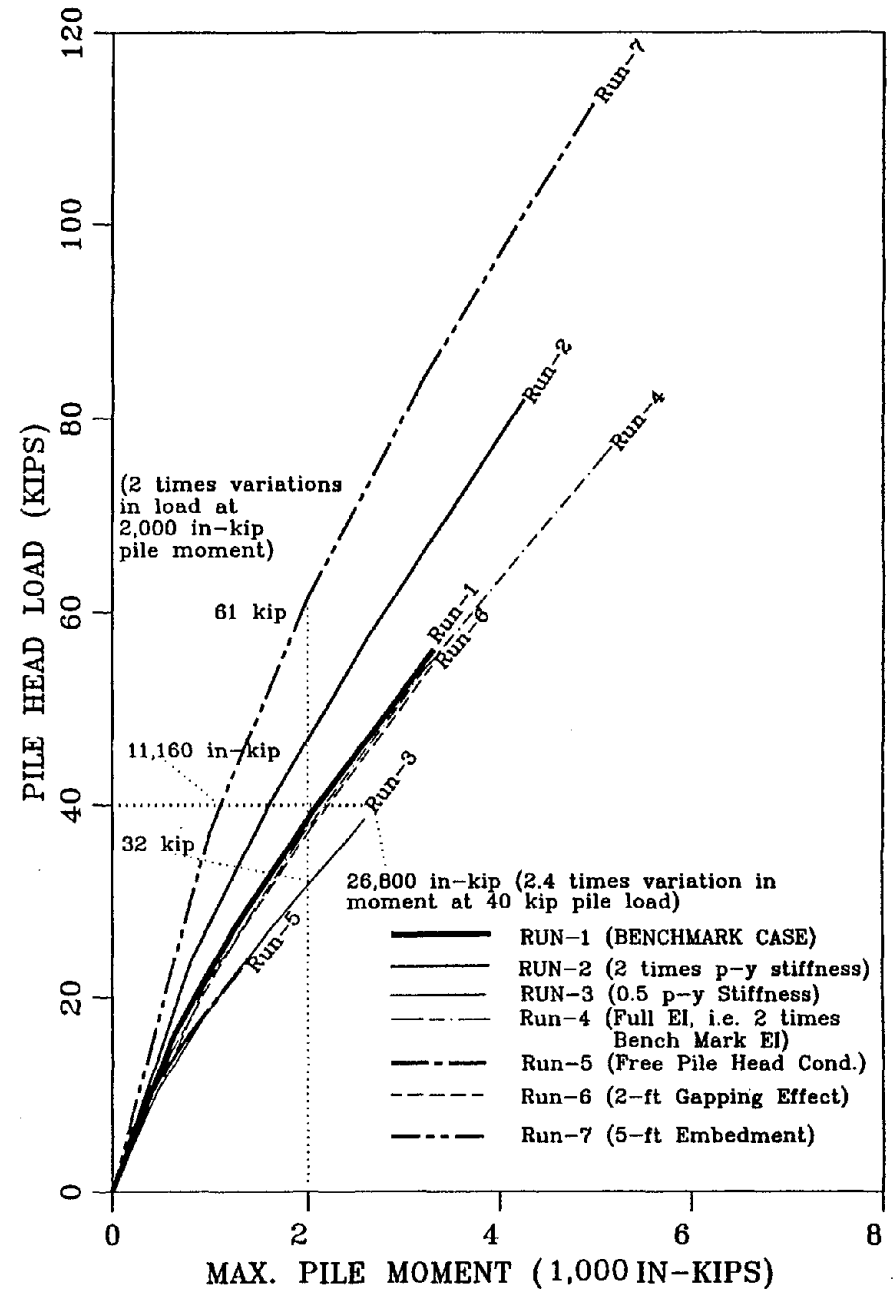
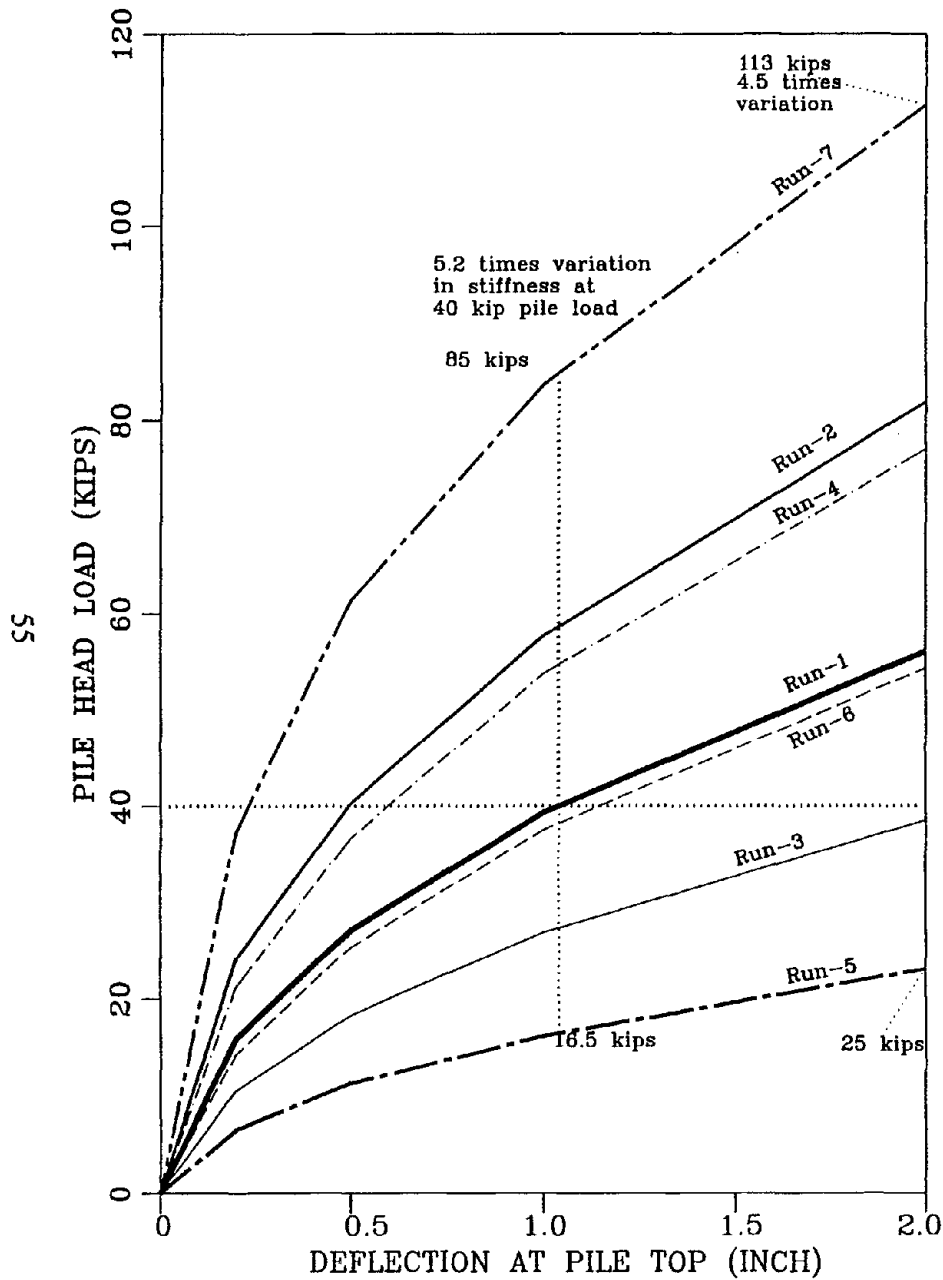


Figure 2-22 Sensitivity Study of Various Uncertainties in Pile Loading Analysis

- (1) There is a wide range in the load-deflection pile stiffness characteristics and load-moment relationships. For example, the pile-head load of the stiffest and softest pile differ by a factor up to over 5 times at a given displacement. The loads for the stiffest and softest piles differ by a factor of about 2 times at a given moment. The fact that the range of variation in load-moment characteristics is more narrow would be more evident if the 5-ft embedment case is excluded from the comparison, leading to a rather unique moment versus shear load relationship for a given pile group configuration.

From this observation, it can be concluded that uncertainties in foundation design largely relates to the foundation stiffness issue and their implication on the dynamic response characteristics of the overall bridge. Uncertainties in structural integrity issues (i.e., the maximum pile moment versus pile load) are relatively minor and are relatively insensitive to many sources of uncertainty. It should also be recognized that in many cases, the dynamic response characteristics of the overall bridge are relatively insensitive to the foundation stiffness (particularly the lateral stiffness in comparison to the rotational stiffness of the foundation) because a significant degree of the overall compliance will be from deformation of the bridge structure (e.g., the bridge column) itself. From our experience, the foundation stiffness issue would be more important for stiffer structures (e.g., the transverse response of pier walls) where the foundation compliance would constitute a significant proportion of the overall compliance. While there is tremendous attention (especially in the academic community) devoted to the pile response issue for lateral loading, the importance and the significance of these issues in the actual design problem might not be as great as it seems.

- (2) In terms of foundation stiffness, it can be observed that uncertainties in p-y curves are actually a rather insignificant problem compared to other sources of uncertainty, including the pile-head fixity, the choice of bending stiffness of the pile and particularly the embedment issue. All of the discussed issues appeared to be more or of equal importance as a two-fold variation in the overall pile-soil stiffness. In the example presented, the gapping effect appeared to be a relatively insignificant issue. However, this is largely because of the choice of a sand site and a relatively insignificant 2-ft gap in the sensitivity study. Gapping effects can be of major significance for clay soil conditions where more substantial gaps (such as over 20 ft) have been observed from past earthquakes.
- (3) Among the presented sensitivity studies, it appears that the effects of embedment could be significant and designers and researchers probably should put more emphasis on this topic.

2.6.4 Pile Group Effects for Typical Pile Footings

The pile group effect has been a popular research topic within the geotechnical community for almost 50 years. At present, there is no common consensus on the approach for group effects. Full-size and model tests by a number of authors show that in general, the lateral capacity of a pile in a pile group versus that of a single pile (termed "efficiency") is reduced as the pile spacing is reduced. Other important factors that affect the efficiency and lateral stiffness of the piles are the type and strength of soil, number of piles, and type and level of loading.

Table 2-1 p-Multipliers (Cycle-1 Loading) from Various Experiments at 3D Center-to-Center Spacing for 3x3 Pile Groups

Pile Test, Soil Description, Reference	p-multiplier on single-pile p-y curves		
	Front Row	Middle Row	Back Row
Free-Head, Medium Dense Sand, $D_r=50\%$ Brown et al. (1988)	0.8	0.4	0.3
Fixed-Head, Medium Dense Sand, $D_r = 55\%$ McVay Centrifuge (1995)	0.8	0.45	0.3
Fixed-Head, Medium Dense Sand, $D_r = 33\%$ McVay Centrifuge (1995)	0.65	0.45	0.35
Free-Head, Soft to Medium Clays and Silts Rollins et al. (1997)	0.6	0.38	0.43

2.6.4.1 Group Effects from Elastic Halfspace Theory

In earlier years, the analysis of group effects were based mostly on elastic halfspace theory due to the absence of costly full-scale pile experiments. These solutions have many shortcomings, including (1) they do not account for changes in the soils from pile installation, (2) they do not account for many aspects of soil-pile interaction phenomena (e.g., gapping effects) and (3) they are based on an elastic halfspace model which does not account for reinforcing effects of the piles within the soil mass, or soil compaction from pile driving. In earlier days (the 1970's), elastic halfspace theory has been used for group effects to soften the elastic stiffness (by introducing y-multipliers on p-y curves). However, as more full-scale pile load test data have become available, it was found that group effects have to be accounted for by introducing p-multipliers on the p-y curves (Brown et al., 1987, 1988, McVay et al., 1995, Rollins et al., 1997, Ruesta and Townsend, 1997).

2.6.4.2 Group Effects from Experimental Studies

In recent years, a number of major studies yielded some high-quality experimental data from either full-scale or centrifuge model pile-load tests (Brown et al., 1987; Brown et al., 1988; McVay et al., 1995; Rollins et al., 1997). These experiments yielded information that largely corroborated each other on the following aspects:

- (1) Most of these experiments first used the single pile data to verify the validity of the widely used Reese's and Matlock's benchmark p-y criteria and all concluded that the Reese and Matlock p-y criteria provide reasonable solutions.
- (2) The observed group effects appeared to be associated with shadowing effects and the various researchers found relatively consistent pile group behavior in that the leading piles would be

loaded more heavily than the trailing piles when all piles are loaded to the same deflection. It was concluded from all reported full-scale or centrifuge model test experiments that the observed group effects cannot be accounted for by merely softening the elastic stiffness of the p-y curves (i.e., using only y-multipliers on p-y curves as those developed from elastic halfspace theory). All referenced researchers recommended to modify the single pile p-y curves by adjusting the resistance value on the single pile p-y curves (i.e. p-multiplier). The p-multipliers were found to be dependent largely on the position of the pile in relation to the pile loading direction. Most of the experiments were conducted on 3x3 pile groups with the center-to-center pile spacing equal to about 3 pile diameters. Table 2-1 summarizes some of the back-calculated p-multiplier values from the individual researchers.

The experiments reported by McVay also included data for pile center-to-center spacing of 5D which showed p-multipliers of 1.0, 0.85 and 0.7 for the front, middle and back row piles, respectively. For such multipliers, the group stiffness efficiency would be about 95% and group effects would be practically negligible.

Rollins et al. (1997) studied group effects for fast rate dynamic loading using the Statnamic loading device, and also studied pile cap-pile interaction behavior. Rollins concluded from the fast rate loading Statnamic test data that "the effects of stress wave phenomena on the pile group are negligible with a large concentrated mass affixed to the top of the pile group." The authors interpret this statement to imply that at the relatively long periods (or wave lengths) which is important for the response of the overall structure, dynamic effects related to scattering of stress waves would be negligible because of the relatively small foundation dimensions. Rollins' pile cap experiment also collaborated nicely with the findings by Gadre and Dobry (Gadre, 1997). The ultimate passive pressure capacity of the pile cap corresponds to a passive earth pressure coefficient K_p of about 18.4, which compared favorably with passive pressure based on the log-spiral method. Again, the base friction from the pile group-pile cap system was found to be small compared to the passive pressure capacity acting on the pile cap (base friction was only about 25% of the passive pressure component of resistance).

To date, Rollins' pile group experiment probably represents the most comprehensive experimental study for clay soils for the rectangular pile group arrangement typical of highway bridges. For pile group effects in sands, the research team at University of Florida probably produced the most updated comprehensive pile group experiments. In addition to the comprehensive suite of centrifuge experiments reported by McVay et al. (1995), which included proper account for pile driving effects as it simulated pile driving in the centrifuge in flight, Ruesta and Townsend (1997) recently presented a full-scale pile group test for a loose sand condition for a 4x4 pile group using 30-inch square concrete piles with a fixed-head condition. This test set up probably represents the biggest size pile group tested to-date.

Figure 2-23 has been extracted from the Ruesta and Townsend's paper to illustrate the group effects in some detail. The figure shows that in addition to geometric effects, pile installation (as reflected by the pile installation sequence) also plays a significant role in affecting the resultant soil resistance. The piles for this experiment were jetted to 7.6 m (25 ft) penetration prior to impact driving, which

probably had a significant effect on the resulting measured pile resistance. From backfitting analyses, Ruesta and Townsend recommended p-multipliers of 0.8, 0.7, 0.3 and 0.3 for the row 1 (front) to the row 4 (trailing row) piles, respectively. They further recommended an overall p-multiplier of 0.55 for fitting the overall behavior of the pile group, which corresponds to a mere 20% reduction in pile-head stiffness efficiency.

Figure 2-24 presents some load-deflection analyses using a range of p-multipliers from the above discussed pile group effect experiments. Solutions are presented using the previous sensitivity analyses for the 16-inch CIDH fixed-head pile embedded in medium sand of 35° friction angle. The figure presents results for five load-deflection analyses:

- (1) A case for the standard static loading p-y curve to illustrate the behavior if one ignores pile group effects.
- (2) Cases for p-multipliers of 0.8, 0.4 and 0.3 to represent analyses including group effects for the front row, the center row and the back row piles, respectively, for the range of p-multipliers from the discussed group effect experiments.
- (3) In the load-deflection plot, a load-deflection curve from averaging the stiffnesses of three piles (the 0.8 p-multiplier case, representing the front row pile, plus two of the 0.3 p-multiplier solutions, representing the middle-row and trailing pile) to develop the resultant average pile stiffness in a 3x3 pile group stiffness.
- (4) An additional case for a p-multiplier of 0.5 which might represent the average adjustment factor to develop an average condition to fit the overall group effect. Such simplification would be needed in practical design for earthquake loading considering the cyclic earthquake loading conditions. The front row pile would become the rear row pile when loading is reversed. Therefore, for cyclic loading conditions, there is relatively little justification to maintain a different p-multiplier specific to the position of the pile. A uniform average multiplier would be adequate to incorporate pile group effects in design practice for typical pile group configurations. This case of 0.5 p-multiplier would have a resultant pile stiffness quite similar to the average pile stiffness discussed in item (3) above.

The solutions show that group effects (as depicted in the average load-deflection curve) represent a maximum of 50% reduction in the resultant pile-head stiffness (depending on the deflection or the load values of interest) when the static single-pile stiffness is used as the reference point. The significance of the portrayed group effect is further diminished in terms of the assessed pile stress as evident by the moment versus shear load characteristics. As shown in figure 2-24, for a specific pile load (say 40 kip per pile), there would only be about a 20 to 30% difference in maximum pile moment between the solution for p-multiplier of 1 (no group effect) and 0.5 (with group effect). This difference would even be further diminished in actual design because the kinematic constraint of the pile cap would enforce all the piles in the group to deflect to the same deflection amplitude. Hence, the stiffer front row pile would carry a higher proportion of pile load as compared to the trailing piles. However, the stiffer front row pile also mobilizes more soil resistance which would

TEST PILE GROUP 0.55

	0.4	0.3	0.3	N/A	
1	8	4	15	16	Row 4 t trailing 0.3
	0.5	0.2	0.2	N/A	
2	7	3	13	14	Row 3 t Middle Trailing 0.3
	0.6	0.7	0.8	N/A	
3	6	2	11	12	Row 2 t Middle Leading 0.7
	1.0	0.6	0.8	1.2	
4	5	1	9	10	Row 1 t Leading 0.8

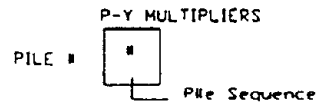


Figure 2-23 Results of 4x4 Pile Group Tests in Sand (Ruesta and Townsend, 1997)

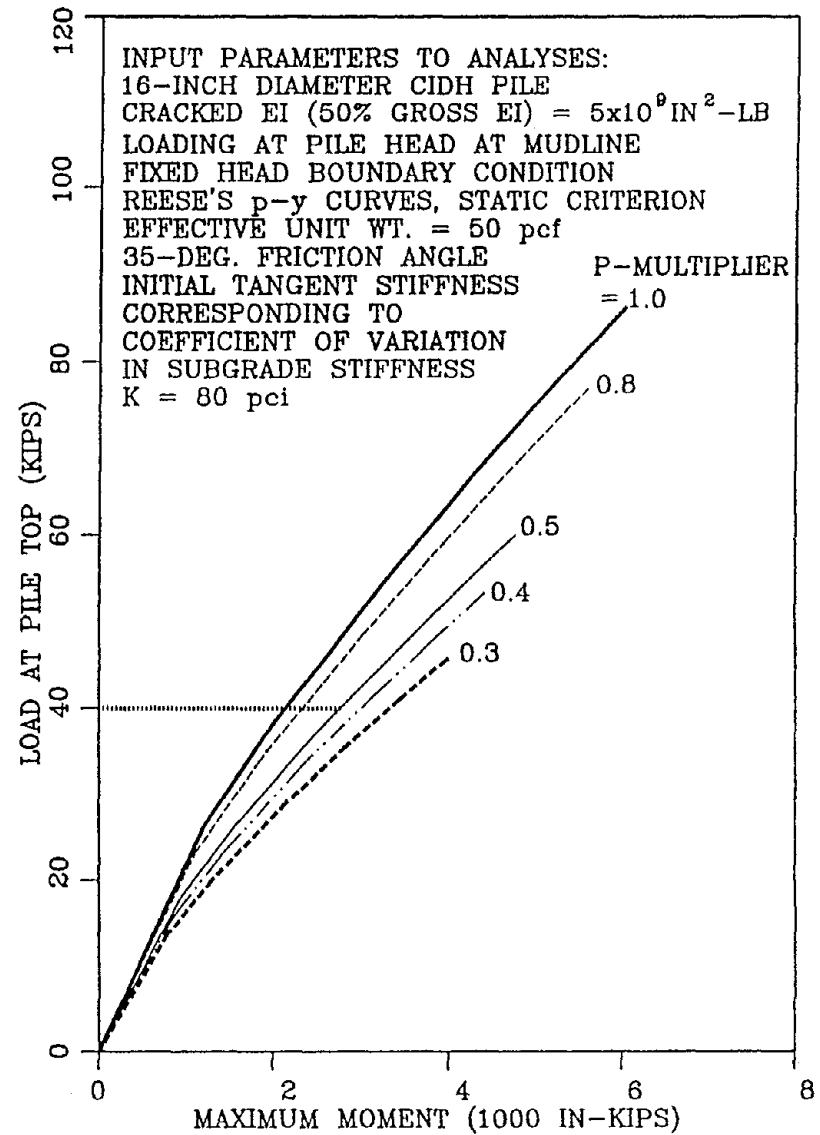
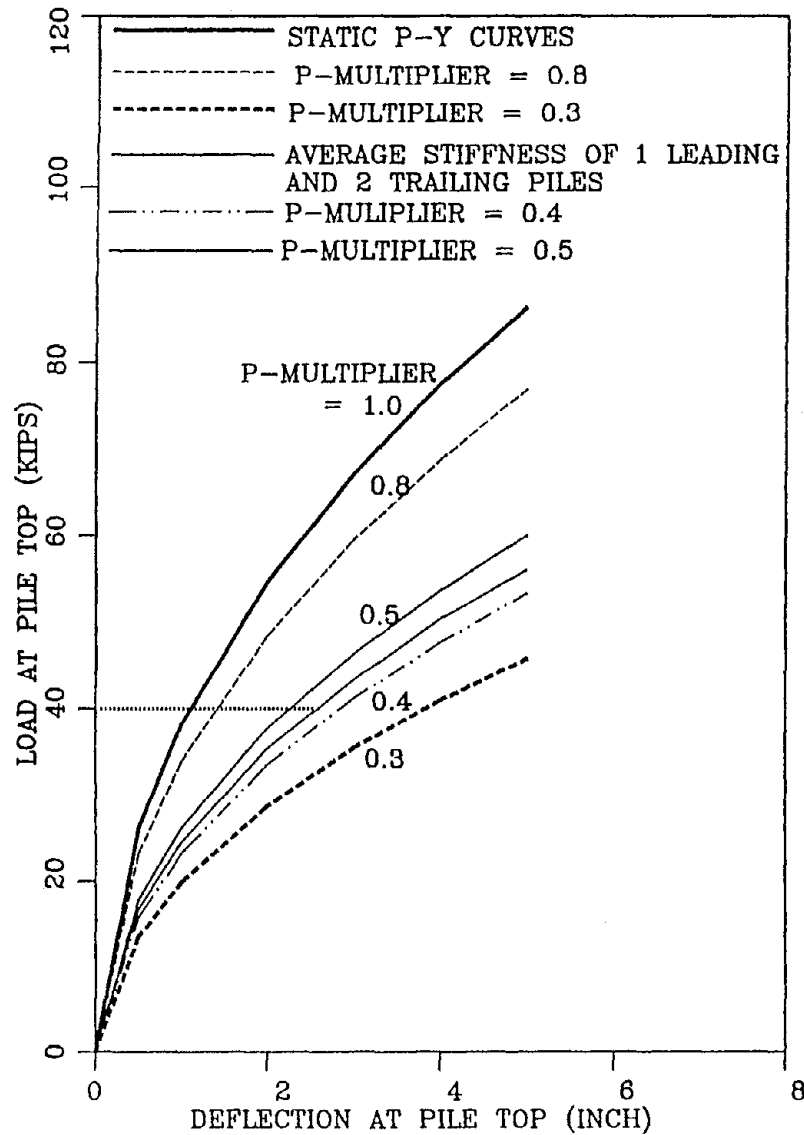


Figure 2-24 Pile Group Effects Reflected by p-y Curve on Pile Response

lower the pile moment. In effect, this kinematic constraint will lead to stiffer piles to compensate for the weaker piles and will result in a more uniform pile moment distribution among each of the piles. Most of the pile group tests also show that upon cyclic loading, the resultant load and moment distribution among individual piles tends to become more uniform as compared to the initial loading condition. In fact, many researchers have speculated or reported that the cyclic loading condition tends to result in a reduction in the so-called group effects.

While the available data suggests that the group effect would result in a systematic softer pile stiffness, it is the authors' experience that other effects (e.g., soil resistance of the pile cap, gapping effects and consideration of cyclic loading effects) also need to be properly accounted for. Some of these effects are as significant as the pile group effects. This suggestion should not be mistaken to infer that the authors advocate to use static loading p-y curves for design because the pile group effect is not deemed to be of overwhelming importance. The authors merely attempt to point out that the observed 50% softening of the pile-head stiffness is relatively small in relation to the overall uncertainties in the design problem. As shown in figure 2-22, other aspects in soil-pile interaction behavior can easily result in as much as a five-fold change in pile stiffness, which render the observed 50% effect relatively mild.

Other factors (including gapping and potential cyclic degradation) should also be considered in pile design for earthquake loading. Recently, some full-scale vibratory pile load tests have been reported by Lam and Cheang (1995) for submerged sands and by Crouse et al. (1993) for peat. These fast-rate vibratory cyclic loading data also suggest a softer pile stiffness. Along with the issue of group effect, there is some justification to implement a p-multiplier less than unity for pile design to account for a variety of considerations, among which the group effect is merely one of the many factors. For this reason, Lam and Cheang (1995) recommended a p-multiplier of 0.5 to be applied on the standard static loading p-y curves involving typical pile groups. For liquefied sites, even lower p-multipliers have been used to allow for a more drastic cyclic degradation effects (Lam and Law, 1994).

2.6.5 Group Effects for Extremely Large Pile Groups

The above discussed pile group effects are empirically determined from pile load tests for relatively small pile groups involving only 9 or 16 piles in the pile groups. Foundations for major water crossings often involves extremely large piers supported by several hundred piles, where the horizontal dimension of the footing can easily be the major dimension in contrast to most cases where the pile length is usually several times the size of the pile cap. The pile-soil system in these configuration resembles a reinforced soil mass. A full-scale experiment for such a huge pile group would be impossible and there is no recourse but to rely on numerical predictions for these problems. Lam and Law (1994) recently utilized the periodic boundary condition to solve for the pile response for an infinite repeating pile pattern. Figure 2-25 describes the periodic boundary condition methodology. Some of the results from such group effect solutions are shown in figure 2-26.

From such three-dimensional nonlinear finite element solutions (which also account for gapping effects), group effects in terms of resultant p-y curves for such huge size pile groups have been

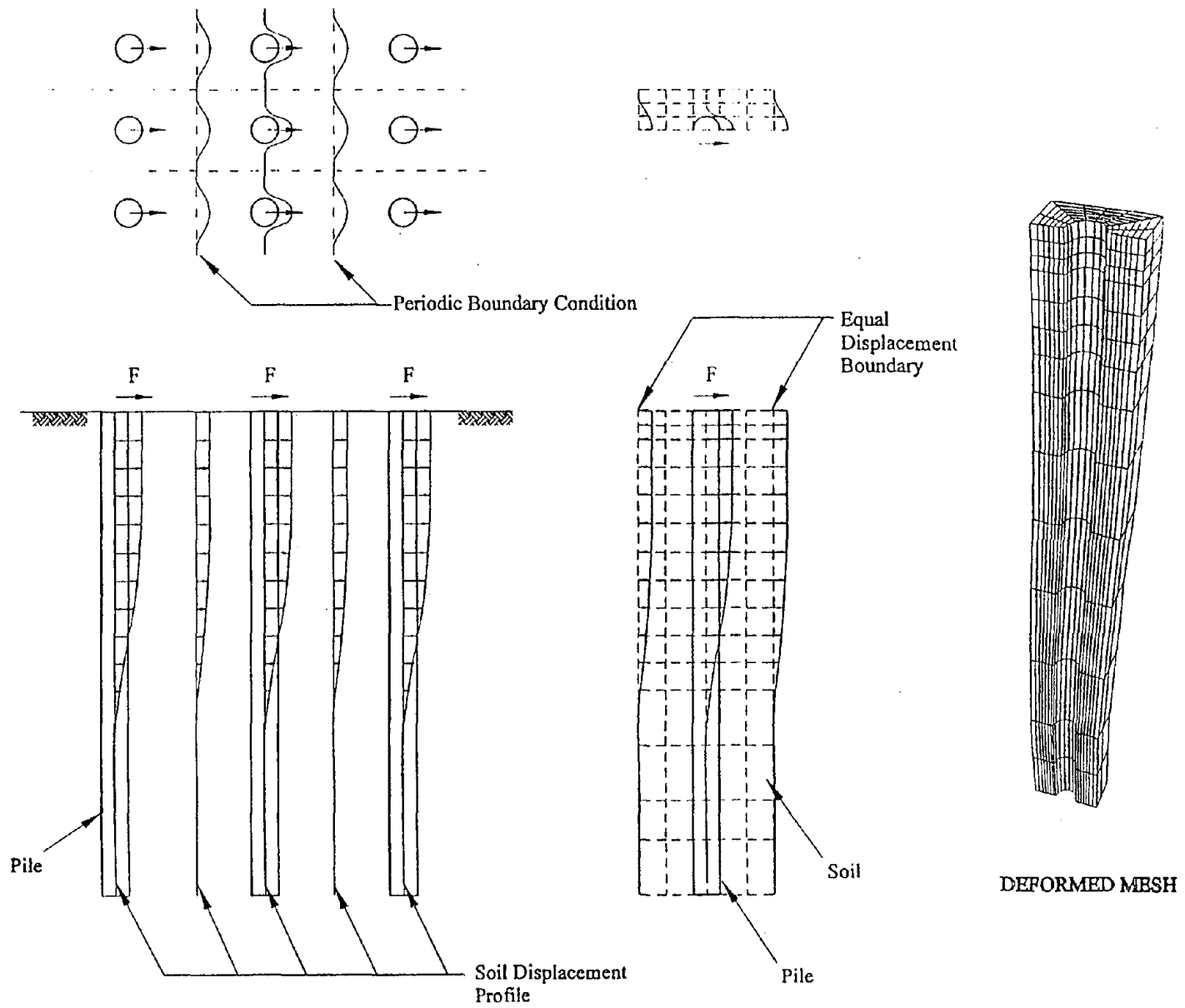


Figure 2-25 3-D FE Analysis using Periodic Boundary Condition for Infinite Pile Groups

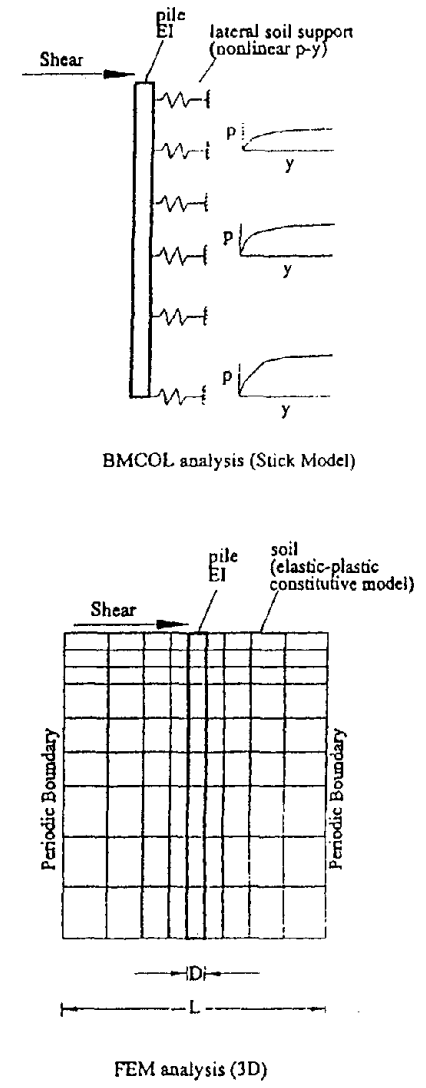
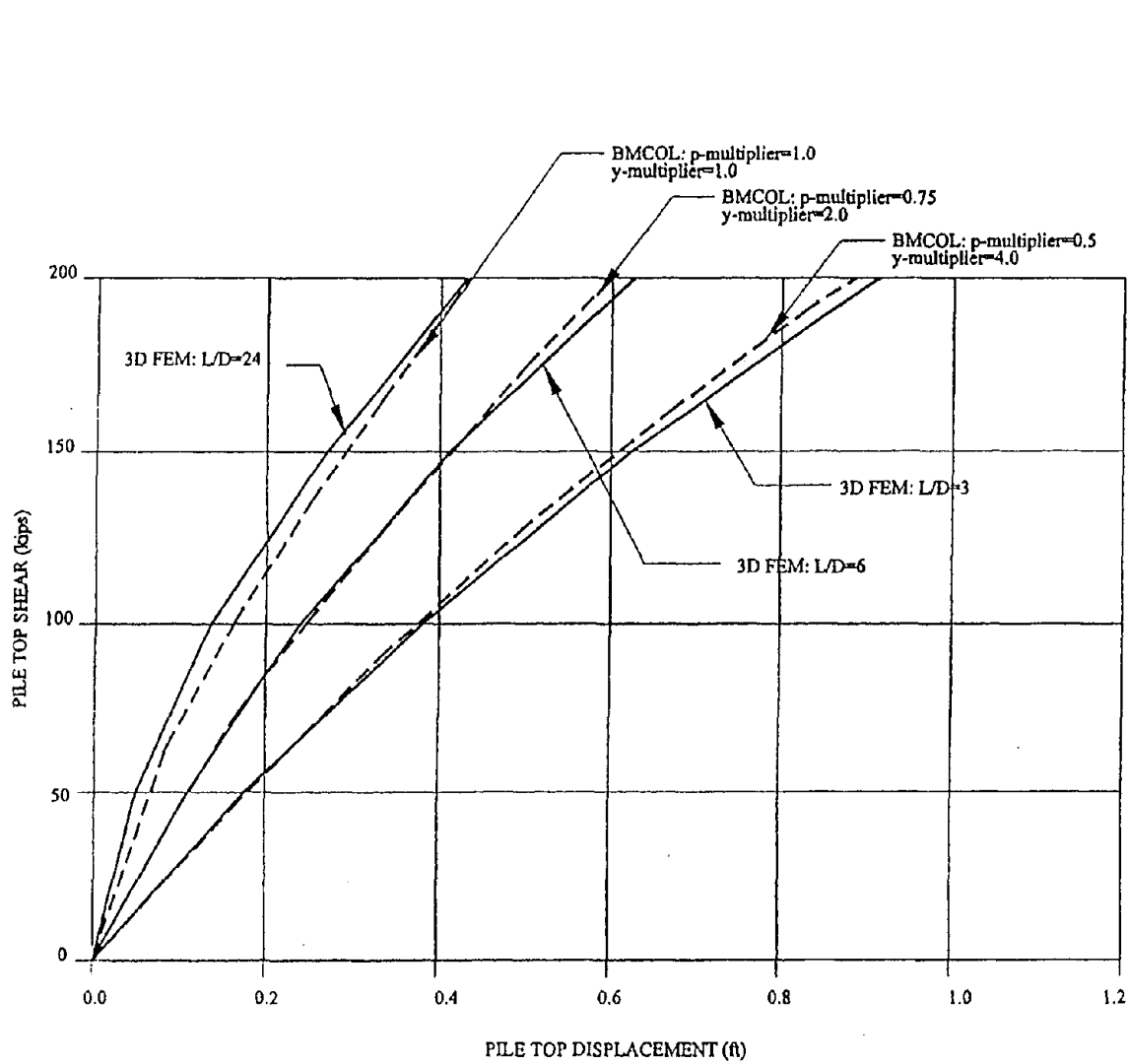


Figure 2-26 Results of Group Effects at 3 Spacings for Infinite Pile Group

studied. From the limited number of solutions, the authors found that for a pile center-to-center spacing of 3 diameters, it is necessary to soften the elastic branch of the p-y curves (by using a y-multiplier larger than unity) in conjunction with the 0.5 p-multiplier. For the 3-diameter center-to-center spacing, y-multiplier values up to 4 have been used in past projects.

2.6.6 Pile Design in Liquefiable Soils

Another major area of advances in the pile design problem from research programs funded by FHWA/NCEER is in the pile design for liquefiable soils. As discussed earlier, pile design in liquefiable soils involves consideration for two load cases: (1) the load case associated with structural loading (e.g., from inertial load induced by the earthquake), and (2) an additional load case arising from earth pressure loading on the embedded piles associated with the lateral ground spread problem. Figure 2-27 schematically illustrates the two loading mechanisms. These two load cases could occur simultaneously during the earthquake, and a rather complicated time-history analysis would be required to account for this problem involving modeling the overall bridge structure and foundation in a total solution analysis approach, coupled with solutions of the ground displacement (including permanent displacement) problem. However, such an analysis approach would be highly complex at the present time and would require teaming experts in the fields of structural engineering and soil-structure interaction. To avoid such complexity, it might be appropriate to uncouple the two load cases into separate analyses. Some comments are provided in the foregoing sections to address design issues for the two load cases.

2.6.6.1 Design for Structural Loading

The overall analytical procedure to support design for structural loading would essentially be the same as the previously discussed procedures. However, the choice of p-y characteristics or the linear subgrade modulus must properly consider liquefaction effects of the soil mass in the vicinity of the pile, with more emphasis given to the significant soil-pile interaction zone at shallow depths adjacent to the structure.

A number of studies have recently been conducted to study the p-y curve characteristics of liquefying soils. The liquefaction phenomena is related to the pore pressure build-up process and its effects on the fundamental stress-strain characteristics of the soil mass. There are two pore pressure generation mechanisms that need to be considered as discussed below.

Pore-Pressure From Local Soil-Pile Interaction

The piles would be loaded by the structure which would induce a stress field in the soil mass locally around the pile at the soil-pile interaction zone adjacent to the structure. Some full-scale vibratory pile load test data has been presented by Lam and Cheang (1995); they found that p-y response under fast-rate vibratory loading could result in a softer overall pile-soil stiffness as compared to the slow static monotonic loading (the basis of the static p-y curve). Hence, Lam and Cheang recommended that a p-multiplier less than unity should be applied to the static loading p-y curves of these soils to allow for the cyclic loading condition in earthquake design.

A similar observation has been made by Crouse et al. (1993) who presented similar vibratory pile load test data for a peat site. Various mechanisms, including a dynamic gapping phenomenon have been postulated by Crouse et al. to explain the softening of the pile stiffness under fast rate vibratory loading, as compared to the parallel slow cyclic loading tests. This softening effect, related to such a gapping phenomenon sustained by the faster vibratory rate, was rather drastic at the small deflection range (a p-multiplier as low as 0.2 was observed at less than 0.3 inch deflection). However, it is speculated that such a dynamic gap might not be sustained at the larger deflection level of design interest. Nevertheless, there is ample evidence from such vibratory loading test data to recommend a softer (as compared to the monotonic static pile load tests) pile stiffness for earthquake design. In conjunction with the pile group effect issue, a p-multiplier of 0.5 applied to the static p-y curve has been adopted for typical design applications.

Pore Pressure from Global Free-Field Site Response

The component of pore pressure response related to cyclic loading on the soil from free-field site response has been investigated by centrifuge model tests first conducted Dobry and others at the Rensselaer Polytechnic Institute. A similar major centrifuge model test program is also currently under way at the University of California at Davis. These experiments were conducted (1) to evaluate the p-y characteristics of soil liquefied because of a global pore-pressure mechanism, and (2) to understand the loading mechanism on the pile from lateral spread of liquefied soils (see figure 6-27b).

Figure 2-28 presents a plot obtained from centrifuge experiments to measure p-y curve characteristics of liquefied soils (Liu and Dobry, 1995). A varying degree of pore pressure is first induced in the saturated sand by subjecting the soil to a free-field shaking loading condition, and then a cyclic pile load test is immediately conducted prior to dissipation of pore pressure to measure the p-y curves for the liquefied sand. These curves are then compared to the nonliquefied p-y curves to develop the scaling factor (degradation coefficient in figure 2-28) for static p-y curves for sands at different pore pressure conditions. In a design problem, upon determination of the pore pressure associated with free-field site response analysis, the figure can be used to estimate the scaling factor to be applied to the initial undegraded p-y curves to develop the p-y curves for the liquefied soils.

It can be seen from figure 2-28 that for a complete liquefied soil condition, the residual p-y curve would be about 0.1 of the initial static p-y curves. This figure illustrates the state of the soil condition after free-field liquefaction at the first cycle of pile loading, and hence degradation from local soil-pile cyclic loading has not been accounted for. As discussed earlier, in addition to the global free-field degradation effect, cyclic loading on the pile from the structure would induce another component of degradation to the soil mass locally around the pile. As discussed earlier, a p-multiplier of 0.5 is recommended to account for such local soil-pile interaction effects. As can be seen in figure 2-28, a degradation coefficient of 0.5 corresponds to about 70% free-field pore pressure. It can be concluded that for denser soils which would have a free-field pore pressure below 70% of the effective overburden, degradation on the p-y curve would be controlled by the local soil-pile interaction mechanism, and the default 0.5 p-multiplier on the p-y curve would apply. At higher pore pressure ratios (above 70% of initial effective overburden) corresponding to almost initial liquefaction, degradation effects will be controlled by free-field pore pressure phenomena and

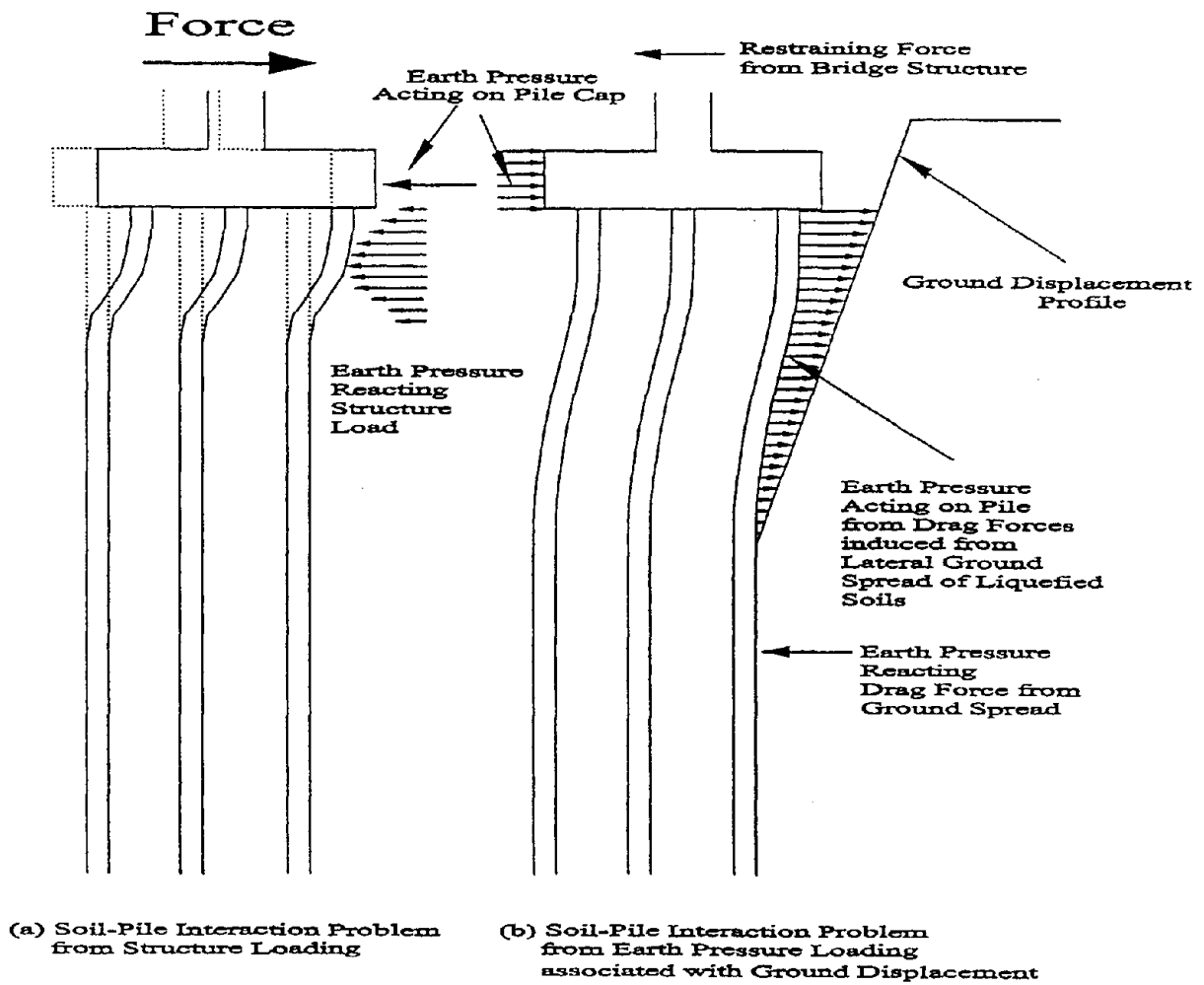


Figure 2-27 Loading Mechanism in Soil-Pile Interaction Problem

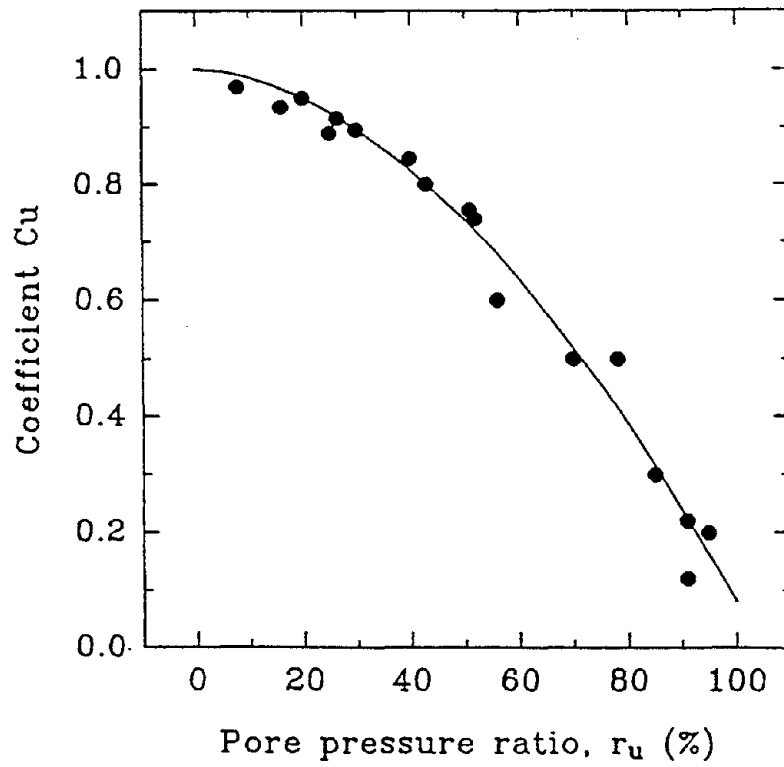


Figure 2-28 Degradation Coefficient C_u versus Pore-Pressure Ratio from Liu and Dobry

the degradation coefficient versus pore pressure ratio shown in figure 2-28 can be used to develop the p-multiplier for pile design.

The centrifuge experiment discussed above was conducted on loose, clean Nevada sand with relative density D_r of 40%. A residual p-y strength of 0.1 can be deemed appropriate for a loose, clean sand soil condition. For other denser sand, or sand with cohesive fines and silts, the residual p-y strength could be higher than 0.1. Some evidence of a higher residual strength of liquefied soil has been observed in parallel centrifuge experiments from the University of California at Davis. P-multipliers for liquefied soil as high as 0.25 have been reported.

Deep Liquefied p-y Curves

So far, Reese p-y curve criteria for sand have been the basis for the benchmark p-y curves. However, Reese p-y curve criteria arose from empirical pile load tests which only yield soil-pile interaction data at very shallow depths (the upper five pile diameters), and the formulation of p-y curves at deeper depths are largely founded on theoretical grounds. P-y stiffness and strength for sands are assumed to be directly proportional to the effective overburden pressure, and hence increase linearly with depth in saturated soil. Lam and Cheang's (1995) observation of deeper p-y curves suggested that such theory might overpredict the p-y curve stiffness at depth.

A similar observation has been made by Chaudhuri (1998) who suggested that soil-pile interaction is a largely undrained loading process and one needs to appreciate the stress-strain characteristics in the undrained loading condition. He utilized a critical-state soil mechanics constitutive model to investigate undrained behavior of sands and concluded that the Reese sand p-y criteria might lead to very stiff p-y curves at depth. This aspect led to some problem on the criteria of residual degraded strength at 0.1 of the static p-y curve at large depths, which would influence the results of soil-pile interaction analysis associated with lateral ground spread problems, where the soil-pile interaction zone could become much more deep-seated than the structural loading problem. To circumvent this problem, following adjustments on liquefied p-y curves are suggested.

In addition to the 0.1 initial p-y criteria, Dobry and his colleagues (Abdoun, 1997) have attempted to backfit typical undrained shear strength values of liquefied soils from the measured drag applied on piles by lateral spreading centrifuge tests. They found that a liquefied loose sand typically has an undrained shear strength of 21 psf. The ultimate passive pressure on the pile (i.e. p_{ult}) has been found to increase from $3cD$ at mudline to $9cD$ at depth (Matlock, 1970). Therefore, p_{ult} value corresponding to an undrained shear strength of 21 psf could vary from 63 psf to 189 psf.

A brief summary of the discussion on treatment of p-y curves for liquefied sands is provided herein:

- (1) A p-multiplier of 0.5 can be set for unliquefied p-y curves to reflect degradation from local soil-pile interaction or softening due to pile group effects.
- (2) Free-field site response analyses should then be conducted to evaluate the free-field pore pressure amplitude and possibly to conclude whether the site has lateral spread or slope instability potential and to solve for the mode and the magnitude of ground deformation.

- (3) For a free-field pore pressure higher than 70%, the degradation coefficient shown in figure 2-28 can be used to establish the p-y curve characteristics of the liquefied (or virtually liquefied) soils.
- (4) The resultant p_{ult} can be checked against the value of $9cD$, where c is the undrained shear strength postulated for liquefied soils equal to 21 psf and D is the pile diameter. If the p_{ult} from Step (3) is higher than this limiting value, the limiting value should be used to develop the p-y curves for the liquefied soil instead.

The above described p-y curve procedures can be used to conduct soil-pile interaction analyses for design against the structural loading conditions in a conventional load-deformation analysis framework. However, it is stressed that the above given residual shear strength was measured from only one experiment, and caution should be exercised in using this value. Residual shear strengths of liquefied sand depend on factors such as void ratio and grain size characteristics. A wide range of values has been backcalculated from case studies (e.g., Seed and Harder, 1991).

The use of the discussed p-y curves in pile integrity analysis associated with the lateral ground spread problem requires some additional considerations as discussed below.

2.6.6.2 Design Issues Related to Lateral Ground Spread

As discussed above, a major liquefaction design issue is related to design for the lateral ground spread problem. When this load case is uncoupled with the dynamic response of the superstructure, the design for this load case involves the following elements for consideration:

- (1) Analysis to predict the mode and amplitude of potential ground spread displacement. A number of research studies is actively underway on this subject. Dobry's centrifuge experiment shows two typical generic modes of ground displacement profiles as shown in figure 2-29. Figure 2-29a represents a two-layer soil profile of liquefied soil above the underlying unliquefied soil. Figure 2-29b presents a three-layer profile of a liquefied soil layer in between unliquefied soils. The upper unliquefied layer might represent a stiffer upper layer or very often represents a soil layer above the ground water table, which therefore is not liquefiable. Recent studies conducted at RPI and Cornell University arrived at the following conclusion; the maximum pile moment is usually at the bottom of the liquefied soil layer, where an abrupt change in the slope of relative ground displacement would occur.

Most current lateral ground spread procedures concentrate on predicting the basic case of free-field ground displacement without considering of the reinforcing effects of the constructed structure. It is found that in some cases, such as the configuration in figure 2-29b, the reinforcing effect of the piles would lead to a significant reduction in the amplitude of permanent ground displacement. Figure 2-29b shows that if the liquefied layer is relatively thin, the pile would act as a fixed-fixed beam and additional stiffness from the pinning effect of the pile would add on the residual shear strength of the liquefied soil layer.

This additional shear strength from pile pinning effect can often be as much or more than the in-situ shear strength of the weak soil layer, and hence its effect must be accounted for in the assessment of the amplitude of ground displacements.

- (2) Soil-pile load-deformation analysis. This analysis can be conducted by establishing the proper pile soil model (i.e., choice of proper pile EI and p-y springs including simulating the proper p-y effect for liquefied soils) and the ground displacement pattern from the analysis in item (1) can be used to prescribe offsets on the p-y curves, and the pile can be allowed to deform to conform with the kinematic effect of the prescribed ground displacement. The resultant solution would yield a deformation pattern and shear and bending moments on the pile which can be used to evaluate the survivability of the pile for the postulated ground movement. Some comments on some aspects of p-y curve in the context of the described analyses are discussed below.

Pile Survivability for the Two-Layer Soil Configuration

For the configuration shown in figure 2-29a, the ultimate pressure capacity of liquefied soils discussed above can be used as input to the kinematic pseudostatic soil-pile interaction in lateral spreading analyses. However, it is cautioned that the resultant pile moment should only be regarded as the lower-bound pile moment because in the case of kinematic soil-pile-interaction analysis, a softer p-y curve actually can lead to unconservative assessment of pile moment for a specified ground displacement. The above discussed p-y curves for liquefied soils (i.e., 0.1 static p-y curves and residual undrained shear strength of 21 psf) represents the minimum residual strength only. As the soil transforms from the stronger unliquefied state to the ultimately liquefied state, there is a transition of stiffer soil to softer soil and at some intermediate stage, the pile can experience moments higher than the ultimate steady state condition. Figure 2-30 was extracted from Dobry's work to illustrate this aspect using fully degraded p-y curves. As shown in the figure, the pile moment is higher at a smaller amplitude of permanent ground displacement (at a time of about 17 sec) than in the ultimate condition (at time of about 32 sec).

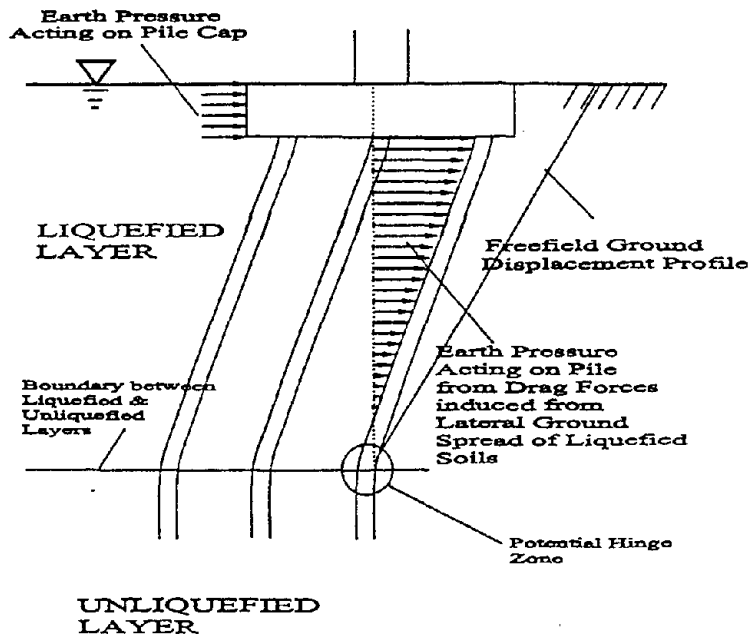
Chaudhuri (1998) utilized critical state soil mechanics theory to predict the transition of the state of p-y curves and simulated the described behavior. However, the procedure utilized in the study involved rather sophisticated constitutive modeling and corresponding soil sampling and testing programs to develop the required soil parameters and would be too complex for practical design. It may be possible, at the current state-of-understanding to conduct the kinematic soil-pile interaction analyses to determine the pile moment at the steady state residual soil strength condition. An additional kinematic soil-pile interaction analysis can be conducted using initial static p-y curves (i.e., the stiffest p-y curve scenario). The two bounding solutions can be used to set the upper and lower-bound pile moment to facilitate the application of engineering judgement in design decision process.

Pile Survivability for the Three-Layer Soil Configuration

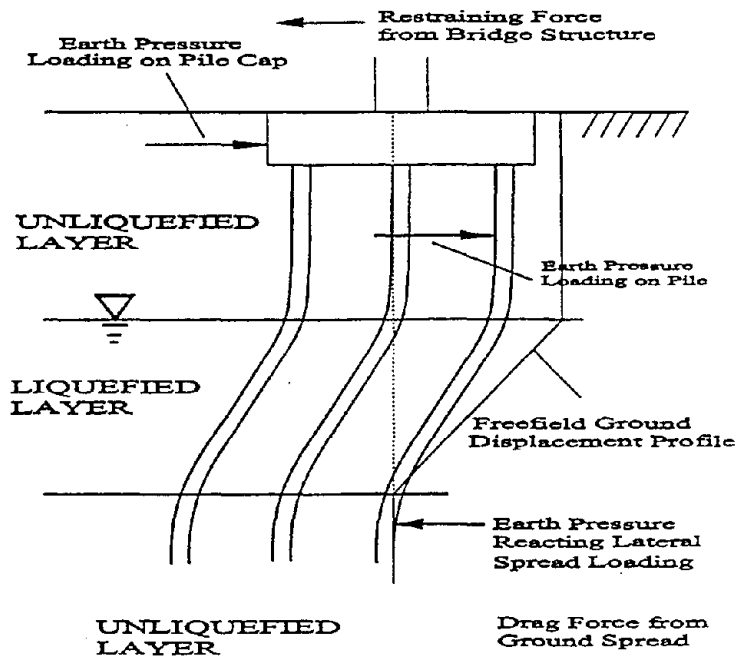
For the configuration shown in figure 2-29b, the kinematic soil-pile interaction analysis involves formulating the appropriate p-y curves for the upper crust of unliquefied soil layer. In most cases, the large cross-sectional area of the pile cap would account for most of the dragged forces constituting the loading mechanism on the underlying piles. The procedure to develop the passive pressure capacity acting on the pile cap discussed in Section 2.5 can provide the upper-bound drag force on the underlying foundation system. This is an upper bound loading scenario because the soil capacity of the upper crust could be eroded as it sits on liquefied soils.

Berrill et al. (1997) reported an actual case history of physically observed lateral ground spread against a pier footing and concluded from backfitting that the passive earth pressure in the upper crust would be approximately equal to that predicted by the Rankine earth pressure theory (a passive pressure coefficient (K_p) of about 1 for the reported soil friction angle of 44° and cohesion of 200 psf). This back-calculated passive pressure capacity is very low compared to the log-spiral passive pressure theory discussed in Section 2.5 (the ratio of Rankine's earth pressure capacity to the log-spiral capacity would be less than 0.1). This case history may suggest an adjustment factor of as small as 0.1 which can be applied to the log-spiral earth pressure capacity (i.e., the original static passive pressure capacity of the pile cap prior to liquefaction). For the kinematic soil-pile interaction shown in figure 2-29b, Berrill also reported that the buttressing effect of the bridge deck which opposes the drag force acting on the pile cap also provided some measure of resistance to oppose the lateral spread loading condition imposed on the pile cap.

Among the two lateral spread configurations shown in figure 2-29a and 2-29b, it appears that the condition shown in figure 2-29a actually might be rather benign because the liquefied soils tends to merely flow around the foundation system, and the dragged force on the foundation system could be rather small. The configuration shown in figure 2-29b could be more hazardous and has been the cause of pile damage or even collapse of bridge structures since this configuration has resulted in very high curvature in the pile. However, the high pile stresses also often lead to significant reinforcing effects of the pile which could significantly reduce the amplitude of ground displacement. It is felt that this latter configuration involves more complex soil-pile interaction issues that are more germane for design consideration and more effort is needed to fine-tune the design problem related to this three-layer lateral spread and soil-pile interaction problem.



(b) Lateral Spread Loading Problem for Liquefied Layer above Unliquefied Layer



(b) Lateral Spread Loading Problem for Unliquefied Layer above Liquefied Layer

Figure 2-29 Two Generic Soil Conditions for Lateral Spread Pile Loading Problem

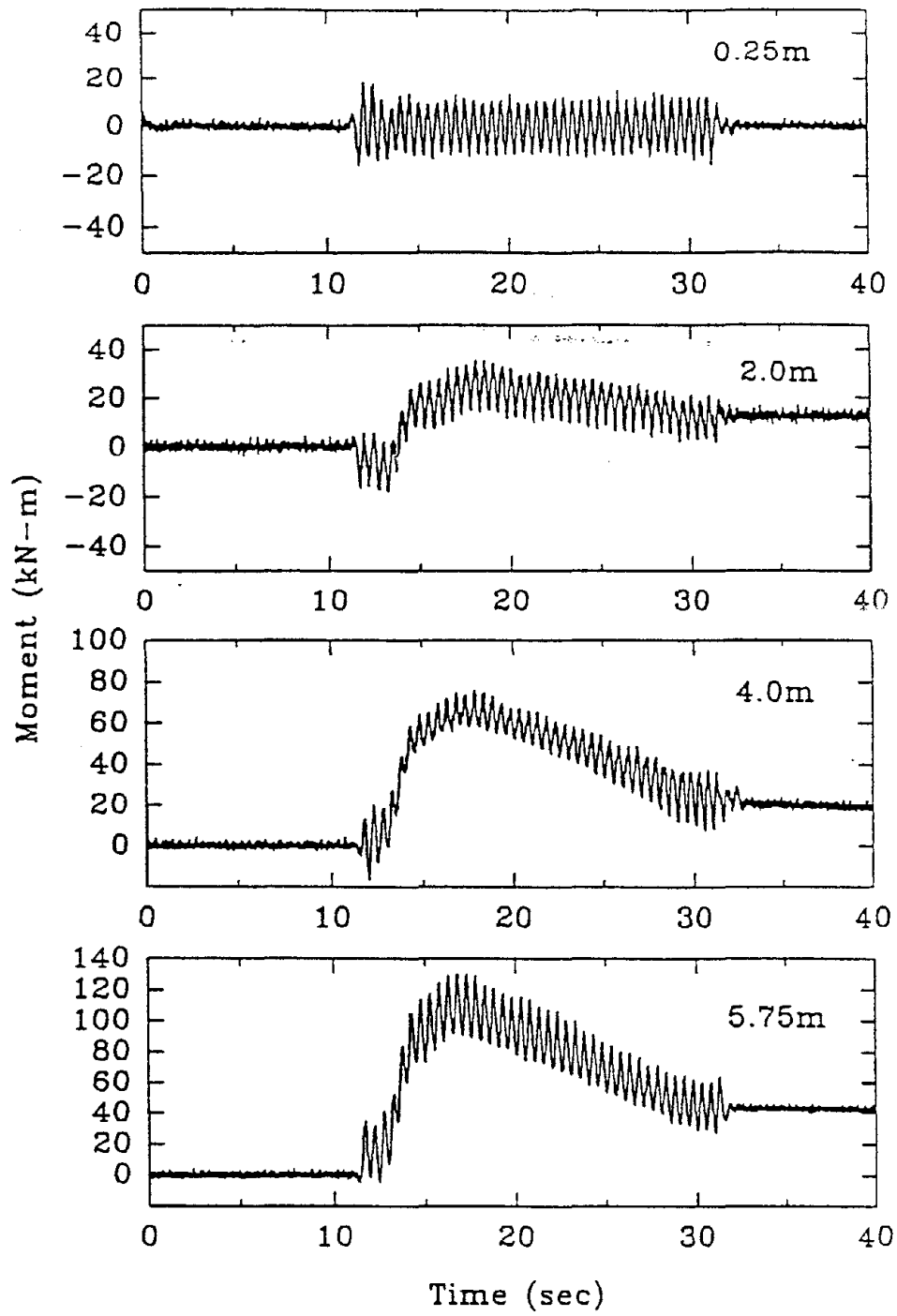


Figure 2-30 Bending Moment from Centrifuge Lateral Spread Loading Experiment

SECTION 3 MODELING OF DRILLED SHAFTS

3.1 Introduction

Drilled shafts are large diameter piles that are used to support high axial loads and overturning moments. They are constructed by drilling/auguring a hole in the ground which may be lined to support the sides of the excavation. Upon completion of drilling, a reinforcement cage is placed and the cavity is filled with concrete. Because of their relatively disturbance-free installation procedure and high load carrying capacity, drilled shafts are often advantageous over conventional small diameter piles. Increased use of this type of foundation can be found for supporting different types of structures such as bridges, transmission towers, and telephone poles. In this section of the report, discussion is focused mainly on seismic design aspects of drilled shaft foundations for bridge structures subjected to lateral loading.

The analysis and design of drilled shafts for the most part are similar to those of conventional-driven piles. Important differences, however, exist due to installation procedure, larger diameter, and small length to diameter ratio compared to typical smaller driven piles. One major difference is that because of these factors, drilled shaft analysis requires some additional considerations, which are later discussed in this section. Also, for bridge structures, the structural arrangement of drilled shaft foundations can be different from conventional structural arrangement. As mentioned before, most bridges on drilled shafts are pile extension type structures (Figure 1-1b). The lateral loads that act on the bridge deck are reacted by the induced shear and bending moment on the drilled shafts. The overall bridge response is relatively insensitive to axial pile response in contrast to pile footings discussed in Section 2.

In developing seismic design guidelines for drilled shaft foundations as well as other types of foundations, various issues related to modeling of actual foundation behavior should be investigated. The effect of modeling assumptions on the design displacement and force demand on the foundation should be evaluated and the limitations should be identified. As mentioned earlier, the most widely used method to analyze pile response under lateral load is by using a p-y model in which soil is replaced by a series of nonlinear springs. A p-y model simply describes the force-displacement relationship of a soil spring, in which p is the soil reaction force per unit length, and y is the corresponding pile displacement. A number of p-y models have been proposed for different soil conditions. The two most commonly used p-y models are those proposed by Matlock (1970) for soft clay and by Reese et al. (1974) for sand. P-y curves for other soil conditions, e.g., stiff clay, rock, can also be found in the literature (e.g., Reese, 1986). The p-y models are essentially semi-empirical and have been developed on the basis of a limited number of full-scale lateral load tests on piles of smaller diameter, ranging from 0.3m to 0.6m (12 to 24 in). To extrapolate p-y criteria to conditions that are different from the one from which these models were developed, requires some judgement and consideration. In fact, several studies (Davidson, 1982; Lam and Martin, 1986) indicated that the p-y models, which were developed from load tests on small diameter piles, might underestimate the soil stiffness for larger diameter drilled shafts. The reasons for such variations are discussed, and a more rational method of estimating drilled shaft stiffness is proposed.

3.2 Seismic Design Procedure for Drilled Shafts

Unlike static loading, dynamic loads on a structure cannot be specified independent of the foundation because they are functions of the foundation stiffness characteristics as well as the structural dynamics properties. It is important to recognize that foundations, being a part of the structural system, influence and modify the overall dynamic response characteristics of the structure. Therefore, a realistic estimation of foundation stiffness and integrating it in the structural analysis is very important. In general, the foundation-soil system responds nonlinearly to the applied load. However, for practical purposes, the foundation is commonly represented as an equivalent linear system which is then incorporated in the analytical model. Structural designers and geotechnical engineers should be aware of the modeling procedure of the foundation system and the inherent limitations posed by the simplifying assumptions.

Seismic design of bridge structures and foundations involves a *two step* procedure. In the *first step*, the geotechnical engineer estimates the soil-foundation stiffness based on the available information on soil properties (e.g., drilling record, in-situ or laboratory test data) and the type of foundation system. The foundation stiffness is then incorporated in the structural model by the structural engineer, who performs a structural analysis (e.g., modal analysis, time-history analysis) to estimate load and displacement demands on the foundation arising from the seismic ground motion. Because the actual foundation is replaced by an equivalent linear model, this first step of analysis might not yield any meaningful information regarding the force and moment distribution in the foundation system, especially at high seismic loads where overshoot of force above the foundation capacity is expected. It should be noted that any overshoot of force above capacity of the system is due largely to the linear assumption in the analytical model. If a nonlinear load-deflection curve is used in an iterative nonlinear response analysis, the predicted load will be compatible to the input load-deflection curve and the overshoot above the assumed capacity will be negligible. Therefore, the only way to evaluate the integrity of the system would be to base it on the computed displacement demand. A second analytical step is needed to calculate the force demand in the system (including foundation forces) realistically.

In the *second step*, the overall foundation system with the surrounding soil is modeled including structural nonlinearity to conduct a quasi-dynamic push over analysis of the bridge system to determine the displacement level where structural yielding is initiated (i.e. to determine yield displacement) and how the load is distributed to structural elements at various load levels (including the design earthquake load level). On the basis of the analyses, foundation capacity (usually based on the displacement level where there is no compromise on the vertical load capacity of the drilled shafts) is evaluated and compared to the displacement demand for the design earthquake for adequacy in structural integrity for earthquake performance. Each step is described and some of the important issues involved in each step are discussed in the following subsections.

3.2.1 Step 1 : Modeling of Foundation Stiffness

According to the current state of practice, the response of drilled shaft foundations to externally applied lateral load and moments are analyzed by idealizing the soil as a series of linear or nonlinear

springs. The force-displacement characteristics of the springs are defined by p-y relationships, and various procedures for developing p-y curves have been proposed by several authors. The most commonly used p-y formulations in practice are the ones based on procedures suggested by Reese et al. (1974) for sand and Matlock (1970) for clay. Another popular method is the one recommended by the American Petroleum Institute (API), which is essentially developed from the above-mentioned methods. Although p-y relationships are semi-empirical in nature, they are found to provide reasonably good prediction of pile response. Another commonly used practice is to adopt a linear approach, and to characterize the subgrade based on the recommended values of coefficient of subgrade modulus by Terzaghi (1955). Lam et al. (1991) indicated that solutions based on linear subgrade modulus theory can adequately represent pile stiffness. They presented design charts to estimate pile head stiffness for piles embedded in a subgrade with linearly increasing modulus. The subgrade modulus, E_s , at a depth z is given as in eq. (2-3) and repeated herein for convenience,

$$E_s = fZ \quad (3-1)$$

in which f is the coefficient of variation in subgrade modulus with depth. Under elastic conditions, subgrade modulus can be related to the Young's modulus of soil. Based on closed form solution of infinitely long beam on an elastic foundation, Vesic(1961) showed that, when subgrade modulus is constant (i.e., constant with depth), it can be related to soil Young's modulus (E_{soil}) as

$$E_s = 0.65 \sqrt[12]{\frac{E_{soil} D^4}{EI} \frac{E_{soil}}{1-\nu^2}} \quad (3-2)$$

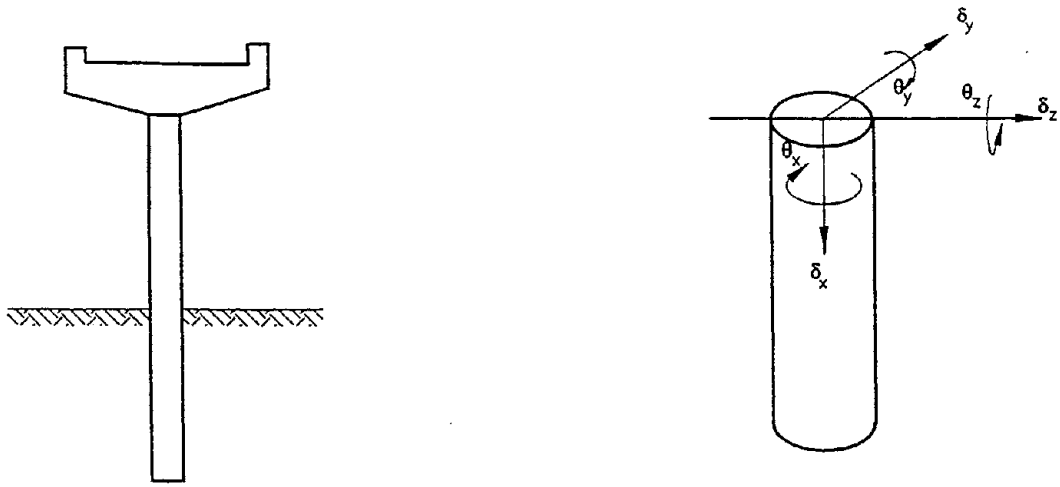
where D is the width of the beam, E is the Young's modulus of pile, I is the moment of inertia of beam, and ν is the Poisson's ratio of soil. It must be noted here that eq. (2-6) is an approximate form of eq. (3-2).

As an alternative to subgrade modulus or p-y approach, some researchers (e.g., Poulos and Davis, 1980) developed solutions by idealizing the soil as an elastic continuum. A comprehensive summary on this particular approach is presented by Pender (1993).

Once the pile response is estimated by one of these methods, pile stiffness can be represented in several ways. Three common methods are 1) coupled foundation stiffness matrix, 2) equivalent cantilever model, and 3) uncoupled base spring model. A brief description of these methods are presented here. For more detailed discussion the reader is referred to the work by Lam and Martin (1986).

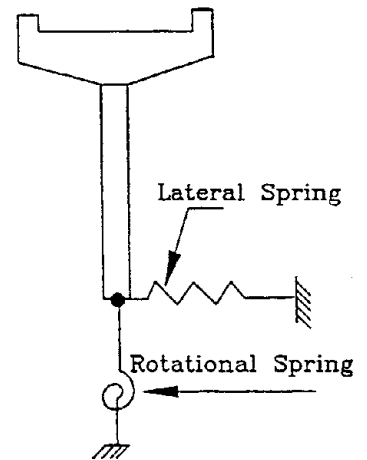
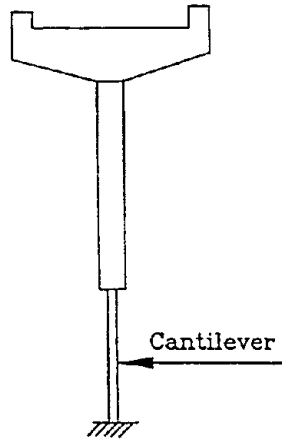
3.2.1.1 Coupled Foundation Stiffness Matrix

Among the three methods mentioned above, the most general method to represent the foundation stiffness is by the coupled foundation stiffness matrix . In this method, the stiffness of a single pile is represented by a 6 x 6 matrix representing stiffnesses associated with all six degrees of freedom at the pile head as illustrated in figure 3-1. The common form of the stiffness matrix in the local pile coordinate system is given in eq. (3-3),



(a) Drilled Shaft and Bridge Superstructure with Local Pile Coordinate System

$$K_{pile} = \begin{pmatrix} K_x & 0 & 0 & 0 & 0 & 0 \\ & K_y & 0 & 0 & 0 & K_{y\theta_z} \\ & & K_z & 0 & -K_{z\theta_y} & 0 \\ & & & K_{\theta_x} & 0 & 0 \\ & & & & K_{\theta_y} & 0 \\ & & & & & K_{\theta_z} \end{pmatrix}$$



(b) Stiffness Matrix

(c) Equivalent Cantilever

(d) Uncoupled Springs

Figure 3-1 Pile Head Stiffness Representation

$$K_{pile} = \begin{bmatrix} K_x & 0 & 0 & 0 & 0 & 0 \\ & K_y & 0 & 0 & 0 & K_{y\theta_z} \\ & & K_z & 0 & -K_{z\theta_y} & 0 \\ & & & K_{\theta_x} & 0 & 0 \\ & & & & K_{\theta_y} & 0 \\ & & & & & K_{\theta_z} \end{bmatrix} \quad (3-3)$$

in which the diagonal terms $K_x, K_y, K_z, K_{\theta_x}, K_{\theta_y}, K_{\theta_z}$ are stiffnesses corresponding to translational and rotational degrees of freedom associated with x (local pile axis), y, and z axes, respectively. The off-diagonal terms represent coupling between two degrees of freedom. For a single vertical pile, the axial and torsional stiffnesses can be uncoupled from other degrees of freedom, and as a result the corresponding off-diagonal terms are zero. For a single pile embedded in a subgrade with linearly increasing subgrade modulus, E_s , the stiffness coefficients can be calculated from the solutions presented by Lam et al. (1991). For piles in layered soils, the pile head stiffness matrix can be computed by conducting static condensation such that all degrees of freedom below the pile-cap are eliminated (Bryant, 1977).

For piles of flexural stiffness EI_p embedded in linearly increasing subgrade modulus, the stiffness matrix at the pile head (grade elevation) was calculated by Lam et al. (1991) and is given by

$$K = \begin{bmatrix} K_y & K_{y\theta_z} \\ sym & K_{\theta_z} \end{bmatrix} = EI_p \begin{bmatrix} \frac{1.06}{\lambda^3} & \frac{0.98}{\lambda^2} \\ sym & \frac{1.48}{\lambda} \end{bmatrix} \quad (3-4)$$

in which λ is the characteristic length of the pile, and can be estimated as

$$\lambda = \sqrt[5]{\frac{EI_p}{f}} \quad (3-5)$$

The procedure for estimating the stiffness matrix for a single pile (along with simplified design charts) and pile group has been described in detail in the previous sections.

3.2.1.2 Equivalent Cantilever Beam

In the equivalent cantilever method, the foundation is replaced by a cantilever beam that has a stiffness equivalent to that of the pile and the surrounding soil. This is represented schematically in figure 3-1c. The California Department of Transportation design manual (Caltrans, 1990) suggests two procedures for estimating the equivalent cantilever length for the pile. The first one is a

simplified procedure, in which equivalent pile length is estimated based on the SPT blow count of the soil stratum as shown in figures 3-2 and 3-3. In the other method, which is termed as the 'rigorous' method, the equivalent length is estimated by matching the pile stiffness (from a Caltrans in-house pile-soil system load-deflection solution) with the stiffness of a cantilever beam by equating displacements and rotations. The equivalent cantilever can also be estimated by equating the maximum moment in the pile. The estimated length, in that case, may be different. The choice of the method to determine the equivalent cantilever model depends on the intended applications. For seismic design, the equivalent cantilever model is normally used to account for foundation stiffnesses in a global dynamic response analysis. As discussed earlier, after the displacement demand is established, a second step pseudo static pushover analysis is needed for capacity evaluation. The state-of-practice is to represent the soils by p-y curves in this second step approach. The equivalent cantilever model is generally considered to be too crude in the second step in which force amplitude and corresponding distribution are evaluated.

It is possible to calculate equivalent length of the cantilever beam by equating the terms of the pile head stiffness matrix with those in the stiffness matrix of a cantilever beam. The corresponding stiffness matrix of a cantilever beam of length L_c and flexural stiffness, EI_c , is given by

$$K_{cantilever} = EI_c \begin{bmatrix} \frac{12}{L_c^3} & \frac{6}{L_c^2} \\ sym & \frac{4}{L_c} \end{bmatrix} \quad (3-6)$$

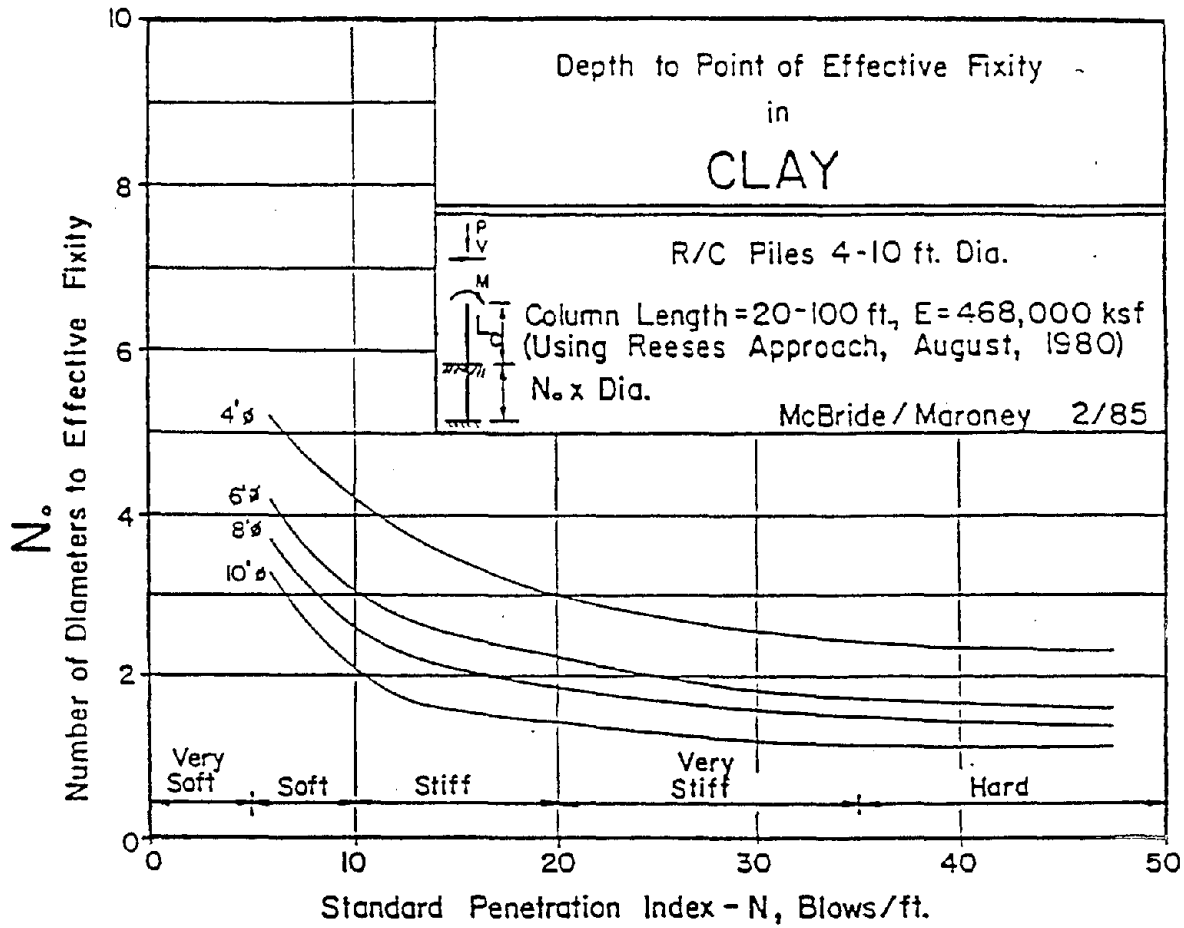
The stiffness matrix of the soil pile system (shown in eq. 3-3) can be approximated by an equivalent cantilever model by choosing the appropriate EI_c and equivalent cantilever length L_c . It is obvious that only two cantilever model parameters are not sufficient to satisfy all three stiffness coefficients (two diagonal stiffness and one cross-coupling stiffness coefficients) in eq. (3-3). The general approach is to match the diagonal stiffness terms which leads to the following cantilever model parameters:

$$L_c = 2.05\lambda \quad (3-7)$$

$$EI_c = 0.757EI_p \quad (3-8)$$

The basis of matching the diagonal stiffness coefficient in the above equivalent cantilever model appears generally sound, especially for a pile extension type configuration (shown in figure 1-1b).

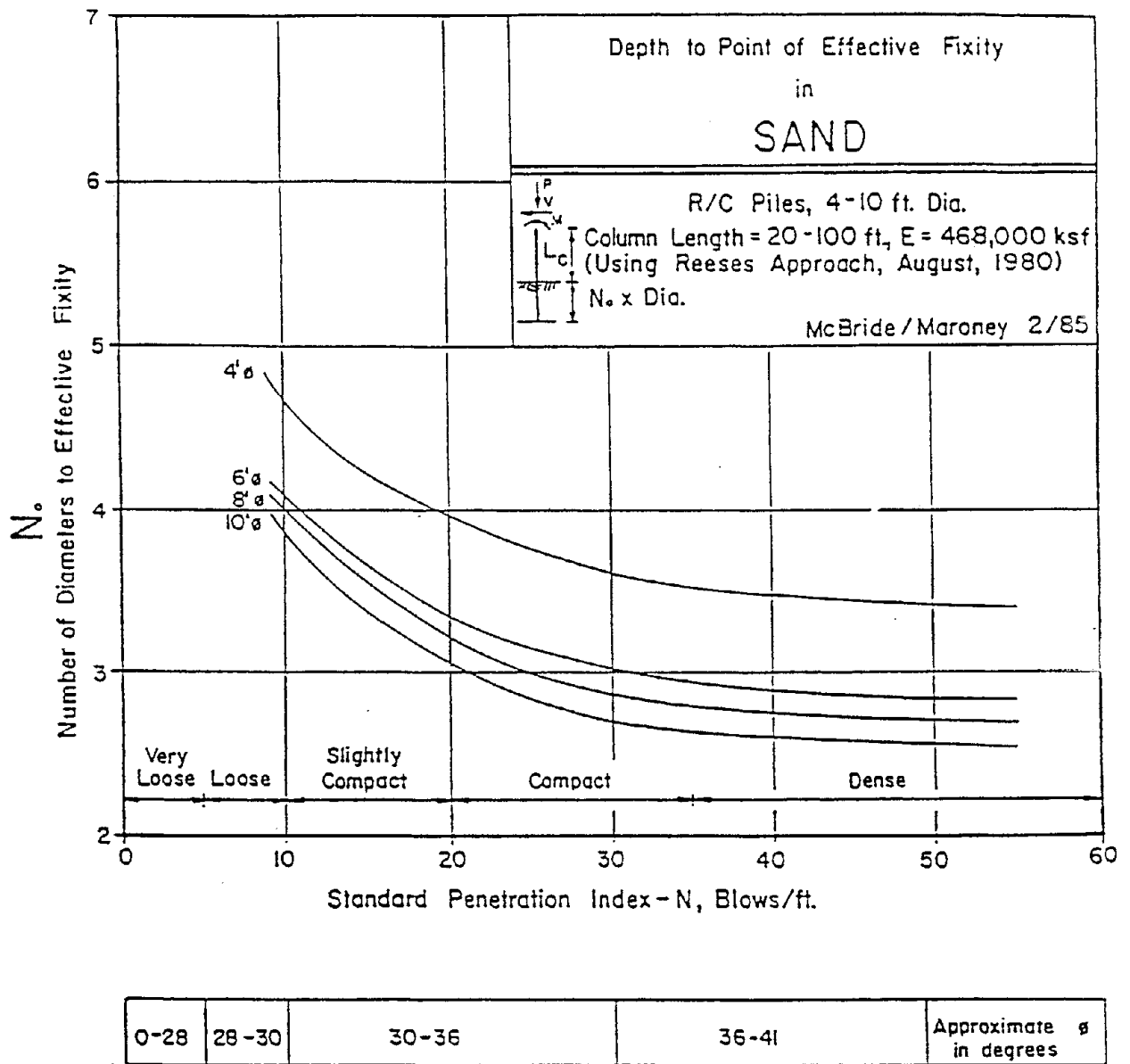
For a pile footing type configuration (figure 1-1a), the rotational stiffness of the pile group tends to be dominated by the axial pile stiffness as compared to the stiffness contribution from the bending stiffness of individual piles. Therefore it might be possible to choose the equivalent cantilever model solely to match the lateral force versus deflection equation (i.e. the first of eq. 3-4 by matching the translational and the cross-coupling stiffness term) resulting in the following cantilever model. This approach can lead to a more appropriate lateral stiffness for a wider range of pile head boundary (fixed and free head) conditions.



0-.5	.5-1	1-2	2-4	4-6	Shear Strength, ksf
------	------	-----	-----	-----	---------------------

1 kip = 4.45 kN
 1 in = 25.4 mm
 1 ft = 0.305 m

Figure 3-2 SPT Blowcount vs. Cantilever Length of Pile in Sand (After Caltrans, 1990)



1 kip = 4.45 kN
 1 in = 25.4 mm
 1 ft = 0.305 m

Figure 3-3 SPT Blowcount vs. Cantilever Length of Pile in Clay (After Caltrans, 1990)

$$L_c = 1.85\lambda \quad (3-9)$$

$$EI_c = 0.556EI_p \quad (3-10)$$

When equivalent cantilever length is determined by matching displacements or stiffness, it represents the foundation stiffness properly. However, the calculated shear and bending moments in the cantilever may not bear any relevance to those in the actual pile. Therefore, this particular modeling approach is only suitable for the *first step* in the design process to represent foundation stiffness in a global dynamic response analysis of the bridge structure. To calculate pile forces, it is necessary to go through the second step, where the complete pile with the surrounding soil is modeled.

3.2.1.3 Uncoupled Foundation Springs

As illustrated in figure 3-1d, the third method of characterizing pile stiffness involves replacement of the pile by two springs, one representing the translational and the other representing the rotational stiffness. In this particular method, the cross-coupling between lateral and rotational movement is not maintained. For deep foundations, especially for a pile extension, the cross-coupling between lateral and rotational foundation stiffness are significant, and therefore, an uncoupled foundation spring model would not be appropriate. Such a model should be restricted for shallow foundations (i.e. spread footings) or pile footing type configuration for smaller piles.

3.2.1.4 Foundation Nonlinearity

The lateral load-deflection response of a drilled shaft with a nonlinear p-y curve representation, but with a linear bending stiffness (EI) assumption was previously shown in figure 2-1. As discussed previously, this type of nonlinear soil pile interaction analyses has become the state-of-practice in the Step 2 nonlinear pushover design process for capacity determination. Such analysis using nonlinear p-y curves can also be used to derive the appropriate foundation stiffness matrix in Step 1. However, use of such nonlinear foundation load-deflection solutions to develop linear foundation stiffness matrices may lead to erroneous solutions if proper precautions are not taken. Some words of cautions are provided below in this aspect.

- (1) **Suitable Stiffness Matrix.** It is important to recognize that a foundation stiffness matrix implies a linear pile and soil system. For example, each point in the nonlinear load-deflection curve in figure 2-1 implies a different tangent stiffness matrix with its own three stiffness coefficients. The foundation stiffness matrix must be positive definite and symmetric for practical analyses and design procedures. The way to ensure that the appropriate stiffness matrix can be developed from pushover analysis would be to first develop equivalent linear soil-springs (suitable to the loading condition) compatible with the secant modulus fitted through the p-y curves at the appropriate deflection values. Subsequent load-deflection analyses can be conducted for the linearized soil spring model to solve for the stiffness matrix coefficients. So long as the pile and soil system has been linearized, a unique positive definite and symmetric stiffness matrix can be obtained

irrespective of the loading condition used for the pushover analysis. One way to ensure that the stiffness matrix is positive definite is to invert the stiffness matrix for the compliance matrix and check that the diagonal terms in the compliance matrix are all positive-real.

- (2) **Linearization of Nonlinear Load-Deflection Curves.** A nonlinear load-deflection solution implies that the stiffness is dependent on the deformation and corresponding load amplitudes. Unlike structural properties, which typically have reasonably well defined elastic stiffnesses, soils are intrinsically nonlinear, starting from extremely small load levels. For this reason, the choice of an equivalent linear soil modulus to develop foundation stiffness involves numerous complexity and uncertainties. In recent years the trend has been to base it on more complicated finite-element analyses using shear wave velocity data. If soil modulus based on shear wave velocity data are used, they must be adjusted by extremely small factors (typically much smaller than those arising from free field wave propagation analyses such as below 0.1, because the soil strain is usually an order of magnitude higher under foundation load as compared to wave propagation problems). It must be noted that strain compatible soil modulus determined from a 1-D site response analysis would only be valid for 1-D shear beam configurations. This approach is typically used where equivalent soil modulus ratio versus shear strain relationships are utilized. Therefore, it cannot be used to establish strain compatible scaling factors for rather complicated 3-D soil-pile configurations which requires rigorous 6-D stress-strain (constitutive) soil modeling. This method is not only complicated but also is not well proven for practical applications. For these reasons, the merits of an inherently complex finite element soil-structure interaction approach will be very questionable. Traditionally, empirical load test data (either Terzaghi's subgrade theory or p-y curves) formed the basis for stiffness evaluation in foundation design which has the problem that they are mostly evaluated from slow rate loading conditions and might not capture some aspects of dynamic effects. Most bridges are long period structures. The discussed foundation dynamic effects would be small as compared to the inertia forces of the superstructure. The traditional p-y approach is simpler to use and also has been proven over its long history of applications.

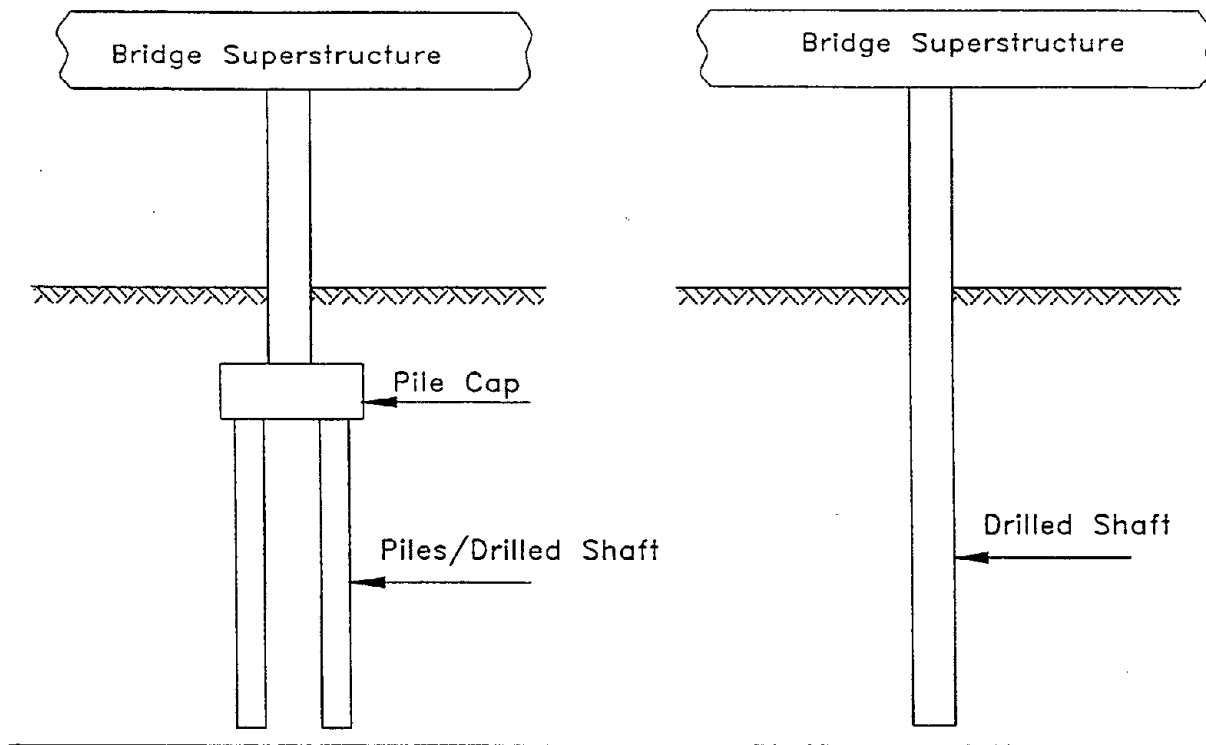
Any nonlinear procedure theoretically requires an iterative process to ensure that the stiffness matrix is compatible to the assumed deflection level. As shown in figure 2-1, a secant stiffness at peak load/deflection would represent the lower bound stiffness occurring only at an infinitesimal duration in time during peak earthquake load. Such a stiffness might be too soft to be representative for the overall duration of the earthquake. A secant stiffness at a smaller deflection might be a better choice to serve as the effective foundation stiffness representative for a longer time frame over the duration of the earthquake. In equivalent linear site response analyses, Idriss and Sun (1992) proposed to establish the equivalent secant soil modulus at an effective strain value equal to the peak strain multiplied by a scaling factor $n = (M_w - 1)/10$ where M_w is the earthquake magnitude (Moment magnitude). The above recommendation by Idriss and Sun, or simply establishing a secant foundation stiffness at 0.5 to 0.65 of peak deflection, would provide a better basis for developing foundation stiffness than the lower bound stiffness at peak deflection.

- (3) **Inherent Limitation.** Various researchers (Miranda, 1991) have concluded that solutions from linear response analysis generally give reasonable peak displacement predictions (referred to as equal displacement principle for long period systems). However, as shown in figure 2-1, a secant stiffness at below peak deflection will always overshoot the predicted load at the peak deflection for a typical nonlinear load-deflection curve. The dilemma is that a secant stiffness at below the peak load should be used in order to rationally capture the stiffness characteristics which in turn forms the basis to predict the proper level of peak displacement, but it would automatically overshoot the predicted load. This is the reason that a pseudo-static nonlinear pushover analysis is needed in a subsequent Step-2 to account for forces corresponding to the displacement demand predicted in Step-1. These inherent limitations in a linear response analysis imply that a nonlinear dynamic response analysis is needed to solve for both forces and displacement simultaneously in a one-step analysis for a system that has significant inherent nonlinearities (both material and geometric nonlinearity).
- (4) **Significance of Foundation Stiffness.** For most bridges supported by drilled shafts or pile extensions, the compliance of the foundation is small compared to the compliance of the unsupported column. For this and the above discussed complexities and uncertainties in foundation behavior, a more simplistic linear approach to incorporate foundation stiffness in the first step dynamic response analysis has many merits and is recommended for general application. The recommendation is intended to minimize errors commonly associated with more complicated approaches. The linear approach includes the use of Terzaghi's linear subgrade reaction to account for soil stiffness in conjunction with an equivalent cantilever model to account for foundation stiffness.

3.2.1.5 Foundation Geometry

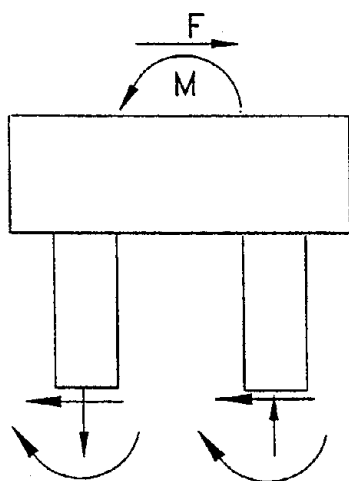
When the foundation system is replaced by any of the methods described in the previous subsection, it is an idealized representation of the actual system which gives a measure of foundation stiffness. Two foundation systems may have comparable stiffness, but the load supporting mechanism may be completely different. Consider, for example, the pile group and the pile extension in figures 3-4a and b. The free-body diagrams of the two systems are shown in figures 3-4c and d, respectively. In the case of a pile group, the overturning moment is resisted by the axial stiffness of individual piles, and the contribution of rotational stiffness of individual piles is relatively small for small diameter piles. Similarly, the torsional moment on the pile group is resisted by the lateral stiffness of individual piles. For pile groups, therefore, coupling exists between axial displacement and overturning rotation. On the other hand, in the case of a pile extension, the lateral load and overturning moment are resisted by the lateral stiffness of the pile shaft alone. Similarly torsional moment is resisted by only the torsional stiffness of the single pile.

In addition, for the pile group, the pile cap contributes to the foundation stiffness due to lateral soil resistance on the bottom and sides of the pile cap. The contribution from the pile cap stiffness may be significant when it is embedded in dense soil.

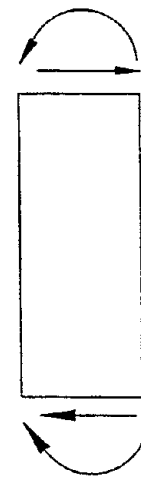


(a) Pile Cap Configuration

(b) Pile Extension



(c) Free Body Diagram for Pile Cap



(d) Free Body Diagram For Pile Extension

Figure 3-4 Pile Configuration and Load Resistance Mechanism

3.2.1.6 Boundary Conditions

The boundary condition at the pile head has a significant effect on pile response and, therefore, on the estimated pile head stiffness. When piles are connected to a rigid pile cap, the condition at the pile head depends on the reinforcement connection detail. The lateral stiffness can increase by a factor of 2 to 3 as the pile head fixity changes from a free (pinned) to a fixed head condition. For moment-resisting connections, the boundary condition at the pile head may be considered to be fixed against rotation, but free to translate. Figure 3-5 shows the influence of the boundary condition on pile response. In this figure pile head displacements and maximum pile moments are plotted for two different boundary conditions, completely free and fixed against rotation only. The plots indicate that, pile head displacement is strongly influenced by the boundary condition at the pile head, whereas the maximum calculated moments do not change significantly. Although the maximum moment for two conditions are comparable as shown in figure 3-5, the distribution of bending moment in these two cases are quite different. For the fixed head condition, the maximum negative moment occurs at the pile head, whereas for the free head condition the maximum positive moment occurs at depth below the ground surface. In reality the pile head condition is usually neither free nor fixed. A possible way to model the pile head condition would be to represent the joint by a moment-resisting rotational spring. As an example, the same pile is modeled with a rotation spring at the head with a rotational stiffness of 1.1×10^5 kN-m/rad. The calculated pile head displacements and maximum pile moments for this condition are also shown in figure 3-5. While the fixed and free head conditions present the upper and lower bound for pile head displacement (therefore, lateral stiffness), the maximum pile moment for the partially restrained condition is not bounded by the above conditions, but usually would be less than either the negative moment at the pile head for the fixed head case and less than the positive moment at depth for the free head case. The more balanced and lower moment for a more realistic representation of the pile head fixity condition usually can lead to more economical design and is an important design issue (both from a foundation stiffness as well as a force and moment assessment standpoint) that is often overlooked by designers and researchers.

For most piles, the boundary conditions at the pile tip do not affect the pile performance because they are sufficiently far from the structure and the piles can be considered as infinitely long piles when the pile length is larger than 3 times the characteristics length λ (eq. 3-5). For large diameter shafts, it is important to check the pile length, especially for soft soil conditions, to determine the need to include the pile tip's boundary conditions as compared to merely using closed form solutions for infinite beam solutions as shown in eq. (3-4). This will be further discussed in Section 3.2.2.4.

In many instances, concrete pavement or traffic barriers are constructed around drilled shafts at the ground level. Unless a gap is maintained around the shaft, the pavement can provide lateral support to the pile, which may in turn influence the pile head stiffness.

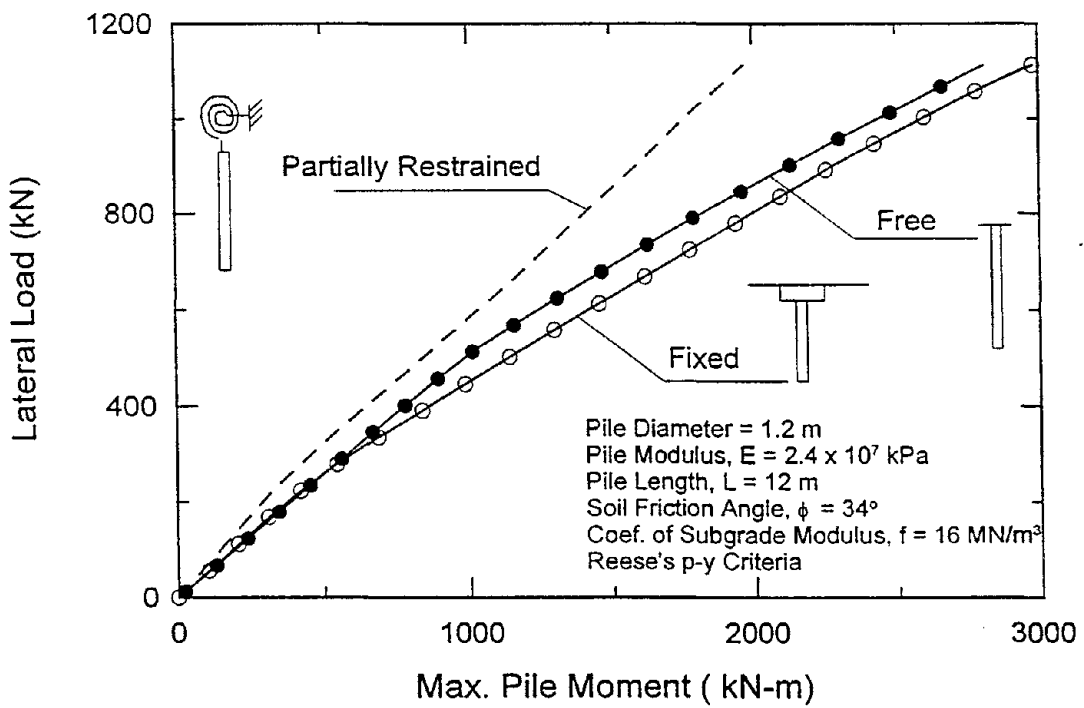
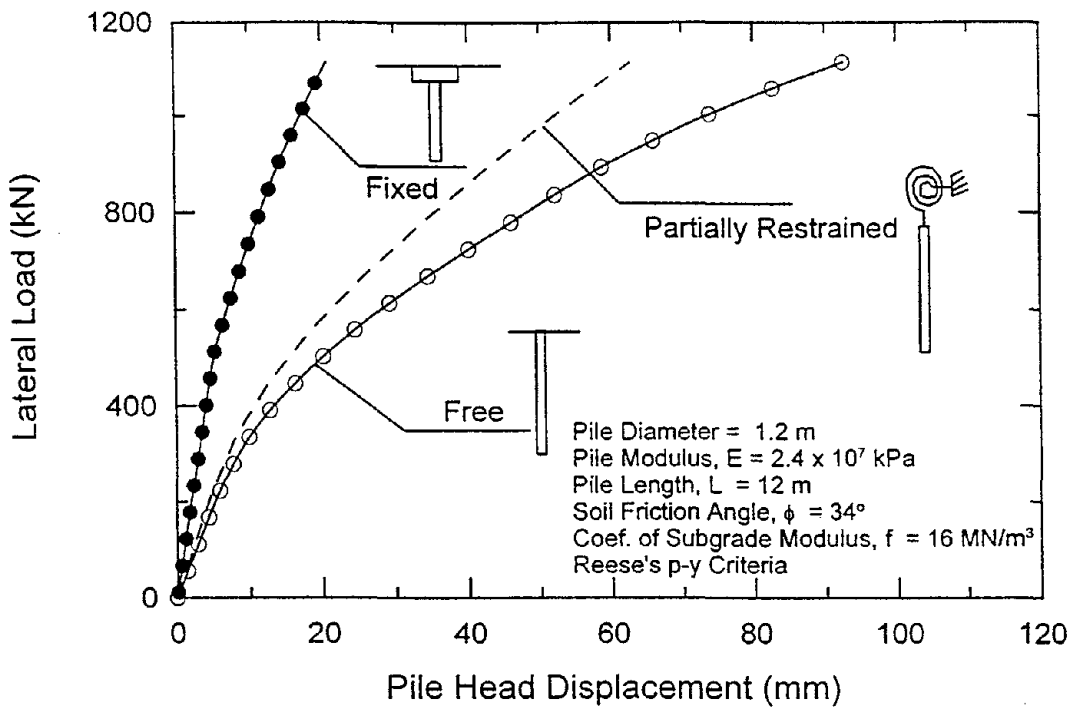


Figure 3-5 Boundary Condition and Pile Response

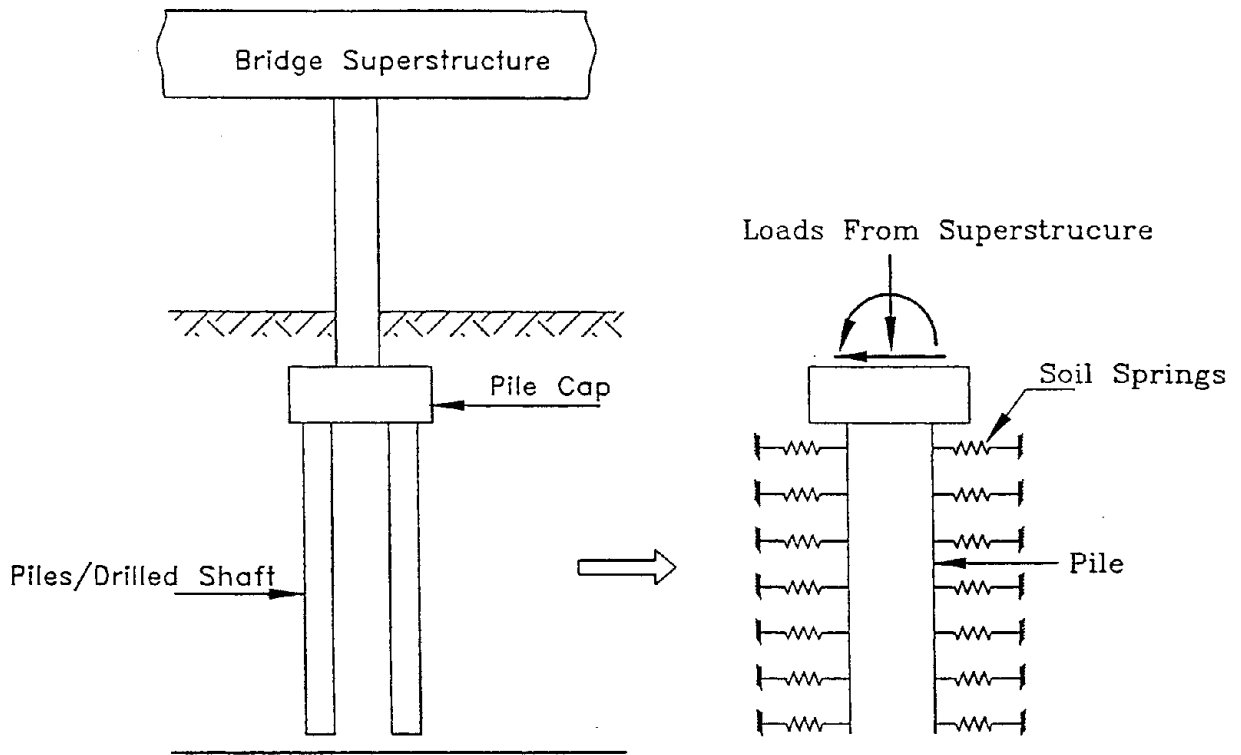
3.2.1.7 Other Considerations

Nonlinear Structural Behavior of Drilled Shaft : The stress-strain response of concrete is not linear and the response deviates from a linear relationship at a relatively small strain. Because the elastic modulus and effective cross-section of concrete piles change with strain, the flexural rigidity of the pile, EI_p , which governs the pile stiffness, changes with applied load level. For large diameter concrete piles, minor cracking develops at a relatively small applied moment and it would be appropriate to use effective section properties for evaluating pile stiffness for seismic design. Based on load tests on large diameter piles, the influence of nonlinear concrete behavior in estimating pile response has been demonstrated by Naramore and Feng (1990). The design charts developed by Priestley (1991), which were presented in figure 2-12, can be used to estimate effective section properties. In the absence of detailed information regarding reinforcing steel and applied axial load, an equivalent cracked section can be estimated by reducing the stiffness of the uncracked section by half. In general, the cracked section is a function of the reinforcement ratio (volume of steel reinforcement versus that of concrete), but is often adequate to assume as one-half of the uncracked section for most pile analyses.

Cyclic Loading Condition: The recommended soil stiffness in terms of subgrade modulus and conventional p-y curves is developed mainly from slow cyclic load tests. Applicability under faster-rate vibratory loading conditions in a seismic event needs to be considered. Based on the findings of several researchers, Pender (1993) concluded that the dynamic pile stiffness at large load levels during the earthquake is smaller than its static stiffness. Lam and Cheang (1995) and Crouse et al. (1993) presented fast-rate dynamic pile test data which confirmed Pender's recommendations.

3.2.2 Step 2: Estimating Foundation Capacity

The second step in the design of drilled shaft foundations involves the analyses of the pile foundation system using the estimated load from the superstructure and proportioning the foundation accordingly. In this step, the actual foundation is modeled with the surrounding soil as shown in figure 3-6. Usually, the soil is modeled as nonlinear springs with force-displacement characteristics of the springs based on given p-y relationships. It can be readily said that realistic nonlinear modeling of structural elements is more essential than that of soil in Step 2 capacity solution. In many cases, linearized representation of soil stiffness, such as the Terzaghi's subgrade modulus approach provides reasonable solutions for design applications. For a laterally loaded pile problem, usually there are ample soil capacities (ultimate passive pressure from soil) over the entire pile length. Therefore, the foundation system capacity is controlled by the structural member capacity. The appropriate analysis to determine the foundation capacity for lateral earthquake load requires an assessment of the magnitude of lateral deflection that can be tolerated by the foundation such that the foundation's ability to provide vertical support to structures within acceptable performance (settlement) is not compromised. For seismic design, which usually implies extremely high load but at a relatively low probability of occurrence, the structural system is expected to be damaged and will undergo some level of yielding. In practice this Step 2 static pushover analysis involves monotonically increasing the load to establish the displacement corresponding to initial yielding to define the yield displacement. Then the analysis is continued to the level of displacement demand determined in Step 1 for the load distribution in various components of the structural and foundation



(a) Complete Structure with Foundation

(b) Pile with Soil Springs
For Step 2 Analysis

Figure 3-6 Modeling Soil-Pile System in Step 2 Analysis

system. The ratio of the displacement demand to yield displacement (i.e. the displacement ductility demand) is then used as a measure of ductility demand on the system. Most often, a lower load (as compared to linear elastic earthquake response solutions) for foundation design can be justified to reflect limit states (load fuses such as plastic hinges in columns) built into the design strategy as discussed below.

3.2.2.1 Prevalent Practice for Conservatism

It is often recommended by the geotechnical engineers that a softer soil stiffness and/or a lower soil capacity be used in the foundation design as it leads to more conservative designs. This is true if the foundation is designed for a *static* loading case in which the design load level is known a priori. As was mentioned previously, pushover analysis is commonly used in the seismic design of foundations. When a displacement controlled pushover analysis is performed, it is obvious that soft soil stiffness assumption leads to unconservative force in the structural components. Moreover, overly soft soil stiffness implies that the plastic hinges on the drilled shaft occur at a deeper location below grade. In such cases shear demand on the structure may be underestimated (see section 3.2.2.2)

It can be concluded from the above discussion that it may be quite counterproductive if arbitrary conservatism is introduced in the general geotechnical recommendation. It is recommended that analysis and design for seismic load cases should be conducted using the least number of assumptions. However, this statement only applies to the seismic load case. Traditional conservatism should be maintained in foundation design for other load cases in which the loading condition is better defined.

3.2.2.2 Formation of Plastic Hinge

The foundation capacity of a drilled shaft is related to the maximum tolerable lateral deformation without compromising the vertical load carrying capacity of the foundation. Therefore, the overall foundation capacity is usually controlled by the structural capacity of the foundation rather than the ultimate soil resistance. The principles of ductile design is often employed in the seismic design of superstructure as well as sizing of the column or the pile extension. Accordingly, in a seismic event plastic hinges can form at a predetermined location that limits the load transfer and also provides an energy dissipation mechanism. It also ensures that there is sufficient displacement ductility capacity. Some examples of plastic hinge locations for typical bridge structures are shown in figure 2-2. These are very sound and necessary design strategies, not just from an economic standpoint. They are necessary because of uncertainty in our knowledge of the earthquake load and therefore it would be good practice to control the behavior for potential over-load conditions such that potential damage would occur at preferred locations and to be associated with a ductile mode of system behavior for the overall system. The locations of plastic hinges should be such that they are easily accessible for repair after the earthquake. Therefore, it is not desirable that hinges form below the ground level where they can not be detected.

For an applied lateral load at the superstructure level, the maximum moment occurs below the ground level as shown in figure 3-7a. The maximum moment occurs approximately at a depth of 0.9λ below the ground level. The parameter λ is the characteristic length of the pile as defined in eq. (3-5). Assuming a circular pile cross-section, and considering Young's modulus, E , of concrete

to be 2.7×10^7 kPa, the depth of maximum moment can be estimated as 1.8 to 3 times the shaft diameter (D) below the ground for loose and dense soil, respectively. For cracked sections with flexural rigidity, EI_{eff} , equal to half of that of the uncracked section, the depth of maximum moment would be at shallower depth, 1.4 to 2.2D for loose and dense soils, respectively.

Because the maximum moment in the pile extension occurs at a depth below the ground, it is still possible to design the plastic hinge above ground as shown in figure 3-7b by the use of proper structural details. The pile moment capacity is increased above that of the column to ensure that the plastic hinge occurs at the base of the column. However, this causes a shorter plastic hinge zone and therefore lower plastic rotational capacity.

3.2.2.3 Shear Capacity

As mentioned in the previous section, plastic hinges are allowed to form in the columns to limit loads and provide ductility to the structure. However, sufficient column shear capacity should be provided to avoid brittle failure of the column which may result in complete collapse of the structure. Because of the severe potential consequences of a shear failure, Caltrans (1990) specifies that the smallest column length which yields largest possible design shear forces should be used. As mentioned earlier, the largest moment for a pile extension and therefore the location of potential plastic hinges are assumed to occur at some depth below the ground level; this situation may be incompatible with the presence of a pavement or road barrier at the ground level. In this case it is possible that the plastic hinge would form at or above ground level, and the design shear force would increase. Also, the location of the plastic hinge may be higher than that indicated in the previous section due to higher stiffness of the soil near the surface. Such situations may arise when there is a stiff desiccated crust at the ground surface.

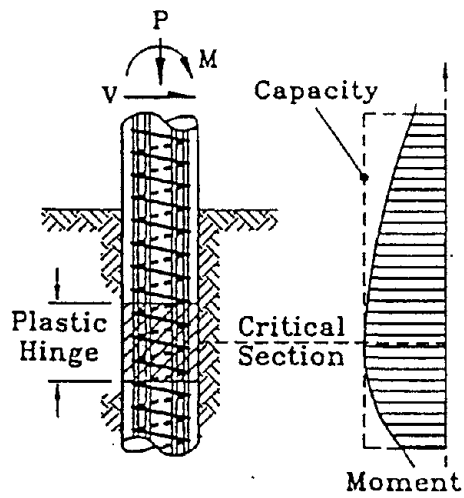
The influence of near ground support on the shear demand of a pile is illustrated in figure 3-8. Figure 3-8b shows a pile extension with pavement at the ground level, whereas in figure 3-8a no pavement or any other supporting structure is present. The location of potential plastic hinges for both situation are also indicated in the figure. Since pavement acts as a supporting structure, there is a likelihood that the plastic hinge would form at the ground level and the design shear, V_2 , in that case would be

$$V_2 = \frac{M_p}{L_2} \quad (3-11)$$

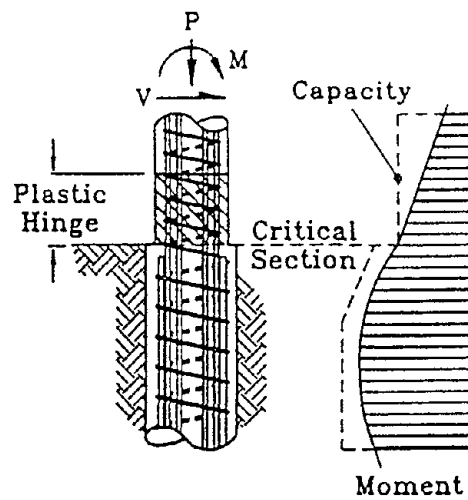
If the ground level support is neglected, and it is assumed that the plastic hinge would form below the ground, then the estimated shear V_1 is calculated as

$$V_1 = \frac{M_p}{L_1} \quad (3-12)$$

Because L_1 is larger than L_2 , the estimated shear would be less than the actual shear that the structure needs to resist. In many instances failure of the pile/column results from assuming an overly deep plastic hinge location L, by neglecting surficial soil/structural constraints. It would be good design



(a) Integrated Pile/Column



(b) Integrated Pile/Column with Oversize Pile

Figure 3-7 Plastic Hinge Formation in Pile (after Priestley et al., 1996)

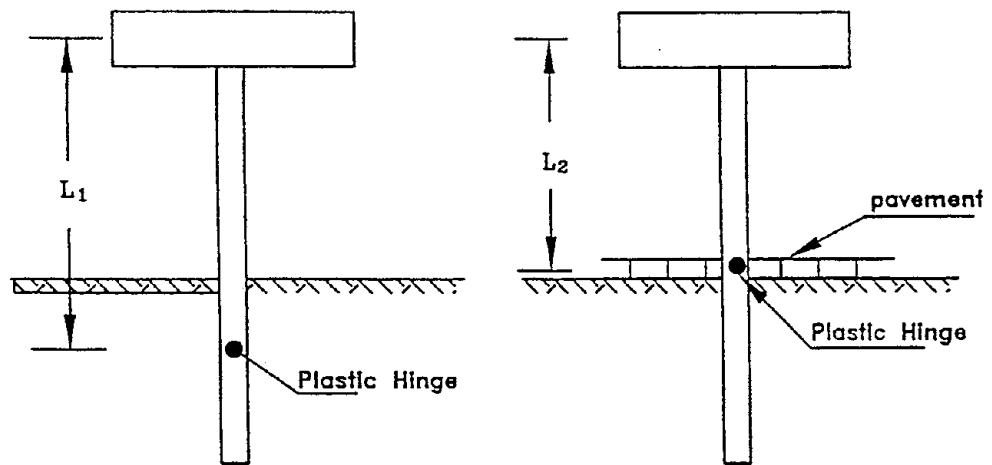


Figure 3-8 Effect of Near Ground Support

practice to provide some gap between the pile and the pavement to ensure that the plastic hinge can be formed at its intended locations or to design for a more conservative shear capacity to take into account the uncertainty of the location of the plastic hinge.

3.2.2.4 Minimum Pile Length

The Caltrans design manual (1990) introduces the concept of ‘stable’ pile foundation and suggests that a minimum pile length should be maintained to ensure stability against excessive rotations. According to this procedure, a pile is assumed to be stable when "...a substantial decrease in pile shaft length does not result in excessive (pile head) deflection". Although ensuring a limit on pile displacement is a rational design approach, the Caltrans ‘stability’ approach requires more time consuming computer analyses and potentially subjective judgement to decide what can be viewed as excessive deflection. On the other hand, although time consuming computer analysis can cover a more general soil pile condition. Some discussion on the subject of minimum pile length is provided below.

The concept of a stable pile is essentially similar to that of a long pile. A long pile under lateral loading is defined as a pile which can be modeled as an infinitely long beam, and application of load at one end has no significant influence on the other end. Whether a pile behave as a long or short pile depends on the ratio of pile length (L) to the characteristic length (λ). The characteristic length λ for a soil profile with linearly increasing subgrade modulus has been defined in eq. (3-5), and that for constant modulus is defined in the following equation as

$$\lambda = \sqrt[4]{\frac{EI_p}{E_s}} \quad (3-13)$$

From analytical solutions (Hetenyi, 1946), a pile may be treated as a long pile when L/λ is greater than π . The pile head displacement remains essentially constant as the pile length, L , is increased beyond $\pi\lambda$. For a relatively large diameter pile with higher EI_p , the pile length needs to be larger to achieve the pile length of $\pi\lambda$. Therefore for a given soil condition, the stable length of a larger diameter pile would be larger than a pile of smaller diameter, although a larger pile would have higher capacity and stiffness to meet the force demand.

This particular aspect is illustrated in figure 3-9. In this figure pile head displacements are plotted against pile length for two piles with diameters 1.2 m and 2.4 m. The stable lengths of these two piles are also indicated in the figure according to the suggested procedure by Caltrans. This figure indicates that the stable length of the smaller pile is about 10 m whereas that for the larger pile is about 15 m.

The above discussion provides the theoretical basis for the minimum pile length under idealized pile soil conditions. The method involves an appreciation of the profile of subgrade modulus (approximately equal to the Young’s modulus of the soil). Lam et al. (1991) provided some guidelines on the subgrade modulus values which can be used to establish the above discussed

characteristic length. A model in which the subgrade modulus varies linearly with depth generally works well with most soil sediment condition (both sand and clay sites) and the characteristic length can be calculated using eq. (3-5). As shown in the above examples, a drilled shaft exceeding 15 m (50 ft) embedment would usually be sufficiently long to qualify for the minimum length.

For very stiff sites including shafts socketed into rock, it is useful to determine a minimum rock socket length. For these stiff soil conditions, a more appropriate soil profile model would be to assume that the subgrade modulus is constant with depth. For these cases, the characteristic length can be determined from eq. (3-13), and can be used to determine the needed minimum length of $\pi\lambda$. Using typical Young's modulus for weathered rocks, a sensitivity study suggests that shafts socketed 4 pile diameters in rock would be sufficient for lateral loading for shafts up to 3.5m in diameter.

Based on our experience and a limited sensitivity study, we have found that the length of most drilled shafts would be controlled by axial load requirements, rather than by the lateral load requirement. Whereas, the above discussed minimum length for stability issues should not be overlooked, they should not be regarded as rigid requirements. If the stable pile length calculation results in an uneconomical design (i.e. if the pile length is controlled by lateral load rather than vertical load), the designer should evaluate the actual lateral stiffness of the drilled shaft and compare it to that required for acceptable performance. If the embedment length and the strength of the drilled shaft is adequate to provide sufficient lateral stiffness with adequate allowance for uncertainties in the soil stiffness parameters, a lower pile length could be justified. As discussed earlier, one artifact in large-diameter shaft design is that it also leads to the requirement for longer length to satisfy the minimum stable pile length requirement, without regards to the actual stiffness and capacity of the drilled shaft itself. In some rare situations, the minimum stable pile length requirement can lead to overly conservative design and may drive the designer to make unreasonable decisions to select smaller diameter drilled shafts solely to avoid the unstable pile length issue.

3.3 p-y Model for Drilled Shafts

As mentioned earlier, the most widely used method to analyze pile response under lateral load is by using a p-y model in which soil is replaced by a series of nonlinear springs. A p-y model simply describes the force-displacement relationship of a soil spring, in which p is the soil reaction force per unit length, and y is the corresponding pile displacement. A number of p-y models have been proposed by different authors for different soil conditions. The two most commonly used p-y models are those proposed by Matlock (1970) for soft clay and by Reese et al. (1974) for sand. P-y curves for other soil conditions, e.g., stiff clay, rock, can also be found in the literature (e.g., Reese, 1986). The p-y models are essentially semi-empirical and have been developed based on a limited number of full-scale lateral load tests on piles of smaller diameter, ranging from 0.3m to 0.6m (12 to 24 in). To extrapolate p-y criteria to conditions that are different from the one from which these models were developed requires some judgement and consideration.

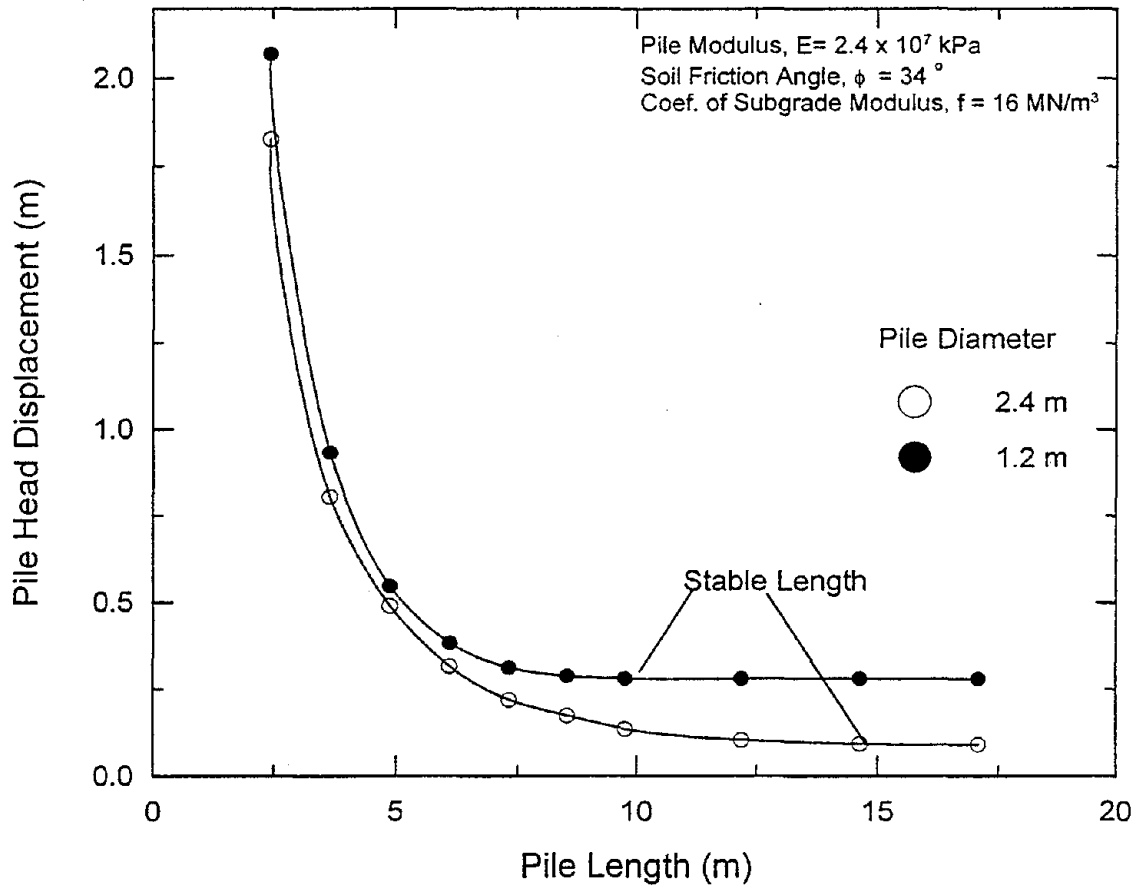


Figure 3-9 Stability Ratios of Two Piles

The nonlinear p-y curve is a form of discrete spring approach to account for the stiffness of the soil mass. Matlock's and Reese's nonlinear p-y approaches can be regarded as an extension of the widely used linear subgrade modulus approach of Terzaghi (1955). Terzaghi's linear subgrade modulus can be regarded as the soil stiffness corresponding to the secant stiffness at normal working load range. If the Matlock's clay and the Reese's sand p-y criteria are used in load deflection analyses for typical smaller piles to develop a nonlinear load-deflection curve, they typically give solutions comparable to results from Terzaghi's linear subgrade modulus at 12 to 50 mm (0.5 to 2 in) pile head deflection. As a matter of fact, Reese's sand p-y criteria utilizes Terzaghi's working load modulus scaled by a factor of 3 to form the initial tangent stiffness in the p-y curves. As a result, solutions from p-y curves and the more simple Terzaghi's linear modulus approach can usually be cross correlated to a reasonable degree. Terzaghi's linear approach can often form the basis in the Step 1 dynamic response analysis and then the nonlinear p-y approach can be used for the Step 2 pushover analysis where results from the apparently different approaches generally give reasonably compatible solutions in the design process.

Based on field load test results, some researchers have indicated that stiffness and ultimate lateral carrying capacity of a large diameter drilled shaft are larger than the values estimated using the conventional subgrade reaction model. Based on the work by Carter (1984) and Ling (1988), Pender (1993) suggests that subgrade modulus would increase linearly with pile diameter. Stevens and Audibert (1979) came to a similar conclusion and suggested that E_s is proportional to the square root of pile diameter. Davidson (1982) and Lam and Martin (1986) attribute the increased stiffness and strength of large diameter shafts to additional soil resistance mobilized due to pile rotation. Lam and Cheang (1995) presented a set of full-scale pile load test data that include variations in loading rate from slow cyclic loading to fast vibratory loading) and different pile head boundary conditions (free head vs. fixed head). Lam and Law (1994) presented nonlinear finite element solutions for both smooth and rough pile surfaces. The above research suggests that the apparent diameter effects on p-y curve are related to the pile rotation and skin friction issues. The apparent diameter effects reported in empirical pile load tests are due in part to the fact that most pile load tests are free-head tests and fixed-head tests are relatively rare. In this section, the applicability of conventional p-y models to drilled shaft foundation design is examined.

3.3.1 Effects of Various Parameters

In this section, the effects of different parameters on pile response are examined and the results are presented in graphical form. The sensitivity study is performed for a generic sand site which is usually stiffer than a typical clay site. A stiffer soil condition has been selected for the sensitivity study because drilled shafts are more appropriate for more competent soil conditions and also because the overall pile soil response would be more sensitive to changes in input soil parameters. For a soft clay site, the overall pile response will be rather insensitive to relatively large variations in p-y curves. The sensitivity study is conducted using the standard Reese sand p-y criteria (Reese, 1974).

3.3.1.1 Soil Properties

The p-y curves are formulated using three soil parameters - unit weight of the soil, γ , angle of friction, ϕ , and the modulus of subgrade reaction, E_s . To estimate the sensitivity of the estimated pile response to the input soil parameters, a parametric study is performed by varying the soil properties. The pile chosen for the study is a 1.2m-(4ft)diameter drilled shaft with a length of 12 m (40 ft). The pile is embedded in a uniform soil deposit. The soil density and friction angle are varied from 18.1 and 18.8 kN/m³ (115 to 120 pcf) and 30 to 36° to represent a variation from loose to medium dense sand. The coefficient of subgrade modulus, f_s , is also varied from 5,500 to 16,000 kN/m³ (20 to 60 pci) to reflect the change in the soil condition from loose to medium dense.

The response of the pile foundation in terms of pile head displacement and maximum pile moment are calculated, and are presented in figure 3-10. Figures 3-10a and 3-10b show the variation of pile head displacement and maximum pile bending moment, respectively, with applied lateral load at the pile head. The estimated pile head displacement decreases significantly with increasing soil density. However, it can be observed that the pile head load-deflection characteristics are linear for the loose and dense sand conditions. The relationship of maximum pile moment versus shear load, however, is not significantly affected by the variations in input p-y curves. The presented example illustrates the earlier comment that, although the soil behavior is nonlinear, its effect on the overall pile response for lateral loading would only be mildly nonlinear because of the linear property of the pile (i.e. linear EI_p) and overly complicated treatment to deal with soil nonlinearity is not needed from a practical point of view. For a softer soil condition, the pile response will even be less sensitive to changes in p-y curves.

3.3.1.2 Degradation Effect

In many instances the p-y curves are degraded to simulate the effect of reduced soil strength and/or stiffness. This is normally achieved by scaling the p-y curves along the p-axis as illustrated in figure 3-11. This scaling factor is generally referred as a p-multiplier. The effect of a p-multiplier is illustrated in figure 3-12. In this figure the pile head displacement and maximum moment of a free-headed pile are plotted for different values of p-multiplier. Pile head displacements (therefore, pile head stiffness) are more strongly influenced by the change in p-y curves, than the relationship of maximum pile moment versus shear load. These two examples illustrate that although pile head stiffness is influenced by changes in p-y curves, the maximum pile moment tends to be insensitive to such changes.

3.3.1.3 Embedment and Gapping or Scouring

Because of the influence of effective confining pressure, the subgrade modulus and the ultimate soil reaction on piles increases with depth. For pile foundations with pile caps, the equivalent foundation stiffness is usually estimated at the pile cap level. The effect of embedment on pile head stiffness in that case could be significant. On the other hand, for piles in a river bed, soil may be removed by scouring which results in a loss of lateral soil restraint. To examine the effects of embedment and scouring, the same pile used in the previous examples is analyzed for two conditions. In one, the

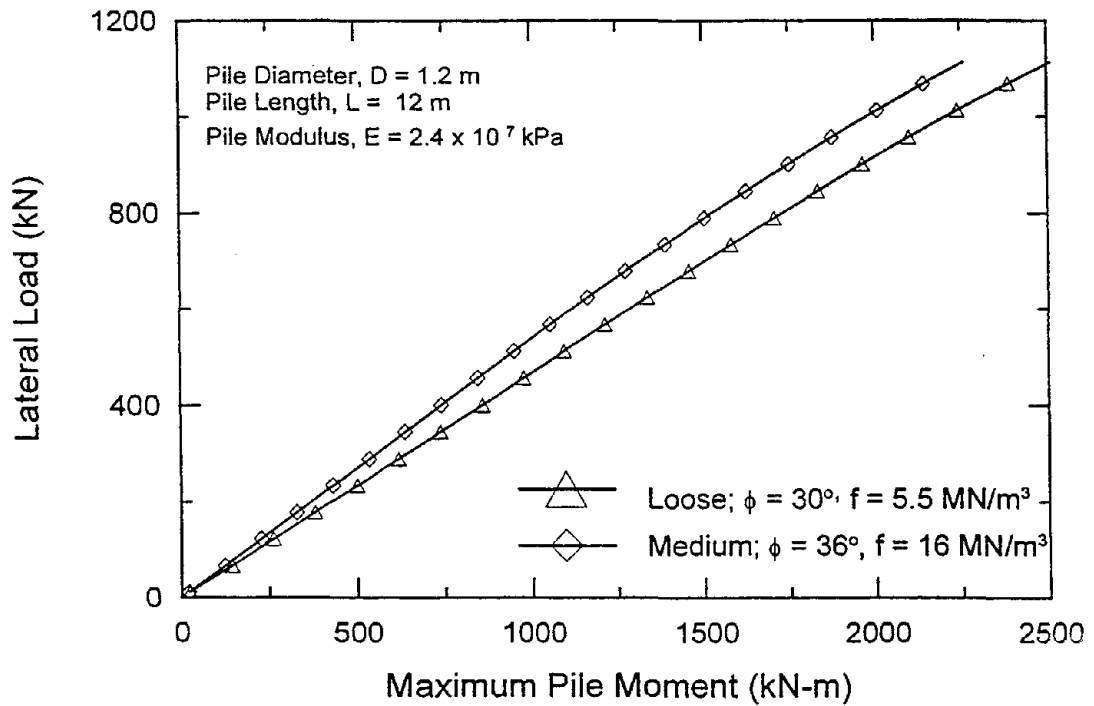
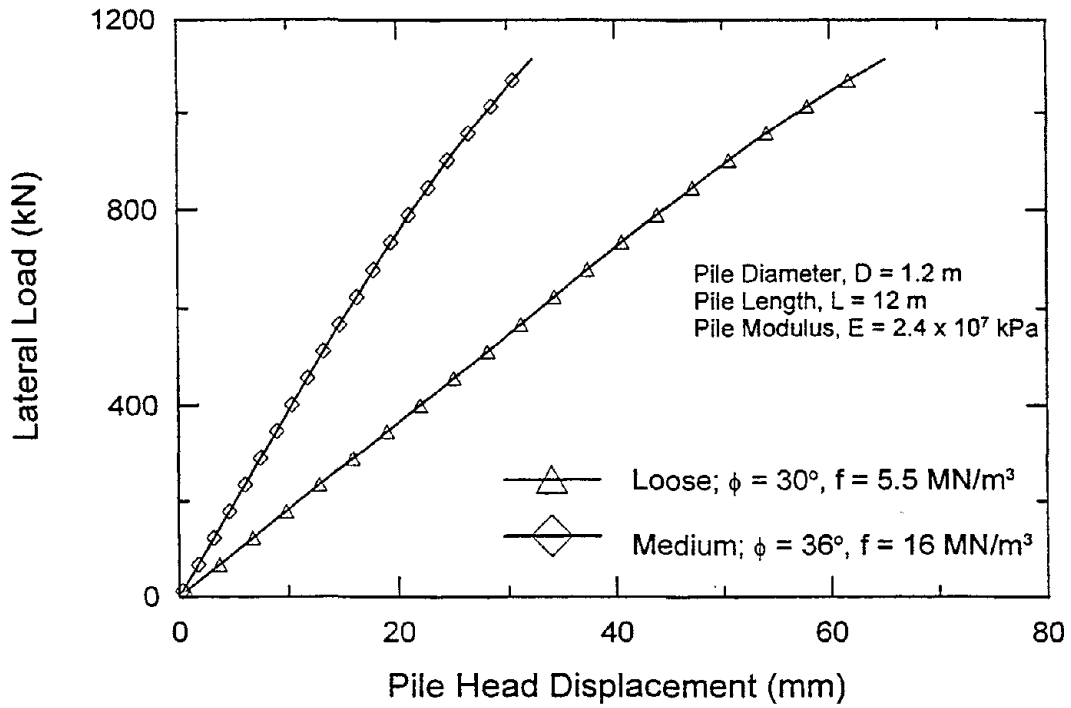


Figure 3-10 Effect of Soil Properties on Pile Response

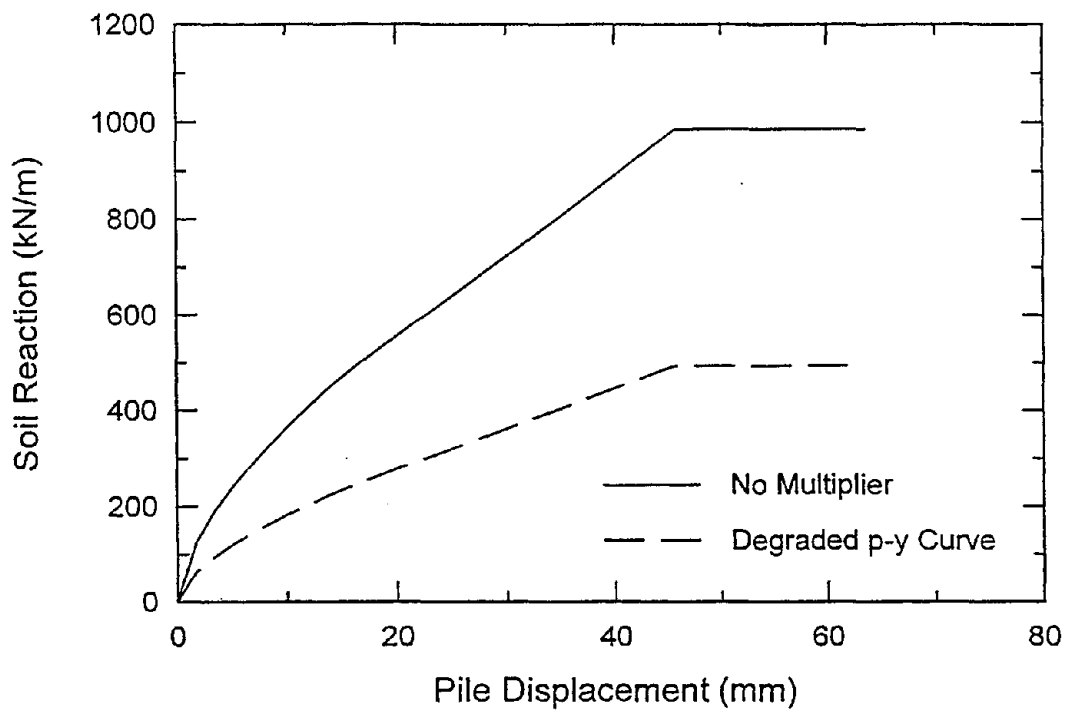


Figure 3-11 Example of p-multiplier on p-y Curves

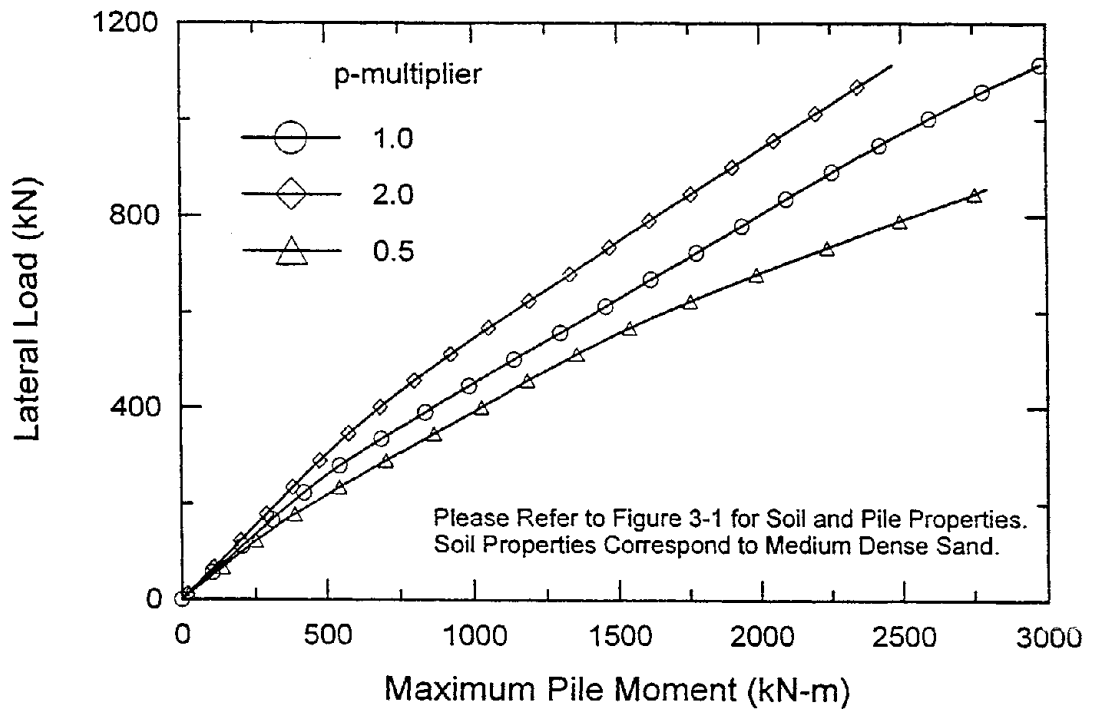
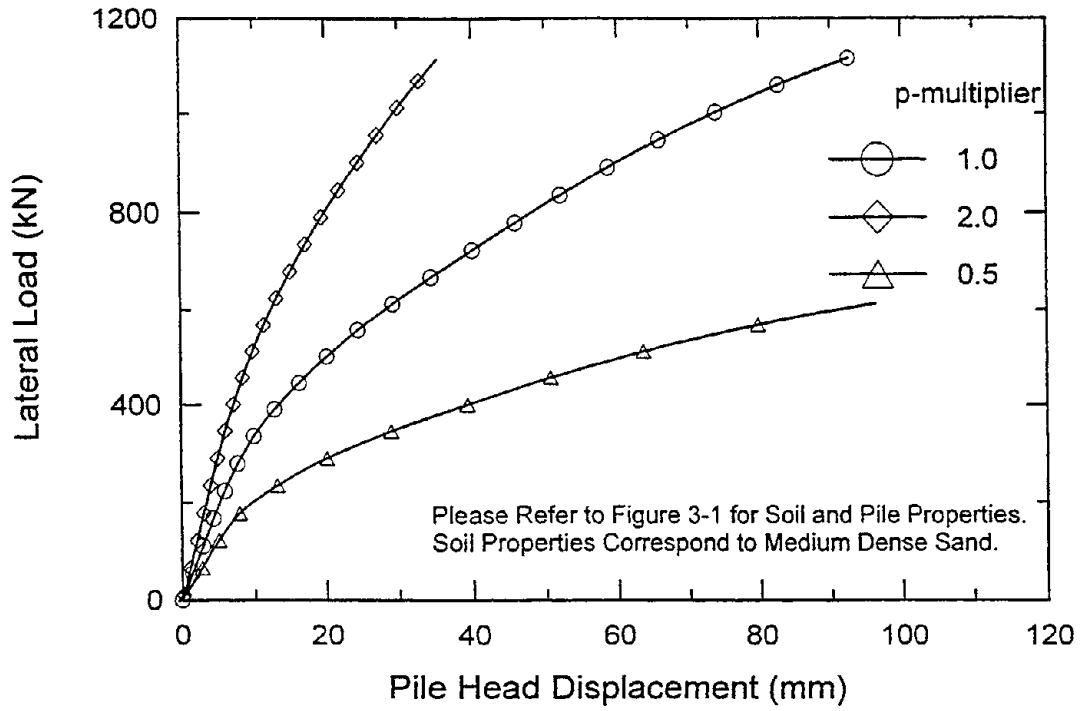


Figure 3-12 Effect of p-multiplier on Pile Response

pile is embedded below the ground level at a depth of 1D (1.2 m), and in the other 1.2 m of soil is removed at the ground level to model embedment and scouring effects, respectively. The calculated pile head displacements and maximum pile bending moments are plotted in figures 3-13a and 3-13b. The results indicate that the gapping (or scouring) effect would be more significant than the above discussed degradation and nonlinearity issue. The presented study assumes that the gapping (or scouring) effect is modeled as a loss of soil resistance to 1 pile diameter. This should be regarded as a lower bound case. Physical evidence from post-earthquake inspections and analytical studies (e.g. Lam and Law, 1994) suggest that gapping can extend to much deeper depths. From the presented sensitivity study, it can be judged that the gapping issue (i.e. geometric nonlinearity) would be more important and deserve more attention in design than the issue of soil nonlinearity, and to some extent, soil degradation.

3.3.2 Load Transfer Mechanism of Laterally Loaded Piles

The load transfer mechanism of laterally loaded piles is complex, and the subgrade reaction or the p-y model is a simplified representation of the mechanism. Lam and Martin (1986) indicate at least six different forms of load transfer between pile and soil under lateral load which are illustrated in figure 3-14. They are :

- (1) Lateral soil resistance due to translation of the pile.
- (2) Shear stresses along the sides of the pile resisting axial movement.
- (3) Axial resistance at the tip of the pile due to end bearing.
- (4) Rotational resistance along the shaft length due to tilting of the pile.
- (5) Rotational resistance at the tip of the pile.
- (6) Lateral resistance at the tip of the pile due to base shear.

In the p-y or any subgrade reaction model the effects of these factors are not accounted for separately; rather they are all lumped into one single parameter that represents lateral springs. For small diameter long piles, the effects of some of these load transfer mechanisms (e.g. items 4, 5) are not pronounced in the overall response of the pile. However, in large diameter shafts some of these effects may be significant. To develop some of these mechanisms, the pile needs to undergo large rotational movement. Single piles, such as those in pile extensions, may rotate significantly, and for these piles consideration of additional soil resistance is justified. However, pile rotation is restricted in a pile cap configuration and such rotational resistance (so-called "diameter effects") may not be justified. In addition, the side skin friction, which generates the rotational resistance, is influenced by installation procedure and the soil-pile interface properties (i.e. much higher unit skin friction when concrete is poured against soils as compared to driven piles). This suggests that the increase in resistance for large diameter shafts is, in part, due to how drilled shafts are constructed. Further comments on these issues are provided below.

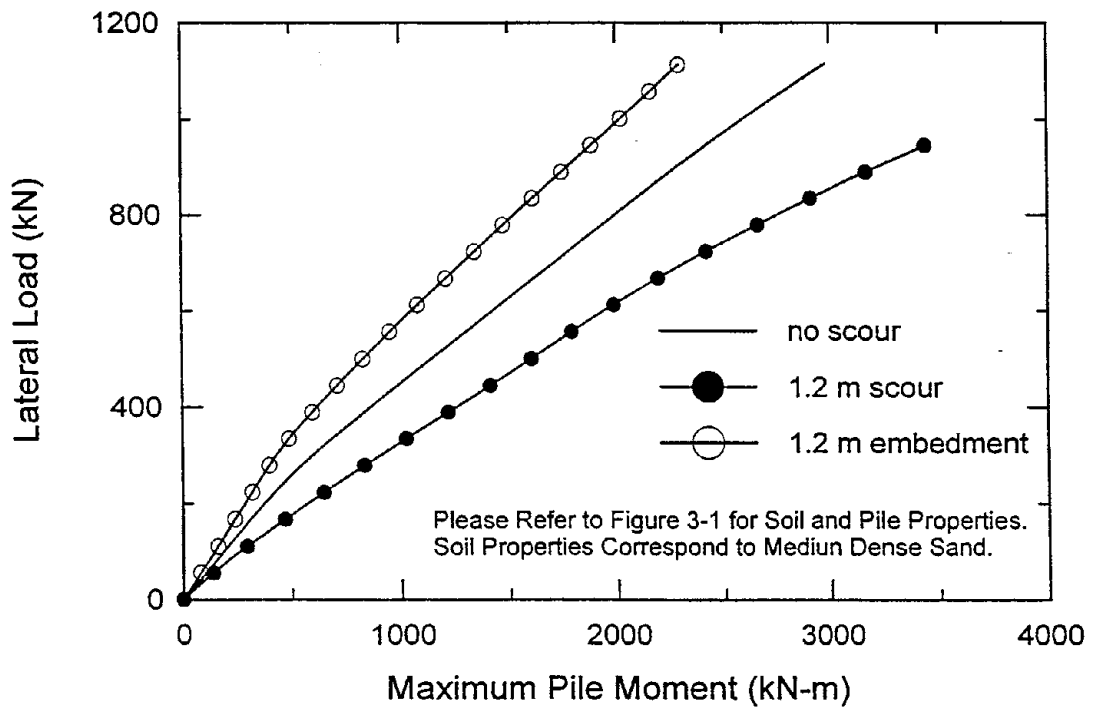
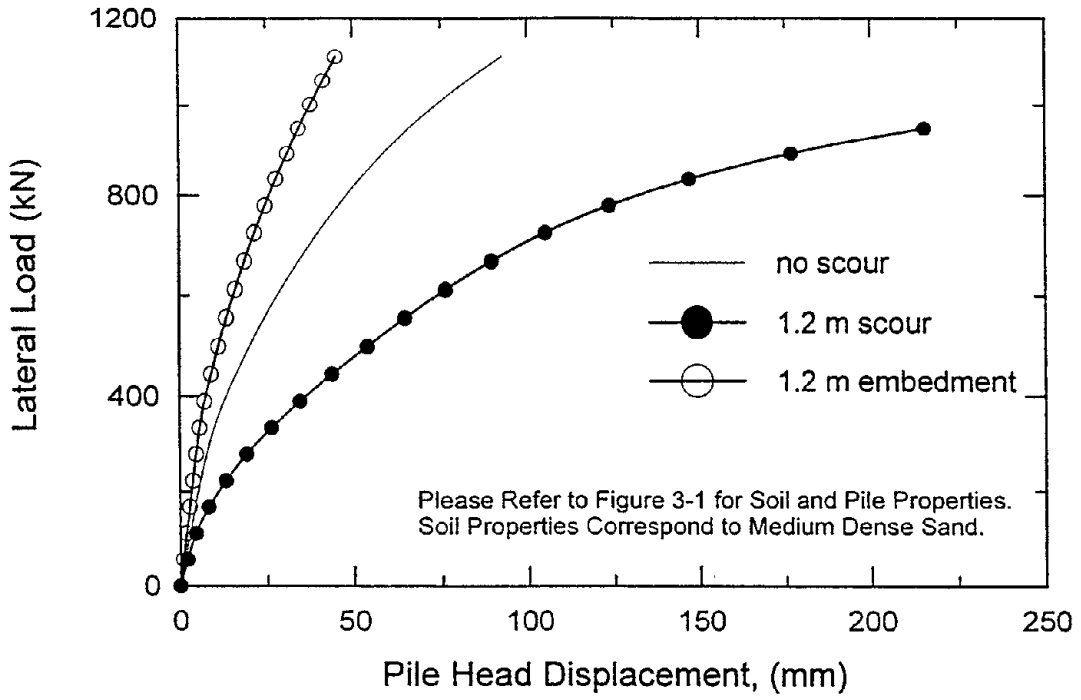


Figure 3-13 Effect of Scouring and Embedment on Pile Response

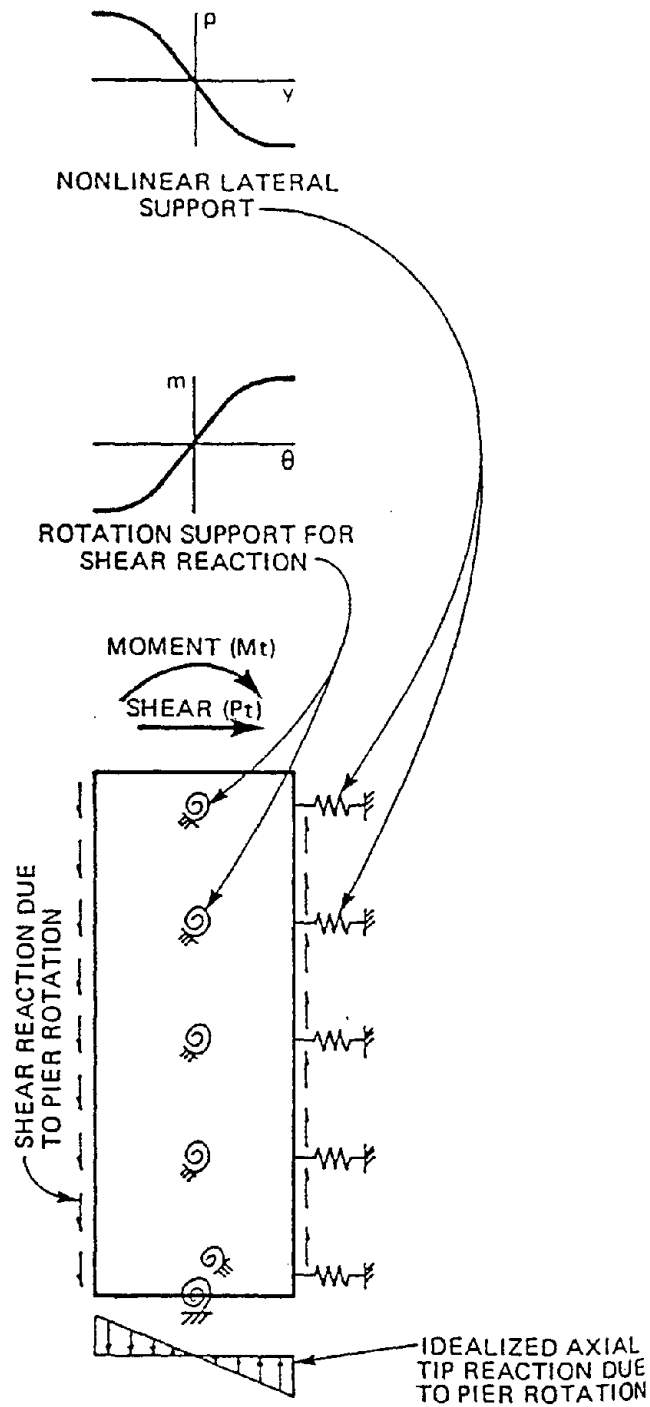


Figure 3-14 Load Transfer Mechanism of Drilled Shaft (after Lam and Martin, 1986)

3.3.3 Installation Procedure

Due to the differences in installation procedures of driven piles versus drilled shafts, the stress condition in the soil surrounding the pile can be quite different. It is possible that the differences in stiffness and the lateral load-carrying capacities of these two types of piles are influenced by the installation procedure. It is common knowledge that a drilled shaft develops higher skin friction capacity if the concrete is poured directly against the soil mass instead of pouring against a casing. This is the reason that any temporary casings must be retrieved in drilled shaft construction practice. The differences in installation method between drilled shafts and driven piles probably contributes to much of the observed differences in load test response of these two types of foundations.

3.3.4 Observation From Load Test Data

Pender (1993) describes lateral load tests on piles having diameter in excess of 1.0 m. From these tests it appears that the back calculated values of subgrade modulus are larger than those proposed by Terzaghi (1955). Pender indicated that the subgrade modulus increases linearly with diameter, and according to the procedure suggested by Carter (1984) and Ling (1988) may be given by

$$E_{s2} = E_{s1} \frac{D_1}{D_2} \quad (3-14)$$

in which E_{s1} and E_{s2} are modulus of subgrade reaction for pile diameter D_1 and D_2 , respectively.

Davidson (1982) performed lateral load tests on drilled shafts of 1.4m-diameter and larger. These load tests were intended for transmission tower applications where large overturning moments are expected. The lateral load were applied at about 24.4 m above the ground level with only 6.1 m pile embedment. The resulting pile displacement and rotation were quite high. He also performed a parametric study based on the finite element method. Based on these studies, he proposed a lateral resistance mechanism consisting of four springs that account for pile rotation as well as lateral translation. The modified model appeared to match the measured pile response reasonably well. These load tests have also been analyzed by Lam and Martin (1986). Their analyses indicate significant contribution from rotational resistance and base shear at the pile tip.

Naramore and Fang (1990) described lateral load tests on drilled shafts having diameter 4 and 8 ft (1.2 and 2.4 m). They also analyzed the piles using the program COM624 which utilizes the conventional Reese/Matlock p-y formulation. Their analyses indicate that the conventional p-y approach predicts a stiffer pile response. This observation differs from those mentioned above. However, the data presented by Naramore and Feng (which is quite different from results from other researchers) require more detailed evaluation and some comments are provided herein. The Naramore and Feng data might be an isolated case and may not appropriate on which to base general design guidelines. Some of the following issues need to be examined in more detail for the presented data:

- (1) The site consisted of very stiff to hard clay where secondary structures in the clay (fissures, etc.) tend to affect the resultant pile load test results. Therefore, one cannot merely assume that the intact shear strength of the clay would control the behavior of the pile soil system. For such very stiff sites, it would not be appropriate to use the intact soil shear strength directly for design when the shear strength exceeds a given threshold.
- (2) The Matlock soft clay and also the Reese stiff clay p-y criteria were all formulated using a parabolic equation which implies an infinite initial tangent stiffness. This shortcoming generally does not lead to significant error for soft clays, but could result in unsatisfactory solutions for the very stiff to hard clay condition.
- (3) There is a tremendous uncertainty in the bending stiffness of the large diameter concrete drilled shaft (i.e., what is the effective bending stiffness, EI_{eff}). Naramore and Feng's backfitting analysis and the calculated p-y curves could be obscured by the choice of the value.

3.3.5 Observations From Analytical Results

To examine the effect of large diameter on drilled shaft response, Lam and Law (1994) performed finite element analyses modeling the soil as a continuum. An elasto-plastic model was chosen for the soil, and the soil-pile interface was modeled as smooth as well as rough to examine the effect of skin friction. They found that for the rough faced pile, skin friction contributes toward rotational stiffness, and the pile response is stiffer. They also concluded that the mobilization of rotational stiffness is affected by the loading and boundary conditions. For fixed head piles with small rotation, the rotational restraint may not be significant.

SECTION 4 SUMMARY AND CONCLUSIONS

4.1 Summary

In Section 2, general modeling guidelines associated with the seismic design of pile foundations is presented. A two-step design process involved in seismic design is introduced and various design parameters that have an effect on the predicted foundation response are identified. Hence, the implications of foundation modeling process in the estimated structural response are described. The applicability of conventional p-y formulations in modeling soil-pile interaction behavior is examined. Some of the most recent research results for pile group effects and design of pile foundations for the lateral spread problem in liquefied soil are reviewed. Finally, modifications of p-y curves to account for cyclic loading conditions, pile group effects and soil-pile interaction behavior in liquefied soils are discussed.

Section 3 presents an overview of the characteristics of drilled shaft foundations. General recommendations are made for the seismic design of this specific type of foundation. The two-step design procedure described in Section 2 is adopted and various related design parameters that influence the foundation response are identified. Similarly, p-y formulations with various modifications are utilized in modeling drilled shaft foundation behavior.

4.2 Conclusions and Recommendations

The following conclusions can be made regarding seismic design of pile footings and drilled shafts from a geotechnical standpoint:

- (1) It is important to recognize how geotechnical recommendations are used by structural designers, particularly in a two-step seismic design process. Seismic demand can be expressed either in terms of displacements or forces imposed on the foundation as well as on the overall structural system. In other words, elements of foundation system can be designed for the deformations or the forces. Hence, when characterizing a foundation system for seismic design, seismic demand should be clearly identified depending on the chosen design criteria. Moreover, various uncertainties involved in defining the seismic demand should be carefully considered at this stage. Consequently, prevalent conservatism should be avoided in geotechnical recommendations for the seismic load case because (i) geotechnical engineers often do not know how their recommendations are implemented by the structural engineers, hence their "conservative" estimate of design parameters may lead to a counterproductive design, and (ii) although it may impose extremely severe demand on the structural and foundation system, occurrence of a seismic load case is very rare. Therefore, an economic decision-making would be necessary with some level of risk implied by the uncertainties in seismic load cases.
- (2) Characterization of the stiffness properties of an individual pile requires an evaluation of the pile load-displacement behavior under axial and lateral loading conditions depending on the pile configuration as well as the dominant load transfer/bearing mechanism. It must be noted

that unlike pile footings, drilled shaft foundations are typically pile extension type foundations in which the overall bridge response is generally insensitive to axial pile response. In fact, the axial pile loading, which is related to the rocking response of the pile group foundations, involves both material and geometric nonlinearities and therefore deserves more attention.

- (3) p-y models which define the nonlinear force-displacement relationship of a "soil spring" to analyze pile response (soil-pile interaction) can be reliably used, provided that the effect of various soil conditions, conditions that arise from different pile configurations, etc, are accounted for by appropriate scaling factors. Nonlinear p-y models are essentially semi-empirical and have been developed based on a limited number of full-scale lateral load tests on smaller diameter piles.
- (4) From the sensitivity study presented in Section 3, it can be concluded that the most important issue in foundation design and analysis relates to the need to properly consider boundary conditions (including scouring, gapping and how liquefaction affects the boundary conditions, as well as the pile head fixity and how it relates to connection details). Soil nonlinearity and, to some extent, variations in soil properties usually do not result in grossly different foundation behavior.
- (5) It can be readily said that uncertainties involved in p-y curves are in fact a rather insignificant problem compared to other sources of uncertainty, including pile-head fixity, the choice of bending stiffness of the piles and particularly the embedment issue which may cause two-fold variations in the predicted soil-pile stiffness.
- (6) In the pile footing design, apart from the individual pile stiffness, pile cap stiffness can also be incorporated in the overall system. In general, pile cap stiffness is defined as the ratio of ultimate soil capacity acting at the face of a pile cap to an estimated displacement to mobilize this capacity. For practical design applications, a passive pressure coefficient of 10 is recommended as a typical value to determine the pile cap resistance. The lateral deflection to mobilize this full passive pressure capacity can be taken as 1% to 2% of the thickness of the embedded pile cap depending on the soil type.
- (7) Pile group effects can be taken into account by p-multipliers. Analytical studies on the pile group effects on the overall response of the foundation systems have revealed that a uniform average multiplier would be adequate to incorporate the pile group effects in the design of typical pile group configurations. A p-multiplier of 0.5 on the standard static loading p-y curves involving typical pile groups is recommended, however, lower p-multipliers may be adopted to account for other factors such as gapping, potential cyclic degradation, etc.
- (8) Seismic design for the structural loading conditions in liquefiable soils requires consideration of the pore pressure build-up process and its effects on the fundamental stress-strain characteristics of the soil mass. In general, a p-multiplier of 0.5 is initially set for unliquefied p-y curves to reflect degradation due to local soil-pile interaction or softening due to pile group effects. The degradation coefficients are then used to establish the p-y curve

characteristics of the liquefied soil as a function of the free-field pore pressure. The resulting ultimate passive pressure, p_{ult} , on the pile is limited by $9cD$, where c is the undrained shear strength and D is the pile diameter.

- (9) It may be concluded that conventional p-y stiffnesses tend to be too soft for drilled shafts. This has been referred to as the "diameter effects" by various researchers. The mechanistic explanation for this diameter effect has been studied. For typical conditions for drilled shafts which include competent soil, concrete poured against soils directly which results in higher unit skin friction and positive moment on the shaft at mudline causing some degree of pile rotation, a higher subgrade stiffness is recommended for larger diameter shafts above 0.6m (24 in). Such scaling factors are recommended for most discrete soil spring approaches, including the linear Terzaghi's subgrade stiffness and the nonlinear p-y curve approach. Therefore, it is recommended that a scaling factor (larger than unity) to either the linear subgrade modulus or on the resistance value of the p-y curves for pile diameters greater than 0.6m (24 in) should be applied. The scaling factor would be the ratio of the pile diameter to 0.6m. For diameters smaller than 0.6m, conventional soil stiffness parameters should be used for design.
- (10) It is cautioned that the recommended diameter effects for the drilled shaft design should not be used blindly, without a sound mechanistic basis. It should be recognized that most offshore piles are large diameter (over 1.2 m or 48 in) driven steel pipe piles. However, poor soil conditions, the installation method and the jacket-leg configuration restrains the pile head against rotation at the mudline and no diameter effects are introduced in offshore pile design. Furthermore, other than Matlock and Reese's test data, a significant amount of pile load test data have been accumulated within the offshore industry (numerous papers presented over the past 30 year history of offshore technology conferences), including tests on 1.5 m (60 in) piles. The diameter effects for offshore piles have either been concluded as not valid or considered insignificant within the offshore industry.

SECTION 5 REFERENCES

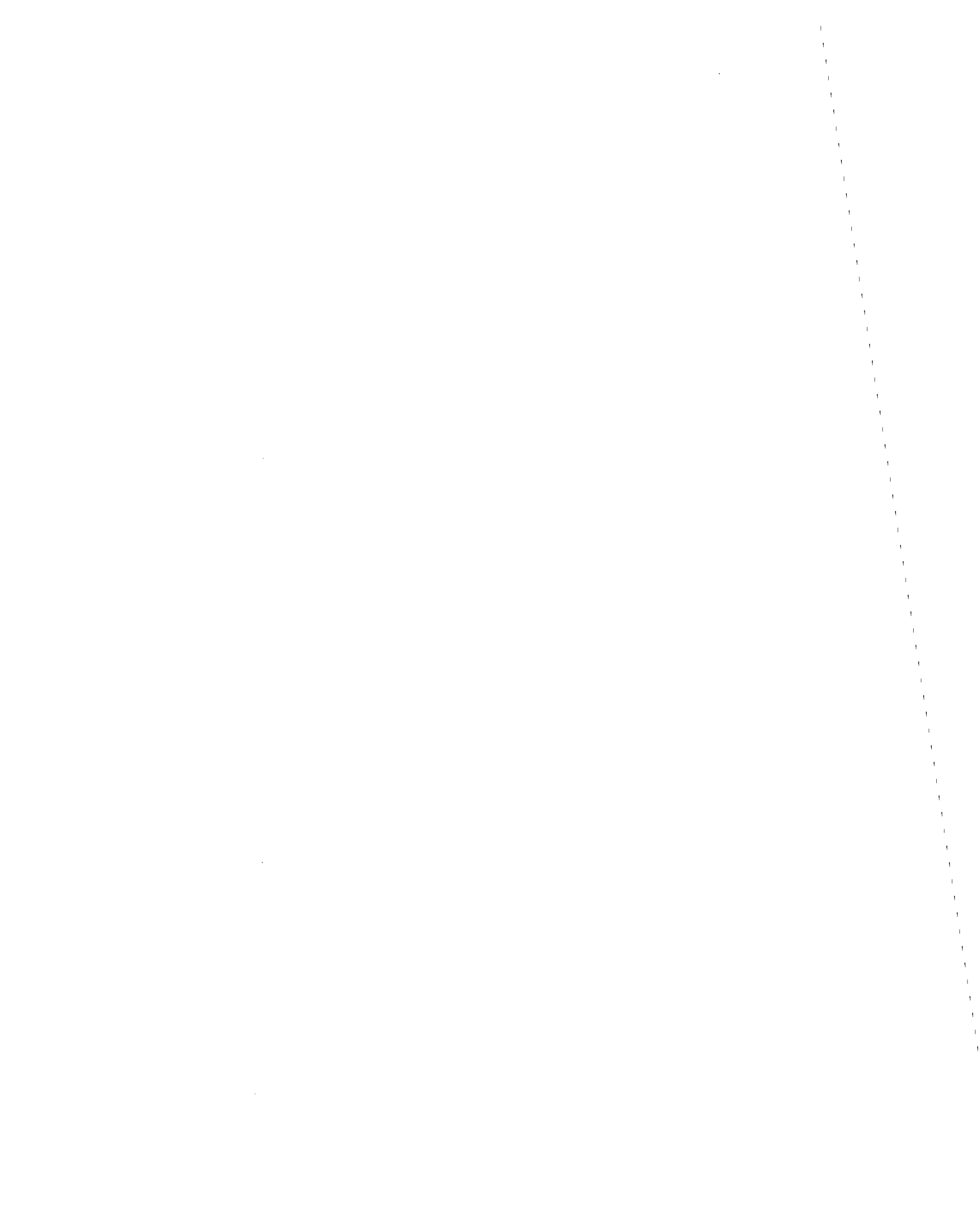
- Abcarius (1991), "Lateral Load Test on Driven Pile Footings," Proceedings, 3rd Bridge Engineering Conference, Denver, Colorado, March 10-13, Transportation Research Record No. 1290, Vol. 2.
- Abdoun, T.H. (1997), "Modeling of Seismically Induced Lateral Spreading of Multi-Layered Soil and Its Effect on Pile Foundations," Ph. D. Dissertation, Rensselaer Polytechnic Institute.
- Applied Technology Council (1996), "ATC-32, Improved Seismic Design Criteria for California Bridges: Provisional Recommendations."
- Bartlett, S.F. and Youd, T.L. (1992), "Empirical Analysis of Horizontal Ground Displacement Generated by Liquefaction-Induced Lateral Spreads", Technical Report NCEER-92-0021, Aug. 17.
- Berrill, J.B., Christensen, S.A., Keenan, R.J., Okada, W. and Pettinga, J.R., (1997), "Lateral-spreading loads on a piled bridge foundation," Seismic Behaviour of Ground and Geotechnical Structures, Seco e Pinto (Editor), Balkema, Rotterdam, ISBN 90 5410 887 8.
- Brown et al. (1987), Reese, L.C., and O'Neill, M.W. (1987), "Cyclic Lateral Loading of a Large-Scale Pile Group," Journal of Geotechnical Engineering, Vol. 113, No. 11, pp.1326-1343, November.
- Brown, D.A., Morrison, C. and Reese, L.C. (1988), "Lateral Load Behavior of a Pile Group in Sand", Journal of Geotechnical Engineering, ASCE, Vol. 114, No. 11.
- Bryant, L.M. (1977), "Three Dimensional Analysis of Framed Structures with Nonlinear Pile Foundation," Ph. D. Dissertation, University of Texas, Austin.
- Bryant, L.M., Lam, I.P.L., and Matlock, H. (1977), "Soil-Pile-Structure Interaction," Documentation for Programs: STAR, Structural Analysis Routines, and PASS, Pile and Structure Solution, Earth Mechanics, Inc.
- Caltrans, (1990), "Seismic Design References," California Department of Transportation, Sacramento, California.
- Caltrans BDS, (1993), "Bridge Design Specifications Manual", State of California, Department of Transportation, Sacramento, California, January.
- Caquot and Kerisel, (1948), "Tables for the Calculation of Passive Pressure, Active Pressure and Bearing Capacity of Foundations." Gauthiers-Villars, Paris.

- Carter, D. P. (1984), "A Nonlinear Soil Model for Predicting Lateral Pile Response", Report No. 359, Civil Engineering Department, University of Auckland.
- Chaudhuri, D. (1998), "Liquefaction and Lateral Soil Movement Effects on Piles," Ph.D. Dissertation, Cornell University, New York.
- Clough, G.W., and Duncan, J.M. (1991), "Chapter 6, Earth Pressures", Foundation Engineering Handbook, Second Edition, Edited by Fang, Hsai-Yang, Van Nostrand Reinhold, New York.
- Crouse, C.B., Kramer, L., Mitchell, R., and Hushmand, B. (1993) "Dynamic Tests of Pipe Pile in Saturated Peat," Journal of Technical Engineering, Vol. 119, No. 10, October 1993,
- Crouse, C.B., Kramer, L., Mitchell, R., and Hushmand, B. (1993), "Dynamic Tests of Pipe Pile in Saturated Peat," Journal of Technical Engineering, Vol. 119, No. 10, October 1993,
- Davidson, H. L. (1982), "Laterally Loaded Drilled Pier Research", Report No. EL-2197, Vol. 2, Electric Power Research Institute, Palo Alto, California.
- Douglas, B.M., and Norris, G.M., (1983), "Bridge Dynamic Tests: Implications for Seismic Design," ASCE Journal of Technical Topics in Civil Engineering, 1983, Vol. 109, No. 1.
- Gadre, A. (1997), Lateral Response of Pile-Cap Foundation Systems and Seat-Type Bridge Abutments in Dry Sand, Ph.D. Dissertation, Rensselaer Polytechnic Institute.
- GROUP (1994), "Documentation of Computer Program GROUP, Version 3.0," Ensoft Inc., Austin, Texas.
- Hetenyi, M. (1946), "Beams on Elastic Foundation", The University of Michigan Press, Ann Arbor.
- Holloway, D.M., Moriwaki, Y., Stevens, J.B., and Perez, J.-Y. (1981) "Response of a Pile Group to Combined Axial and Lateral Loading," Proceedings, 10th International Conference on Soil Mechanics and Foundation Engineering, Boulimia Publishers, Stockholm, Sweden, Vol 2.
- Idriss, I. M. and Sun, J. I. (1992), "User's Manual for SHAKE91," Center for Geotechnical Modeling, Department of Environmental Engineering, University of California, Davis, California.
- Lam, I. P. and Kapuskar, M. M. (1998), "Modeling of Pile Footings for Seismic Design" Technical Report to NCEER, not yet published.
- Lam, I. P. and Law, H. (1994), "Soil-Foundation-Structure Interaction - Analytical Considerations by Empirical p-y Methods", 4th CALTRANS Seismic Research Workshop, California Department of Transportation, Sacramento.
- Lam, I. P. and Martin, G. R. (1986), "Seismic Design of Highway Bridge Foundations, Vol. 2, Report No. FHWA/RD-86/102, Federal Highway Administration, McLean, Virginia.

- Lam, I. P., Martin, G. R., and Imbsen, R. (1991), "Modeling Bridge Foundations for Seismic Design and Retrofitting", Transportation Research Record 1290.
- Lam, I.P. (1994), Soil-Structure Interaction Related to Piles and Footings, Proceedings, Second International Workshop in Queenstown, New Zealand, Aug. 9-12.
- Lam, I.P., and Cheang, L.C. (1995), "Dynamic Soil-Pile Interaction Behavior in Submerged Sands," Proceedings, Earthquake-Induced Movements and Seismic Remediation of Existing Foundations and Abutments, ASCE Convention, San Diego, California, October 23-27, ASCE Geotechnical Special Publication No. 55.
- Ling, L. F. (1988), "Back Analysis of Lateral Load Tests on Piles", M. E. Thesis, Civil Engineering Department, University of Auckland.
- Liu, L. and Dobry, R., (1995), "Effect of liquefaction on Lateral Response of Piles by Centrifuge model Tests, Report submitted to NCEER.
- LPILE (1995), "Program LPILE Plus, Version 2.0" Ensoft Inc., Austin, Texas.
- Maroney, B., Kutter, B., Romstad, K., Chai, Y.H., and Vanderbilt, E. (1994), "Interpretation of Large Scale Bridge Abutment Test Results," Proceedings, Third Annual Seismic Workshop, Caltrans, Sacramento, California, June 27-29.
- Martin, G.R., Yan, L., and Lam, I.P. (1997), "Development and Implementation of Improved Seismic Design and Retrofit Procedures for Bridge Abutments," University of Southern California, Dept. Of Civil Engineering, Report to California Dept. of Transportation, Contract No. DOT 59Q121, Sept.
- Matlock, H. (1970), "Correlations for Design of Laterally Loaded Piles in Soft Clay", 2nd Offshore Technology Conference, Vol. 1, Houston, pp. 579-594.
- Matlock, H. and Reese, L. C. (1960), "Generalized Solutions for Laterally Loaded Piles", Journal of the Soil Mechanics and Foundation Division, ASCE, Vol. 86, No. SM5, pp. 63-91.
- Matlock, H., Bogard, D., Lam, I.P. (1981), "BMCOL 76, A Computer Program for the Analysis of Beam-Columns under Static Axial and Lateral Loading," University of Texas, Austin.
- McVay, M., Casper, R. and Shang, Te-I (1995), "Lateral Response of Three-Row Groups in Loose to Dense Sands at 3D and 5D Pile Spacing," Journal of Geotechnical Engineering, ASCE, Vol. 121, No. 5.
- Miranda E (1991), "Seismic Evaluation and Upgrading of Existing Buildings", Ph. D. Thesis, Department of Civil Engineering, University of California, Berkeley.

- Moulton, L.K., GangaRao, H.V.S., and Halvorsen, G.T. (1985), "Tolerable Movement Criteria for Highway Bridges," Report No. FHWA/RD-85/107, Federal Highway Administration, Washington, D.C.
- Murchison, J. M. and O'Neill, M. W. (1984), "Evaluation of p-y Relationships in Cohesionless Soils", Analysis and Design of Pile Foundations, ASCE, New York, pp. 174-191.
- Murchison, J.M., and O'Neill, M.W. (1983), "An Evaluation of p-y Relationships in Sands," Report No. PRAC 82-41-1 to the American Petroleum Institute, May.
- Naramore, S. A. and Feng, F. Y. (1990), "Field Tests of Large Diameter Drilled Shafts, Part I- Lateral Loads", Report No. FHWA/CA/SD-88/02, California Department of Transportation, Sacramento, California.
- NAVFAC, (1986), "Foundations & Earth Structures," Naval Facilities Engineering Command, Design Manual 7.02.
- NCHRP (1991), "Manuals for the Design of Bridge Foundations," Cooperative Highway Research Program Report 343, Dec.
- O'Neill, M.W. and Gazioglu, S.M., (1984), "An Evaluation of p-y Relationships in Clays," Report No. PRAC 82-41-2, American Petroleum Institute, April.
- Pender, M. J. (1993), "Aseismic Pile Foundation Design and Analysis", Bulletin of the New Zealand National Society for Earthquake Engineering, Vol. 26, No. 1, pp. 49-160.
- Poulos, H. G. and Davis, E. H. (1980), "Pile Foundation Analysis and Design", John Wiley and Sons, New York.
- Priestley, M. J. N. (1991), "Seismic Assessment of Existing Concrete Bridges", Seismic Assessment and Retrofit of Bridges, Report No. SSRP-91/03, Priestley and Seible Ed., pp. 84-149, University of California, San Diego, California.
- Priestley, M. J. N., Seible, F. and Calvi, G.M. (1996), "Seismic Design and Retrofit of Bridges", John Wiley and Sons, New York.
- Reese, L. C., Cox, W. R. and Koop, F. D. (1974), "Analysis of Laterally Loaded Piles in Sand", 6th Offshore Technology Conference, Houston, Vol. 2, pp. 473-483.
- Reese, L.C. and Sullivan, W.R., (1980), "Documentation of Computer Program COM624," Geotechnical Engineering Center, University of Texas, Austin.
- Rollins, K.M., Peterson, K.T., Weaver, T.J. (1997), "Lateral Load Behavior of a Full-Scale Pile Group in Clay", Submitted to ASCE Journal of Geotechnical Engineering for Publication.

- Ruesta, P.F., and Townsend, F.C. (1997), "Evaluation of Laterally Loaded Pile Group at Roosevelt Bridge," ASCE, Journal of Geotechnical Engineering, December, Vol. 123, No. 12.
- Seed, R.B., and Harder, L.F. Jr. (1991), SPT-Based Analysis of Cyclic Pore-Pressure Generation and Undrained Residual Strength," in Evaluation and Mitigation of Earthquake Induced Liquefaction Hazards, Seismic Short Course, San Francisco State University and University of Southern California, Los Angeles.
- Stevens, J. B. and Audibert, J. M. E. (1979), "Re-Examination of p-y Curve Formulations", 11th Offshore Technology Conference, Houston, pp.397-401.
- Terzaghi, K. (1955), "Evaluation of Coefficients of Subgrade Reaction", Geotechnique, Vol. 5, No. 4, pp. 297-326.
- Vesic, A. B. (1961), "Beams on Elastic Subgrade and Winkler's Hypothesis", 5th International Conference on Soil Mechanics and Foundation Engineering, Paris, Vol. 1, pp.845-850.
- Wilson, J.C. (1988), "Stiffness of Non-Skew Monolithic Bridge Abutments for Seismic Analysis," Earthquake Engineering and Structural Dynamics, Vol. 16.
- Yashinsky, and Zelinski (1993), Personal Communication.



Multidisciplinary Center for Earthquake Engineering Research List of Technical Reports

The Multidisciplinary Center for Earthquake Engineering Research (MCEER) publishes technical reports on a variety of subjects related to earthquake engineering written by authors funded through MCEER. These reports are available from both MCEER Publications and the National Technical Information Service (NTIS). Requests for reports should be directed to MCEER Publications, Multidisciplinary Center for Earthquake Engineering Research, State University of New York at Buffalo, Red Jacket Quadrangle, Buffalo, New York 14261. Reports can also be requested through NTIS, 5285 Port Royal Road, Springfield, Virginia 22161. NTIS accession numbers are shown in parenthesis, if available.

- NCEER-87-0001 "First-Year Program in Research, Education and Technology Transfer," 3/5/87, (PB88-134275, A04, MF-A01).
- NCEER-87-0002 "Experimental Evaluation of Instantaneous Optimal Algorithms for Structural Control," by R.C. Lin, T.T. Soong and A.M. Reinhorn, 4/20/87, (PB88-134341, A04, MF-A01).
- NCEER-87-0003 "Experimentation Using the Earthquake Simulation Facilities at University at Buffalo," by A.M. Reinhorn and R.L. Ketter, to be published.
- NCEER-87-0004 "The System Characteristics and Performance of a Shaking Table," by J.S. Hwang, K.C. Chang and G.C. Lee, 6/1/87, (PB88-134259, A03, MF-A01). This report is available only through NTIS (see address given above).
- NCEER-87-0005 "A Finite Element Formulation for Nonlinear Viscoplastic Material Using a Q Model," by O. Gyebi and G. Dasgupta, 11/2/87, (PB88-213764, A08, MF-A01).
- NCEER-87-0006 "Symbolic Manipulation Program (SMP) - Algebraic Codes for Two and Three Dimensional Finite Element Formulations," by X. Lee and G. Dasgupta, 11/9/87, (PB88-218522, A05, MF-A01).
- NCEER-87-0007 "Instantaneous Optimal Control Laws for Tall Buildings Under Seismic Excitations," by J.N. Yang, A. Akbarpour and P. Ghaemmaghami, 6/10/87, (PB88-134333, A06, MF-A01). This report is only available through NTIS (see address given above).
- NCEER-87-0008 "IDARC: Inelastic Damage Analysis of Reinforced Concrete Frame - Shear-Wall Structures," by Y.J. Park, A.M. Reinhorn and S.K. Kunnath, 7/20/87, (PB88-134325, A09, MF-A01). This report is only available through NTIS (see address given above).
- NCEER-87-0009 "Liquefaction Potential for New York State: A Preliminary Report on Sites in Manhattan and Buffalo," by M. Budhu, V. Vijayakumar, R.F. Giese and L. Baumgras, 8/31/87, (PB88-163704, A03, MF-A01). This report is available only through NTIS (see address given above).
- NCEER-87-0010 "Vertical and Torsional Vibration of Foundations in Inhomogeneous Media," by A.S. Veletsos and K.W. Dotson, 6/1/87, (PB88-134291, A03, MF-A01). This report is only available through NTIS (see address given above).
- NCEER-87-0011 "Seismic Probabilistic Risk Assessment and Seismic Margins Studies for Nuclear Power Plants," by Howard H.M. Hwang, 6/15/87, (PB88-134267, A03, MF-A01). This report is only available through NTIS (see address given above).
- NCEER-87-0012 "Parametric Studies of Frequency Response of Secondary Systems Under Ground-Acceleration Excitations," by Y. Yong and Y.K. Lin, 6/10/87, (PB88-134309, A03, MF-A01). This report is only available through NTIS (see address given above).
- NCEER-87-0013 "Frequency Response of Secondary Systems Under Seismic Excitation," by J.A. HoLung, J. Cai and Y.K. Lin, 7/31/87, (PB88-134317, A05, MF-A01). This report is only available through NTIS (see address given above).

- NCEER-87-0014 "Modelling Earthquake Ground Motions in Seismically Active Regions Using Parametric Time Series Methods," by G.W. Ellis and A.S. Cakmak, 8/25/87, (PB88-134283, A08, MF-A01). This report is only available through NTIS (see address given above).
- NCEER-87-0015 "Detection and Assessment of Seismic Structural Damage," by E. DiPasquale and A.S. Cakmak, 8/25/87, (PB88-163712, A05, MF-A01). This report is only available through NTIS (see address given above).
- NCEER-87-0016 "Pipeline Experiment at Parkfield, California," by J. Isenberg and E. Richardson, 9/15/87, (PB88-163720, A03, MF-A01). This report is available only through NTIS (see address given above).
- NCEER-87-0017 "Digital Simulation of Seismic Ground Motion," by M. Shinozuka, G. Deodatis and T. Harada, 8/31/87, (PB88-155197, A04, MF-A01). This report is available only through NTIS (see address given above).
- NCEER-87-0018 "Practical Considerations for Structural Control: System Uncertainty, System Time Delay and Truncation of Small Control Forces," J.N. Yang and A. Akbarpour, 8/10/87, (PB88-163738, A08, MF-A01). This report is only available through NTIS (see address given above).
- NCEER-87-0019 "Modal Analysis of Nonclassically Damped Structural Systems Using Canonical Transformation," by J.N. Yang, S. Sarkani and F.X. Long, 9/27/87, (PB88-187851, A04, MF-A01).
- NCEER-87-0020 "A Nonstationary Solution in Random Vibration Theory," by J.R. Red-Horse and P.D. Spanos, 11/3/87, (PB88-163746, A03, MF-A01).
- NCEER-87-0021 "Horizontal Impedances for Radially Inhomogeneous Viscoelastic Soil Layers," by A.S. Veletsos and K.W. Dotson, 10/15/87, (PB88-150859, A04, MF-A01).
- NCEER-87-0022 "Seismic Damage Assessment of Reinforced Concrete Members," by Y.S. Chung, C. Meyer and M. Shinozuka, 10/9/87, (PB88-150867, A05, MF-A01). This report is available only through NTIS (see address given above).
- NCEER-87-0023 "Active Structural Control in Civil Engineering," by T.T. Soong, 11/11/87, (PB88-187778, A03, MF-A01).
- NCEER-87-0024 "Vertical and Torsional Impedances for Radially Inhomogeneous Viscoelastic Soil Layers," by K.W. Dotson and A.S. Veletsos, 12/87, (PB88-187786, A03, MF-A01).
- NCEER-87-0025 "Proceedings from the Symposium on Seismic Hazards, Ground Motions, Soil-Liquefaction and Engineering Practice in Eastern North America," October 20-22, 1987, edited by K.H. Jacob, 12/87, (PB88-188115, A23, MF-A01). This report is available only through NTIS (see address given above).
- NCEER-87-0026 "Report on the Whittier-Narrows, California, Earthquake of October 1, 1987," by J. Pantelic and A. Reinhorn, 11/87, (PB88-187752, A03, MF-A01). This report is available only through NTIS (see address given above).
- NCEER-87-0027 "Design of a Modular Program for Transient Nonlinear Analysis of Large 3-D Building Structures," by S. Srivastav and J.F. Abel, 12/30/87, (PB88-187950, A05, MF-A01). This report is only available through NTIS (see address given above).
- NCEER-87-0028 "Second-Year Program in Research, Education and Technology Transfer," 3/8/88, (PB88-219480, A04, MF-A01).
- NCEER-88-0001 "Workshop on Seismic Computer Analysis and Design of Buildings With Interactive Graphics," by W. McGuire, J.F. Abel and C.H. Conley, 1/18/88, (PB88-187760, A03, MF-A01). This report is only available through NTIS (see address given above).
- NCEER-88-0002 "Optimal Control of Nonlinear Flexible Structures," by J.N. Yang, F.X. Long and D. Wong, 1/22/88, (PB88-213772, A06, MF-A01).

- NCEER-88-0003 "Substructuring Techniques in the Time Domain for Primary-Secondary Structural Systems," by G.D. Manolis and G. Juhn, 2/10/88, (PB88-213780, A04, MF-A01).
- NCEER-88-0004 "Iterative Seismic Analysis of Primary-Secondary Systems," by A. Singhal, L.D. Lutes and P.D. Spanos, 2/23/88, (PB88-213798, A04, MF-A01).
- NCEER-88-0005 "Stochastic Finite Element Expansion for Random Media," by P.D. Spanos and R. Ghanem, 3/14/88, (PB88-213806, A03, MF-A01).
- NCEER-88-0006 "Combining Structural Optimization and Structural Control," by F.Y. Cheng and C.P. Pantelides, 1/10/88, (PB88-213814, A05, MF-A01).
- NCEER-88-0007 "Seismic Performance Assessment of Code-Designed Structures," by H.H-M. Hwang, J-W. Jaw and H-J. Shau, 3/20/88, (PB88-219423, A04, MF-A01). This report is only available through NTIS (see address given above).
- NCEER-88-0008 "Reliability Analysis of Code-Designed Structures Under Natural Hazards," by H.H-M. Hwang, H. Ushiba and M. Shinozuka, 2/29/88, (PB88-229471, A07, MF-A01). This report is only available through NTIS (see address given above).
- NCEER-88-0009 "Seismic Fragility Analysis of Shear Wall Structures," by J-W Jaw and H.H-M. Hwang, 4/30/88, (PB89-102867, A04, MF-A01).
- NCEER-88-0010 "Base Isolation of a Multi-Story Building Under a Harmonic Ground Motion - A Comparison of Performances of Various Systems," by F-G Fan, G. Ahmadi and I.G. Tadjbakhsh, 5/18/88, (PB89-122238, A06, MF-A01). This report is only available through NTIS (see address given above).
- NCEER-88-0011 "Seismic Floor Response Spectra for a Combined System by Green's Functions," by F.M. Lavelle, L.A. Bergman and P.D. Spanos, 5/1/88, (PB89-102875, A03, MF-A01).
- NCEER-88-0012 "A New Solution Technique for Randomly Excited Hysteretic Structures," by G.Q. Cai and Y.K. Lin, 5/16/88, (PB89-102883, A03, MF-A01).
- NCEER-88-0013 "A Study of Radiation Damping and Soil-Structure Interaction Effects in the Centrifuge," by K. Weissman, supervised by J.H. Prevost, 5/24/88, (PB89-144703, A06, MF-A01).
- NCEER-88-0014 "Parameter Identification and Implementation of a Kinematic Plasticity Model for Frictional Soils," by J.H. Prevost and D.V. Griffiths, to be published.
- NCEER-88-0015 "Two- and Three- Dimensional Dynamic Finite Element Analyses of the Long Valley Dam," by D.V. Griffiths and J.H. Prevost, 6/17/88, (PB89-144711, A04, MF-A01).
- NCEER-88-0016 "Damage Assessment of Reinforced Concrete Structures in Eastern United States," by A.M. Reinhorn, M.J. Seidel, S.K. Kunnath and Y.J. Park, 6/15/88, (PB89-122220, A04, MF-A01). This report is only available through NTIS (see address given above).
- NCEER-88-0017 "Dynamic Compliance of Vertically Loaded Strip Foundations in Multilayered Viscoelastic Soils," by S. Ahmad and A.S.M. Israil, 6/17/88, (PB89-102891, A04, MF-A01).
- NCEER-88-0018 "An Experimental Study of Seismic Structural Response With Added Viscoelastic Dampers," by R.C. Lin, Z. Liang, T.T. Soong and R.H. Zhang, 6/30/88, (PB89-122212, A05, MF-A01). This report is available only through NTIS (see address given above).
- NCEER-88-0019 "Experimental Investigation of Primary - Secondary System Interaction," by G.D. Manolis, G. Juhn and A.M. Reinhorn, 5/27/88, (PB89-122204, A04, MF-A01).

- NCEER-88-0020 "A Response Spectrum Approach For Analysis of Nonclassically Damped Structures," by J.N. Yang, S. Sarkani and F.X. Long, 4/22/88, (PB89-102909, A04, MF-A01).
- NCEER-88-0021 "Seismic Interaction of Structures and Soils: Stochastic Approach," by A.S. Veletsos and A.M. Prasad, 7/21/88, (PB89-122196, A04, MF-A01). This report is only available through NTIS (see address given above).
- NCEER-88-0022 "Identification of the Serviceability Limit State and Detection of Seismic Structural Damage," by E. DiPasquale and A.S. Cakmak, 6/15/88, (PB89-122188, A05, MF-A01). This report is available only through NTIS (see address given above).
- NCEER-88-0023 "Multi-Hazard Risk Analysis: Case of a Simple Offshore Structure," by B.K. Bhartia and E.H. Vanmarcke, 7/21/88, (PB89-145213, A05, MF-A01).
- NCEER-88-0024 "Automated Seismic Design of Reinforced Concrete Buildings," by Y.S. Chung, C. Meyer and M. Shinozuka, 7/5/88, (PB89-122170, A06, MF-A01). This report is available only through NTIS (see address given above).
- NCEER-88-0025 "Experimental Study of Active Control of MDOF Structures Under Seismic Excitations," by L.L. Chung, R.C. Lin, T.T. Soong and A.M. Reinhorn, 7/10/88, (PB89-122600, A04, MF-A01).
- NCEER-88-0026 "Earthquake Simulation Tests of a Low-Rise Metal Structure," by J.S. Hwang, K.C. Chang, G.C. Lee and R.L. Ketter, 8/1/88, (PB89-102917, A04, MF-A01).
- NCEER-88-0027 "Systems Study of Urban Response and Reconstruction Due to Catastrophic Earthquakes," by F. Kozin and H.K. Zhou, 9/22/88, (PB90-162348, A04, MF-A01).
- NCEER-88-0028 "Seismic Fragility Analysis of Plane Frame Structures," by H.H.M. Hwang and Y.K. Low, 7/31/88, (PB89-131445, A06, MF-A01).
- NCEER-88-0029 "Response Analysis of Stochastic Structures," by A. Kardara, C. Bucher and M. Shinozuka, 9/22/88, (PB89-174429, A04, MF-A01).
- NCEER-88-0030 "Nonnormal Accelerations Due to Yielding in a Primary Structure," by D.C.K. Chen and L.D. Lutes, 9/19/88, (PB89-131437, A04, MF-A01).
- NCEER-88-0031 "Design Approaches for Soil-Structure Interaction," by A.S. Veletsos, A.M. Prasad and Y. Tang, 12/30/88, (PB89-174437, A03, MF-A01). This report is available only through NTIS (see address given above).
- NCEER-88-0032 "A Re-evaluation of Design Spectra for Seismic Damage Control," by C.J. Turkstra and A.G. Tallin, 11/7/88, (PB89-145221, A05, MF-A01).
- NCEER-88-0033 "The Behavior and Design of Noncontact Lap Splices Subjected to Repeated Inelastic Tensile Loading," by V.E. Sagan, P. Gergely and R.N. White, 12/8/88, (PB89-163737, A08, MF-A01).
- NCEER-88-0034 "Seismic Response of Pile Foundations," by S.M. Mamoon, P.K. Banerjee and S. Ahmad, 11/1/88, (PB89-145239, A04, MF-A01).
- NCEER-88-0035 "Modeling of R/C Building Structures With Flexible Floor Diaphragms (IDARC2)," by A.M. Reinhorn, S.K. Kunnath and N. Panahshahi, 9/7/88, (PB89-207153, A07, MF-A01).
- NCEER-88-0036 "Solution of the Dam-Reservoir Interaction Problem Using a Combination of FEM, BEM with Particular Integrals, Modal Analysis, and Substructuring," by C-S. Tsai, G.C. Lee and R.L. Ketter, 12/31/88, (PB89-207146, A04, MF-A01).
- NCEER-88-0037 "Optimal Placement of Actuators for Structural Control," by F.Y. Cheng and C.P. Pantelides, 8/15/88, (PB89-162846, A05, MF-A01).

- NCEER-88-0038 "Teflon Bearings in Aseismic Base Isolation: Experimental Studies and Mathematical Modeling," by A. Mokha, M.C. Constantinou and A.M. Reinhorn, 12/5/88, (PB89-218457, A10, MF-A01). This report is available only through NTIS (see address given above).
- NCEER-88-0039 "Seismic Behavior of Flat Slab High-Rise Buildings in the New York City Area," by P. Weidlinger and M. Ettouney, 10/15/88, (PB90-145681, A04, MF-A01).
- NCEER-88-0040 "Evaluation of the Earthquake Resistance of Existing Buildings in New York City," by P. Weidlinger and M. Ettouney, 10/15/88, to be published.
- NCEER-88-0041 "Small-Scale Modeling Techniques for Reinforced Concrete Structures Subjected to Seismic Loads," by W. Kim, A. El-Attar and R.N. White, 11/22/88, (PB89-189625, A05, MF-A01).
- NCEER-88-0042 "Modeling Strong Ground Motion from Multiple Event Earthquakes," by G.W. Ellis and A.S. Cakmak, 10/15/88, (PB89-174445, A03, MF-A01).
- NCEER-88-0043 "Nonstationary Models of Seismic Ground Acceleration," by M. Grigoriu, S.E. Ruiz and E. Rosenblueth, 7/15/88, (PB89-189617, A04, MF-A01).
- NCEER-88-0044 "SARCF User's Guide: Seismic Analysis of Reinforced Concrete Frames," by Y.S. Chung, C. Meyer and M. Shinozuka, 11/9/88, (PB89-174452, A08, MF-A01).
- NCEER-88-0045 "First Expert Panel Meeting on Disaster Research and Planning," edited by J. Pantelic and J. Stoyke, 9/15/88, (PB89-174460, A05, MF-A01).
- NCEER-88-0046 "Preliminary Studies of the Effect of Degrading Infill Walls on the Nonlinear Seismic Response of Steel Frames," by C.Z. Chrysostomou, P. Gergely and J.F. Abel, 12/19/88, (PB89-208383, A05, MF-A01).
- NCEER-88-0047 "Reinforced Concrete Frame Component Testing Facility - Design, Construction, Instrumentation and Operation," by S.P. Pessiki, C. Conley, T. Bond, P. Gergely and R.N. White, 12/16/88, (PB89-174478, A04, MF-A01).
- NCEER-89-0001 "Effects of Protective Cushion and Soil Compliancy on the Response of Equipment Within a Seismically Excited Building," by J.A. HoLung, 2/16/89, (PB89-207179, A04, MF-A01).
- NCEER-89-0002 "Statistical Evaluation of Response Modification Factors for Reinforced Concrete Structures," by H.H-M. Hwang and J-W. Jaw, 2/17/89, (PB89-207187, A05, MF-A01).
- NCEER-89-0003 "Hysteretic Columns Under Random Excitation," by G-Q. Cai and Y.K. Lin, 1/9/89, (PB89-196513, A03, MF-A01).
- NCEER-89-0004 "Experimental Study of 'Elephant Foot Bulge' Instability of Thin-Walled Metal Tanks," by Z-H. Jia and R.L. Ketter, 2/22/89, (PB89-207195, A03, MF-A01).
- NCEER-89-0005 "Experiment on Performance of Buried Pipelines Across San Andreas Fault," by J. Isenberg, E. Richardson and T.D. O'Rourke, 3/10/89, (PB89-218440, A04, MF-A01). This report is available only through NTIS (see address given above).
- NCEER-89-0006 "A Knowledge-Based Approach to Structural Design of Earthquake-Resistant Buildings," by M. Subramani, P. Gergely, C.H. Conley, J.F. Abel and A.H. Zaghaw, 1/15/89, (PB89-218465, A06, MF-A01).
- NCEER-89-0007 "Liquefaction Hazards and Their Effects on Buried Pipelines," by T.D. O'Rourke and P.A. Lane, 2/1/89, (PB89-218481, A09, MF-A01).

- NCEER-89-0008 "Fundamentals of System Identification in Structural Dynamics," by H. Imai, C-B. Yun, O. Maruyama and M. Shinozuka, 1/26/89, (PB89-207211, A04, MF-A01).
- NCEER-89-0009 "Effects of the 1985 Michoacan Earthquake on Water Systems and Other Buried Lifelines in Mexico," by A.G. Ayala and M.J. O'Rourke, 3/8/89, (PB89-207229, A06, MF-A01).
- NCEER-89-R010 "NCEER Bibliography of Earthquake Education Materials," by K.E.K. Ross, Second Revision, 9/1/89, (PB90-125352, A05, MF-A01). This report is replaced by NCEER-92-0018.
- NCEER-89-0011 "Inelastic Three-Dimensional Response Analysis of Reinforced Concrete Building Structures (IDARC-3D), Part I - Modeling," by S.K. Kunnath and A.M. Reinhorn, 4/17/89, (PB90-114612, A07, MF-A01). This report is available only through NTIS (see address given above).
- NCEER-89-0012 "Recommended Modifications to ATC-14," by C.D. Poland and J.O. Malley, 4/12/89, (PB90-108648, A15, MF-A01).
- NCEER-89-0013 "Repair and Strengthening of Beam-to-Column Connections Subjected to Earthquake Loading," by M. Corazao and A.J. Durrani, 2/28/89, (PB90-109885, A06, MF-A01).
- NCEER-89-0014 "Program EXKAL2 for Identification of Structural Dynamic Systems," by O. Maruyama, C-B. Yun, M. Hoshiya and M. Shinozuka, 5/19/89, (PB90-109877, A09, MF-A01).
- NCEER-89-0015 "Response of Frames With Bolted Semi-Rigid Connections, Part I - Experimental Study and Analytical Predictions," by P.J. DiCorso, A.M. Reinhorn, J.R. Dickerson, J.B. Radzimirski and W.L. Harper, 6/1/89, to be published.
- NCEER-89-0016 "ARMA Monte Carlo Simulation in Probabilistic Structural Analysis," by P.D. Spanos and M.P. Mignolet, 7/10/89, (PB90-109893, A03, MF-A01).
- NCEER-89-P017 "Preliminary Proceedings from the Conference on Disaster Preparedness - The Place of Earthquake Education in Our Schools," Edited by K.E.K. Ross, 6/23/89, (PB90-108606, A03, MF-A01).
- NCEER-89-0017 "Proceedings from the Conference on Disaster Preparedness - The Place of Earthquake Education in Our Schools," Edited by K.E.K. Ross, 12/31/89, (PB90-207895, A012, MF-A02). This report is available only through NTIS (see address given above).
- NCEER-89-0018 "Multidimensional Models of Hysteretic Material Behavior for Vibration Analysis of Shape Memory Energy Absorbing Devices, by E.J. Graesser and F.A. Cozzarelli, 6/7/89, (PB90-164146, A04, MF-A01).
- NCEER-89-0019 "Nonlinear Dynamic Analysis of Three-Dimensional Base Isolated Structures (3D-BASIS)," by S. Nagarajaiah, A.M. Reinhorn and M.C. Constantinou, 8/3/89, (PB90-161936, A06, MF-A01). This report has been replaced by NCEER-93-0011.
- NCEER-89-0020 "Structural Control Considering Time-Rate of Control Forces and Control Rate Constraints," by F.Y. Cheng and C.P. Pantelides, 8/3/89, (PB90-120445, A04, MF-A01).
- NCEER-89-0021 "Subsurface Conditions of Memphis and Shelby County," by K.W. Ng, T-S. Chang and H-H.M. Hwang, 7/26/89, (PB90-120437, A03, MF-A01).
- NCEER-89-0022 "Seismic Wave Propagation Effects on Straight Jointed Buried Pipelines," by K. Elhadi and M.J. O'Rourke, 8/24/89, (PB90-162322, A10, MF-A02).
- NCEER-89-0023 "Workshop on Serviceability Analysis of Water Delivery Systems," edited by M. Grigoriu, 3/6/89, (PB90-127424, A03, MF-A01).
- NCEER-89-0024 "Shaking Table Study of a 1/5 Scale Steel Frame Composed of Tapered Members," by K.C. Chang, J.S. Hwang and G.C. Lee, 9/18/89, (PB90-160169, A04, MF-A01).

- NCEER-89-0025 "DYNA1D: A Computer Program for Nonlinear Seismic Site Response Analysis - Technical Documentation," by Jean H. Prevost, 9/14/89, (PB90-161944, A07, MF-A01). This report is available only through NTIS (see address given above).
- NCEER-89-0026 "1:4 Scale Model Studies of Active Tendon Systems and Active Mass Dampers for Aseismic Protection," by A.M. Reinhorn, T.T. Soong, R.C. Lin, Y.P. Yang, Y. Fukao, H. Abe and M. Nakai, 9/15/89, (PB90-173246, A10, MF-A02). This report is available only through NTIS (see address given above).
- NCEER-89-0027 "Scattering of Waves by Inclusions in a Nonhomogeneous Elastic Half Space Solved by Boundary Element Methods," by P.K. Hadley, A. Askar and A.S. Cakmak, 6/15/89, (PB90-145699, A07, MF-A01).
- NCEER-89-0028 "Statistical Evaluation of Deflection Amplification Factors for Reinforced Concrete Structures," by H.H.M. Hwang, J-W. Jaw and A.L. Ch'ng, 8/31/89, (PB90-164633, A05, MF-A01).
- NCEER-89-0029 "Bedrock Accelerations in Memphis Area Due to Large New Madrid Earthquakes," by H.H.M. Hwang, C.H.S. Chen and G. Yu, 11/7/89, (PB90-162330, A04, MF-A01).
- NCEER-89-0030 "Seismic Behavior and Response Sensitivity of Secondary Structural Systems," by Y.Q. Chen and T.T. Soong, 10/23/89, (PB90-164658, A08, MF-A01).
- NCEER-89-0031 "Random Vibration and Reliability Analysis of Primary-Secondary Structural Systems," by Y. Ibrahim, M. Grigoriu and T.T. Soong, 11/10/89, (PB90-161951, A04, MF-A01).
- NCEER-89-0032 "Proceedings from the Second U.S. - Japan Workshop on Liquefaction, Large Ground Deformation and Their Effects on Lifelines, September 26-29, 1989," Edited by T.D. O'Rourke and M. Hamada, 12/1/89, (PB90-209388, A22, MF-A03).
- NCEER-89-0033 "Deterministic Model for Seismic Damage Evaluation of Reinforced Concrete Structures," by J.M. Bracci, A.M. Reinhorn, J.B. Mander and S.K. Kunnath, 9/27/89, (PB91-108803, A06, MF-A01).
- NCEER-89-0034 "On the Relation Between Local and Global Damage Indices," by E. DiPasquale and A.S. Cakmak, 8/15/89, (PB90-173865, A05, MF-A01).
- NCEER-89-0035 "Cyclic Undrained Behavior of Nonplastic and Low Plasticity Silts," by A.J. Walker and H.E. Stewart, 7/26/89, (PB90-183518, A10, MF-A01).
- NCEER-89-0036 "Liquefaction Potential of Surficial Deposits in the City of Buffalo, New York," by M. Budhu, R. Giese and L. Baumgrass, 1/17/89, (PB90-208455, A04, MF-A01).
- NCEER-89-0037 "A Deterministic Assessment of Effects of Ground Motion Incoherence," by A.S. Veletsos and Y. Tang, 7/15/89, (PB90-164294, A03, MF-A01).
- NCEER-89-0038 "Workshop on Ground Motion Parameters for Seismic Hazard Mapping," July 17-18, 1989, edited by R.V. Whitman, 12/1/89, (PB90-173923, A04, MF-A01).
- NCEER-89-0039 "Seismic Effects on Elevated Transit Lines of the New York City Transit Authority," by C.J. Costantino, C.A. Miller and E. Heymsfield, 12/26/89, (PB90-207887, A06, MF-A01).
- NCEER-89-0040 "Centrifugal Modeling of Dynamic Soil-Structure Interaction," by K. Weissman, Supervised by J.H. Prevost, 5/10/89, (PB90-207879, A07, MF-A01).
- NCEER-89-0041 "Linearized Identification of Buildings With Cores for Seismic Vulnerability Assessment," by I-K. Ho and A.E. Aktan, 11/1/89, (PB90-251943, A07, MF-A01).
- NCEER-90-0001 "Geotechnical and Lifeline Aspects of the October 17, 1989 Loma Prieta Earthquake in San Francisco," by T.D. O'Rourke, H.E. Stewart, F.T. Blackburn and T.S. Dickerman, 1/90, (PB90-208596, A05, MF-A01).

- NCEER-90-0002 "Nonnormal Secondary Response Due to Yielding in a Primary Structure," by D.C.K. Chen and L.D. Lutes, 2/28/90, (PB90-251976, A07, MF-A01).
- NCEER-90-0003 "Earthquake Education Materials for Grades K-12," by K.E.K. Ross, 4/16/90, (PB91-251984, A05, MF-A05). This report has been replaced by NCEER-92-0018.
- NCEER-90-0004 "Catalog of Strong Motion Stations in Eastern North America," by R.W. Busby, 4/3/90, (PB90-251984, A05, MF-A01).
- NCEER-90-0005 "NCEER Strong-Motion Data Base: A User Manual for the GeoBase Release (Version 1.0 for the Sun3)," by P. Friberg and K. Jacob, 3/31/90 (PB90-258062, A04, MF-A01).
- NCEER-90-0006 "Seismic Hazard Along a Crude Oil Pipeline in the Event of an 1811-1812 Type New Madrid Earthquake," by H.H.M. Hwang and C-H.S. Chen, 4/16/90, (PB90-258054, A04, MF-A01).
- NCEER-90-0007 "Site-Specific Response Spectra for Memphis Sheahan Pumping Station," by H.H.M. Hwang and C.S. Lee, 5/15/90, (PB91-108811, A05, MF-A01).
- NCEER-90-0008 "Pilot Study on Seismic Vulnerability of Crude Oil Transmission Systems," by T. Ariman, R. Dobry, M. Grigoriu, F. Kozin, M. O'Rourke, T. O'Rourke and M. Shinozuka, 5/25/90, (PB91-108837, A06, MF-A01).
- NCEER-90-0009 "A Program to Generate Site Dependent Time Histories: EQGEN," by G.W. Ellis, M. Srinivasan and A.S. Cakmak, 1/30/90, (PB91-108829, A04, MF-A01).
- NCEER-90-0010 "Active Isolation for Seismic Protection of Operating Rooms," by M.E. Talbott, Supervised by M. Shinozuka, 6/8/9, (PB91-110205, A05, MF-A01).
- NCEER-90-0011 "Program LINEARID for Identification of Linear Structural Dynamic Systems," by C-B. Yun and M. Shinozuka, 6/25/90, (PB91-110312, A08, MF-A01).
- NCEER-90-0012 "Two-Dimensional Two-Phase Elasto-Plastic Seismic Response of Earth Dams," by A.N. Yiagos, Supervised by J.H. Prevost, 6/20/90, (PB91-110197, A13, MF-A02).
- NCEER-90-0013 "Secondary Systems in Base-Isolated Structures: Experimental Investigation, Stochastic Response and Stochastic Sensitivity," by G.D. Manolis, G. Juhn, M.C. Constantinou and A.M. Reinhorn, 7/1/90, (PB91-110320, A08, MF-A01).
- NCEER-90-0014 "Seismic Behavior of Lightly-Reinforced Concrete Column and Beam-Column Joint Details," by S.P. Pessiki, C.H. Conley, P. Gergely and R.N. White, 8/22/90, (PB91-108795, A11, MF-A02).
- NCEER-90-0015 "Two Hybrid Control Systems for Building Structures Under Strong Earthquakes," by J.N. Yang and A. Danielians, 6/29/90, (PB91-125393, A04, MF-A01).
- NCEER-90-0016 "Instantaneous Optimal Control with Acceleration and Velocity Feedback," by J.N. Yang and Z. Li, 6/29/90, (PB91-125401, A03, MF-A01).
- NCEER-90-0017 "Reconnaissance Report on the Northern Iran Earthquake of June 21, 1990," by M. Mehrain, 10/4/90, (PB91-125377, A03, MF-A01).
- NCEER-90-0018 "Evaluation of Liquefaction Potential in Memphis and Shelby County," by T.S. Chang, P.S. Tang, C.S. Lee and H. Hwang, 8/10/90, (PB91-125427, A09, MF-A01).
- NCEER-90-0019 "Experimental and Analytical Study of a Combined Sliding Disc Bearing and Helical Steel Spring Isolation System," by M.C. Constantinou, A.S. Mokha and A.M. Reinhorn, 10/4/90, (PB91-125385, A06, MF-A01). This report is available only through NTIS (see address given above).

- NCEER-90-0020 "Experimental Study and Analytical Prediction of Earthquake Response of a Sliding Isolation System with a Spherical Surface," by A.S. Mokha, M.C. Constantinou and A.M. Reinhorn, 10/11/90, (PB91-125419, A05, MF-A01).
- NCEER-90-0021 "Dynamic Interaction Factors for Floating Pile Groups," by G. Gazetas, K. Fan, A. Kaynia and E. Kausel, 9/10/90, (PB91-170381, A05, MF-A01).
- NCEER-90-0022 "Evaluation of Seismic Damage Indices for Reinforced Concrete Structures," by S. Rodriguez-Gomez and A.S. Cakmak, 9/30/90, PB91-171322, A06, MF-A01).
- NCEER-90-0023 "Study of Site Response at a Selected Memphis Site," by H. Desai, S. Ahmad, E.S. Gazetas and M.R. Oh, 10/11/90, (PB91-196857, A03, MF-A01).
- NCEER-90-0024 "A User's Guide to Strongmo: Version 1.0 of NCEER's Strong-Motion Data Access Tool for PCs and Terminals," by P.A. Friberg and C.A.T. Susch, 11/15/90, (PB91-171272, A03, MF-A01).
- NCEER-90-0025 "A Three-Dimensional Analytical Study of Spatial Variability of Seismic Ground Motions," by L-L. Hong and A.H.-S. Ang, 10/30/90, (PB91-170399, A09, MF-A01).
- NCEER-90-0026 "MUMOID User's Guide - A Program for the Identification of Modal Parameters," by S. Rodriguez-Gomez and E. DiPasquale, 9/30/90, (PB91-171298, A04, MF-A01).
- NCEER-90-0027 "SARCF-II User's Guide - Seismic Analysis of Reinforced Concrete Frames," by S. Rodriguez-Gomez, Y.S. Chung and C. Meyer, 9/30/90, (PB91-171280, A05, MF-A01).
- NCEER-90-0028 "Viscous Dampers: Testing, Modeling and Application in Vibration and Seismic Isolation," by N. Makris and M.C. Constantinou, 12/20/90 (PB91-190561, A06, MF-A01).
- NCEER-90-0029 "Soil Effects on Earthquake Ground Motions in the Memphis Area," by H. Hwang, C.S. Lee, K.W. Ng and T.S. Chang, 8/2/90, (PB91-190751, A05, MF-A01).
- NCEER-91-0001 "Proceedings from the Third Japan-U.S. Workshop on Earthquake Resistant Design of Lifeline Facilities and Countermeasures for Soil Liquefaction, December 17-19, 1990," edited by T.D. O'Rourke and M. Hamada, 2/1/91, (PB91-179259, A99, MF-A04).
- NCEER-91-0002 "Physical Space Solutions of Non-Proportionally Damped Systems," by M. Tong, Z. Liang and G.C. Lee, 1/15/91, (PB91-179242, A04, MF-A01).
- NCEER-91-0003 "Seismic Response of Single Piles and Pile Groups," by K. Fan and G. Gazetas, 1/10/91, (PB92-174994, A04, MF-A01).
- NCEER-91-0004 "Damping of Structures: Part 1 - Theory of Complex Damping," by Z. Liang and G. Lee, 10/10/91, (PB92-197235, A12, MF-A03).
- NCEER-91-0005 "3D-BASIS - Nonlinear Dynamic Analysis of Three Dimensional Base Isolated Structures: Part II," by S. Nagarajaiah, A.M. Reinhorn and M.C. Constantinou, 2/28/91, (PB91-190553, A07, MF-A01). This report has been replaced by NCEER-93-0011.
- NCEER-91-0006 "A Multidimensional Hysteretic Model for Plasticity Deforming Metals in Energy Absorbing Devices," by E.J. Graesser and F.A. Cozzarelli, 4/9/91, (PB92-108364, A04, MF-A01).
- NCEER-91-0007 "A Framework for Customizable Knowledge-Based Expert Systems with an Application to a KBES for Evaluating the Seismic Resistance of Existing Buildings," by E.G. Ibarra-Anaya and S.J. Fenves, 4/9/91, (PB91-210930, A08, MF-A01).

- NCEER-91-0008 "Nonlinear Analysis of Steel Frames with Semi-Rigid Connections Using the Capacity Spectrum Method," by G.G. Deierlein, S-H. Hsieh, Y-J. Shen and J.F. Abel, 7/2/91, (PB92-113828, A05, MF-A01).
- NCEER-91-0009 "Earthquake Education Materials for Grades K-12," by K.E.K. Ross, 4/30/91, (PB91-212142, A06, MF-A01). This report has been replaced by NCEER-92-0018.
- NCEER-91-0010 "Phase Wave Velocities and Displacement Phase Differences in a Harmonically Oscillating Pile," by N. Makris and G. Gazetas, 7/8/91, (PB92-108356, A04, MF-A01).
- NCEER-91-0011 "Dynamic Characteristics of a Full-Size Five-Story Steel Structure and a 2/5 Scale Model," by K.C. Chang, G.C. Yao, G.C. Lee, D.S. Hao and Y.C. Yeh," 7/2/91, (PB93-116648, A06, MF-A02).
- NCEER-91-0012 "Seismic Response of a 2/5 Scale Steel Structure with Added Viscoelastic Dampers," by K.C. Chang, T.T. Soong, S-T. Oh and M.L. Lai, 5/17/91, (PB92-110816, A05, MF-A01).
- NCEER-91-0013 "Earthquake Response of Retaining Walls; Full-Scale Testing and Computational Modeling," by S. Alampalli and A-W.M. Elgamal, 6/20/91, to be published.
- NCEER-91-0014 "3D-BASIS-M: Nonlinear Dynamic Analysis of Multiple Building Base Isolated Structures," by P.C. Tsopelas, S. Nagarajaiah, M.C. Constantinou and A.M. Reinhorn, 5/28/91, (PB92-113885, A09, MF-A02).
- NCEER-91-0015 "Evaluation of SEAOC Design Requirements for Sliding Isolated Structures," by D. Theodossiou and M.C. Constantinou, 6/10/91, (PB92-114602, A11, MF-A03).
- NCEER-91-0016 "Closed-Loop Modal Testing of a 27-Story Reinforced Concrete Flat Plate-Core Building," by H.R. Somaprasad, T. Toksoy, H. Yoshiyuki and A.E. Aktan, 7/15/91, (PB92-129980, A07, MF-A02).
- NCEER-91-0017 "Shake Table Test of a 1/6 Scale Two-Story Lightly Reinforced Concrete Building," by A.G. El-Attar, R.N. White and P. Gergely, 2/28/91, (PB92-222447, A06, MF-A02).
- NCEER-91-0018 "Shake Table Test of a 1/8 Scale Three-Story Lightly Reinforced Concrete Building," by A.G. El-Attar, R.N. White and P. Gergely, 2/28/91, (PB93-116630, A08, MF-A02).
- NCEER-91-0019 "Transfer Functions for Rigid Rectangular Foundations," by A.S. Veletsos, A.M. Prasad and W.H. Wu, 7/31/91, to be published.
- NCEER-91-0020 "Hybrid Control of Seismic-Excited Nonlinear and Inelastic Structural Systems," by J.N. Yang, Z. Li and A. Danielians, 8/1/91, (PB92-143171, A06, MF-A02).
- NCEER-91-0021 "The NCEER-91 Earthquake Catalog: Improved Intensity-Based Magnitudes and Recurrence Relations for U.S. Earthquakes East of New Madrid," by L. Seeber and J.G. Armbruster, 8/28/91, (PB92-176742, A06, MF-A02).
- NCEER-91-0022 "Proceedings from the Implementation of Earthquake Planning and Education in Schools: The Need for Change - The Roles of the Changemakers," by K.E.K. Ross and F. Winslow, 7/23/91, (PB92-129998, A12, MF-A03).
- NCEER-91-0023 "A Study of Reliability-Based Criteria for Seismic Design of Reinforced Concrete Frame Buildings," by H.H.M. Hwang and H-M. Hsu, 8/10/91, (PB92-140235, A09, MF-A02).
- NCEER-91-0024 "Experimental Verification of a Number of Structural System Identification Algorithms," by R.G. Ghanem, H. Gavin and M. Shinozuka, 9/18/91, (PB92-176577, A18, MF-A04).
- NCEER-91-0025 "Probabilistic Evaluation of Liquefaction Potential," by H.H.M. Hwang and C.S. Lee," 11/25/91, (PB92-143429, A05, MF-A01).

- NCEER-91-0026 "Instantaneous Optimal Control for Linear, Nonlinear and Hysteretic Structures - Stable Controllers," by J.N. Yang and Z. Li, 11/15/91, (PB92-163807, A04, MF-A01).
- NCEER-91-0027 "Experimental and Theoretical Study of a Sliding Isolation System for Bridges," by M.C. Constantinou, A. Kartoum, A.M. Reinhorn and P. Bradford, 11/15/91, (PB92-176973, A10, MF-A03).
- NCEER-92-0001 "Case Studies of Liquefaction and Lifeline Performance During Past Earthquakes, Volume 1: Japanese Case Studies," Edited by M. Hamada and T. O'Rourke, 2/17/92, (PB92-197243, A18, MF-A04).
- NCEER-92-0002 "Case Studies of Liquefaction and Lifeline Performance During Past Earthquakes, Volume 2: United States Case Studies," Edited by T. O'Rourke and M. Hamada, 2/17/92, (PB92-197250, A20, MF-A04).
- NCEER-92-0003 "Issues in Earthquake Education," Edited by K. Ross, 2/3/92, (PB92-222389, A07, MF-A02).
- NCEER-92-0004 "Proceedings from the First U.S. - Japan Workshop on Earthquake Protective Systems for Bridges," Edited by I.G. Buckle, 2/4/92, (PB94-142239, A99, MF-A06).
- NCEER-92-0005 "Seismic Ground Motion from a Haskell-Type Source in a Multiple-Layered Half-Space," A.P. Theoharis, G. Deodatis and M. Shinozuka, 1/2/92, to be published.
- NCEER-92-0006 "Proceedings from the Site Effects Workshop," Edited by R. Whitman, 2/29/92, (PB92-197201, A04, MF-A01).
- NCEER-92-0007 "Engineering Evaluation of Permanent Ground Deformations Due to Seismically-Induced Liquefaction," by M.H. Baziar, R. Dobry and A-W.M. Elgamal, 3/24/92, (PB92-222421, A13, MF-A03).
- NCEER-92-0008 "A Procedure for the Seismic Evaluation of Buildings in the Central and Eastern United States," by C.D. Poland and J.O. Malley, 4/2/92, (PB92-222439, A20, MF-A04).
- NCEER-92-0009 "Experimental and Analytical Study of a Hybrid Isolation System Using Friction Controllable Sliding Bearings," by M.Q. Feng, S. Fujii and M. Shinozuka, 5/15/92, (PB93-150282, A06, MF-A02).
- NCEER-92-0010 "Seismic Resistance of Slab-Column Connections in Existing Non-Ductile Flat-Plate Buildings," by A.J. Durrani and Y. Du, 5/18/92, (PB93-116812, A06, MF-A02).
- NCEER-92-0011 "The Hysteretic and Dynamic Behavior of Brick Masonry Walls Upgraded by Ferrocement Coatings Under Cyclic Loading and Strong Simulated Ground Motion," by H. Lee and S.P. Prawel, 5/11/92, to be published.
- NCEER-92-0012 "Study of Wire Rope Systems for Seismic Protection of Equipment in Buildings," by G.F. Demetriades, M.C. Constantinou and A.M. Reinhorn, 5/20/92, (PB93-116655, A08, MF-A02).
- NCEER-92-0013 "Shape Memory Structural Dampers: Material Properties, Design and Seismic Testing," by P.R. Witting and F.A. Cozzarelli, 5/26/92, (PB93-116663, A05, MF-A01).
- NCEER-92-0014 "Longitudinal Permanent Ground Deformation Effects on Buried Continuous Pipelines," by M.J. O'Rourke, and C. Nordberg, 6/15/92, (PB93-116671, A08, MF-A02).
- NCEER-92-0015 "A Simulation Method for Stationary Gaussian Random Functions Based on the Sampling Theorem," by M. Grigoriu and S. Balopoulou, 6/11/92, (PB93-127496, A05, MF-A01).
- NCEER-92-0016 "Gravity-Load-Designed Reinforced Concrete Buildings: Seismic Evaluation of Existing Construction and Detailing Strategies for Improved Seismic Resistance," by G.W. Hoffmann, S.K. Kunnath, A.M. Reinhorn and J.B. Mander, 7/15/92, (PB94-142007, A08, MF-A02).

- NCEER-92-0017 "Observations on Water System and Pipeline Performance in the Limón Area of Costa Rica Due to the April 22, 1991 Earthquake," by M. O'Rourke and D. Ballantyne, 6/30/92, (PB93-126811, A06, MF-A02).
- NCEER-92-0018 "Fourth Edition of Earthquake Education Materials for Grades K-12," Edited by K.E.K. Ross, 8/10/92, (PB93-114023, A07, MF-A02).
- NCEER-92-0019 "Proceedings from the Fourth Japan-U.S. Workshop on Earthquake Resistant Design of Lifeline Facilities and Countermeasures for Soil Liquefaction," Edited by M. Hamada and T.D. O'Rourke, 8/12/92, (PB93-163939, A99, MF-E11).
- NCEER-92-0020 "Active Bracing System: A Full Scale Implementation of Active Control," by A.M. Reinhorn, T.T. Soong, R.C. Lin, M.A. Riley, Y.P. Wang, S. Aizawa and M. Higashino, 8/14/92, (PB93-127512, A06, MF-A02).
- NCEER-92-0021 "Empirical Analysis of Horizontal Ground Displacement Generated by Liquefaction-Induced Lateral Spreads," by S.F. Bartlett and T.L. Youd, 8/17/92, (PB93-188241, A06, MF-A02).
- NCEER-92-0022 "IDARC Version 3.0: Inelastic Damage Analysis of Reinforced Concrete Structures," by S.K. Kunnath, A.M. Reinhorn and R.F. Lobo, 8/31/92, (PB93-227502, A07, MF-A02).
- NCEER-92-0023 "A Semi-Empirical Analysis of Strong-Motion Peaks in Terms of Seismic Source, Propagation Path and Local Site Conditions, by M. Kamiyama, M.J. O'Rourke and R. Flores-Berrones, 9/9/92, (PB93-150266, A08, MF-A02).
- NCEER-92-0024 "Seismic Behavior of Reinforced Concrete Frame Structures with Nonductile Details, Part I: Summary of Experimental Findings of Full Scale Beam-Column Joint Tests," by A. Beres, R.N. White and P. Gergely, 9/30/92, (PB93-227783, A05, MF-A01).
- NCEER-92-0025 "Experimental Results of Repaired and Retrofitted Beam-Column Joint Tests in Lightly Reinforced Concrete Frame Buildings," by A. Beres, S. El-Borgi, R.N. White and P. Gergely, 10/29/92, (PB93-227791, A05, MF-A01).
- NCEER-92-0026 "A Generalization of Optimal Control Theory: Linear and Nonlinear Structures," by J.N. Yang, Z. Li and S. Vongchavalitkul, 11/2/92, (PB93-188621, A05, MF-A01).
- NCEER-92-0027 "Seismic Resistance of Reinforced Concrete Frame Structures Designed Only for Gravity Loads: Part I - Design and Properties of a One-Third Scale Model Structure," by J.M. Bracci, A.M. Reinhorn and J.B. Mander, 12/1/92, (PB94-104502, A08, MF-A02).
- NCEER-92-0028 "Seismic Resistance of Reinforced Concrete Frame Structures Designed Only for Gravity Loads: Part II - Experimental Performance of Subassemblages," by L.E. Aycardi, J.B. Mander and A.M. Reinhorn, 12/1/92, (PB94-104510, A08, MF-A02).
- NCEER-92-0029 "Seismic Resistance of Reinforced Concrete Frame Structures Designed Only for Gravity Loads: Part III - Experimental Performance and Analytical Study of a Structural Model," by J.M. Bracci, A.M. Reinhorn and J.B. Mander, 12/1/92, (PB93-227528, A09, MF-A01).
- NCEER-92-0030 "Evaluation of Seismic Retrofit of Reinforced Concrete Frame Structures: Part I - Experimental Performance of Retrofitted Subassemblages," by D. Choudhuri, J.B. Mander and A.M. Reinhorn, 12/8/92, (PB93-198307, A07, MF-A02).
- NCEER-92-0031 "Evaluation of Seismic Retrofit of Reinforced Concrete Frame Structures: Part II - Experimental Performance and Analytical Study of a Retrofitted Structural Model," by J.M. Bracci, A.M. Reinhorn and J.B. Mander, 12/8/92, (PB93-198315, A09, MF-A03).
- NCEER-92-0032 "Experimental and Analytical Investigation of Seismic Response of Structures with Supplemental Fluid Viscous Dampers," by M.C. Constantinou and M.D. Symans, 12/21/92, (PB93-191435, A10, MF-A03). This report is available only through NTIS (see address given above).

- NCEER-92-0033 "Reconnaissance Report on the Cairo, Egypt Earthquake of October 12, 1992," by M. Khater, 12/23/92, (PB93-188621, A03, MF-A01).
- NCEER-92-0034 "Low-Level Dynamic Characteristics of Four Tall Flat-Plate Buildings in New York City," by H. Gavin, S. Yuan, J. Grossman, E. Pekelis and K. Jacob, 12/28/92, (PB93-188217, A07, MF-A02).
- NCEER-93-0001 "An Experimental Study on the Seismic Performance of Brick-Infilled Steel Frames With and Without Retrofit," by J.B. Mander, B. Nair, K. Wojtkowski and J. Ma, 1/29/93, (PB93-227510, A07, MF-A02).
- NCEER-93-0002 "Social Accounting for Disaster Preparedness and Recovery Planning," by S. Cole, E. Pantoja and V. Razak, 2/22/93, (PB94-142114, A12, MF-A03).
- NCEER-93-0003 "Assessment of 1991 NEHRP Provisions for Nonstructural Components and Recommended Revisions," by T.T. Soong, G. Chen, Z. Wu, R-H. Zhang and M. Grigoriu, 3/1/93, (PB93-188639, A06, MF-A02).
- NCEER-93-0004 "Evaluation of Static and Response Spectrum Analysis Procedures of SEAOC/UBC for Seismic Isolated Structures," by C.W. Winters and M.C. Constantinou, 3/23/93, (PB93-198299, A10, MF-A03).
- NCEER-93-0005 "Earthquakes in the Northeast - Are We Ignoring the Hazard? A Workshop on Earthquake Science and Safety for Educators," edited by K.E.K. Ross, 4/2/93, (PB94-103066, A09, MF-A02).
- NCEER-93-0006 "Inelastic Response of Reinforced Concrete Structures with Viscoelastic Braces," by R.F. Lobo, J.M. Bracci, K.L. Shen, A.M. Reinhorn and T.T. Soong, 4/5/93, (PB93-227486, A05, MF-A02).
- NCEER-93-0007 "Seismic Testing of Installation Methods for Computers and Data Processing Equipment," by K. Kosar, T.T. Soong, K.L. Shen, J.A. HoLung and Y.K. Lin, 4/12/93, (PB93-198299, A07, MF-A02).
- NCEER-93-0008 "Retrofit of Reinforced Concrete Frames Using Added Dampers," by A. Reinhorn, M. Constantinou and C. Li, to be published.
- NCEER-93-0009 "Seismic Behavior and Design Guidelines for Steel Frame Structures with Added Viscoelastic Dampers," by K.C. Chang, M.L. Lai, T.T. Soong, D.S. Hao and Y.C. Yeh, 5/1/93, (PB94-141959, A07, MF-A02).
- NCEER-93-0010 "Seismic Performance of Shear-Critical Reinforced Concrete Bridge Piers," by J.B. Mander, S.M. Waheed, M.T.A. Chaudhary and S.S. Chen, 5/12/93, (PB93-227494, A08, MF-A02).
- NCEER-93-0011 "3D-BASIS-TABS: Computer Program for Nonlinear Dynamic Analysis of Three Dimensional Base Isolated Structures," by S. Nagarajaiah, C. Li, A.M. Reinhorn and M.C. Constantinou, 8/2/93, (PB94-141819, A09, MF-A02).
- NCEER-93-0012 "Effects of Hydrocarbon Spills from an Oil Pipeline Break on Ground Water," by O.J. Helweg and H.H.M. Hwang, 8/3/93, (PB94-141942, A06, MF-A02).
- NCEER-93-0013 "Simplified Procedures for Seismic Design of Nonstructural Components and Assessment of Current Code Provisions," by M.P. Singh, L.E. Suarez, E.E. Matheu and G.O. Maldonado, 8/4/93, (PB94-141827, A09, MF-A02).
- NCEER-93-0014 "An Energy Approach to Seismic Analysis and Design of Secondary Systems," by G. Chen and T.T. Soong, 8/6/93, (PB94-142767, A11, MF-A03).
- NCEER-93-0015 "Proceedings from School Sites: Becoming Prepared for Earthquakes - Commemorating the Third Anniversary of the Loma Prieta Earthquake," Edited by F.E. Winslow and K.E.K. Ross, 8/16/93, (PB94-154275, A16, MF-A02).

- NCEER-93-0016 "Reconnaissance Report of Damage to Historic Monuments in Cairo, Egypt Following the October 12, 1992 Dahshur Earthquake," by D. Sykora, D. Look, G. Croci, E. Karaesmen and E. Karaesmen, 8/19/93, (PB94-142221, A08, MF-A02).
- NCEER-93-0017 "The Island of Guam Earthquake of August 8, 1993," by S.W. Swan and S.K. Harris, 9/30/93, (PB94-141843, A04, MF-A01).
- NCEER-93-0018 "Engineering Aspects of the October 12, 1992 Egyptian Earthquake," by A.W. Elgarnal, M. Amer, K. Adalier and A. Abul-Fadl, 10/7/93, (PB94-141983, A05, MF-A01).
- NCEER-93-0019 "Development of an Earthquake Motion Simulator and its Application in Dynamic Centrifuge Testing," by I. Krstelj, Supervised by J.H. Prevost, 10/23/93, (PB94-181773, A-10, MF-A03).
- NCEER-93-0020 "NCEER-Taisei Corporation Research Program on Sliding Seismic Isolation Systems for Bridges: Experimental and Analytical Study of a Friction Pendulum System (FPS)," by M.C. Constantinou, P. Tsopelas, Y-S. Kim and S. Okamoto, 11/1/93, (PB94-142775, A08, MF-A02).
- NCEER-93-0021 "Finite Element Modeling of Elastomeric Seismic Isolation Bearings," by L.J. Billings, Supervised by R. Shepherd, 11/8/93, to be published.
- NCEER-93-0022 "Seismic Vulnerability of Equipment in Critical Facilities: Life-Safety and Operational Consequences," by K. Porter, G.S. Johnson, M.M. Zadeh, C. Scawthorn and S. Eder, 11/24/93, (PB94-181765, A16, MF-A03).
- NCEER-93-0023 "Hokkaido Nansei-oki, Japan Earthquake of July 12, 1993, by P.I. Yanev and C.R. Scawthorn, 12/23/93, (PB94-181500, A07, MF-A01).
- NCEER-94-0001 "An Evaluation of Seismic Serviceability of Water Supply Networks with Application to the San Francisco Auxiliary Water Supply System," by I. Markov, Supervised by M. Grigoriu and T. O'Rourke, 1/21/94, (PB94-204013, A07, MF-A02).
- NCEER-94-0002 "NCEER-Taisei Corporation Research Program on Sliding Seismic Isolation Systems for Bridges: Experimental and Analytical Study of Systems Consisting of Sliding Bearings, Rubber Restoring Force Devices and Fluid Dampers," Volumes I and II, by P. Tsopelas, S. Okamoto, M.C. Constantinou, D. Ozaki and S. Fujii, 2/4/94, (PB94-181740, A09, MF-A02 and PB94-181757, A12, MF-A03).
- NCEER-94-0003 "A Markov Model for Local and Global Damage Indices in Seismic Analysis," by S. Rahman and M. Grigoriu, 2/18/94, (PB94-206000, A12, MF-A03).
- NCEER-94-0004 "Proceedings from the NCEER Workshop on Seismic Response of Masonry Infills," edited by D.P. Abrams, 3/1/94, (PB94-180783, A07, MF-A02).
- NCEER-94-0005 "The Northridge, California Earthquake of January 17, 1994: General Reconnaissance Report," edited by J.D. Goltz, 3/11/94, (PB193943, A10, MF-A03).
- NCEER-94-0006 "Seismic Energy Based Fatigue Damage Analysis of Bridge Columns: Part I - Evaluation of Seismic Capacity," by G.A. Chang and J.B. Mander, 3/14/94, (PB94-219185, A11, MF-A03).
- NCEER-94-0007 "Seismic Isolation of Multi-Story Frame Structures Using Spherical Sliding Isolation Systems," by T.M. Al-Hussaini, V.A. Zayas and M.C. Constantinou, 3/17/94, (PB193745, A09, MF-A02).
- NCEER-94-0008 "The Northridge, California Earthquake of January 17, 1994: Performance of Highway Bridges," edited by I.G. Buckle, 3/24/94, (PB94-193851, A06, MF-A02).
- NCEER-94-0009 "Proceedings of the Third U.S.-Japan Workshop on Earthquake Protective Systems for Bridges," edited by I.G. Buckle and I. Friedland, 3/31/94, (PB94-195815, A99, MF-A06).

- NCEER-94-0010 "3D-BASIS-ME: Computer Program for Nonlinear Dynamic Analysis of Seismically Isolated Single and Multiple Structures and Liquid Storage Tanks," by P.C. Tsopelas, M.C. Constantinou and A.M. Reinhorn, 4/12/94, (PB94-204922, A09, MF-A02).
- NCEER-94-0011 "The Northridge, California Earthquake of January 17, 1994: Performance of Gas Transmission Pipelines," by T.D. O'Rourke and M.C. Palmer, 5/16/94, (PB94-204989, A05, MF-A01).
- NCEER-94-0012 "Feasibility Study of Replacement Procedures and Earthquake Performance Related to Gas Transmission Pipelines," by T.D. O'Rourke and M.C. Palmer, 5/25/94, (PB94-206638, A09, MF-A02).
- NCEER-94-0013 "Seismic Energy Based Fatigue Damage Analysis of Bridge Columns: Part II - Evaluation of Seismic Demand," by G.A. Chang and J.B. Mander, 6/1/94, (PB95-18106, A08, MF-A02).
- NCEER-94-0014 "NCEER-Taisei Corporation Research Program on Sliding Seismic Isolation Systems for Bridges: Experimental and Analytical Study of a System Consisting of Sliding Bearings and Fluid Restoring Force/Damping Devices," by P. Tsopelas and M.C. Constantinou, 6/13/94, (PB94-219144, A10, MF-A03).
- NCEER-94-0015 "Generation of Hazard-Consistent Fragility Curves for Seismic Loss Estimation Studies," by H. Hwang and J.R. Huo, 6/14/94, (PB95-181996, A09, MF-A02).
- NCEER-94-0016 "Seismic Study of Building Frames with Added Energy-Absorbing Devices," by W.S. Pong, C.S. Tsai and G.C. Lee, 6/20/94, (PB94-219136, A10, A03).
- NCEER-94-0017 "Sliding Mode Control for Seismic-Excited Linear and Nonlinear Civil Engineering Structures," by J. Yang, J. Wu, A. Agrawal and Z. Li, 6/21/94, (PB95-138483, A06, MF-A02).
- NCEER-94-0018 "3D-BASIS-TABS Version 2.0: Computer Program for Nonlinear Dynamic Analysis of Three Dimensional Base Isolated Structures," by A.M. Reinhorn, S. Nagarajaiah, M.C. Constantinou, P. Tsopelas and R. Li, 6/22/94, (PB95-182176, A08, MF-A02).
- NCEER-94-0019 "Proceedings of the International Workshop on Civil Infrastructure Systems: Application of Intelligent Systems and Advanced Materials on Bridge Systems," Edited by G.C. Lee and K.C. Chang, 7/18/94, (PB95-252474, A20, MF-A04).
- NCEER-94-0020 "Study of Seismic Isolation Systems for Computer Floors," by V. Lambrou and M.C. Constantinou, 7/19/94, (PB95-138533, A10, MF-A03).
- NCEER-94-0021 "Proceedings of the U.S.-Italian Workshop on Guidelines for Seismic Evaluation and Rehabilitation of Unreinforced Masonry Buildings," Edited by D.P. Abrams and G.M. Calvi, 7/20/94, (PB95-138749, A13, MF-A03).
- NCEER-94-0022 "NCEER-Taisei Corporation Research Program on Sliding Seismic Isolation Systems for Bridges: Experimental and Analytical Study of a System Consisting of Lubricated PTFE Sliding Bearings and Mild Steel Dampers," by P. Tsopelas and M.C. Constantinou, 7/22/94, (PB95-182184, A08, MF-A02).
- NCEER-94-0023 "Development of Reliability-Based Design Criteria for Buildings Under Seismic Load," by Y.K. Wen, H. Hwang and M. Shinozuka, 8/1/94, (PB95-211934, A08, MF-A02).
- NCEER-94-0024 "Experimental Verification of Acceleration Feedback Control Strategies for an Active Tendon System," by S.J. Dyke, B.F. Spencer, Jr., P. Quast, M.K. Sain, D.C. Kaspari, Jr. and T.T. Soong, 8/29/94, (PB95-212320, A05, MF-A01).
- NCEER-94-0025 "Seismic Retrofitting Manual for Highway Bridges," Edited by I.G. Buckle and I.F. Friedland, published by the Federal Highway Administration (PB95-212676, A15, MF-A03).

- NCEER-94-0026 "Proceedings from the Fifth U.S.-Japan Workshop on Earthquake Resistant Design of Lifeline Facilities and Countermeasures Against Soil Liquefaction," Edited by T.D. O'Rourke and M. Hamada, 11/7/94, (PB95-220802, A99, MF-E08).
- NCEER-95-0001 "Experimental and Analytical Investigation of Seismic Retrofit of Structures with Supplemental Damping: Part I - Fluid Viscous Damping Devices," by A.M. Reinhorn, C. Li and M.C. Constantinou, 1/3/95, (PB95-266599, A09, MF-A02).
- NCEER-95-0002 "Experimental and Analytical Study of Low-Cycle Fatigue Behavior of Semi-Rigid Top-And-Seat Angle Connections," by G. Pekcan, J.B. Mander and S.S. Chen, 1/5/95, (PB95-220042, A07, MF-A02).
- NCEER-95-0003 "NCEER-ATC Joint Study on Fragility of Buildings," by T. Anagnos, C. Rojahn and A.S. Kiremidjian, 1/20/95, (PB95-220026, A06, MF-A02).
- NCEER-95-0004 "Nonlinear Control Algorithms for Peak Response Reduction," by Z. Wu, T.T. Soong, V. Gattulli and R.C. Lin, 2/16/95, (PB95-220349, A05, MF-A01).
- NCEER-95-0005 "Pipeline Replacement Feasibility Study: A Methodology for Minimizing Seismic and Corrosion Risks to Underground Natural Gas Pipelines," by R.T. Eguchi, H.A. Seligson and D.G. Honegger, 3/2/95, (PB95-252326, A06, MF-A02).
- NCEER-95-0006 "Evaluation of Seismic Performance of an 11-Story Frame Building During the 1994 Northridge Earthquake," by F. Naeim, R. DiSulio, K. Benuska, A. Reinhorn and C. Li, to be published.
- NCEER-95-0007 "Prioritization of Bridges for Seismic Retrofitting," by N. Basöz and A.S. Kiremidjian, 4/24/95, (PB95-252300, A08, MF-A02).
- NCEER-95-0008 "Method for Developing Motion Damage Relationships for Reinforced Concrete Frames," by A. Singhal and A.S. Kiremidjian, 5/11/95, (PB95-266607, A06, MF-A02).
- NCEER-95-0009 "Experimental and Analytical Investigation of Seismic Retrofit of Structures with Supplemental Damping: Part II - Friction Devices," by C. Li and A.M. Reinhorn, 7/6/95, (PB96-128087, A11, MF-A03).
- NCEER-95-0010 "Experimental Performance and Analytical Study of a Non-Ductile Reinforced Concrete Frame Structure Retrofitted with Elastomeric Spring Dampers," by G. Pekcan, J.B. Mander and S.S. Chen, 7/14/95, (PB96-137161, A08, MF-A02).
- NCEER-95-0011 "Development and Experimental Study of Semi-Active Fluid Damping Devices for Seismic Protection of Structures," by M.D. Symans and M.C. Constantinou, 8/3/95, (PB96-136940, A23, MF-A04).
- NCEER-95-0012 "Real-Time Structural Parameter Modification (RSPM): Development of Innervated Structures," by Z. Liang, M. Tong and G.C. Lee, 4/11/95, (PB96-137153, A06, MF-A01).
- NCEER-95-0013 "Experimental and Analytical Investigation of Seismic Retrofit of Structures with Supplemental Damping: Part III - Viscous Damping Walls," by A.M. Reinhorn and C. Li, 10/1/95, (PB96-176409, A11, MF-A03).
- NCEER-95-0014 "Seismic Fragility Analysis of Equipment and Structures in a Memphis Electric Substation," by J-R. Huo and H.H.M. Hwang, (PB96-128087, A09, MF-A02), 8/10/95.
- NCEER-95-0015 "The Hanshin-Awaji Earthquake of January 17, 1995: Performance of Lifelines," Edited by M. Shinozuka, 11/3/95, (PB96-176383, A15, MF-A03).
- NCEER-95-0016 "Highway Culvert Performance During Earthquakes," by T.L. Youd and C.J. Beckman, available as NCEER-96-0015.

- NCEER-95-0017 "The Hanshin-Awaji Earthquake of January 17, 1995: Performance of Highway Bridges," Edited by I.G. Buckle, 12/1/95, to be published.
- NCEER-95-0018 "Modeling of Masonry Infill Panels for Structural Analysis," by A.M. Reinhorn, A. Madan, R.E. Valles, Y. Reichmann and J.B. Mander, 12/8/95.
- NCEER-95-0019 "Optimal Polynomial Control for Linear and Nonlinear Structures," by A.K. Agrawal and J.N. Yang, 12/11/95, (PB96-168737, A07, MF-A02).
- NCEER-95-0020 "Retrofit of Non-Ductile Reinforced Concrete Frames Using Friction Dampers," by R.S. Rao, P. Gergely and R.N. White, 12/22/95, (PB97-133508, A10, MF-A02).
- NCEER-95-0021 "Parametric Results for Seismic Response of Pile-Supported Bridge Bents," by G. Mylonakis, A. Nikolaou and G. Gazetas, 12/22/95, (PB97-100242, A12, MF-A03).
- NCEER-95-0022 "Kinematic Bending Moments in Seismically Stressed Piles," by A. Nikolaou, G. Mylonakis and G. Gazetas, 12/23/95.
- NCEER-96-0001 "Dynamic Response of Unreinforced Masonry Buildings with Flexible Diaphragms," by A.C. Costley and D.P. Abrams, 10/10/96.
- NCEER-96-0002 "State of the Art Review: Foundations and Retaining Structures," by I. Po Lam, to be published.
- NCEER-96-0003 "Ductility of Rectangular Reinforced Concrete Bridge Columns with Moderate Confinement," by N. Wehbe, M. Saiidi, D. Sanders and B. Douglas, 11/7/96, (PB97-133557, A06, MF-A02).
- NCEER-96-0004 "Proceedings of the Long-Span Bridge Seismic Research Workshop," edited by I.G. Buckle and I.M. Friedland, to be published.
- NCEER-96-0005 "Establish Representative Pier Types for Comprehensive Study: Eastern United States," by J. Kulicki and Z. Prucz, 5/28/96, (PB98-119217, A07, MF-A02).
- NCEER-96-0006 "Establish Representative Pier Types for Comprehensive Study: Western United States," by R. Imbsen, R.A. Schamber and T.A. Osterkamp, 5/28/96, (PB98-118607, A07, MF-A02).
- NCEER-96-0007 "Nonlinear Control Techniques for Dynamical Systems with Uncertain Parameters," by R.G. Ghanem and M.I. Bujakov, 5/27/96, (PB97-100259, A17, MF-A03).
- NCEER-96-0008 "Seismic Evaluation of a 30-Year Old Non-Ductile Highway Bridge Pier and Its Retrofit," by J.B. Mander, B. Mahmoodzadegan, S. Bhadra and S.S. Chen, 5/31/96.
- NCEER-96-0009 "Seismic Performance of a Model Reinforced Concrete Bridge Pier Before and After Retrofit," by J.B. Mander, J.H. Kim and C.A. Ligozio, 5/31/96.
- NCEER-96-0010 "IDARC2D Version 4.0: A Computer Program for the Inelastic Damage Analysis of Buildings," by R.E. Valles, A.M. Reinhorn, S.K. Kunnath, C. Li and A. Madan, 6/3/96, (PB97-100234, A17, MF-A03).
- NCEER-96-0011 "Estimation of the Economic Impact of Multiple Lifeline Disruption: Memphis Light, Gas and Water Division Case Study," by S.E. Chang, H.A. Seligson and R.T. Eguchi, 8/16/96, (PB97-133490, A11, MF-A03).
- NCEER-96-0012 "Proceedings from the Sixth Japan-U.S. Workshop on Earthquake Resistant Design of Lifeline Facilities and Countermeasures Against Soil Liquefaction, Edited by M. Hamada and T. O'Rourke, 9/11/96, (PB97-133581, A99, MF-A06).

- NCEER-96-0013 "Chemical Hazards, Mitigation and Preparedness in Areas of High Seismic Risk: A Methodology for Estimating the Risk of Post-Earthquake Hazardous Materials Release," by H.A. Seligson, R.T. Eguchi, K.J. Tierney and K. Richmond, 11/7/96.
- NCEER-96-0014 "Response of Steel Bridge Bearings to Reversed Cyclic Loading," by J.B. Mander, D-K. Kim, S.S. Chen and G.J. Premus, 11/13/96, (PB97-140735, A12, MF-A03).
- NCEER-96-0015 "Highway Culvert Performance During Past Earthquakes," by T.L. Youd and C.J. Beckman, 11/25/96, (PB97-133532, A06, MF-A01).
- NCEER-97-0001 "Evaluation, Prevention and Mitigation of Pounding Effects in Building Structures," by R.E. Valles and A.M. Reinhorn, 2/20/97, (PB97-159552, A14, MF-A03).
- NCEER-97-0002 "Seismic Design Criteria for Bridges and Other Highway Structures," by C. Rojahn, R. Mayes, D.G. Anderson, J. Clark, J.H. Hom, R.V. Nutt and M.J. O'Rourke, 4/30/97, (PB97-194658, A06, MF-A03).
- NCEER-97-0003 "Proceedings of the U.S.-Italian Workshop on Seismic Evaluation and Retrofit," Edited by D.P. Abrams and G.M. Calvi, 3/19/97, (PB97-194666, A13, MF-A03).
- NCEER-97-0004 "Investigation of Seismic Response of Buildings with Linear and Nonlinear Fluid Viscous Dampers," by A.A. Seleemah and M.C. Constantinou, 5/21/97, (PB98-109002, A15, MF-A03).
- NCEER-97-0005 "Proceedings of the Workshop on Earthquake Engineering Frontiers in Transportation Facilities," edited by G.C. Lee and I.M. Friedland, 8/29/97, (PB98-128911, A25, MR-A04).
- NCEER-97-0006 "Cumulative Seismic Damage of Reinforced Concrete Bridge Piers," by S.K. Kunnath, A. El-Bahy, A. Taylor and W. Stone, 9/2/97, (PB98-108814, A11, MF-A03).
- NCEER-97-0007 "Structural Details to Accommodate Seismic Movements of Highway Bridges and Retaining Walls," by R.A. Imbsen, R.A. Schamber, E. Thorkildsen, A. Kartoum, B.T. Martin, T.N. Rosser and J.M. Kulicki, 9/3/97.
- NCEER-97-0008 "A Method for Earthquake Motion-Damage Relationships with Application to Reinforced Concrete Frames," by A. Singhal and A.S. Kiremidjian, 9/10/97, (PB98-108988, A13, MF-A03).
- NCEER-97-0009 "Seismic Analysis and Design of Bridge Abutments Considering Sliding and Rotation," by K. Fishman and R. Richards, Jr., 9/15/97, (PB98-108897, A06, MF-A02).
- NCEER-97-0010 "Proceedings of the FHWA/NCEER Workshop on the National Representation of Seismic Ground Motion for New and Existing Highway Facilities," edited by I.M. Friedland, M.S. Power and R.L. Mayes, 9/22/97.
- NCEER-97-0011 "Seismic Analysis for Design or Retrofit of Gravity Bridge Abutments," by K.L. Fishman, R. Richards, Jr. and R.C. Divito, 10/2/97, (PB98-128937, A08, MF-A02).
- NCEER-97-0012 "Evaluation of Simplified Methods of Analysis for Yielding Structures," by P. Tsopelas, M.C. Constantinou, C.A. Kircher and A.S. Whittaker, 10/31/97, (PB98-128929, A10, MF-A03).
- NCEER-97-0013 "Seismic Design of Bridge Columns Based on Control and Repairability of Damage," by C-T. Cheng and J.B. Mander, 12/8/97.
- NCEER-97-0014 "Seismic Resistance of Bridge Piers Based on Damage Avoidance Design," by J.B. Mander and C-T. Cheng, 12/10/97.
- NCEER-97-0015 "Seismic Response of Nominally Symmetric Systems with Strength Uncertainty," by S. Balopoulou and M. Grigoriu, 12/23/97, (PB98-153422, A11, MF-A03).

- NCEER-97-0016 "Evaluation of Seismic Retrofit Methods for Reinforced Concrete Bridge Columns," by T.J. Wipf, F.W. Klaiber and F.M. Russo, 12/28/97.
- NCEER-97-0017 "Seismic Fragility of Existing Conventional Reinforced Concrete Highway Bridges," by C.L. Mullen and A.S. Cakmak, 12/30/97, (PB98-153406, A08, MF-A02).
- NCEER-97-0018 "Loss Assessment of Memphis Buildings," edited by D.P. Abrams and M. Shinozuka, 12/31/97.
- NCEER-97-0019 "Seismic Evaluation of Frames with Infill Walls Using Quasi-static Experiments," by K.M. Mosalam, R.N. White and P. Gergely, 12/31/97, (PB98-153455, A07, MF-A02).
- NCEER-97-0020 "Seismic Evaluation of Frames with Infill Walls Using Pseudo-dynamic Experiments," by K.M. Mosalam, R.N. White and P. Gergely, 12/31/97.
- NCEER-97-0021 "Computational Strategies for Frames with Infill Walls: Discrete and Smeared Crack Analyses and Seismic Fragility," by K.M. Mosalam, R.N. White and P. Gergely, 12/31/97, (PB98-153414, A10, MF-A02).
- NCEER-97-0022 "Proceedings of the NCEER Workshop on Evaluation of Liquefaction Resistance of Soils," edited by T.L. Youd and I.M. Idriss, 12/31/97.
- MCEER-98-0001 "Extraction of Nonlinear Hysteretic Properties of Seismically Isolated Bridges from Quick-Release Field Tests," by Q. Chen, B.M. Douglas, E.M. Maragakis and I.G. Buckle, 5/26/98.
- MCEER-98-0002 "Methodologies for Evaluating the Importance of Highway Bridges," by A. Thomas, S. Eshenaur and J. Kulicki, 5/29/98.
- MCEER-98-0003 "Capacity Design of Bridge Piers and the Analysis of Overstrength," by J.B. Mander, A. Dutta and P. Goel, 6/1/98.
- MCEER-98-0004 "Evaluation of Bridge Damage Data from the Loma Prieta and Northridge, California Earthquakes," by N. Basoz and A. Kiremidjian, 6/2/98.
- MCEER-98-0005 "Screening Guide for Rapid Assessment of Liquefaction Hazard at Highway Bridge Sites," by T. L. Youd, 6/16/98.
- MCEER-98-0006 "Structural Steel and Steel/Concrete Interface Details for Bridges," by P. Ritchie, N. Kahl and J. Kulicki, 7/13/98.
- MCEER-98-0007 "Capacity Design and Fatigue Analysis of Confined Concrete Columns," by A. Dutta and J.B. Mander, 7/14/98.
- MCEER-98-0008 "Proceedings of the Workshop on Performance Criteria for Telecommunication Services Under Earthquake Conditions," edited by A.J. Schiff, 7/15/98.
- MCEER-98-0009 "Fatigue Analysis of Unconfined Concrete Columns," by J.B. Mander, A. Dutta and J.H. Kim, 9/12/98.
- MCEER-98-0010 "Centrifuge Modeling of Cyclic Lateral Response of Pile-Cap Systems and Seat-Type Abutments in Dry Sands," by A.D. Gadre and R. Dobry, 10/2/98.
- MCEER-98-0011 "IDARC-BRIDGE: A Computational Platform for Seismic Damage Assessment of Bridge Structures," by A.M. Reinhorn, V. Simeonov, G. Mylonakis and Y. Reichman, 10/2/98.
- MCEER-98-0012 "Experimental Investigation of the Dynamic Response of Two Bridges Before and After Retrofitting with Elastomeric Bearings," by D.A. Wendichansky, S.S. Chen and J.B. Mander, 10/2/98.

- MCEER-98-0013 "Design Procedures for Hinge Restrainers and Hinge Sear Width for Multiple-Frame Bridges," by R. Des Roches and G.L. Fenves, 11/3/98.
- MCEER-98-0014 "Response Modification Factors for Seismically Isolated Bridges," by M.C. Constantinou and J.K. Quarshie, 11/3/98.
- MCEER-98-0015 "Proceedings of the U.S.-Italy Workshop on Seismic Protective Systems for Bridges," edited by I.M. Friedland and M.C. Constantinou, 11/3/98.
- MCEER-98-0016 "Appropriate Seismic Reliability for Critical Equipment Systems: Recommendations Based on Regional Analysis of Financial and Life Loss," by K. Porter, C. Scawthorn, C. Taylor and N. Blais, 11/10/98.
- MCEER-98-0017 "Proceedings of the U.S. Japan Joint Seminar on Civil Infrastructure Systems Research," edited by M. Shinozuka and A. Rose, 11/12/98.
- MCEER-98-0018 "Modeling of Pile Footings and Drilled Shafts for Seismic Design," by I. PoLam, M. Kapuskar and D. Chaudhuri, 12/21/98.



MULTIDISCIPLINARY CENTER FOR EARTHQUAKE ENGINEERING RESEARCH

A National Center of Excellence in Advanced Technology Applications

University at Buffalo, State University of New York
Red Jacket Quadrangle ■ Buffalo, New York 14261-0025
Phone: 716/645-3391 ■ Fax: 716/645-3399
E-mail: mceer@acsu.buffalo.edu ■ WWW Site: <http://mceer.buffalo.edu>

ISSN 1520-295X